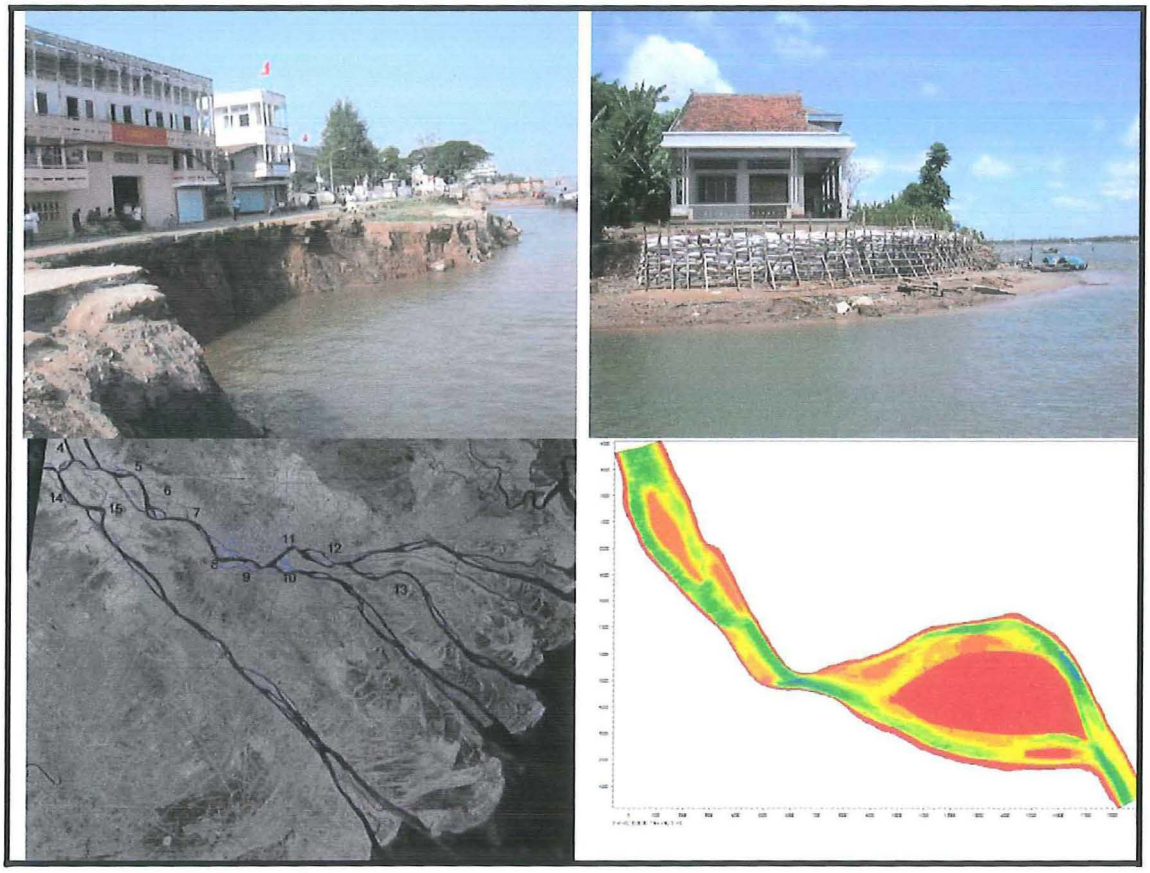

BANK EROSION PREDICTION AND MITIGATION MEASURES ALONG THE LOWER MEKONG RIVER

DRAFT REPORT

Nguyen Nghia Hung
Msc Thesis WSE-HERBD
May 2006

BANK EROSION PREDICTION AND MITIGATION MEASURES ALONG THE LOWER MEKONG RIVER

Master of Science thesis

by

Nguyen Nghia Hung

Supervisor

Ir.G.J.Klaassen

Examination committee:

Chairman: Prof.Dr. N. Wright

Members: Ir.K.W.Pilarczyk

Ir.G.J.Klaassen

The research is done for the partial fulfillment of requirements for the Master of Science degree at UNESCO-IHE Institute for Water education, Delft, The Netherlands

Delft, May 2006

The findings, interpretations and conclusion expressed in this study do neither necessarily reflect the views of the UNESCO_IHE Institute for Water Education, nor of the individual members of the Msc committee, nor of their respective employers.

ACKNOWLEDGMENTS

I would like to take this opportunity to express my sincere thanks and appreciation to all the people who directly or indirectly contributed to the completion of my Master of Science study at UNESCO-IHE Institute for Water Education, The Netherlands. Both NUFFIC and the Ministry of Transport and Water Management - Rijkswaterstaat, Road and Hydraulic Engineering Institute of The Netherlands kindly provided funding for my 20-month study in The Netherlands.

I wish to gratefully acknowledge my supervisor Ass. Prof. Ir. G.J.Klaassen for his valuable advices, meticulous guidance, and regular encouragement during the entire study. The best thanks are given to Ir. K.Pilarczyk for his advice and encouragement, for providing relevant literature, and for the careful revision of the draft text. Also, I would like to thank Prof.Dr. N.Wright for chairing my examination committee and for his valuable comments on the draft report.

My sincere thanks go to all other lecturers, who provided valuable knowledge and information during their lectures and Ir. G.H. Geurtsen the course coordinator for his support during my study in the Netherlands.

Many thanks are certainly due to Prof.Dr. Le Sam, Director, and Ass.Prof.Dr. Le Manh Hung, Dr. Tang Duc Thang, Ass. Prof.Dr. Hoang Van Huan, Vice Directors of SIWRR (Southern Institute of Water Resource Research) – Vietnam for their support and encouragement.

Thanks also given to Dr.B. Lief, and G. Henrick, M.sc, and Dr. D.C. San, for their providing MIKE dongle, and their valuable advice during the MIKE21C modelling.

My gratefulness goes to all Vietnamese, Dutch and foreign friends in the Netherlands. Thanks also given to my colleagues, and PhD student Nguyen Anh Duc for his revision of the draft text, advice, and his encouragement.

Lastly but most importantly, I would like to express my deepest gratefulness to my parents, and my dear wife. *My Love, beside a success man is a great wife!*

Nguyen Nghia Hung
Delft, May 2006

Abstract

The Lower Mekong River area is a zone with plenty of natural resources and it has the highest agricultural production in Vietnam. The river passes though six provinces in the Southern part of Vietnam, with more than 16 million in habitants in total. However, serious riverbank erosion problems occur and there is no master plan or mitigation strategy to prevent this problem. Given these conditions, the first objective of this Master of Science study was to study bank erosion prediction by means of both empirical methods and numerical methods. The second objective is to study possible mitigation measures, especially the use of revetments, bend cut-off, and permeable groynes.

Based on a number of satellite images (1987, 1996, 2000), old map (1937, 1966) and the observed topography data at some locations, empirical methods to predict riverbank erosion were studied, tested and modified. It appeared not possible to derive an empirical method which in generally applicable in the Lower Mekong River. A numerical model was developed amongst others to make of riverbank erosion predictions. This model was properly calibrated and verified against data from measurements. In an early state of numerical model development, riverbank erosion prediction along the Lower Mekong River was tested with the model. In this testing, the sensitive of parameters in the bank erosion module of MIKE21C were checked for the Tan Chau -Hong Ngu reach.

To prevent (predict and mitigate) riverbank erosion is a very challenging task in river engineering. The mitigation measures were studied by a comprehensive approach, which reviewed the existing mitigation measures in the lower Mekong river, and subsequently fare an overview of possibility preventive measures in this area. Finally, one case study, notably the critical reach near Tan Chau, was taken considering three kinds of measures: a revetment, a bend cut and permeable groynes. The numerical model was used to predict (i) the scour hole in front of revetment, and (ii) the effect of the bend cut. Also the application of the permeable groynes was studied, but these appear to be less suitable for the specific conditions at Tan Chau.

Hopefully, the study results will on the lay sum contribute to the master plan study for the sustainable development in the lower Mekong river system. It has definitely contributed to the author's knowledge and professional career.

TABLE OF CONTENTS

LIST OF FIGURES

LIST OF TABLES

LIST OF SYMBOLS

Symbols	Define	Unit
A	Cross-section area	m^2
A_{bf}	Area of cross-section at bankfull level	m^2
C	Chezy roughness coefficient	$m^{1/2}/s$
D	Particle diameter	mm
i	The slope of river	-
h_b	Bank height, the distance from lowest point to flood plain level	m
h	Water depth	m
E	Riverbank erosion rate	m/year
R	Radius of curvature	m
λ	Meandering length	m
λ_{max}	Meandering length	m
$\overline{\lambda}$	Average meandering length	m
B_s	River width at the average discharge	m
W	Bankfull width	m
$E_{2.5}$	Riverbank erosion rate at R/W=2.5	m/year
Ω	Stream power	watt/m'
Q	Discharge	m^3/s
Q_5	The five-year flood	m^3/s
Y_b	Bank strength parameter	N/m^2
E_{max}	Maximum riverbank erosion rate	m/year
ρ	Density of water	kg/m^3
g	Acceleration due to gravity	m/s^2
w_s	Particle fall velocity	m/s
$u*$	Bed-shear velocity	m/s
$D*$	Dimensionless particle parameter	(-)
ν	Kinematic viscosity coefficient	kg/m/s
Re	Shear Reynold number	-
$\tau_{0,cr}$	Critical shear stress	N/m^2
i_s	Helical flow intensity	-
Δ	Specific density	-

T	Transport stage parameter	-
q_b	Volumetric bed load transport rate	m^2/s
q_s	Volumetric suspended load transport rate	m^2/s
q_{total}	Total load transport (without wash load)	m^2/s
u	depth average velocity	m/s
ε	Porosity of bed material	-
z_b	Bed level	m
α, β, γ	Bank erosion calibration parameter	-
s, n	Co-ordinates in the curvilinear co-ordinate system	-
R_s	Radius of curvature of streamlines	m
c	Concentration of suspended sediment	mg/m^3
G	Transverse slope coefficient	-
θ	Shields parameter	-
E	Turbulent (eddy) viscosity coefficient	m^2/s
J	Number of grid along the streamline	-
K	Number of grid transverse the streamline	-
L_G	Length of permeable groyne	m
y_s	Scour depth	m
$y_{s\ local}$	Local scour depth	m
$y_{s,0}$	Total scour depth	m
P	Permeability of groyne	-
l_s	Length of scour hole	m
C_D	Drag coefficient	-

1. INTRODUCTION

1.1 General information of Mekong River

Through the ages, river has played a central role in the evolution of human societies. The Mekong River is one of the ten biggest rivers of the world, which crosses six countries of South East Asia: China, Myanmar, Laos, Cambodia, Thailand, and Vietnam. It originates in China in the Tibetan Tanggula mountain range at an altitude of about 5,000m and drains itself into the South China Sea in Vietnam. The total length is about 4,800 km with the catchment area about 795,500 km^2 (source: MRC). The Mekong River takes an extremely important part in ecosystem balance for South East Asia.

Historically, the river has five different names in the different languages through which it runs: Dza Chu (water of rock) at its origin in China's Tibetang Tanggula, Lan Cang (Mighty River) in Yunnan province in China, Lancang Jiang in Myanmar, Mea Nam Khong (the Mother of Waters or Mekong) in Laos and Thailand, Tonle Thom (Big River) in Cambodia. Then it goes to the South China Sea in nine branches, thence Cuu Long (Nine Dragons) is called by Vietnamese (Hoang Dinh Co, 2003). Nowadays, Mekong is an international name of river.

In 1866, a French named Francis Garnier with his team decided a heroic expedition in an attempt to find the water way from Saigon to China, that was known one of the earliest understanding of Mekong river (Louis Delaporte / Francis Garnier 1866-1868). In 1995, the Mekong river commission was formed between four countries, Thai Land, Laos, Cambodia and Vietnam. In 2000, China and Myanmar are two countries of observation. They are working in a framework with good cooperation. In the figure 1 below, the summary of Mekong river information is shown.

Short information Mekong River
- Total length: 4800 km
- River basin area: 795,000 km^2.
- Area integrated:
  About 2 million ha of net area.
- Area of wetlands:
60,400-83,700 km ^{2}
- Main products: Rice, cassava, maize, vegetables, fruit, coffee, tea, rubber, livestock, fish and timber.
- Population: 60-65 million inhabitants

Lower part of Mekong River in Vietnam
- Total length: about 230 km
- Region area: 39,000km2.
- Population: about 16.3 million inhabitants
- Number of outlets: 9 (Dai, Tieu, Ba Lai, Bassac, Cung Hau, Cung Hay, Co chien, Dinh An and TranDe.
- Main products: Rice, fish, fruit, vegetables, construction material etc.

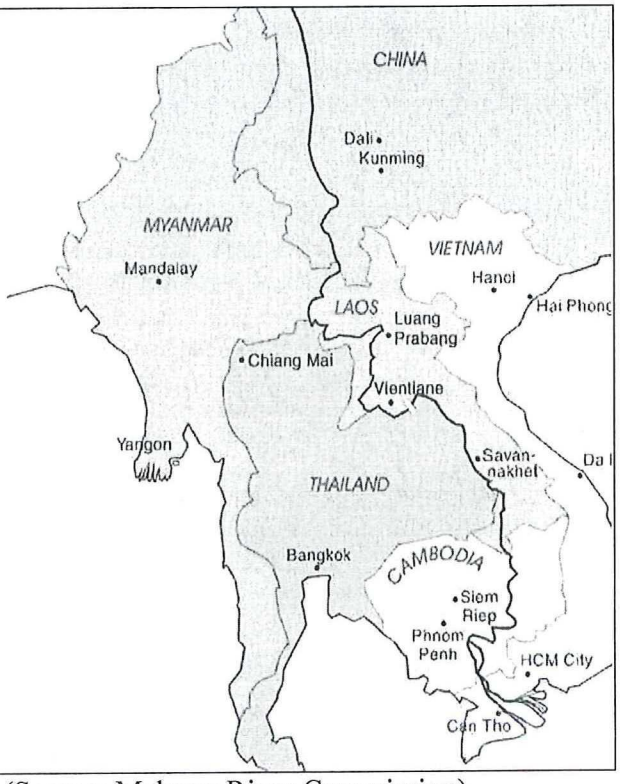

Figure 1.1 Overview of Mekong River (Source: Mekong River Commission)

Although, the Mekong River is a gift of nature but it is not for free. The flooding and riverbank erosion always are two threatens to people who are living there. The following sections explain about riverbank erosion phenomena and some general theoretical research.

1.2 Problem statement

Despite many efforts from various governmental agencies on different levels, riverbank erosion and its consequences still remain as one of the critical issues in the lower Mekong river. To prevent the riverbank erosion problems substantially is a challenging task, which needs broad and profound studies. In chapter 3, the riverbank erosion at some special places are reported in riverbank erosion assessment section.

River bank erosion is a natural phenomenon of rivers. It is a random and dynamic process in time and space. It happens randomly. The results are damages at the locations on riverbank are house collapses, land loss, etc. Definitely, river bank erosion can be causes by flow of river, seepage of bank soil material, waves, loading on the river bank, propagation of flood or tidal, the soil material of river bank etc. It is most prominent in river bends due to the increase of velocities in the outer bend and the spiral flow, which tends to deepen the outer bend. Because of a complex phenomenon, many factors involve, so that riverbank erosion becomes a difficult task for river engineering.

In time and space, river changes itself due to the interaction between plan form and flow. As a result of river width changes, riverbank erosion has many factors, which play a major role. They are sedimentology, geology, hydrology, morphology and vegetation as well. In addition, riverbank erosion expresses from the balance of resistant forces and slip forces of mass of riverbank. The flow attaches to the riverbank by scouring and movable of the scour hole in front of riverbank are two main reasons that make riverbank collapse.

Moreover, the rates of lateral erosion for various rivers are greatly different due to variation in geological structure and sediment composition of the valley material. Rates of lateral migration from a few meters per year (Brice 1984, USA Rivers) via some tens of meters per year (Mahakam River, Kalimantan, Indonesia), and 50-75 m/year (Missouri, Mississipi), to values of 302-750m/years for Brahmaputra river, occurring mainly during the flood season (Coleman, 1969; Klaassen & Masselink, 1992). The Lower Mekong river is about 5-50m/year for Mekong river (Le Manh Hung et al, 2003).

Until now, there is not many theoretical or even empirical works related to quantitative prediction of riverbank erosion. It is easy to understand that because of many limitations: Firstly, to understand clearly all causes and quantification it is not always easy. Secondly, riverbank erosion is the random phenomena and very difficult to survey its geometry. The physical modeling research is not relevant to apply in this phenomenon. Lastly, the movable boundary is still a difficult task in mathematical modeling.

Annually, people are died, houses and lands loss due to of riverbank erosion in lower Mekong river in Vietnam. Because of the critical problems, the Vietnamese government have been spent a lot of money and labour to limit the damage from the riverbank erosion. In all of those efforts, this study tries to understand the phenomena as well as the predictable tools and research some suitable mitigation measures in the lower Mekong river. Hopefully, this study contributes and updates the research on riverbank erosion of the Mekong River.

1.3 Objective of study

☆ ***Research on prediction of riverbank erosion by using GIS analysis, mathematical modeling in the lower part of Mekong River.***

☆ ***Research on mitigation measures with preventive measures, notably revetment, bend cut and permeable groyne.***

1.4 Methodology

1.4.1 Riverbank erosion prediction

In order to predict the mobilization of riverbank, the methodology can be expressed by figure below:

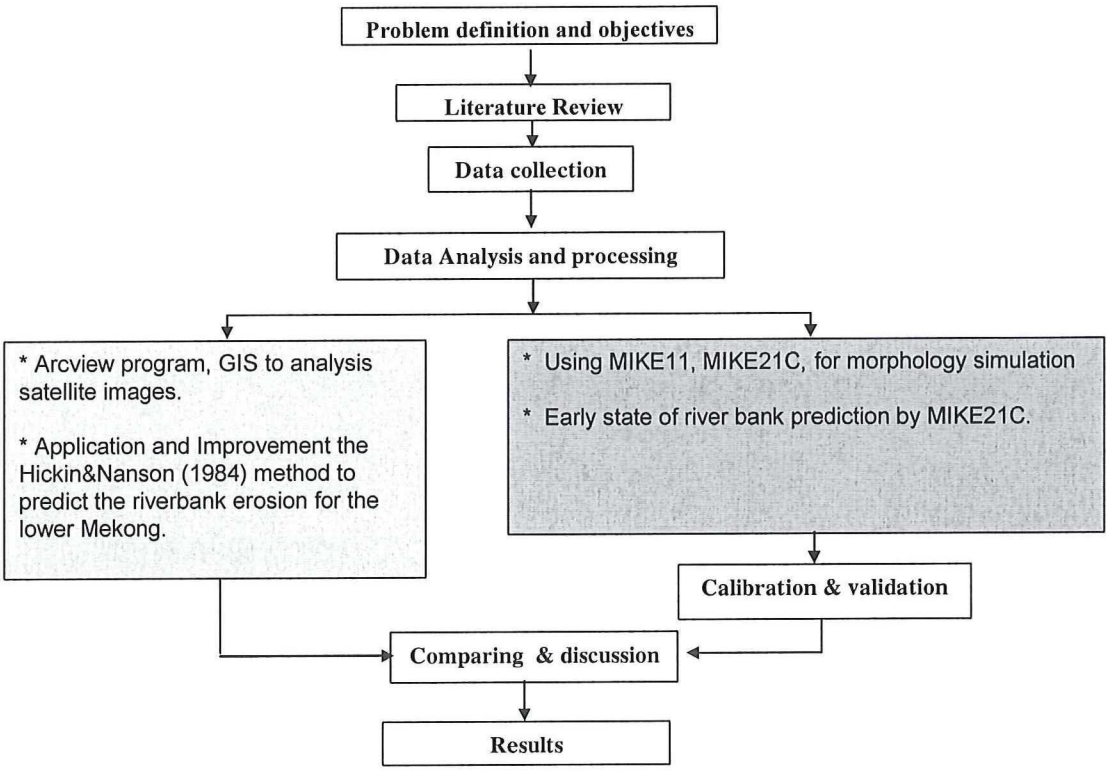

Figure 1.2 Methodology of riverbank erosion prediction

The figure shows that, to predict the riverbank erosion in two ways. One ways can be use the satellite images, old maps to apply the Hickin & Nanson (1984). The other way is possible to use mathematical model (MIKE21C), which can update the grid cells, bathymetry during computation process. The results of two ways will be discussed and conclusion, recommendation and draw the lesions learn from it.

1.4.2 Mitigation measures

In recent years, efforts to mitigate riverbank erosion and stabilize floodplain land were carried out on the main channel using usually high-cost protection measures. However, with a large-scale area, lack of the funds, these measures have been applied only for the critical locations.

Nevertheless, whatever strategies to mitigate the riverbank erosion that have to take into account the economic aspect, technology aspect and the biology aspect as well. The best mitigation measure could only be found at the specific location with specific causes and its effects. In other words, it depends on the characteristic of locations, the causes of riverbank erosion, and the impacts of riverbank erosion to the riverine society.
Up to now, a master-plan is not implemented in the lower Mekong. The long-term sustainable development should be studied, which's based on the number of variables such as history, problem statements, predictable method, biology, the view of future development, ect…

In order to supply for the clear Master-plan, this study can recommend where is critical problem, and some possibility prevent structures were introduced. The mitigation measures focus on the scour in front of revetment, the bend cut solution and design the permeable groyn at Tan Chau location, where riverbank erosion occurs yearly with high rates. Furthermore, under the critical problems, the Vietnamese government has spent about 9 millions euro from 2001 to 2004 to protect the TanChau town. It is a button neck in the Tien River. The project was the highest cost of riverbank protection construction in the lower Mekong. However, it has not taken into account the physical modeling and mathematical modeling research in the pre-feasibility of the project. In other words, to check the stability of this revetment by computing the scour depth is an important task in this report. In addition, a mathematical modelling established to study the design boundary condition of this revetment. The bend cut solution is also considering for this sharp bend in MIKE21C model.

2. LITERATURE REVIEW

2.1 Riverbank erosion and its process, causes and effects

2.1.1 Bank erosion process

Bank erosion can be due to fluvial entrainment of individual particles (mainly by large velocities and shear stress on the banks), undermining of the toe of the bank and subsequent soil-mechanical failure or liquefaction by over pressure in fine sand during falling water level. Non-cohesive material of riverbank usually involves the flowing process (Nagata, Hosoda, Muramoto. 2000):

- Bed scouring at the side bank
- Bank collapse due to instability of the scoured bank
- Deposition of the collapsed bank materials at the front of the bank
- Transportation of the deposited material

Cohesive banks erode by mass failure under gravity during discrete events when a critical stability condition exceed. Debris from mass failure accumulates at the toe were removed by the flow. Moreover, vegetation has a significant influence on bank erodibility, because of its roots and the roughness (Nicholas et al, 2005).

Darby. S (2004) classified the bank erosion process to fourth steps below:
Weathering and weakening
Particle by particle removal by flow
Large –scale mass failure of bank material
Removal of failed debris by the flow.
The riverbank erosion has many kinds of mechanisms of bank collapse:
- Planar-type failures (e.g. Osman and Thorne, 1988)
- Rotational failures (e.g. Bishop, 1955)
- Cantilever-type failures (e.g. Thorne & Tovey, 1981)
- Piping and sapping related failures (e.g. Hagerty, 1991)

In conclusion, riverbank erosion is generally to understand that a dynamical process can be address in following circle.

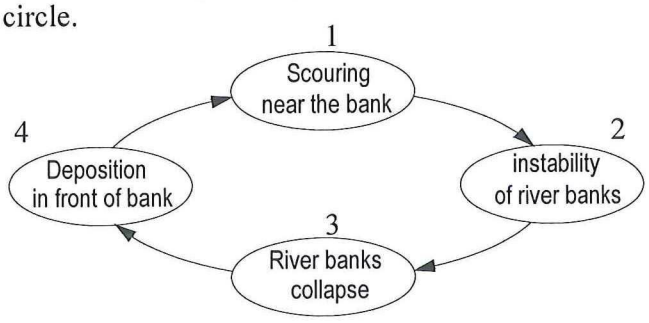

Figure 2.1 The circle of riverbank erosion process

2.1.2. Cause and effects of bank erosion

"The cake of causes and effects" of riverbank erosion was built from a series of materials, which most of them are different taste. However in combining all causes, there are two

common kinds of riverbank process, were shown in figure19 and figure 20 below. The figure 19 shows that, cause of surfaces erosion are gulleying, surface run-off, waves, seepage due to boundary changes, uplift due to seepages and high shear stress. The mass failure mentioned in figure 20. In addition, mass failure was determined by surcharge loading, cracking, seepage, scour, flood, and tidal recession.

In the other ways, Le Manh Hung et al (2003) explained the combination of all cause factors of riverbank erosion in figure 21, in the view of mass balance, increasing the driving forces, and decreasing the resistant forces. The combinations with all factors show that, in term of many factors most of them have the relationship to others.
The effect of riverbank erosion is not only the morphology changes itself but also the environment changes of river systems, the obstacle in transportation, etc. D.J.Hagerty et al (1991) reported concerning the seepage phenomena influences to erosion.

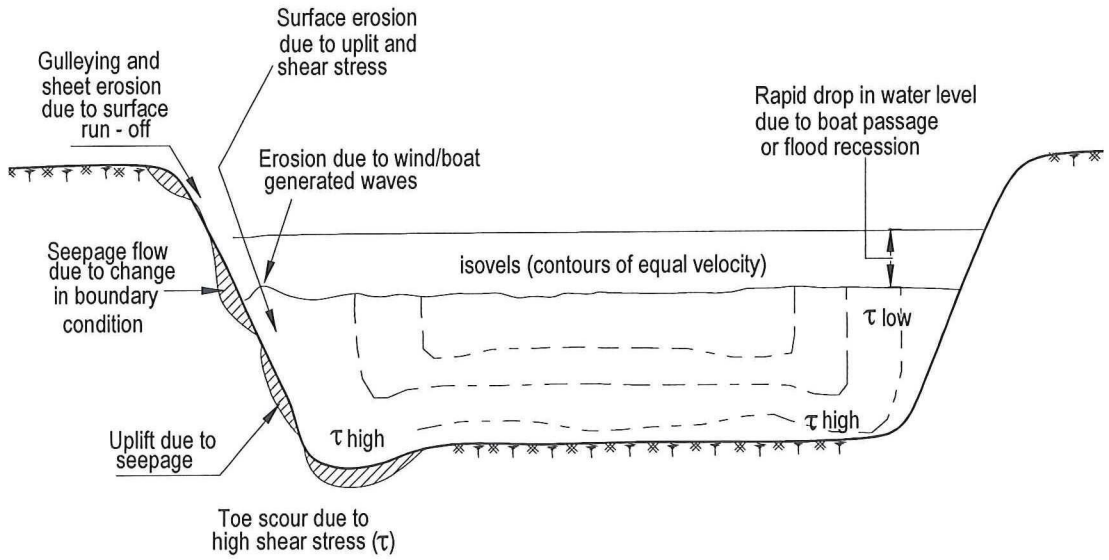

Figure 2.2 Surface erosion process

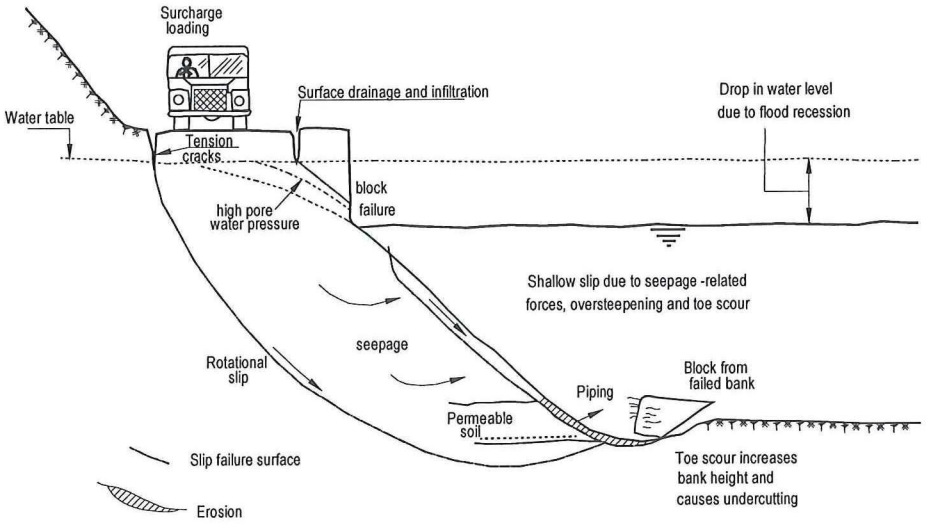

Figure 2.3 Mass failure process

The riverbank erosion is considered as a serious socio-economic problem in the lower Mekong river. Problems are especially severe at Tanchau on the Tien branch where the rates attain more than 30m/year, and approximately 400households have had to be relocated recently due to the bank collapsed.
Moreover, bank erosion has resulted in major disruption to local livelihoods and financial burden on the provincial government by spent money to relocation of inhabitants and building the bank protection works. The impacts due to the riverbank erosion to the infrastructures such as port, road, and embankment are very costly.

The other impact of bank erosion is the influence of transportation capacity. Because of the mass debris from the river bank material that sliced into the riverbed and it has significant impact to the riverbed.

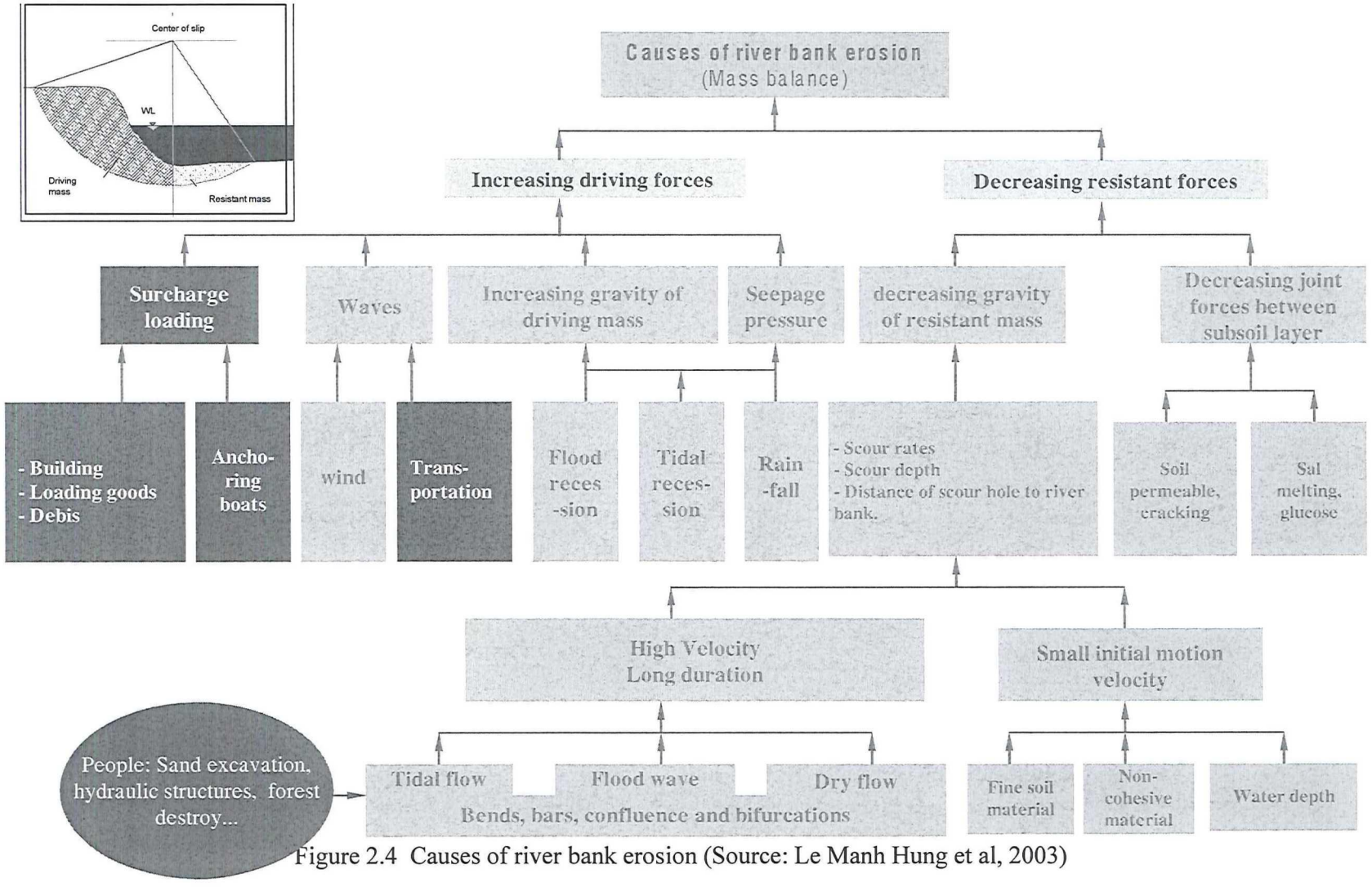

Figure 2.4 Causes of river bank erosion (Source: Le Manh Hung et al, 2003)

2.2 Prediction of riverbank erosion

Although riverbank erosion has many factors, and it plays a center role and it occurs randomly, but in principle riverbank erosion can be predicted based on the history, the influence factors, the understanding in terms of causes and effects, and the available data of the phenomena. Riverbank can be observed from history from the old map, the satellite images, or some proofs of river at the erosion locations. The influence factors could be the causes and effects of phenomena such as high velocity, poor mechanical condition of bank material, waves due to win or transportation, etc. In addition, a good understanding and suitable data can have a successful empirical relationship. Nowadays, both empirical method and the numerical method are used to predict the riverbank erosion.

2.2.1 Empirical method

In 1984, Hickin and Nanson (1984) used the observation data of 189 bends in Western Canada to find the relation between rates of channel migration, bend radius, and channel width. Specially, he found that the maximum rate of channel migration when the ratios of r/B=2.5, that relation can be rewritten as

$M(R/B) = M_{2.5}.f(R/B)$ (2.1)

For f(R/B) an empirical relation was derived:

for $1<R/B<2.5$ $f(R/B)=2/3(R/B-1)$ (2.2)

for $R/B>2.5$ $f(R/B)=2.5\ B/R$ (2.3)

The maximum erosion rate occurs for R/B=2.5 and is defined as $M_{2.5}$ (in m/year) and this maximum rate is proportional to total stream power Ω which is defined as:

$\Omega = Q_5.\tau.h^{-1}=\rho.g.Q_5.i$ (2.4)

where Ω= total stream power (in watt/m), Q_5= discharge exceeded once in 5 years (m^3/s).

$M_{2.5}$ is inversely proportional to a bank-strength parameter Y_B (dimension N/m^2) which is a function of bed material size:

$$M_{2.5} = \frac{\Omega}{h.Y_B} \quad (2.5)$$

Example: Given $Q_5=15000m^3/s$, h=22m, $i=10^{-3}$, D_{bank} =1mm, R/B=4.

Solution: D_{bank}= 1 mm -> Y_B -> $80N/m^2$

R/B=4 -> f(R/B)=2.5 B/R=2.5/4=0.625

$\Omega=\rho.g.Q_5.i$ =150 000 watt/m

$$M_{2.5} = \frac{\Omega}{h.Y_B} = \frac{150000}{20x80} = 94m/year$$

$M(R/B) = M_{2.5}.f(R/B)$ =94x0.625= 59m/year

This was known a valuable study because it included all aspects of the bend such as the geometry and soil condition as well as the hydraulic condition to predict the phenomena. In other words, the power stream Ω (watt/m) is included five years flood discharge and the value Y_B is depended on the grain size diameters of bank material.

Hudson and Richard (2000) have examined the channel migration and meander-bend morphology for lower Mississippi river in the period from 1877 to 1924. At that moment, the river had not disturbed by mankind such as channel cutoffs, revetments and changes the sediment regime. This study repeated again the relationship between maximum migration rate correspond to ratios of R/W (ratio between meander bends radius to channel width). The result of this study reported that, the highest migration rates occurred with meander bend having a curvature R/W around 1.0 to 2.0. The conclusion of this study also delineated that

river with a complex flood plain deposits exhibit patterns and relationship that deviate from models in homogeneous flood plain deposits.

Empirical method is applied to predict riverbank erosion that is normally to find the relationship between the proofs of riverbank erosion with the flow condition as well as riverbank material condition. By doing so, it normally needs many data from the field of objectives. In other words, the proofs of riverbank erosion can observed and valuated by planform change assessment or topography surveyed or even base on the old map Hudson and Richard (2000) or from the satellite images below.

Since the early 1960s, numerous satellite sensors have been launched into orbit to observe and monitor the Earth and its environment. Most early satellite sensors acquired data for meteorological purposes. The mapping and monitoring purposes of satellite images was occurred when the first Landsat satellite was launched in July 1972. Currently, more than a dozen orbiting satellites of various types provide data crucial to improving our knowledge of the Earth's atmosphere, oceans, ice and snow, and land.

However, the ideas of using satellite images to predict riverbank erosion had been known since the lately 1980s. Notably, the early methodology towards the development of a predictive model for channel changes and related bank erosion, morphological process, a large chaotic behaviour river – Jamuna in Banladesh was a nice case studied by Klaassen and Masselink(1992). In this research, there were six LANDSAT MSS images in the same location have been used in the period from 1976 to 1987 with combination of a series of cross-section in this area. The improved understanding relates especially to the relation between the erosion and the relative curvature, the negligible important of vegetation on bank erosion, the occurrence of channel shifts and the important of sand bars, the propagation in upstream direction of bifurcation when the two channels are of almost equal importance, and the stability of major confluences. Nevertheless, it was impossible to develop such a deterministic model because of at least two reasons (Klaassen and Masselink, 1992). The one of those reasons was the limited understanding of prevailing process and the other was the observed chaotic behaviour of the system. In addition, studying more continuous series of satellite images, included other aspects in the analysis like duration of yearly hydrograph, carrying out of special study into the possible chaotic behaviour of river system were recommended (Klaassen and Masselink, 1992).

At the same moment, the prediction of planform changes can only be done by the probability of occurrence of the different potential developments by Klaassen, Mosselman & Brušhl (1992). The satellite images of Jamuna River were used to identify underlying process and to derive prediction method. However, the limitations of accuracy were listed below:
- The resolution (pixel size) of satellite image was on the order 50m;
- There were no data on the morphological changes during a flood (only the net end result can be seen on the satellite images taken in the dry season);
- Cross-sections were not available for every channel in such big river. In addition, even cross-section were available for a certain channel, it was not representative because of the strong non-uniformity of the channel.
- Inundated banks cannot be distinguished from eroded banks on the satellite images.

Later on, the sedimentary features are a new prediction tool by Sarker et al (2002). This study aims to develop and update the existing prediction tools using a series of annual dry - season satellite images with a relatively fine resolution of 30 x 30m, collected during the period 1992-2000. Base on those images, more accurate prediction could be made of such

morphological process as: channel abandonment, migration of bifurcation, and bank erosion along outflanking curved channels. Sarker et al (2002) have tried to separate the sedimentary features such as contraction bar, sharpened bar, sand wing, sand tongue, etc.

In recent studies, detailed topographic data collected with an airborne laser scanner can help determine the extent of bank erosion and identify banks that are more vulnerable to bank collapse and thus require stabilization efforts the quantifying of riverbank erosion by using scanning laser altimetry (Thoma, Gupta and Bauer, 2001).

Other study on the Mekong river, Le Manh Hung et al,(2003) researched on river bank erosion at a series of cross-section in the lower part of Mekong river. The yearly bank erosion rates have the relation with many factors below.

$B_{xi}=f(\alpha,\beta F, L, T, H_{max}, H_0)$

where B_{xi} = yearly bank erosion at cross-section i in the bend (m/yr), F =total eroded area (m^2); L(m) is the length of eroding area. T= eroded time yearly, $H_{max,i}$=the maximum water depth in cross-section i, H_{max} the maximum of bend scour depth, H_0 is the stable depth at transfer cross-section between two curve, α, β are empirical parameters. This study gives a complex formula with combination many parameters such as hydraulic parameters, eroded time, and eroded area, etc. However, the calibration of this formula does not implemented and the eroded area (F) is not a accuracy number.

In conclusion, the rates of river bank erosion not only depends on many factors which play a major role but also be influenced by the characteristics of each river, under a such situation the empirical relations of some parameters of river bank erosion is still an opening issue till this present. The satellite images have advantage to give us a large area of land surface in time and place. However, the high accuracy of riverbank erosion prediction should implement in combining with satellite images or airborne laser scanner, surveyed map, hydraulic conditions, soil material of riverbank and the sedimentary features, etc. In addition, when using the satellite images in riverbank erosion prediction, it is necessary to combine with the mathematical modeling.

2.2.2 Mathematical modeling researches

Up to now, riverbank erosion has been an interested topic with many publications nearby the '60s to '80s. Late '80s, mathematical modeling was used to analysis, and simulated the river morphology with take into account the sediment due to riverbank erosion. Recently, under the helps of computer science, the development of mathematical modeling deals with river morphology changes is more accuracy. There are many of famous names of program such as, Delft 3D (WL/Delft Hydraulics), MIKE21C (Danish Hydraulic Institute), and many individual programs were built by researchers on over the world such as Darby and Thorne (1996), Mosselman (1992), and Nagata, Hosoda and Muramoto (2000), etc. However, fixed-width numerical morphological models are commonly used in engineering practice to obtain predictions of channel adjustment in response to changes in the independent variables of flow and sediment discharge.

Further more, fixed-width numerical models are limited in applicability to cases where width adjustment are not significant in the prototype channel. To address this deficiency number of attempts to account for time-dependent width adjustments in numerical morphological models have been made.

Simple models to predict mass-wasting: Introduces the basic principles of river bank stability analysis. It is important to understand that a specific analysis is required to model each different type of failure mechanism. The following mechanisms will be discussed:
- Planar-type failures (e.g. Osman and Thorne, 1988)
- Rotational failures (e.g. Bishop, 1955)
- Cantilever-type failures (e.g. Thorne & Tovey, 1981)
- Piping and sapping related failures (e.g. Hagerty, 1991)

Despite the fact that natural riverbanks are liable to failure by a number of specific mechanisms of bank collapse, however the modeling approaches have been solely on analysis of planar failures. The mass-wasting was reported in Osman and Thorne (1988) for the bank profile geometry associate with nature. Darby and Thorne (1996) adopted a quasi -2D method with lateral distribution of flow velocity and boundary shear stress were estimated at each cross section via numerical solution of a version of the flow momentum and continuity equations. By using mass failure method, Darby and Thorne (1999) already taken into account the effect of strength balance on mass of riverbank, which was included the pore- water and hydrostatic confining pressure terms.
The 2D depth –averaged flow sub-model of RIPA (Mosselman, 1992) is based on the differential equations expressing the conservation of mass and momentum of the water. The lateral variation of flow field in natural channels has been made by BRI-STARS (Simon et al, 1991).

Specially, an analysis of a 2-D bed topography model for river was presented by Struiksma, Crosato (1989). This study was known as a deep understanding of the process of river deformation of river meandering with two main characteristics of the bed deformation, the point bar and pool development in the inner and outer bend. They reported that with non-steady state analysis the occurrence and behavior of propagating alternate bars are described. Due to the relatively large propagation velocity of these bars, this type of perturbation cannot give an explanation for the much more steady meandering process, which is characterized by point bar-pool configuration. A steady state analysis turns out more appropriate to describe the meandering process.

Other study, which used MIKE21C is presented by K.W.Olesen & S.Tjerry (2002). This study was taken into account the influence of erosion material to morphology change at Chaktomuk Junction (the bifurcation in the Mekong River). By using MIKE11 to support the boundary for MIKE21C, and using the strongly tools of MIKE21C that is update grid during computation time to simulate the riverbank erosion. The results are directed two important areas named Koh Norea bank in upper Bassac and Monivong Bridge.

For more details of some mathematical models show in table 2 in this table, the bank process and bank material are normally two main parts of the mathematical model. The bank process can understand such as the type of bank failure, the way of deposition in front of riverbank.

Model	Bank process				Bank material		
	Deposition	Fluvial Entrainment	Types of bank failure	Longitudinal extent of failure included	Cohesive	Non cohesive	Layered
Darby-Thorne	No	Yes	Planar curved	Yes	Yes	No	No
RIPA	No	Yes	Planar	No	Yes	No	No
Simon et al	No	No	Planar	No	Yes	No	No
WIDTH	No	Yes	Planar Curved	No	Yes	No	No
MIKE21C	Yes	Yes		Yes	Yes	Yes	No
Delft 3D	Yes	Yes		Yes	Yes	Yes	No

Table 2.1 Sub-Mathematical modeling on river bank erosion research.

In the author's point of view, a simulation of morphology change with the riverbank erosion phenomena has some different parameters in the sediment transport continuity equation. Because of each understanding of the material from riverbank erosion, the mathematical model was made in the different ways.

For instance, MIKE21C: Bank erosion and plan form changes: The bank erosion is computed by a formula relating near-bank conditions to bank erosion rates. The accumulated bank erosion can be used for updating the bank lines, and for updating the curvilinear grid (extent of the modeling area) at every time step. By defining a silt factor, the bank erosion products can be included in the sediment budget for the adjacent riverbed, or it can be disregarded depending on the composition of the bank material. The modules can run interactively, incorporating feedback from variations in the alluvial resistance, bed topography and bank line geometry to the flow hydrodynamics and sediment transport.

+ Sediment transport continuity equation in MIKE21C
The following is the calculation of sediment transport of bed material (Bed load and suspended load) the bed level change can be computed from the equation:

$$(1-n)\frac{\partial z}{\partial t}+\frac{\partial S_x}{\partial x}+\frac{\partial S_y}{\partial y}=\Delta S_e \qquad (2.6)$$

where

S_x total sediment transport in x - direction
S_y total sediment transport in y - direction
n Bed porosity
z Bed level
t time
(x,y) Cartesian co-ordinate system
ΔS_e Lateral sediment supply from bank erosion.

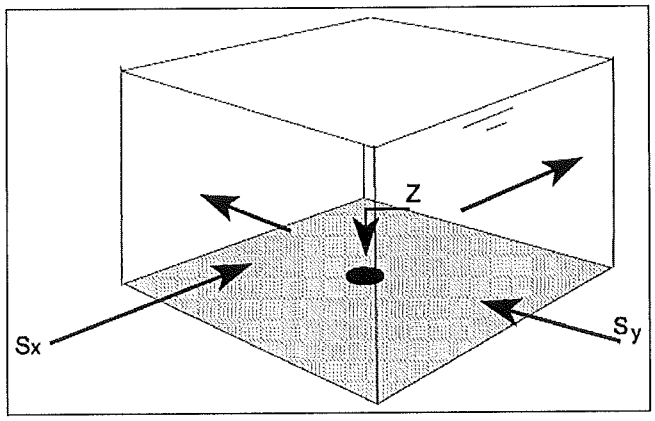

Figure 2.5 Solution of sediment continuity equation (Source: MIKE21C reference manual)

+ Sediment transport included riverbank erosion.

$$E_b = -\alpha \frac{\partial z}{\partial t} + \beta \frac{S}{h} + \gamma \qquad (2.7)$$

Where

E_b the bank erosion rate m/s

z the local bed level

S near bank sediment transport

h local water level

α, β, γ Calibration coefficient specified in the model.

The extra sediment released when riverbank erosion occurs contributes to the sediment balance of equation (2.6). The contribution is following relation.

$$\Delta S_e = \frac{E_b (h + h_b)}{\Delta n} \qquad (2.8)$$

where

h_b high of the bank above water level

Δn Width of cell next to bank line.

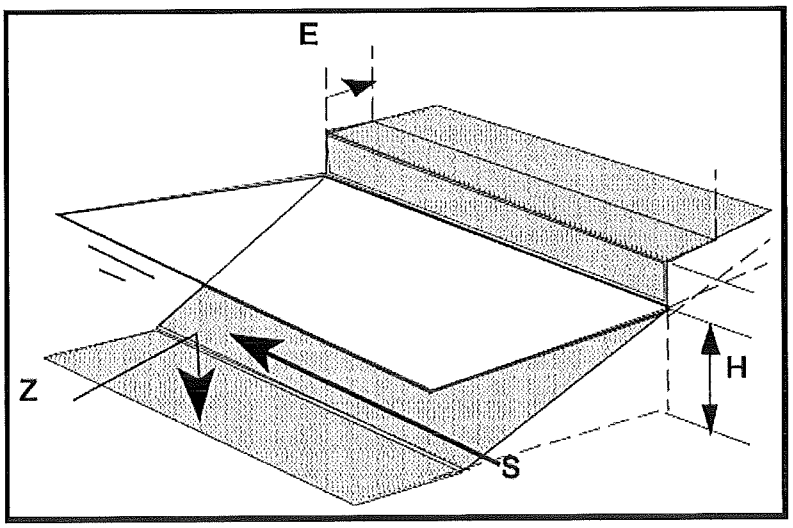

Figure 2.6 Bank erosion (Source: MIKE21C reference manual)

In the equation (2.7), the near bank slope dependency is included in the first term. The dependency upon the near bank shear stress exerted from the river flow is implicitly included in the second term. The last term γ represents a constant erosion rate, which is independent of the hydraulic conditions.

The first term is based on the assumption that the shape of the transverse bed profile is preserved. Therefore, from geometrical considerations the bank erosion rate is proportional to the bed erosion. The α coefficient corresponds to the transverse bed slope at the bank. Transverse bed slopes in natural rivers are typically of the order of 5-20 along eroding banks. This means that the α coefficient should be chosen in the range from 0 to 20.

The second term is derived by considering that the eroded material E_b, is moved downstream by the flow determined sediment transport rate S, or at least a fraction β of it. This means that the β coefficient should be chosen in the range from 0 to 1. Note that the bank erosion module assumes that the bank material is the same as the sediment on the river bed.

Observed bank erosion rates are used to calibrate the coefficients α and β. If no evidence for a relationship to dz/dt or to S is found, it is possible to specify a constant bank erosion rate γ.

Bank erosion is computed at every time step, and the debris is included in the sediment continuity equation along the bank, see eq 2.6. If the accumulated bank erosion at a certain location exceeds a predefined critical width (related to the width of a computational grid cell along the bank), the curvilinear grid is updated with new bank lines. This implies the following steps in the model:
- Generation of a new orthogonal grid based on the new bank lines.
- Recalculation of grid parameters, such as space step Δs, Δn, and radius of curvature of gridlines R_s and R_n.
- Transformation of the model bathymetry from the old to the new curvilinear grid.
- Initialization of accumulated bank erosion record, (which is being used to test, when grid updating is required).

Updating of the plan form can be excluded if bank erosion only influences the morphological development very close to the eroding bank and not the overall hydraulics.

Other instance reported by Darby, Thorne, Affiliate (1996). This study research on Numerical simulation of widening and bed deformation of straight sand-bed rivers.

The model is applicable to straight, sand-bed streams with cohesive bank materials, and non-uniform bathymetry and width in the longitudinal direction. The flow field is obtained by solving versions of the flow resistance, flow momentum, and continuity equations, which account for the influence of gradually varied flow and lateral shear in the near bank zones. Secondary and over bank flows are excluded. Predicted flow is used to compute for stream wise and transverse sediment transport fluxes. Numerical solution of the sediment continuity equation allows temporal variation in bed-material size, bed morphology, and bank geometry to be simulated. A probabilistic approach is used to estimate the longitudinal extent of mass failures within modeled reaches, and mixed layer theory is used to model transport of the resulting bed and bank material mixture.

+ Sediment transport fluxes
Sediment continuity equations in Cartesian co-ordinate.

$$\frac{\partial Z}{\partial t}+\frac{1}{1-\lambda}\left(\frac{\partial q_x}{\partial x}+\frac{\partial q_y}{\partial y}\right)=V_{fi} \qquad (2.9)$$

where
- Z elevation of the bed (m)
- λ Porosity of the sediment
- q_z total streamwise volumetric sediment transport flux per unit channel width (m^2/s)
- q_y total transverse volumetric sediment transport flux per unit channel width (m^2/s)
- V_{fi} Loading term representing volumetric inflow of eroding bank material (m^2/s)

+ With bank erosion.
In modeling bed evolution through use of continuity equation (2.9), estimates of the total volumetric inflow of sediment from bank erosion along the length of the modeled reach are required. However, two- dimesional bank stability theories of the type described in the preceding provide at –a – point estimates only of failure block dimensions per unit reach length. The volumetric inflow of eroding bank material is estimated using:

$$V_{fi}=\frac{V_f \Delta x}{\Delta T} \qquad (2.10)$$

where
V_{fi} total volumetric bank material inflow flux due to mass failure (m^3/s)
Δx length of model reach (m)
ΔT Chosen time step over which the total volumetric inflow of bank material is time averaged (s).
V_f the volume of the failure block per unit channel length (m^3/m).

Application of equation (2.10) assumes that once failure is detected at a computational node, banks along the entire length of the model reach fail. However, mass failures over bank lengths of more than a few meters or tens of meters are rare. When the reach length us larger than the scale of the mass failure, the estimated bank material inflow rate will be unrealistically large. In other words, the fundamental problem is misapplication of 2-D bank stabilities theories. With 3-D riverbank stability analysis, it is hypothesized that more realistic predictions of reach scale bank stability can be obtained by using a probability 2-D river bank stability analysis. More detail is reported in Darby, Thorne and Affiliate (1996). So, V_{ft} was determined in 3-D analysis in following:

$$V_{fi}=\frac{V_m \Delta x}{\Delta T} \qquad (2.11)$$

where
V_{fi} total volumetric bank material inflow flux due to mass failure (m^3/s)
Δx length of model reach (m)
ΔT Chosen time step over which the total volumetric inflow of bank material is time averaged (s).
V_m total mass-failure bank material influx per unit length of reach (m^2/s)
$V_m = \mathrm{RPr}(FS<1)V_f$ (2.12)

Where RPr(FS<1) = reach-scale probability of failure.
Two instances above gave us the all view of mathematical model experts who applied different river bank erosion process for their model.

However, the conclusion is that the obstacle is the way of collapse of river bank in term of combination all factors involve erosion process. The mathematical model are improving in the future. Hopefully, the better understanding and better simplicity can get the best solution in coming time.

3. BACKGROUND AND AVAILABLE DATA OF RESEARCH AREA

3.1 Background of lower Mekong River in Viet Nam

This study focus only focuses on the part of the lower Mekong river in Vietnam. The Northern branch is called Tien River and Southern branch is Hau River, both parallel branches are about 230 km. From these two main branches, they are divided by nine outlets to drainage water into South China Sea. Nowadays, only 8 branches exist, the ninth once disappeared longtime ago.

The lower Mekong crosses over 6 provinces in the Southern part of Vietnam. It is the basis of life for about 16.3 millions inhabitants.

3.1.1 The natural functions

Draining floods is one of the natural functions. Yearly, the duration time of flood season is 4 months (August, September, October, and November). The average volume of water is nearly 250 billons cubic meters and the average flooding discharge is nearly 35,000m3/s. Flood is removed in different ways: by the main rivers, by the channel systems, and passing over the land with maximum surface velocity about 3m/s at Tan Chau station. Inundation area is about 10,000 km^2. Water level in flood season is higher than ground level in a vast area is the reason why people here have to face with many difficulties such as transportation, the environment degradation, etc.

Moreover, River forms an alluvium of high potential for crop production at the end of flooding season. There is about one billion cubic meters of sediment per year. The alluvium is all kind of erosion product from the upstream, and along riverbanks. Although, the flood makes some problems to the people's lives, at the same time it brings sediment to the land and makes the crop production better after the flood season.

In addition, the lower part of the Mekong River system has a complex channel system and many lagoon forest as well as salt marches. The biggest lagoon forest of Vietnam in Kien Giang province, which is believed to be the "Lung" of Southern Vietnam, gains its beauties from the natural function of the river.

Figure 3.1 shows the sediment concentrate in the water and one of the special trees in Southern of Vietnam.

Figure 3.1 Ecosystem in lower part Mekong River

3.1.2 Use of the lower part of Mekong River

The lower part of Mekong River is the location, where people can see both Rice and Water exist together. More than 50% of nation agriculture products are from this area. Nowadays, Vietnam is known the second nation of the world in exporting rice (the first is Thailand).

In addition, fish is also the second main product of this area. Fish exports of Vietnam to Europe, America, and many other countries are from this area. Along the river, there are a lot of fish cases, where people feed the fish (see Fig 3.2). Figure 3.3 shows that the people harvest their crop in the flood plain.

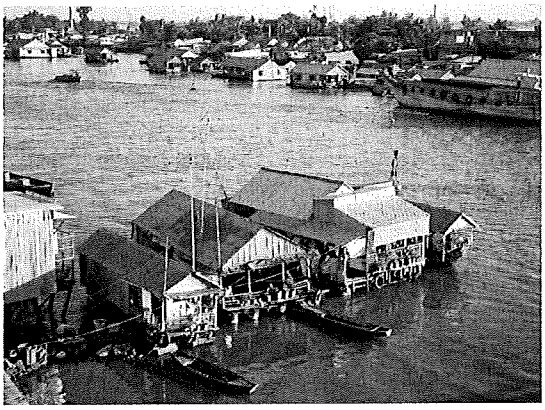

Figure 3.2. Fish cases in lower Mekong River

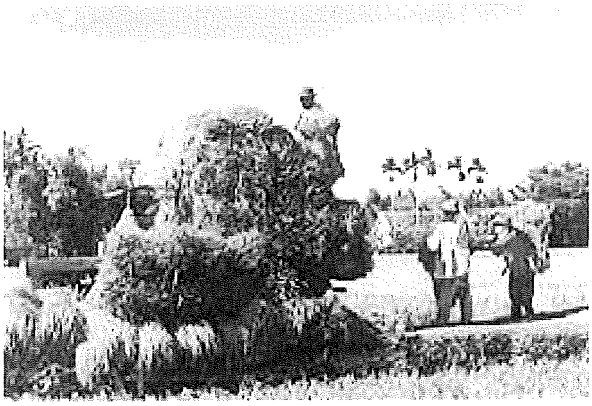

Figure 3.3. Crop production on flood plain

Beside that, the Mekong River is also the main route for outlet of agricultural export items. Water way is used for internal transport and connects neighboring countries. Most of the goods coming to Cambodia and Laos are through this river system.
Specially, river not only brings rice, fish, construction material such as brick and sand (figure 3.4) but also boat markets (see Fig 3.5).

Figure 3.4. Exploiting the sand in the river

Figure 3.5. Float market

3.2 Riverbank erosion impact assessment

Learning from history, reading papers, experience from local people, it is true that riverbank erosion not only occurs in the river system but also the reaches, the creeks system in Mekong Delta, moreover it not only occurred now but also in the past. Normally, the higher risk of riverbank erosion that always happens in flood season. In other words, due to of higher water level, the saturated material of river bank and the higher velocity in main channel are the main causes of higher risk of river bank failures. Moreover, the lower part of Mekong River is a

vast alluvium area with the different land level is not too big from 0.3 to 0.5m, the riverbank is mobilized due to of poor criteria of soil mechanic.
The flowing classes of erosion are often applied for classification of erosion problems:

I	1-5 m/year	Weak
II	5-10m/year	Average
III	10-20m/year	Strong
IV	>20m/year	Very strong

Table 3.1 Classification of riverbank erosion (Le Manh Hung, at al 2003)

There are many special locations, which have appeared urgent problems such as Tan Chau, Hong Ngu, Thuong Phuoc, Sa Dec, Vam Nao, Long Xuyen, and Vinh Long. The erosion rate is nearly 40m/year. The government spent a lot of money for Tan Chau, Long Xuyen, and Sa Dec riverbank protection works. Nevertheless, people still are threatening by this kind of phenomena, loss of Land, loss of house occurred in the lower Mekong river in Vietnam.

The lower of Mekong River is nearly a natural river. There are a lot of vegetation along the river, the crops, and tree along the riverbank. There are only some riverbank protection works along riverbank in Vietnam. When flooding, series of problem come together with it. They are riverbank erosion, transportation, crop, foundation of house trouble due to water inundation, the negative impact of environment etc. In Fig 3.6, it is a common solution when people need to cross the flooding area. The flood season lasts from August to November every year. Flood propagation is slow, water fills large land area the risk of occurrence of riverbank erosion become higher in nearly end of flood season.

Figure 3.6. The trouble in flood season

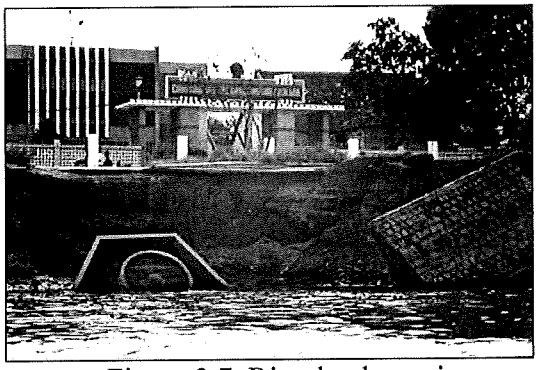

Figure 3.7. Riverbank erosion

Undoubtedly, riverbank erosion is the critical threat of the lower part of Mekong River but it normally occurs during the flood and tidal recession time. The land is loss and many people have to remove their houses. In Fig 3.7, that was riverbank erosion at Tan Chau in 1999. According to the statistic data, there are about 250 people were died. There were three towns that had to rebuild in other place and many infrastructures were damaged due to the bank erosion. According to Le Manh Hung, at al (2003) there are five major types of riverbank erosion:

- Riverbank erosion at river bend has 18 locations (example Tan Chau, Sa Dec, Vinh Long, etc).
- Riverbank erosion at Island has 19 locations (example: Long Khanh island, Tay island, etc)
- Riverbank erosion at bifurcation has 17 locations (example: Hong Ngu, Vam Nao, ect)
- Riverbank erosion due to the waves (shipping, wind) 14 locations (Dai outlet, Tieu outlet...)

Le Manh Hung and his group also pointed out there were 29 locations of riverbank erosion damaged the infrastructure and about 72 locations attacked to house.
- Riverbank erosion in connecting canal due to widening 5 locations.

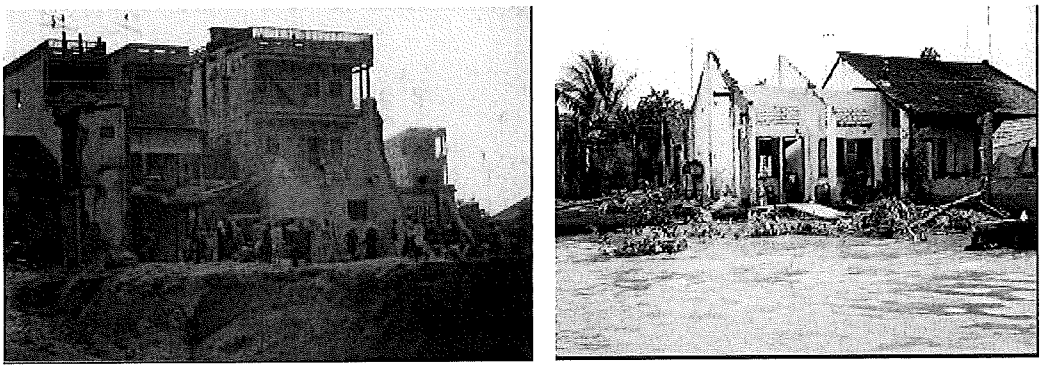

Figure 3.8 House collapsed in lower part of Mekong River

For more understanding of riverbank erosion in some particulars locations, following sections are described some special locations were threaten by riverbank erosion.

3.2.1 River bank erosion in Tan Chau – Hong Ngu

Along 15 km in length of Tien River, bank erosion is unforgettable in the heart of people who are living there. From 1970 to 1998 fifteen people have died and 7 people have been missing. Especially, one building of Hong Ngu community and one big commercial Bank were collapsed at 8 AM on February 8th 1992, 8 peoples were hurt, and 10 people were died in this event(Le Manh Hung, at al, 2003). Tan Chau town is located at outer bend of northern branch of Mekong River, the narrowest of width of river is about 300-350m. The rate of riverbank erosion of this location is about 50-100m/yr. Due to the crowded urban area, people live nearly the riverbanks, and many building are located near the river so the riverbank erosion becomes more dangerous. The deepest scour hole of lower part of Mekong river is about 45->52m. Nowadays, the Vietnamese government has spent a lot of money to protect this location, but the biggest challenge is lack of deep understanding situation.

From Fig 3.9, it indicates much riverbank erosion along the bend, the confluence on this location. The morphology changes here are more complex and variable in time. Soil material of riverbank falls into the riverbed because of erosion process. It makes the sediment transport more complex for the whole area.

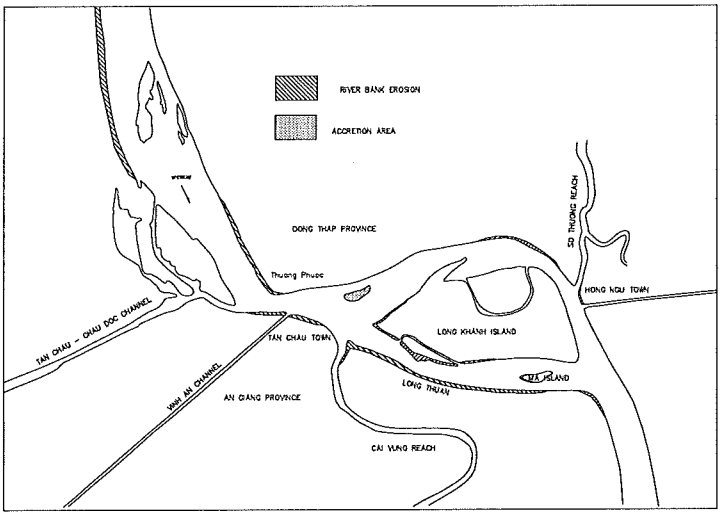

Figure 3.9. Area of case study and riverbank erosion and accretion in period 1999-2002.

3.2.2 River bank erosion in Sa Dec

Sa Dec city is located in the outer bank of Tien River. The system of river, reaches are very complex. Yearly, Sa Dec is threatening by the riverbank erosion phenomena, which erosion rate is about 20-40m/year. The length of river bank erosion lasts nearly 10 km. Notably, there are two big bridges, a hospital, and road were damaged in 1994. Total costs were estimated about 1.9 million USD. Before, Sa Dec is the capital of Dong Thap province; due to erosion of riverbank erosion threatens people who are living there, so Cao Lanh town became the capital in 1998. After the history flood 2000, the riverbank erosion was critical problem. Three kilometers of riverbank change at outer bend is the maximum number was found here (Le Manh Hung, at al 2003).

In Fig 3.10, houses were damaged. In addition, for poor people a house is the big patrimony. Unpredictable what would be causes if they loss land, loss of house even loss of themselves because of riverbank erosion.
Figure 3.11 shows the location of riverbank erosion at the bend and the strong erosion area is in Sa Dec city.

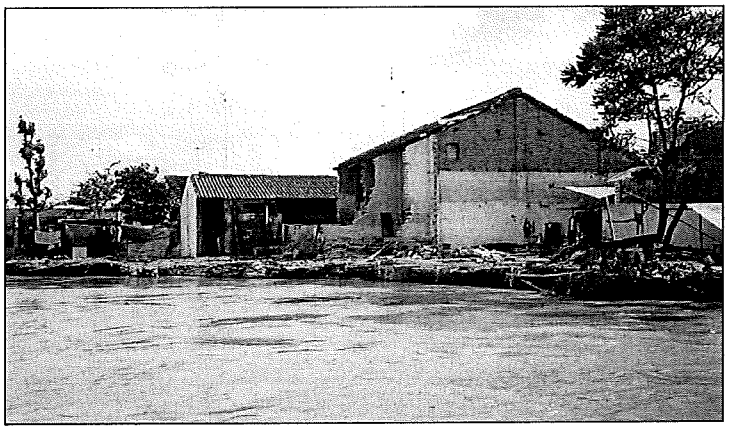

Figure 3.10. River bank erosion was damage house in Sa Dec 2000.

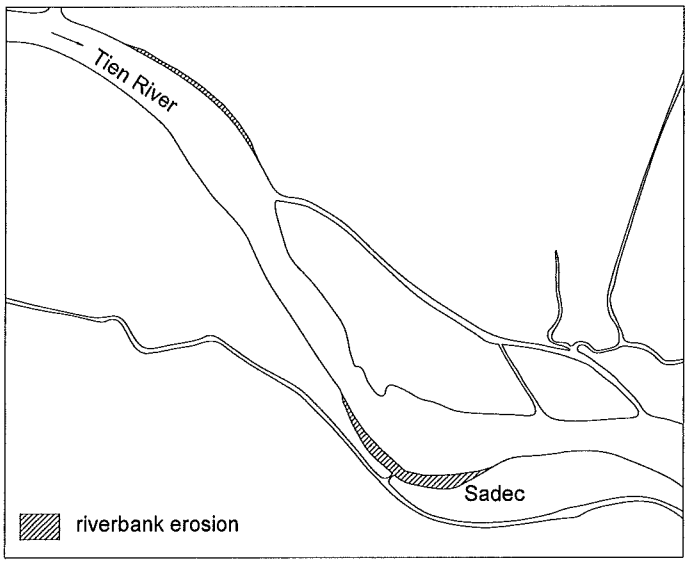

Figure 3.11. The riverbank erosion in Sa Dec city.

3.2.3 River bank erosion in Vam Nao

Vam Nao is a connection between the Tien River and the Hau River. Previously, it is a small reach and now, river width is 600m with 16m in depth in average. The length of this branch is about 7 km, and riverbank erosion happens along of 7 km, specially at both upstream and downstream junctions.

River bank erosion is not only the major in term of economic loss but also it takes a very important role in term of flow distribution between two rivers. If the Vam Nao branch is strongly widened so that the flood risk and change of morphology in downstream of the Hau river would be more danger for Long Xuyen, Can Tho city.

The riverbank erosion rate is about 10-15m/year; in figure 3.12 shows the plan form of Vam Nao branch.

Notably, there is a ferry in upstream conjunction, and it has to move every year with costly funding.

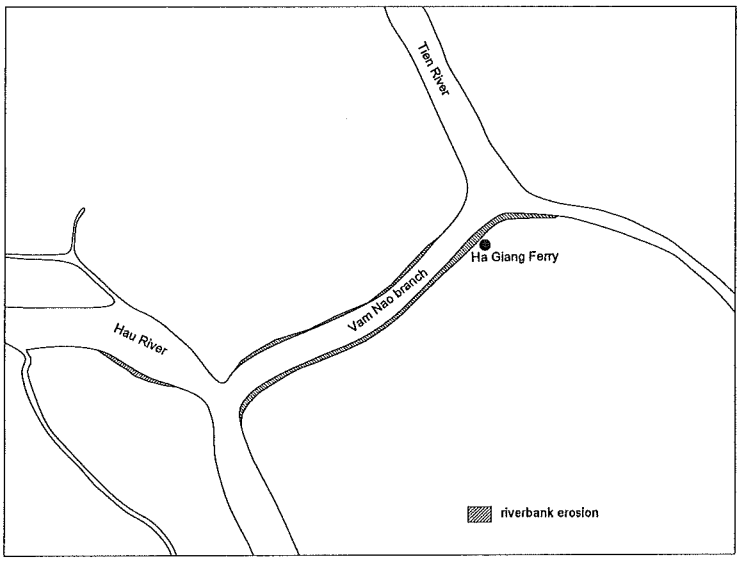

Figure 3.12. River bank erosion in Vam Nao branch

3.2.4 River bank erosion in Long Xuyen

Long Xuyen city is the capital of An Giang province. It looks like the same to Tan Chau – Hong Ngu in term of plan view, but Tan Chau - Hong Ngu is located in upstream of Tien and Long Xuyen locates in the Hau River. The riverbank erosion rate is about 10-15m/year.

In addition, Long Xuyen is a big city in the lower Mekong delta with high population distributions and structures along riverbank. There was a project to build a revetment system to protection river bank here. However, riverbank erosion in other locations still happens.

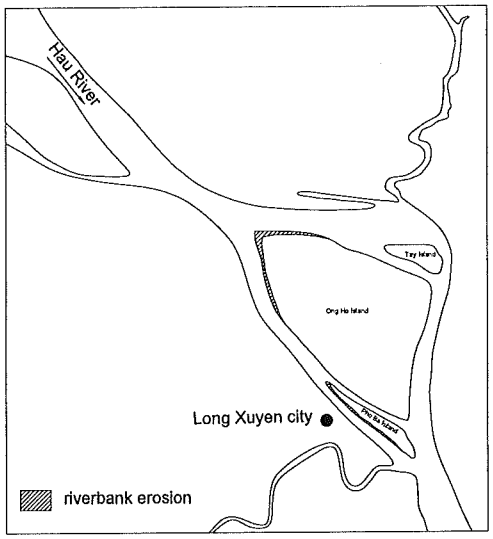

Figure 3.13. River bank erosion in Long Xuyen city

3.3 Available data

3.3.1 The satellite images

The satellite images from are requirement for riverbank erosion research in table 3.2

Number	Time	Type of sensors	Format	Name of Satellite	Number of Bands	Resolution (m x m) & scale
1	1937-1939		Vector	Map		1/254,465
2	1966-1968		Vector	Map (UTM)		1/ 50,000
3	02.04.1987	Optics	Digital	Landsat MSS	4	80 x 80
4	04.12.1989	Optics	Digital	Messr (MOS-1b)	4	50 x 50
5	13.03.1995	Radar	Digital	Radarsat	1	30 x 30
6	22.12.1995	Optics	Digital	Spot 1	1	10 x 10
7	21.02.1996	Optics	Digital	Landsat TM	3	30 x 30
8	13.02.2001	Optics	Digital	Landsat 7 ETM	8	30 x 30

Table 3.2 The old map and satellite images data

3.3.2 The old map and bed topography

River bank erosion in lower part of the Mekong River has been happening for long time, the change of river plan form, the change of bed topography is influenced to the river width. However, long time ago in such poor condition of Vietnamese, there is no money for any survey. Specially, this study collected an old map of French, they surveyed for navigation in 1937 and updated in 1939. This information was known as the oldest of this study and the map in appendix A-1 – available data.

+ The riverbed topography map scale 1/20,000 from Vietnam-Cambodia border to My Thuan dated 1995 (include Tan Chau-Hong Ngu reach). Source Hydrographic atlas Mekong River in Vietnam 1998, published by Ministry of Transport, Vietnam.

+ The cross-sections of the Lower Mekong River, on average 1 Km/ section from Vietnam – Cambodia border to My Thuan in 1995. Source Hydrographic atlas Mekong River in Vietnam 1998, published by Ministry of Transport, Vietnam.

+ The bathymetry maps from Tan Chau to Hong Ngu, scale 1/10,000, dated 2002, 2003, 2004, source survey data of " Research on river bank sliding, prediction and solutions in Mekong delta", Nation project published by Southern Institute of Water Resource Research, Viet Nam.

Nº	Location	Name of rivers	Time of survey	Scale
1	Tan Chau- Hong Ngu	Tien River	1995; 8/2003	Vertical 1/500, Horizontal 1/2000
2	Chau Doc – Nang Gu ferry	Hau River	9/2002	Vertical 1/100, Horizontal 1/500
3	Vam Nao	Vam nao	1995; 6/2003	Vertical 1/200, Horizontal 1/1000
4	Long Xuyen	Hau River	1991; 8/2003	Vertical 1/200, Horizontal 1/1000
5	Sa Dec	Tien River	1991; 3/2003	Vertical 1/500 and 1/200, Horizontal 1/2000
6	My Thuan	Tien River	1995; 11/2003	Vertical 1/500, Horizontal 1/1500

Table 3.3 The cross-section data in the lower Mekong River.

3.3.3 *The hydrology*

The lower Mekong River has 5 key basic hydrology stations. From these stations, data can be water levels, discharges, which have the time step is hourly, and sediment data but it is not too much data and the time series are not continuously.

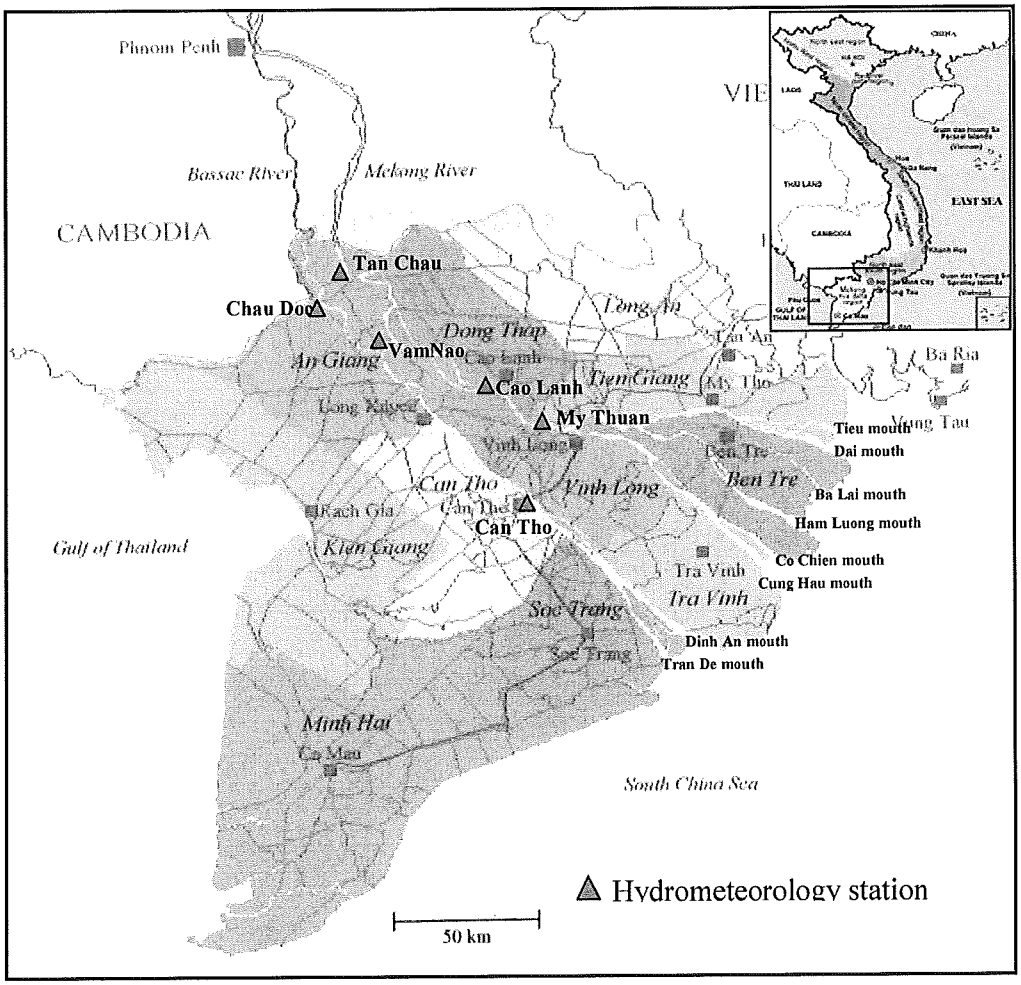

Figure 3.14 Overview of hydrometeorology station in lower Mekong

N^{o}	Stations	Name of rivers	Discharges (Q)		Water level (Z)	
			Time of survey	Types	Time of survey	Types
1	Tan Chau	Tien River	Since 1996 to 2004	Hourly	Since 1996 to 2004	Hourly
2	Cao Lanh	Tien River			Since 1996 to 2004	Hourly
3	My Thuan	Tien River	Since 2000 to 2003	Hourly	Since 1996 to 2004	Hourly
4	Vam Nao	Vam Nao River	Since 1996 to 2003	Hourly	Since 1996 to 2004	Hourly
5	Chau Doc	Hau River	Since 2000 to 2003	Hourly	Since 2000 to 2003	Hourly
6	Can Tho	Hau River	Since 2000 to 2003	Hourly	Since 2000 to 2003	Hourly

Table 3.4 Hydrology data available

The 2D flow velocity distributions (by ADCP surveyed) at Tan Chau - Hong Ngu in October 2001, March 2003 and October 2004.
The sediment transport

+ Suspended sediment at Tan Chau stations in 1998, 2000, 2001, 2002 and 2003, it is not continuously data (see appendix A - 1).

+ Sediment grain size distribution along the Tien River (see appendix A-1).

3.3.4 The geology and soil samples

The faults map of geology in the lower Mekong River, with tectonic active faults . (see figure.. Appendix A-1).
The soil samples at Tanchau in Tien River (see Appendix A-1).

4. EMPIRICAL METHOD IN RIVERBANK EROSION PREDICTION

4.1 Definition of objectives

The prediction of bank erosion rates along the river is very important for suitable development of society along the river. It helps the decision maker not only to prepare good master plans for future river basin management but also to limit the damages due to riverbank erosion, especially concerning settlements and infrastructure.

Despite of the complication in the prediction of riverbank erosion in terms of space and time, empirical methods still play an extremely important role in this process. Over the last decades, several empirical methods have been developed to predict the riverbank erosion rates, such as Hickin & Nanson (1984), Klaassen & Masselink (1992), Sarker et al (2002), and Hudson & Kesel (2000).

However, the application of empirical method is restricted only to local conditions for which have been established. Hence, based on these previous studies, especially Hickin &Nanson (1984), the two old maps (1937, 1966) and a number of satellite images, the adaptation and improvement of empirical method are discussed in this study for the lower Mekong river.

4.2 Methodology

The methodology used here to determine bank line changes over the years and hence (average yearly) bank erosion rates is similar to the method applied by Klaassen& Masselink (1992) for Brahmaputra river in Bangladesh. The major difference is that planform changes and bank erosion rates along the lower Mekong river are much slower than along the Brahmaputra river. Hence, the time intervals up to several decades were acceptable whereas in the case of the Brahmaputra river yearly intervals were used.

The combination between maps and satellite images, and bed topography, and hydrology has been made to find the relation between all parameters, which could be taken into account related to river bank erosion rates of 15 bends in total. (see figure 4.1 for their location). For each of bend the subsequent bank line position was determined from either old maps or the satellite images. The data consisted of two old maps (1937, 1966) and number of satellite images from 1987 to 2001 from the dry season of the lower Mekong river, when the banks are not flooded and the sky is clear (reduce the cloud problem). Chapter 3 can provides more detail information on the data used (see, i.e. table 3.1).

During GIS analysis, two old survey maps (1937 and 1966) were scanned to a raster image and converted to a vector file via heads up digitizing in a geographic information system (Arcview). These were combined with the satellite images that were called geo-corrected in UTM projection. Based on the old map of 1966, which have the scale 1:50.000 in UTM zone 48, projection Transverse Mercator, vertical datum is at HaTien, and horizontal datum Indian datum1960. All bank line information was entered in the same view in Arcview, thus indicating the bank erosion rates and the different morphological parameters.

In the case of the lower Mekong river in principle also the tidal influence should be accounted for as this influence is quite strong during the dry season and especially near the sea. The maximum tidal different in this area is about 3-4m. However, due to the limited resolutions of

satellite images, the effects of tide on planform characteristics are difficult to define; therefore, in this analysis, the tidal effects are neglected.

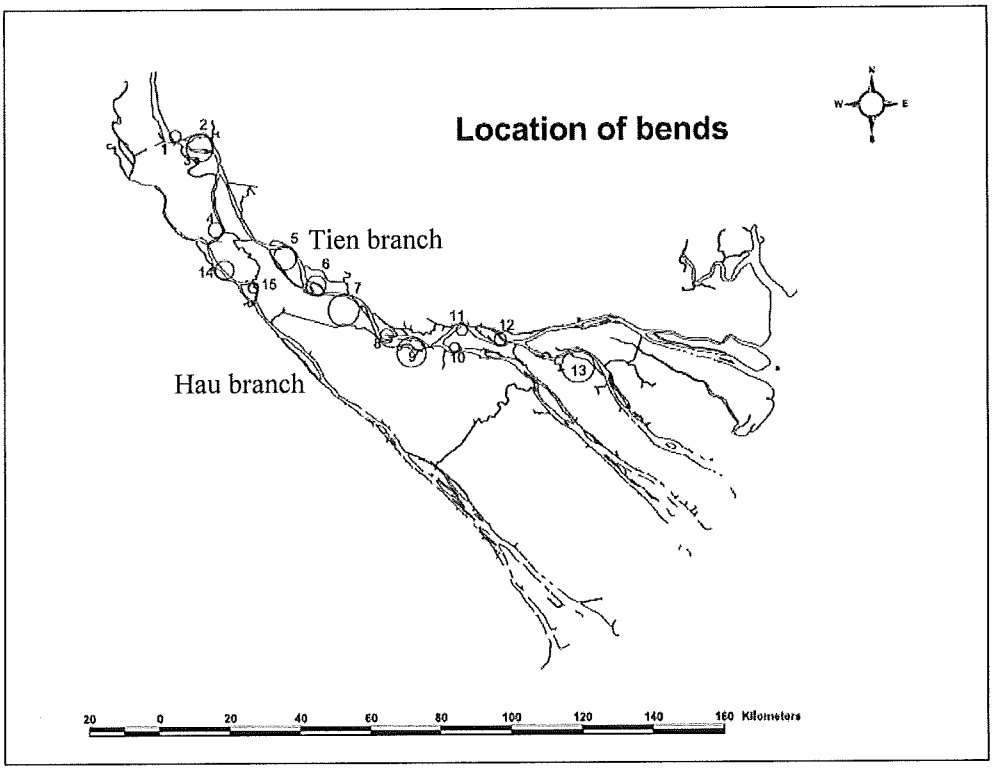

Figure 4.1 Location of bends

4.3 Mekong characteristics

Some characteristics of the lower Mekong in Vietnam are presented hereafter. The total catchment area of Mekong river is about 800,000km^2, from which only about 65,000km^2 is in Vietnam. The length of the lower Mekong river in Vietnam is only 230km, whereas the total length o the Mekong river is about 4,800km. (see figure 1.1 in chapter 1 introduction part)

The lower Mekong is characterised by two main parallel branches, the Tien and the Hau branch (see Fig 4.1, where the branch of the Hau river in Cambodia is indicated as the Bassac river). The average discharge of these two branches combined is about 15,000m^3/s. The flood discharge of the Mekong river varies over between 20,000 to 35,000m^3/s. Hence, the ratio between the flood and average discharge in the lower Mekong river is quite small. In figure 4.2 the discharge at Tan Chau station along the Tien branch during the years 1996 through 2004 is reported. In this period, the maximum discharge occurred in the year 2000 and it corresponds to about 26000m^3/s. The combined discharge of both branches was about 34,000m^3/s. Every year the flood plain is flooded on both sides of river.

The maximum water levels near the Vietnamese Cambodian border are about 4m above mean sea level (MSL) and almost about MSL during the lowest discharges. As the length of the Mekong river in Vietnam is about 230km, the slope is very gentle (variance from 1.25x10^{-5} in dry season to 4x10^{-5} in flood season). Tidal influence is noticeable even at Tan Chau (200 km from the sea) when the discharges are below about 10,000m^3/s.

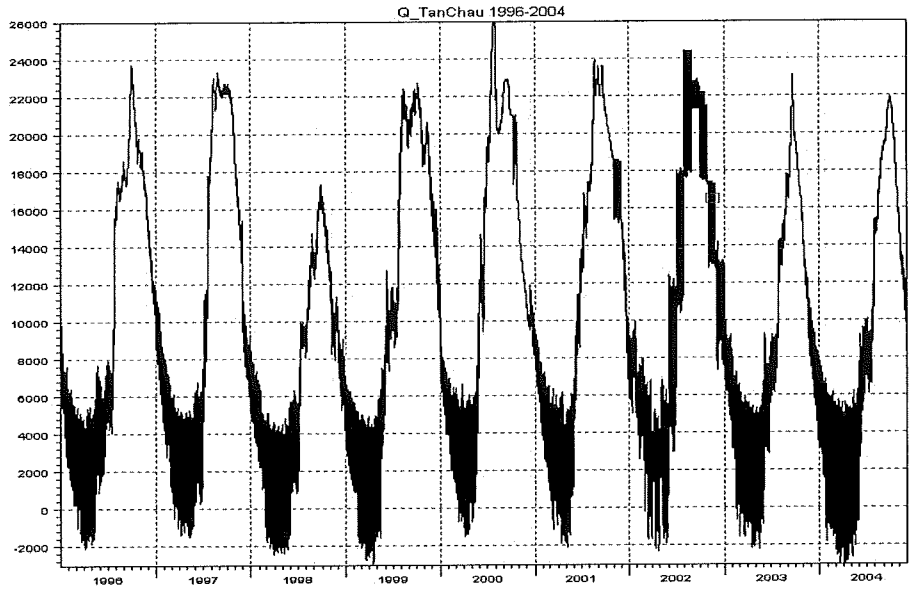

Figure 4.2. The variation of discharge from 1996 to 2004 at Tan Chau station (Tien branch)

The alluvial reach of the lower Mekong is composed of sand with mud and clay. The bed material of Mekong river is fine sand. Le Manh Hung et al (2003) reported that the D_{50} of the Tien channel reduces in VietNam from 0.25 to 0.1mm (see Fig 4.3)

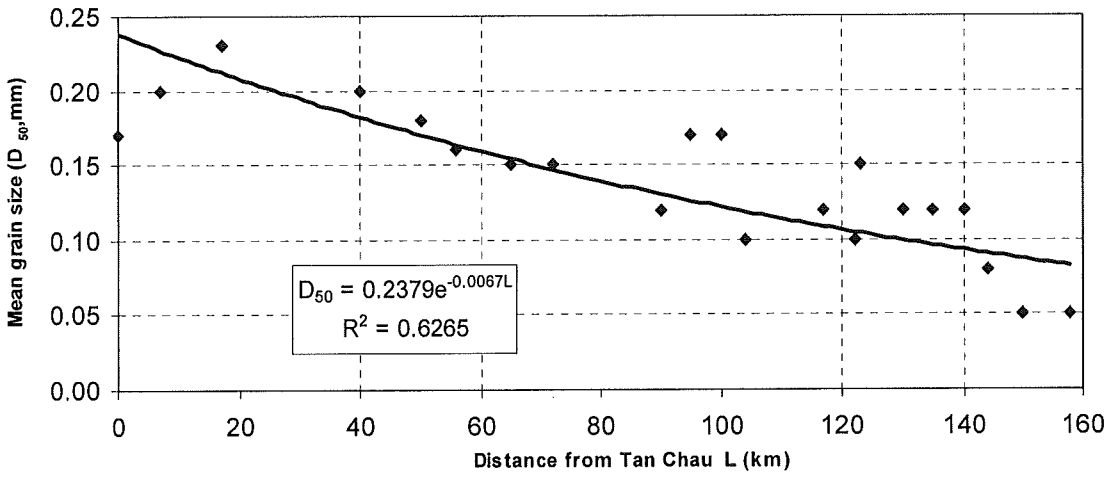

Figure 4.3 The grain size distribution from Tan Chau to downstream

The sediment load of the Mekong river is low. According to data provided in Jansen et al (1979), the average sediment concentration in Mekong is about 200 ppm and the sediment load of the river at its mouth is about 80Mtons per year. In view of the catchment area of about 0.8 million km^2, this corresponds to an average denudation rate of only 0.07 mm/yr. Many other rivers in South East Asia have much higher denudation rates (Yangtze 0.2mm/yr, Yellow river almost 2mm/yr) but the Chao Phrya in Thailand has a comparable denudation rate of about 0.05mm/yr.

The width of the two branches and the interconnecting channels is quite variable, both in space and, as far as the interconnecting branches is concerned, also in time. The width of two branches of the Mekong varies in downstream direction from 400m to 3000m. The water depth varies in longitudinal direction from about 15-20m near the sea to the maximum water depth measured in the Tien branch near Tan Chau about 45m.

Particularly in the Tien branch some large islands are present where the river bifurcates. These islands are not completely stable: erosion occurs at the upstream part and deposition at the tail of these islands, though the rate of erosion and deposition is fair low (see appendix A.2)

Serious bank erosion occurs at a number of places along the Tien branch. Le Manh Hung et al (2003) show the the bank erosion rates are typically from 10m/yr up to 40m/yr. Bank protection works were implemented in some of the most important critical locations, like Tan Chau, Long Xuyen, Sa Dec. At other places, which are less important, the population is removed from the eroding areas and resettled more inland.

4.4 Planform and planform changes of the lower Mekong

4.4.1 Planform disscusion

Before analyzing the planform changes of the Lower Mekong, the planform of the Lower Mekong is discussed here. This is done because there is strong evidence that the lower part might be affected substantially by active tectonics, by past changes in the river system and possibly by extreme heterogeneity of the deposits in the alluvial delta.

The planform of the lower Mekong is characterized by two separate branches (called Tien for Northern branch, and Hau for Southern branch). The conjunction of these two branches and Tonle Sap Lake is Chaktomuk at Phnom Penh in Cambodia. In addition, in concerning of the water discharge distribution at Chaktomuk, the Tien branch is normally carrying larger amount of water than Hau branch.

Another important aspect is that the Tien river is slightly meandering whereas the Hau river is virtually straight. Figure 4.4 suggests that the Lower Mekong river is influenced by neotecnotics and in particular by active faults. The southern branch might follow such active fault and this might explain why the river is quite straight. The Northern branch might also be influenced by active faults. The evidence of that is the river has some very sharp bends such as at Tan Chau and Sa Dec.

The lower Mekong river cannot be compare with Brahmaputra or Jamuna in Bangladesh and other dynamic rivers in over the word in term of the morphological change rates. In other words, the morphological change in lower Mekong river can take long period of time. That the reason why in this study, the map 1937 to 1966 (29years) is used to observed the planform change in for lower part (near the sea). The year of 1966, 1987, 1996 and 2001 for upper part of lower Mekong river.

It is about 230km in the lower Mekong river in Viet Nam, the river is running in two parallel branches. The distance between those branches is about 10 km in upstream part and 35 km nearly the sea. The Hau river is quite straight and the Tien river is lightly meandering. The question is why the distance between two branches is not so large but the planform between them is quite different. The possible answer can be found in figure 4.4 namely: the tectonic

impact, especial is the fault A, B indicated in figure 4.4 can be a reason that Hau river is a straight branch. The river is running along those faults that can make it more straightly.

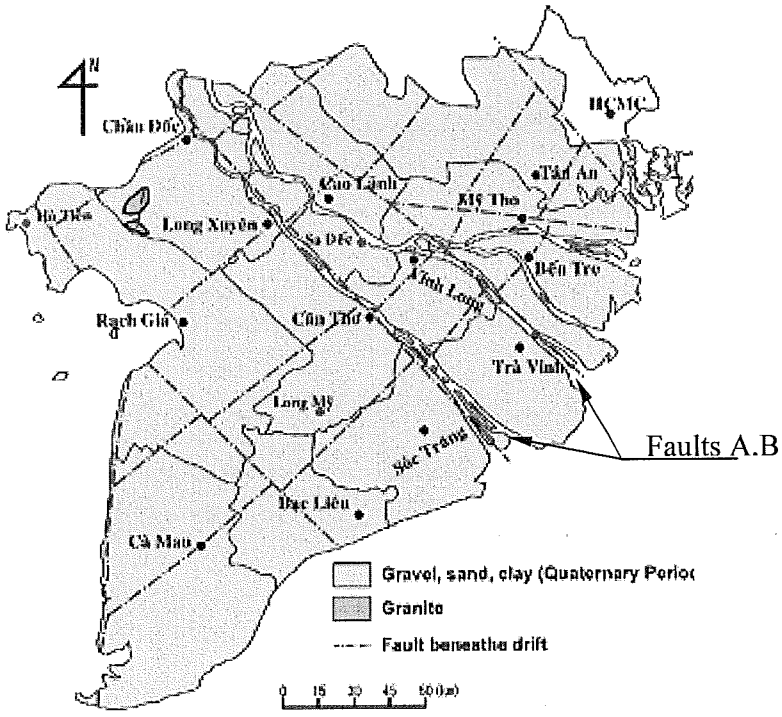

Figure 4.4. The geological faults in lower Mekong

Moreover, there are a number of man - made canals, which can be other influence reason of the straight planform of lower Mekong river. The man-made canals systems defined here a very complex irrigation system. It is estimated about 5000 km length of this system. The density of the canal system over lands surface is about 1250 km/km^2.

Other possible reason that, the river might be influence due to the vast area of alluvial, which contains the fine sand and clay box. The grain size varies from 0.1mm to 0.25mm.
The history of lower Mekong delta used to be a vast of salt marches, lagoon, forest, and the flat delta can be more reason of this area.

Meandering characteristics

The meandering of Tien river has some characteristics following observation data from figure 4.1:
The maximum meandering length $\lambda_{max} = 40$km.
The meandering length between bend number 5 to bend number 7 (indicated in figure 4.1) λ_{5-7}=22.5km; $\lambda_{7-9} = 21.5$km.
The average meandering length $\overline{\lambda}$=22km.
The average amplitude of meandering: a= 6.2km
The width of river variance: W=600-1100m.
The radius of curvature variance: R=3.5-9.6km

Application of predictor method to research on the meandering length of Tien river

- *Inglis (1949), Furguson data*

$\lambda = 6.5.B_s^{0.99}$; where B_s denotes the width at the average discharge .
Estimate : B_s= 800(m) -> λ = 4863(m)

- Zeller (1967a)

$\lambda = 10.B_s^{1.025}$ -> λ = 9455(m)

- Leopold and Wolman (1960)

$\lambda = 11.B_s^{1.01}$ -> λ = 9408(m)
or
$\lambda = 4.6.R^{0.98}$ where R is the radius of curvature

Estimate:
R = 9600m -> λ = 36760 (m)
R = 3500m -> λ = 13675(m)

In comparision with the observation data, the Leopold and Wolman (1960) with the second formula provides acceptable results.

However, these results are strongly influence by existence of the secondary branches only limited number of the bends in Tien river consists of a single bend.

4.4.2 Riverbank erosion from satellite images and old maps and data analysis

4.4.2.1 River bank erosion

The observed erosion rates (E) as a function of the ratios of radius of curvature and river width (R/W) are shown in figure 4.5.

The maximum erosion rate of about 51,2m/yr found at Sadec bend in the periods of 1996 - 2001 corresponds to the ratio of R/W=1.51.(see Fig 4.5 and for more detail in table A.2.2 appendix A.2).
Most of the rates of riverbank erosion varies from 5 to 15 m/yr, and the ratios of R/W vary from 1.5 to 6.

The highest rates happen for the ratios R/W between 1.5 to 3, in this area; the rates of river bank erosion can be very high and vary dynamically. It seems increased from R/W =1 to 1.5 and decrease fater R/W>1.5; from the figure 4.5 also can see the rates of riverbank erosion is about 5-15m/yr when R/W from 3 to 6.
In figure A.2.7 a,b,c; A.2.8 a,b,c; A.2.9 a,b,c; A.2.10 a,b,c in appendix A.2, the planform change of Mekong river is shown for some particular locations such as Tan Chau, Sadec, Vamnao, My Thuan.

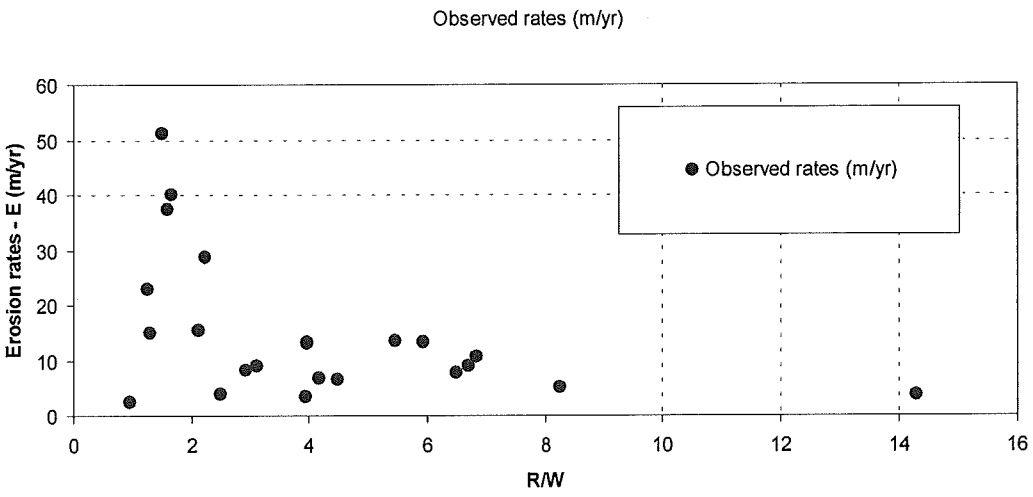

Figure 4.5. Observed erosion rates and R/W ratios data

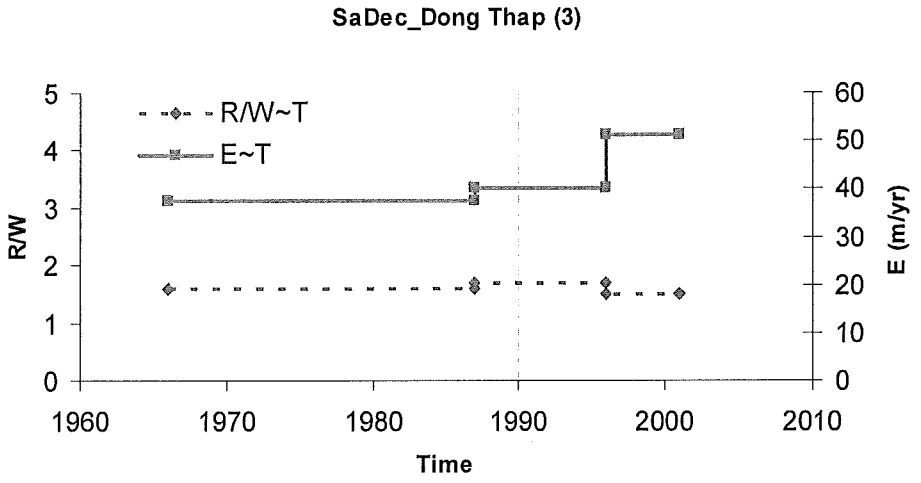

Figure 4.6 a) The variance R/W and E in time at Sadec-Dong Thap

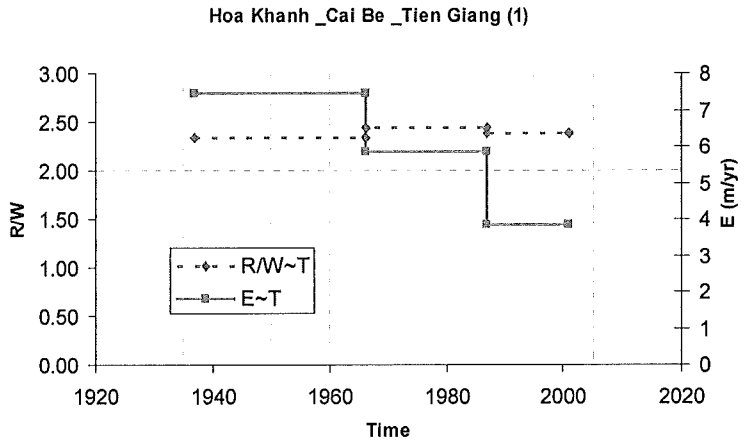

Figure 4.6 b) The variance R/W and E in time at Khanh Hoa-Cai Be-Tien Giang

From the figure 4.6 a) it can be seem that the ratios R/W vary only little with the time, but the erosion rates increase largely in the last decades. However, the erosion rates at Khanh Hoa – Cai Be –Tien Giang in figure 4.6 b) located also more in downstream part of lower Mekong decrease while the variance of R/W is very small. That means that the morphological mobilization of the downstream part of lower Mekong river is decreasing.

Moreover, as indicated by Le Manh Hung et al (2003), most of the riverbank erosion occurs during the flood recession or combination with tidal recession, when the water level is very close to the bankfull level, and the currents are high. Figure 4.7 a) and b) present the erosion progress at Tan chau town within about 1 month period.

a) Riverbank on 18th December, 2005

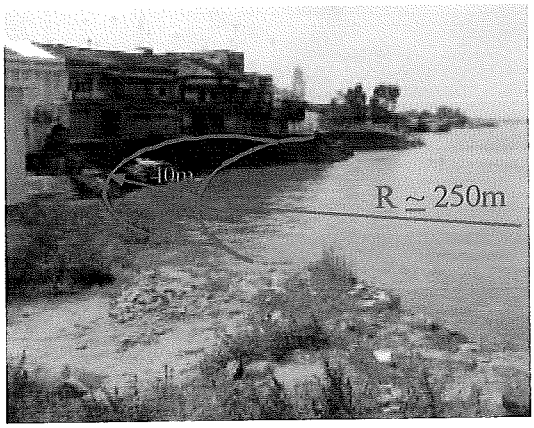

b) Riverbank on 23rdJanuary, 2006

Figure 4.7 Riverbank erosion at upstream of Tan Chau revetment.

4.4.2.2 Data analysis

Based on the data from satellite images and old maps, the erosion rates E(m/yr), the radius and width of river section, and the five year flood discharge, are shown in table A.2.1 and A.2.2 in appendix A.2.
The bank hight and the water depth in each of cross-sections are determined base on the topography data of 1996 for 15 bends. Based on these data the following empirical formula is derived to present the relation between the scour hole depth and the ratios of radius of curvature and bankfull width for the lower Mekong.

$$\frac{h_b}{h} = -0.7091 \ln(\frac{R}{W}) + 3.3792 \qquad (4\text{-}1)$$

The results are plotted in figure 4.8 together with Maynord and USACE formula for comparison. These results show good agreement with the Maynord formula and USACE:

$$\frac{h_b}{h} = -0.36 \ln(\frac{R}{W}) + 2.57 \qquad (4\text{-}2)$$

and the formula of USACE:

$$\frac{h_b}{h} = -0.71 \ln(\frac{R}{W}) + 3.377 \qquad (4\text{-}3)$$

From this comparison, we found that the ratio of scour hole depth and water depth as a function of *R/W* are similar with USACE prediction in lower Mekong river. More detail in table A.2.6. of appendix A.2, results of GIS.

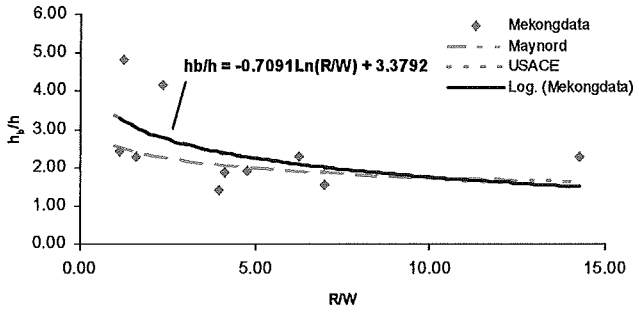

Figure 4.8 The empirical formula for scour hole in lower Mekong river.

The bankfull discharge in 15 bends is determined by following formula (see more detail in table A.2.6 in appendix A.2)

$$Q_{bf} = A_{bf}.C\sqrt{h_{bf}i} \quad (4\text{-}4)$$

where as:

A_{bf} : Area of cross-section at bankfull level (m^2)

h_{bf} : The bankfull depth, $hbf=A_{bf}/W_{bf}$, W_{bf} is the bankfull width

i : The slope of river, $i=4x10^{-5}$

C : Chezy coefficient ($m^{1/2}/s$)

C is computed base on the Englund –Hansen (1967)

$$C = 18\left(\frac{h'}{h}\right)^{0.5}\log\frac{12h'}{2.5D_{50}} \quad (4\text{-}5)$$

where

C - Chezy roughness coefficient ($m^{1/2}/s$)

h - water depth (m)

D_{50} – mean diameter of particle (m)

h' is a parameter (m) defined as:

$$h' = \left(\frac{\theta'}{\theta}\right)h \quad (4\text{-}6)$$

$$\theta = \frac{u_*^2}{\Delta g D_{50}} \quad (4\text{-}7)$$

$\theta \leq 0.7$ $\Rightarrow \theta' = 0.06 + 0.4.\theta^2$ (4-8)

$0.7<\theta<1$ $\Rightarrow \theta' = \theta$

$\theta \geq 1$ $\Rightarrow \theta' = (0.3 + 0.7.\theta^{-1.8})^{-0.56}$ (4-9)

The results of bankfull discharges can be found in table A.2.5 of appendix A.2

4.5 Application of Hickin & Nanson (1984) for Lower Mekong

Hickin & Nanson (1984) reported that the riverbank erosion at bends can be predicted following equation:

$$E(R/W) = E_{2.5}.f(R/W) \quad (4\text{-}10)$$

For $f(R/W)$ an empirical relation was derived:

For $1<R/W<2.5$ $f(R/W) = 2/3(R/W-1)$

For $R/W>2.5$ $f(R/W) = 2.5W/R$

The maximum erosion rate occurs for R/W=2.5 and is defined as $E_{2.5}$ (in m/yr) and this maximum rate is proportional to total stream power Ω which is denoted as:

$$\Omega=Q_5 \gamma h_b^{-1}=\rho g Q_5 i \text{ (watt/m')} \quad (4\text{-}11)$$

$$E_{2.5}=\frac{\Omega}{h_b Y_b} \quad (4\text{-}12)$$

Where as

E(R/W): Erosion rates as function of ratio of curvature radius and width

R : Radius of curvature (m) is determined from old map and satellites images see table A.2.1 in Appendix A.2.

W : Bank full width of river (m) is determined from old map and satellites images see table A.2.1 in Appendix A.2.

Q_5 : The five year flood discharge (m^3/s) is estimated from the width of river at 15 bends above see table A.2.1 in Appendix A.2.

i :slope of river i=$4x10^{-5}$ for lower Mekong river was determined based on the hourly data of water level from 1996 to 1999.

h_b : the bank height determined from the cross-section of the data 1996 at the bend locations, see table A.2.3 in Appendix A.2.

Y_b : the bank strength parameter (N/m^2), base on the database established by Hickin & Nanson for the grain size variance from 0.001mm to 100mm, see table A.2.3 in Appendix A.2.

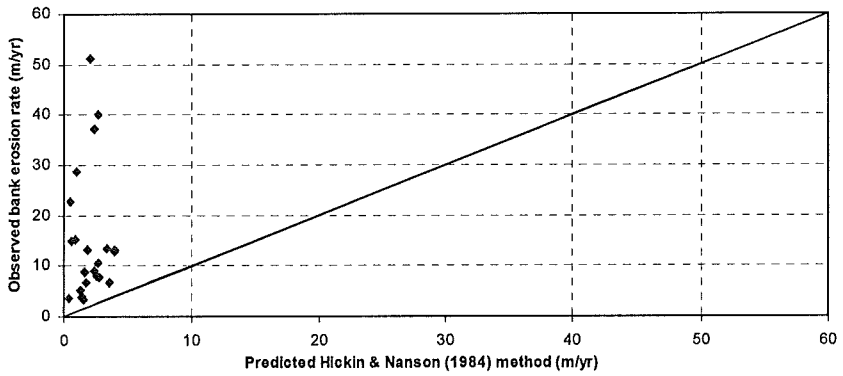

Figure 4.9 Comparison between observed bank erosion rates and Hickin & Nanson (1984)

When applying Hickin & Nanson (1984) method, the maximum rate of only 5m/yr is founding comparison with 51.2 m/yr of observed data. In addition, figure 4.9 shows that the results by applying Hickin & Nanson (1984) are smaller than observed data.

The results by application of Hickin & Nanson (1984) could be explained that:

The lower Mekong is flooded every year (see Fig.4.2) and the different between each flood peak is not so large. So that, the five year flood discharge is not relevant to the lower Mekong river. Moreover, the riverbank erosion occurs every year and specially most of them occur when flood recession or flood recession combine with tidal influence; In applying Hickin & Nanson (1984), the bank strength parameter (Yb) has been found based on grain size of material (D_{50}), but D_{50} was varied in very small range of 0.25mm to 0.1mm in lower Mekong river. The other reason that show in figure 4.5, the maximum observed riverbank erosion rates was found at R/W≈1.5-2.0 but Hickin & Nanson (1984) found R/W=2.5 when E_{max} occurs. Other possible reason is the impact of tectonic fault.

Nevertheless, it could be conclusion that applying the method of Hickin & Nanson (1984), the improvement of this method for local lower Mekong conditions is needed, and the additional future study is necessary.

4.6 Improvement of the Hickin & Nanson (1984) for lower Mekong conditions

4.6.1 The ideas of improved Hickin & Nanson (1984)

As the first stage for improvement of prediction of riverbank erosion in the lower Mekong river, the backgrounds of the Hickin & Nanson (1984) method will be adopted. This method assumes that the riverbank erosion rate is likely dependent on the variable listed in:

$$E = f(\Omega, Y_b, h_b, R, W) \quad (4\text{-}13)$$

in which, Ω = stream power per unit bed area, Y_b= the opposing force per unit boundary area resisting migration, h_b = bank height, R= radius of curvature of bend, W = river width of bend. The sediment transport should be taken into account in equation 4-13. However, it is impossible due to the lack of sediment data in the lower Mekong river.

The improvement version of Hickin & Nanson (1984) is only focus on two parameters:

- The stream power Ω is depend on bankfull discharge. $\Omega=\rho g Q_{bf} i$ (watt/m') (In original Hickin & Nanson (1984) method used five year flood discharges).

- The h_b is dependent variable with riverbank erosion rate, (In original Hickin & Nanson (1984) method h_b is independent parameter).

The reasons lead to improve the stream power by using bankfull discharge instead for five years discharge are:

- By looking the 15bends, many of them are located in the second branch, that means the discharge distribution is change in time, and the five years flood discharge at 15 locations could be only estimated.
- The observed riverbank erosion rates (see appendix A.2) suggests that the riverbank erosion rate is not only depend on the radius of curvature, the width of river but also depend on the local condition of cross-section.

Although, the bankfull discharge does not occur dominantly in the river but it seems acceptable for the prediction of yearly riverbank erosion rate.

In table 4.1 is compare between original Hickin & Nanson (1984) and improvement version

Original Hickin & Nanson (1984)	Improvement version
$E(R/W) = E_{2.5}.f_1(R/W)$ (4-14) * $f_1(R/W)$ an empirical relation was derived: For $1<R/W<2.5$ $f_1(R/W) = 2/3(R/W-1)$ For $R/W>2.5$ $f_1(R/W) = 2.5W/R$ * $E_{2.5} = \frac{\Omega}{h_b Y_b}$ * $\Omega=Q_5 \tau h_b^{-1}=\rho g Q_5 i$ (watt/m') * Y_b found from empirical relation with D_{50} was establised by Hickin & Nanson (1984)	$E(R/W, h_b) = E_{2.5}.f_1(R/W).f_2(R/W, h_b)$ (4-15) * $f_1(R/W)$ an empirical relation was derived: For $1<R/W<2.5$ $f_1(R/W) = 2/3(R/W-1)$ For $R/W>2.5$ $f_1(R/W) = 2.5W/R$ * $E_{2.5} = \frac{\Omega}{h_b Y_b}$ * $\Omega=Q_{bf} \tau h_b^{-1}=\rho g Q_{bf} i$ (watt/m') * Y_b found from empirical relation with D_{50} was establised by Hickin & Nanson (1984) * $f_2(R/W,h_b)$ the empirical relation was found in the lower Mekong river.

Table 4.1 The different between original Hickin & Nanson (1984) and improvement version for the lower Mekong river

Where as:

$E(R/W, h_b)$	: The riverbank erosion rates (m/yr)
R	: Radius of curvature (m) is determined from old map and satellites images see table A.2.1 in Appendix A.2.
W	: Bank full width of river (m) is determined from old map and satellites images see table A.2.1 in Appendix A.2.
Q_{bf}	: The bankfull discharge (m^3/s) calculated at 15 bends above see table A.2.5 in Appendix A.2.
i	: Slope of river $i=4x10^{-5}$ for lower Mekong river was determined base on the hourly data of water level from 1996 to 1999.
h_b	: The bank height determined from the cross-section of the data 1996 at the bend locations, see table A.2.3 in Appendix A.2.
Y_b	: The bank strength parameter (N/m^2), base on the database established by Hickin & Nanson (1984) the grain size variance from 0.001mm to 100mm, see table A.2.3 in Appendix A.2.

4.6.2 The establishing an empirical relationship $f_2(R/W,h_b)$ for the lower Mekong river

From equation (4-15), function $f_2(R/W,h_b)$ can be determined by:

$f_2(R/W, h_b) = E(R/W, h_b) / E_{H\text{-}N}$

Where as:

$E(R/W, h_b)$ is the observed erosion rate at 15 bends.

$E_{H\text{-}N}$ is determined based on original Hickin& Nanson (1984), which the stream power (Ω) computed based on bankfull discharge (Q_{bf}).

The observed riverbank erosion rates data and the bank high (h_b) is available for 10 bends in different period. (see table 4.2). In figure 4.10 a, b the bank high (h_b) is not change so much in time was shown. Because of lack data of bank high overall 10 bends in different time, it was assumed that h_b does not change in time (see table 4.2).

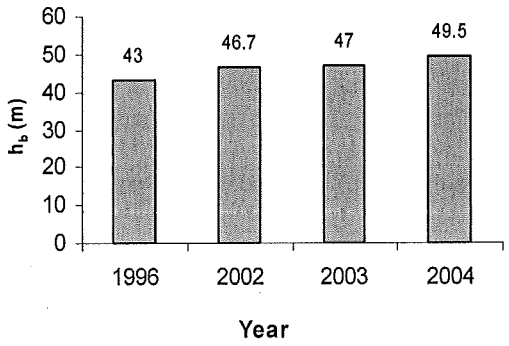

a) The bank high (h_b) at Tan Chau bend in time

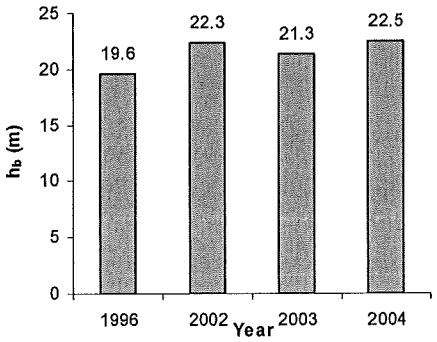

b) The bank high (h_b) at Hong Ngu bend in time

Figure 4.10 The bank high change in time at Tan Chau bend, and Hong Ngu bend

N°	Locations	Observed Time	Observed erosion rates E (m/yr)	R/W	h_b (m)
1	Tan Chau _ outer bend	1996-2003	22.86	1.25	44.00
2	Hong Ngu-Dong Thap	1966-1996	3.90	2.50	19.67
		1996-2001	15.33	2.12	19.67
		2001-2003	28.67	2.23	19.67
3	Phu An _ Lach Vung _ An Giang	1966-2001	3.43	3.96	6.10
5	Thanh Binh - Dong Thap	1966-1987	5.14	8.25	18.60
		1987-1996	8.89	6.69	18.60
		1996-2001	13.20	5.94	18.60
6	My An _ Lap Vo_Dong Thap	1966-1987	6.67	4.17	20.40
		1987-1996	8.11	2.94	20.40
		1996-2001	9.00	3.11	20.40
7	My Xuong -Cao Lanh - Dong Thap	1966-1987	6.62	4.49	20.03
		1987-1996	13.00	3.97	20.03
		1996-2001	13.16	3.96	20.03
8	Sadec -Dong Thap	1966-1987	37.33	1.60	21.90
		1987-1996	40.00	1.68	21.90
		1996-2001	51.20	1.51	21.90
9	Chau Thanh - Dong Thap	1966-1987	10.62	6.85	17.00
		1987-1996	7.78	6.49	17.00
		1996-2001	13.50	5.47	17.00
14	Binh An - Long Xuyen - An Giang	1966-2001	3.69	14.28	9.60
15	An Thanh Trung-Long Xuyen-An Giang	1966-1987	2.48	0.96	10.37
		1987-1996	15.00	1.32	10.37

Table 4.2 The observed data from GIS analysis

From the observed data in table 4.2, it is divided in two parts, one part was used for establishing formula $f_2(h_b, R/W)$ and the other part was used for calibrating of formula.

In order to limit the risk of formula from the lower Mekong condition, the data used for establish formula that must be covered upstream part, downstream part of area and different time of observation. The formula have been found in fig. 4.11 and more detail in see table 4.3.

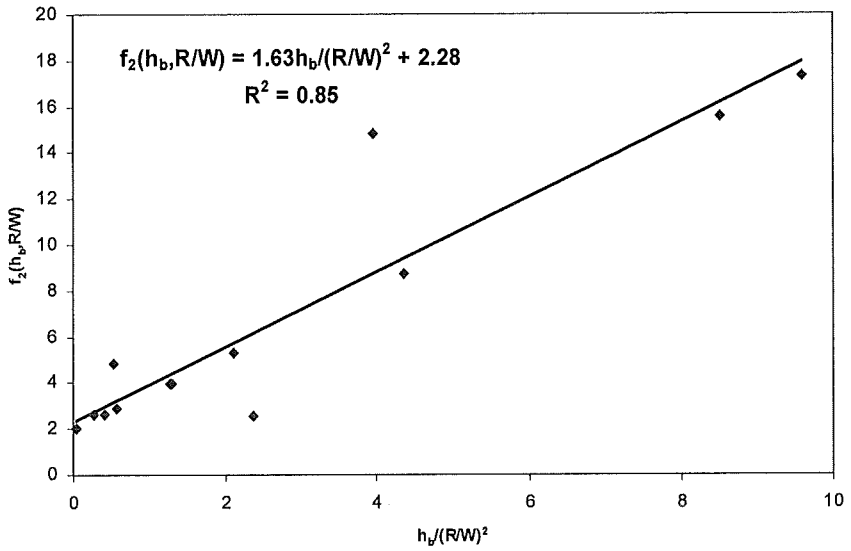

Figure 4.11 Improvement empirical formula of $f_2(h_b, R/W)$

No	Locations	Observed Time	Observed erosion rates E (m/yr)	R/W	Qbf (m3/s)	Ω(watt/m')	Yb (N/m^2)	hb (m)	f_1(R/W)	E2.5	E_{H-N} (m/yr)	$h_b/(R/W)^2$	$f_2(h_b, R/W)$
(1)	(2)	(3)	(4)	(5)	(6)	(7)	(8)	(9)	(10)	(11)	(12)	(13)	(14)
2	Hong Ngu-Dong Thap	1996-2001	15.33	2.12	6347.60	2539.04	55.00	19.67	0.75	2.35	1.76	4.36	8.72
		2001-2003	28.67	2.23	6347.60	2539.04	55.00	19.67	0.82	2.35	1.93	3.94	14.86
5	Thanh Binh - Dong Thap	1966-1987	5.14	8.25	15105.68	6042.27	50.00	18.60	0.30	6.50	1.97	0.27	2.61
		1996-2001	13.20	5.94	15105.68	6042.27	50.00	18.60	0.42	6.50	2.74	0.53	4.82
6	My An _ Lap Vo_Dong Thap	1987-1996	8.11	2.94	9178.49	3671.39	48.00	20.40	0.85	3.75	3.19	2.36	2.55
		1996-2001	9.00	3.11	9178.49	3671.39	48.00	20.40	0.80	3.75	3.01	2.11	5.32
7	My Xuong -Cao Lanh - Dong Thap	1987-1996	13.00	3.97	19390.24	7756.10	47.00	20.03	0.63	8.24	5.18	1.27	3.98
		1996-2001	13.16	3.96	19390.24	7756.10	47.00	20.03	0.63	8.24	5.20	1.27	3.99
8	Sadec -Dong Thap	1966-1987	37.33	1.60	17541.69	7016.68	46.00	21.90	0.40	6.97	2.81	8.50	15.56
		1996-2001	51.20	1.51	17541.69	7016.68	46.00	21.90	0.34	6.97	2.37	9.59	17.30
9	Chau Thanh - Dong Thap	1987-1996	7.78	6.49	21485.15	8594.06	45.00	17.00	0.39	11.23	4.33	0.40	2.60
		1996-2001	13.50	5.47	21485.15	8594.06	45.00	17.00	0.46	11.23	5.14	0.57	2.86
14	Binh An - Long Xuyen - An Giang	1966-2001	3.69	14.28	14260.12	5704.05	50.00	9.60	0.18	11.88	2.08	0.05	2.03
15	An Thanh Trung-Long Xuyen-An Giang	1966-1987	2.48	0.96	15914.56	6365.83	49.00	10.37		12.53	-	-	-

Table 4.3 The results of establishing $f_2(h_b, R/W)$ equation

Explain the table:

Column (1). The name of bend are shown in figure 4.1

Column (4), (5) is observed data from GIS analysis, see more detail in appendix A-2

Column (6), Q_{bf} – bankfull discharge, it is computed at cross-section of the bend, see part 4.4.2 b. and appendix A-2 table

Column (7), Ω - stream power (watt/m') $\Omega=Q_{bf}\gamma h_b^{-1}=\rho g Q_{bf} i$ (watt/m'), see Appendix 17

Column (8), Y_b – strength of riverbank is defined in Hickin & Nanson (1984) based on D_{50} (see more detail in table A.2.6 appendix A-2)

Column (10), $f_1(R/W)$ – the function was found by Hickin & Nanson (1984), see table 4.1

Column (11), $E_{2.5}$ – the maximum rate found at R/W=2.5 by Hickin & Nanson (1984), see table 4.1

Column (12), $E_{H\&N}$- The riverbank erosion rates (m/yr) by applying Hickin & Nanson (1984), Column (12)= Column (10) x Column (11)

Column (13), the observed data

Column (14), $f2(h_b, R/W)$ =Observed erosion rates/E_{H-N}, Column (14)=Column (4)/ Column (12)

At bend number 15, because of R/W=0.96 <1 then applying Hickin & Nanson (1984) is not available.

4.6.3 Calibration of the empirical relationship $f_2(R/W,h_b)$ for the lower Mekong river

From section 4.6.2 the empirical relation was derived:

$$f_2(h_b,R/W)=\frac{E_{obseverved}}{E_{H-N}}=1.63\frac{h_b}{\left(\frac{R}{W}\right)^2}+2.28 \qquad (4\text{-}16)$$

Where as

$f_2(h_b, R/W)$: a empirical relation to adopted the Hickin & Nanson (1984) for the lower Mekong river.

$E_{Observed}$: the observed riverbank erosion rate (m/yr)

E_{H-N} : The apply Hickin &Nanson (1984), which stream power $\Omega = \rho g Q_{bf} i$ (watt/m')

Q_{bf} : the bankfull discharge (m^3/s)

h_b : the bank hight (m)

R : the Radius of curvature (m)

W : the width of river (m)

The formula (4-16) is calibrated with the last part of data. The result is shown in figure 4.12 and more detail information in table 4.4.

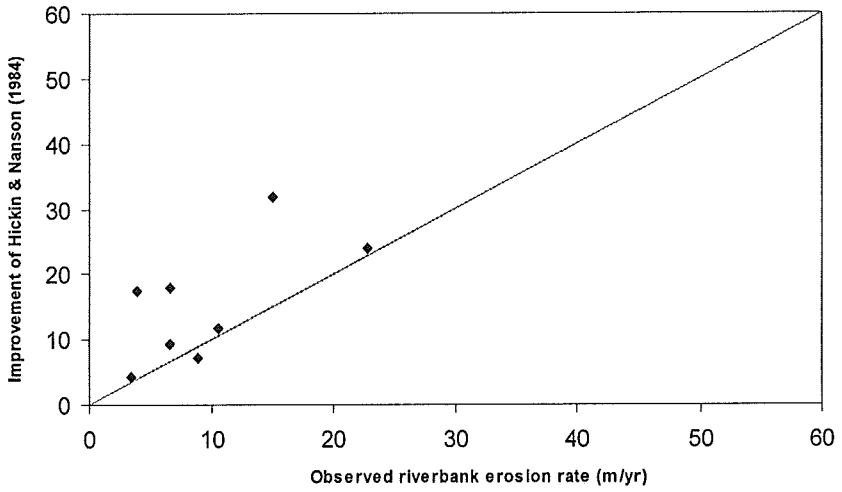

Figure 4.12 Result of calibration the improvement Hickin & Nanson (1984)

In figure 4.12, the results of improvement Hickin & Nanson (1984) is higher than observed data. It seems more safety results for prediction of riverbank erosion. With these results, the improvement Hickin &Nanson (1984) is reasonable.

The maximum error between prediction and observed data is about 78%, and minimum error is about 5%. However, if we look at the bend where has higher errors (see table 4.4), the prediction rates are higher than observed one, so that, could be possible for safety reason.

The errors of improvement can be explain that, because of the limitation of observed data, and the bank high is assumed constant in time at bend, the bankfull discharge is also assumed constant in time at bend. This is two main parameters could be lead the results with larger error. However, the luckily that, the prediction riverbank erosion rates is larger than observed data, so that in the tendency, this improvement version is accepted.

No	Locations	Observed Time	Observed erosion rates E (m/yr)	R/W	Q_{bf} (m3/s)	Ω(watt/m')	Yb (N/m^2)	hb (m)	f_1 (R/W)	E2.5	$E_{H\&N}$ (m/yr)	$h_b/(R/W)^2$	$f_2(h_b, R/W)$	Semin E_{H-N} (m/yr)	Error (%)
(1)	(2)	(3)	(4)	(5)	(6)	(7)	(8)	(9)	(10)	(11)	(12)	(13)	(14)	(15)	(16)
1	Tan Chau _ outer bend	1996-2003	22.86	1.25	19111.71	7644.68	60.00	45.00	0.17	2.90	0.49	28.61	48.91	24.00	4.75%
2	Hong Ngu-Dong Thap	1966-1996	3.90	2.50	6347.60	2539.04	55.00	19.67	1.00	2.35	2.35	3.15	7.41	17.39	77.58%
3	Phu An _ Lach Vung _ An Giang	1966-2001	3.43	3.96	2000.00	800.00	55.00	6.10	0.63	2.38	1.51	0.39	2.91	4.39	21.89%
5	Thanh Binh - Dong Thap	1987-1996	8.89	6.69	15105.68	6042.27	50.00	18.60	0.37	6.50	2.43	0.42	2.96	7.18	19.28%
6	My An _ Lap Vo_Dong Thap	1966-1987	6.67	4.17	9178.49	3671.39	48.00	20.40	0.60	3.75	2.25	1.18	4.20	9.44	29.37%
7	My Xuong -Cao Lanh - Dong Thap	1966-1987	6.62	4.49	19390.24	7756.10	47.00	20.03	0.56	8.24	4.59	0.99	3.90	17.91	63.04%
8	Sadec -Dong Thap	1987-1996	40.00	1.68	17541.69	7016.68	46.00	21.90	0.45	6.97	3.16	7.75	14.92	47.15	15.17%
9	Chau Thanh - Dong Thap	1966-1987	10.62	6.85	21485.15	8594.06	45.00	17.00	0.37	11.23	4.10	0.36	2.87	11.77	9.80%
15	An Thanh Trung-Long Xuyen-An Giang	1987-1996	15.00	1.32	15914.56	6365.83	49.00	10.37	0.21	12.53	2.66	5.97	12.01	31.90	52.97%

Table 4.4 The results of calibration equation (4-16)

Explain the table:

Column (1). The name of bend are shown in figure 4.1
Column (4), (5) is observed data from GIS analysis, see more detail in appendix A-2
Column (6), Q_{bf} – bankfull discharge, it is computed at cross-section of the bend, see part 4.4.2 b. and appendix A-2 table
Column (7), Ω – stream power (watt/m') $\Omega=Q_{bf}\tau h_b^{-1}=\rho g Q_{bf} i$ (watt/m'), see appendix A-2
Column (8), Y_b – strength of riverbank is defined in Hickin & Nanson (1984) based on D_{50} (see more detail in table A.2.6 appendix A-2)
Column (10), $f_1(R/W)$ – the function was found by Hickin & Nanson (1984), see table 4.1
Column (11), $E_{2.5}$ – the maximum rate found at R/W=2.5 by Hickin & Nanson (1984), see table 4.1
Column (12), $E_{H\&N}$- The riverbank erosion rates (m/yr) by applying Hickin & Nanson (1984), Column (12)= Column (10) x Column (11)
Column (13), the ratios of hb/(R/W)^2 computed from data
Column (14), $f2(h_b,R/W)$- the empirical relation in equation (4-16)
Column (15), Prediction riverbank erosion rates results based on the improvement Hickin & Nanson (1984), Colum (15)= Column(12)x Column (14)

4.6.4 The Simplified improvement of Hickin & Nanson (1984) and results

Based on table 4.1 and equation (4-16), the simplified improvement of Hickin & Nanson(1984) are rewrited:
The riverbank erosion can be predicted in lower Mekong river based on following equation:

$$E(R/W, h_b) = E_{2.5}.f_1(R/W).f_2(R/W, h_b) = \frac{\Omega}{Y_b.h_b}.f(R/W).\left(1.63.\frac{h_b}{\left(\frac{R}{W}\right)^2} + 2.28\right) \quad (4\text{-}17)$$

$$\Rightarrow E(R/W, h_b) = \frac{\Omega}{Y_b}.f(R/W).\left[\frac{1.63}{\left(\frac{R}{W}\right)^2} + \frac{2.28}{h_b}\right] \quad (4\text{-}18)$$

For *f(R/W)* an empirical relation was derived:

For $1<R/W<2.5$ $f(R/W) = 2/3(R/W-1)$

For $R/W>2.5$ $f(R/W) = 2.5W/R$

$\Omega = Q_{bf}\tau h_b^{-1} = \rho g Q_{bf} i$ (watt/m')

Y_b determined by Hickin & Nanson (1984)

From equation (4-18) by assume value h_b from range of 10-40m. The riverbank erosion can be predicted from figure 4.13.

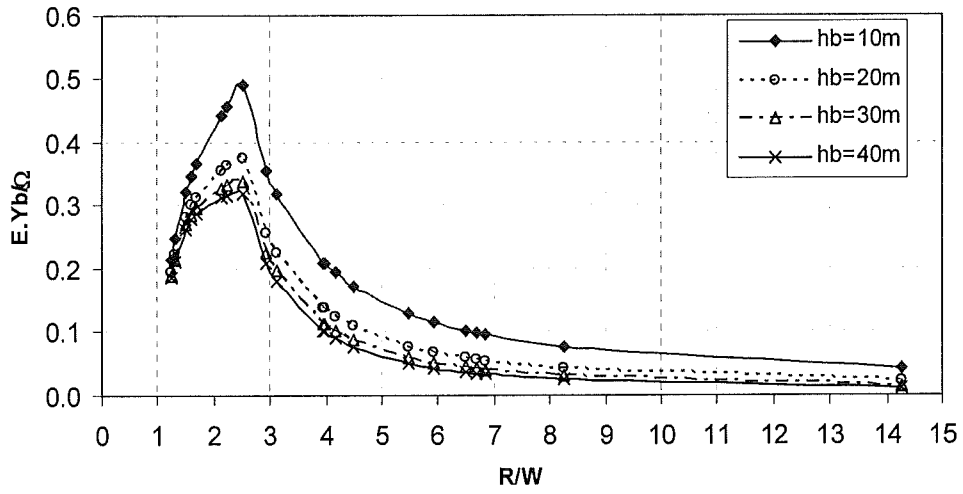

Figure 4.13 The relation of E.Yb/Ω and R/W at different h_b

Where as:
h_b – the bank high counted from deepest point to bank level of cross-section (m)
R – the radius of curvature (m)
W – the river width at bend (m)
Y_b – The bank strength defined as Hickin & Nanson (1984) based on bank material.
Ω – The stream power, $\Omega = \rho g Q_{bf} i$ (watt/m')
ρ - Density of water
g – gravity of acceleration (m/s^2)
Q_{bf} – Bankfull discharge (m3/s)
i – river slope (-)

4.6.5 Re-application of improvement of Hickin & Nanson (1984) for all data in Mekong

Application the improvement of Hickin & Nanson (1984) for all data again we have the results show in figure 4.13 a, b, c , (see more detail in table A.2.4 in appendix A.2)

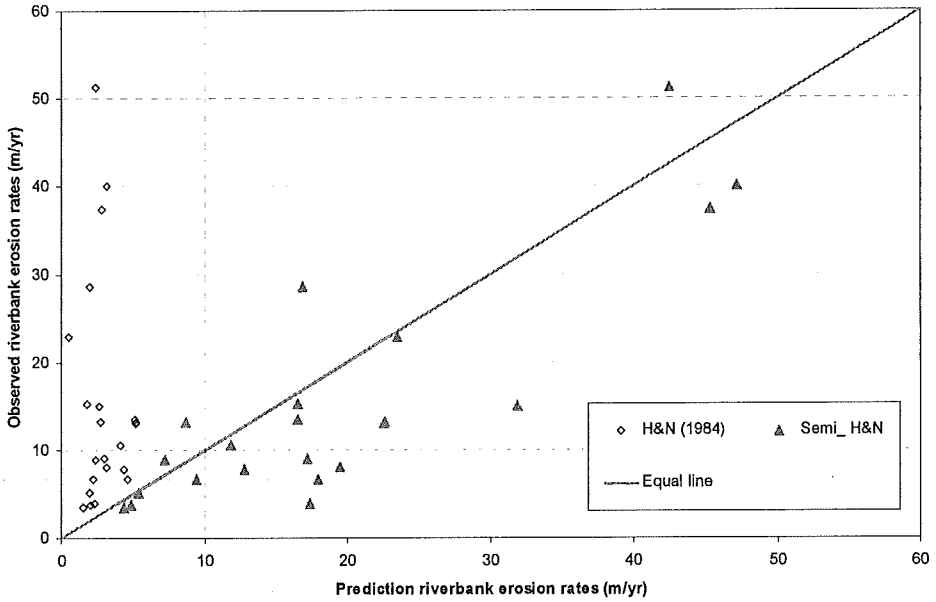

Figure 4.14 a) The results of improvement Hickin & Nanson (1984)

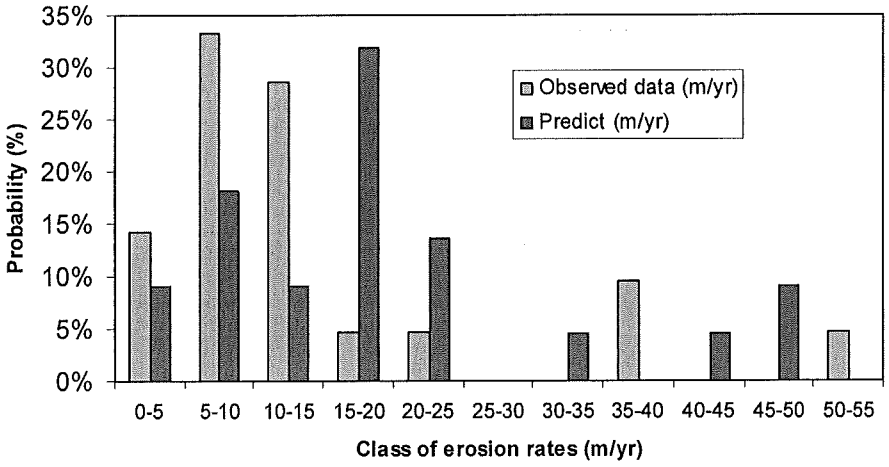

Figure 4.14b) The results of improvement Hickin & Nanson (1984)

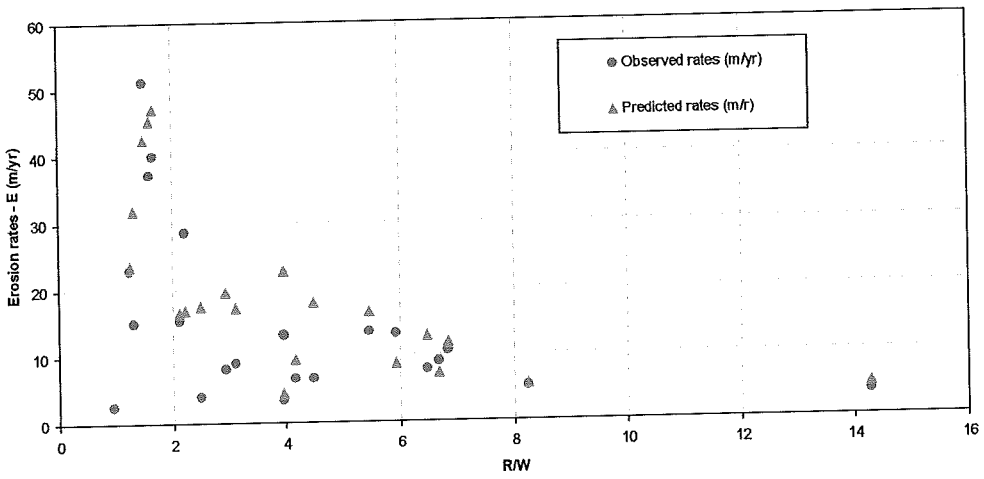

Figure 4.14c) The results of improvement Hickin & Nanson (1984)

The result of improvement Hickin& Nanson (1984) based on the lower Mekong conditions show in figure 4.14 a) is acceptable. The different between observed data and predicted value is not so large, and the class of erosion rates is quite nearly the observed erosion rates.

Figure 4.14.b) shows that, the class of erosion rates is 15-20 m/yr are the highest probability of occurrence. It might be higher than observation data but for safety reason, it could be accepted.
Figure 4.14.c) shows that, the maximum observed rates happens when the ratios of *R/W* is about 1.5 and when comparing to the predicted maximum rate, it also happens when the radius of R/W is in this area.

The results of improvement Hickin and Nanson (1984) opened a new approach for study of riverbank erosion in the lower Mekong river. However, as mentioned above, this is an early stage of riverbank erosion prediction in lower Mekong river. This results still need to be improved, because of the limitation of resolutions of satellite images, also the limitation of number of bends, and periods of time, the bankfull discharge, bank high data used is the same for every period of time in separate bend, (see more detail in table A.2.4).
The equation (4-16) is calibrated. However, the lack data is reason suggest for future, formula (4-16) should verify against with observed data.

5.MIKE 21C, SCHEMATIZATION, CALIBRATION AND VALIDATION

5.1 Objectives

A model is a physical or mathematical schematization of a physical system, including the interaction with its outside world, which can be used to simulate the effect of changes in system itself or the effect of changes in the conditions imposed upon it. However, there are a number of assumptions in the mathematical modelling so that needs calibration and validation steps.

In chapter 4, a number of empirical methods and the improvement of Hickin & Nanson (1984) method by using the old maps and a number of satellite images under the analysis of GIS tool were discussed. However, there are still many limitations of this method, as discussed above. These were the poor resolution of images, the lack of combination between flow and riverbed. Especially, the influence of bank protection works as well as the influence of riverbank erosion material on the morphology of river was not taken into account.

Consequently, it is decided to use mathematical modelling (MIKE21C) for a specific location (Tan Chau –Hong Ngu) to get insight the flowing objectives:

1) To establish the early state of riverbank erosion prediction by using Mike21C in lower Mekong river and notably, to predict the riverbank erosion in Tan Chau-Hong Ngu area.

2) To compute the scour hole in front of Tan Chau revetment in order to predict the stability of Tan Chau revetment on long term.

3) To check whether bend cut to be better solution or not in case the Tan Chau bend continues to develop.

In this chapter, the first objective of modelling is reported after a complex model, which included morphology change, riverbank erosion, and Tan Chau revetment. This model was calibrated for flood seasons 2002, 2003, and verified for a period of August 2003 to July 2004. The second and the third objective are achieved after the model verification process and reported in chapter 6.

5.2 Study area

In the lower Mekong river, there are many locations where riverbank erosion occurs critically. However, Tan Chau-Hong Ngu was known as the most critical location. The whole view of riverbank erosion in this location is reported in chapter 3, part III.2.1.
The computational area is from km248, nearly Vietnam-Cambodia frontier to km218 in Hong Ngu town (the distance is counted from the sea to upstream, Tan Chau at Km317).Total length of area is about 30km from upstream boundary to downstream boundary and river width from 500m to 2400m. The grid consists of 512 cells in length and 45 cells in width. The average cell width is about 30mx30m in the curvilinear grid. Figure 5.1 shows the curvilinear grid of simulation area.
The lowest point is about -40m a.m.s.l (above mean sea level).
This location is very complex, which included islands, bend, and the change of river direction with an angle nearly 90degree. The reason for riverbank erosion is not only bend development but also the high velocity near the bank, as well as the bifurcation.

The maximum flood discharge observed at Tan Chau station is about 26000m^3/s in the year of 2000.
The minimum discharge in the dry season can be 1300m^3/s.
Table 5.1 is the maximum water level in the flood season from 1926 to 1999.

Year	1937	1939	1940	1961	1966	1978	1984	1991	1996	2000
Maximum water level (m) a.m.s.l	4.49	4.89	4.89	5.11	5.03	4.78	4.81	5.02	4.87	5.06
Month occurrence	-	-	-	Oct.	Sept.	Oct.	Sept.	Sept.	Oct.	Sept.

Table 5.1 Maximum water level in flood season.

Note:
Sept=September
Oct=October
- No available information
In figure 5.3, there are five locations where the riverbank erosion occurred and these five locations have the different erosion rates (see table 5.2)

Nº	Name	Observed erosion rates (m/year)
1	Vinh Hoa village	8
2	Thuong Phuoc village	30
3	Tan Chau upstream Tanan Canal	5
4	Hong Ngu town	10
5	Long Thuan village	6

Table 5.2 River bank erosion in the computational area

Notes: The observed data from the satellite images

Tan Chau revetment was implemented from August 2001 with the design of six impermeable groyne 2001 to end of the September, the construction have stopped for change the design due to of flood 2001. Then on February, 2003 it is restarted again with the underwater part. The upper water part was constructed from March, 2004 and finished on August 2004. The figure 5.4 shows the activities at Tan Chau from 2001 to 2004 in both aspects the real world and the activities in this study. The total length of structure is about 650m from Tan An canal to downstream part. The typical design cross-section showed in figure below.

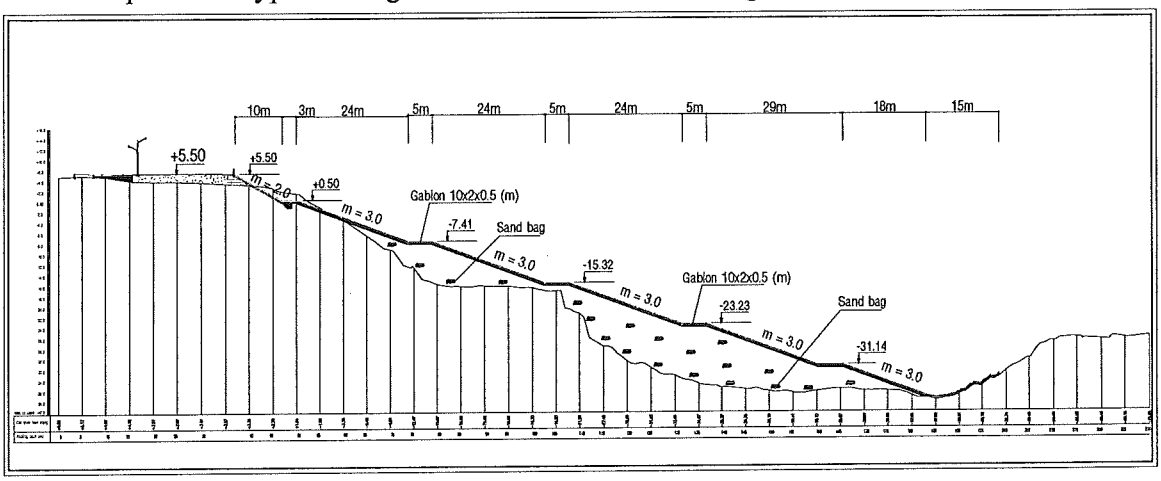

Figure 5.1 The typical design cross-section of Tan Chau revetment

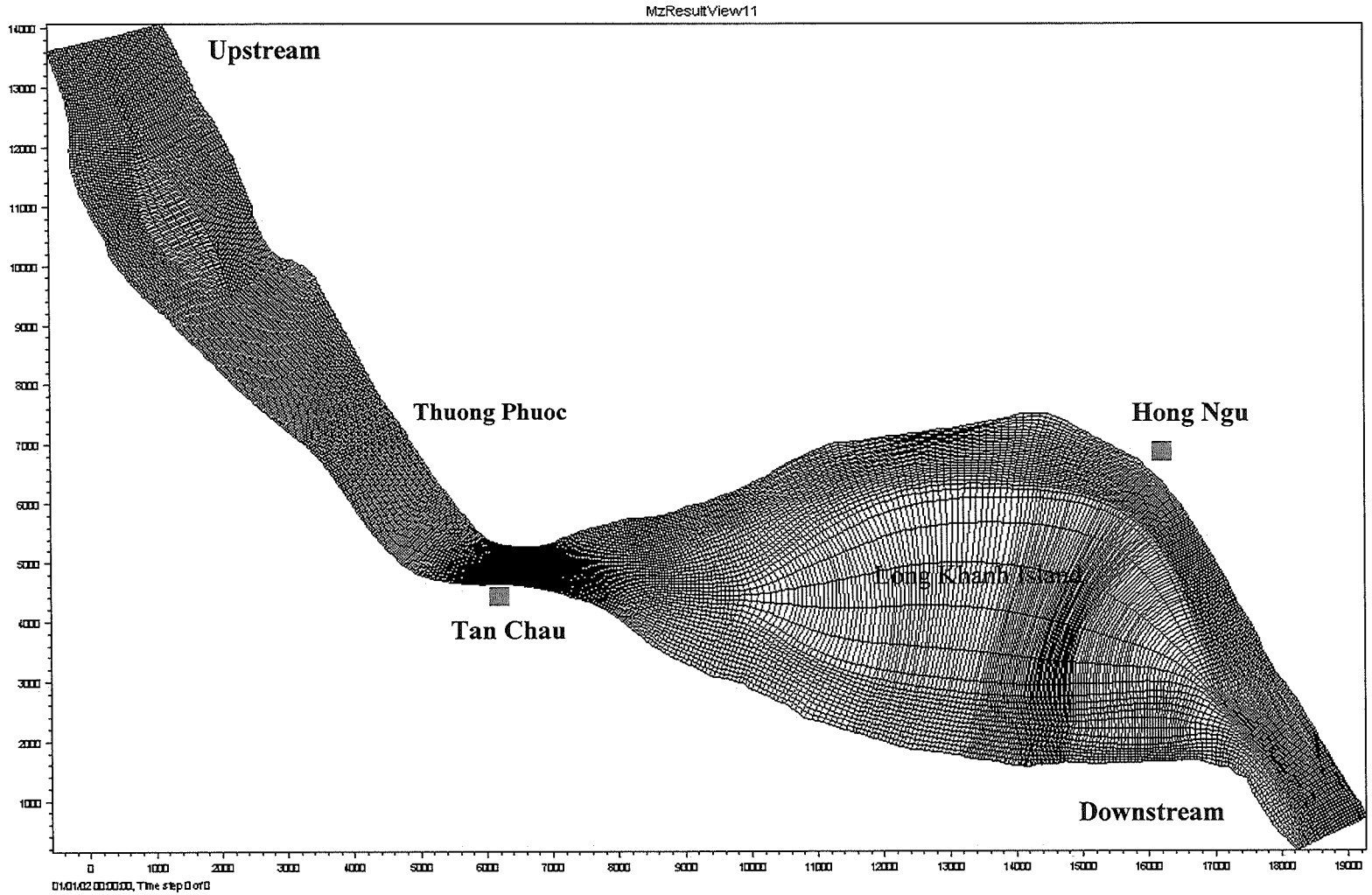

Figure 5.2 The grid of simulation base on the riverbank line of 2002.

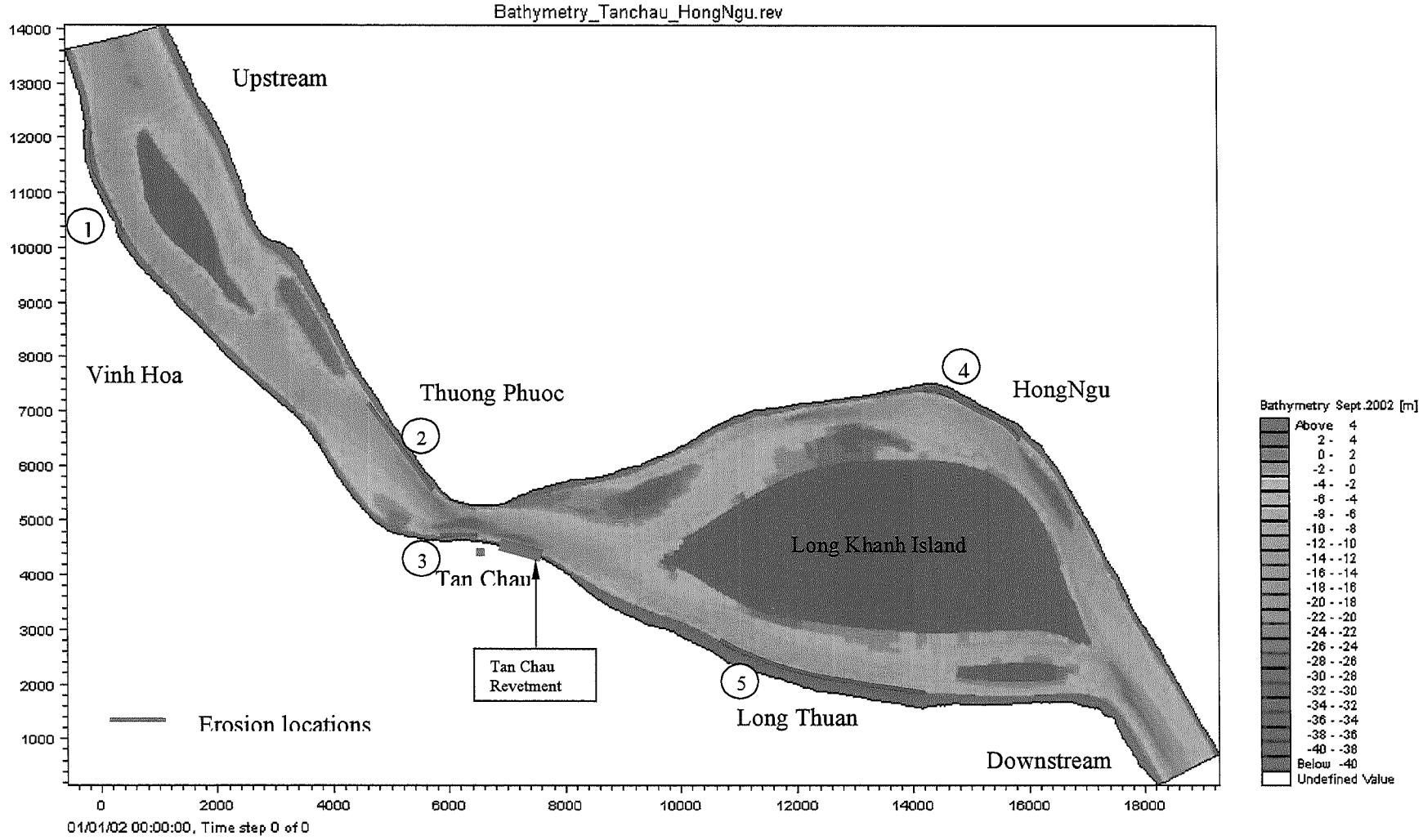

Figure 5.3 The bathymetry, location of bank erosions of simulation based on topography September 2002.

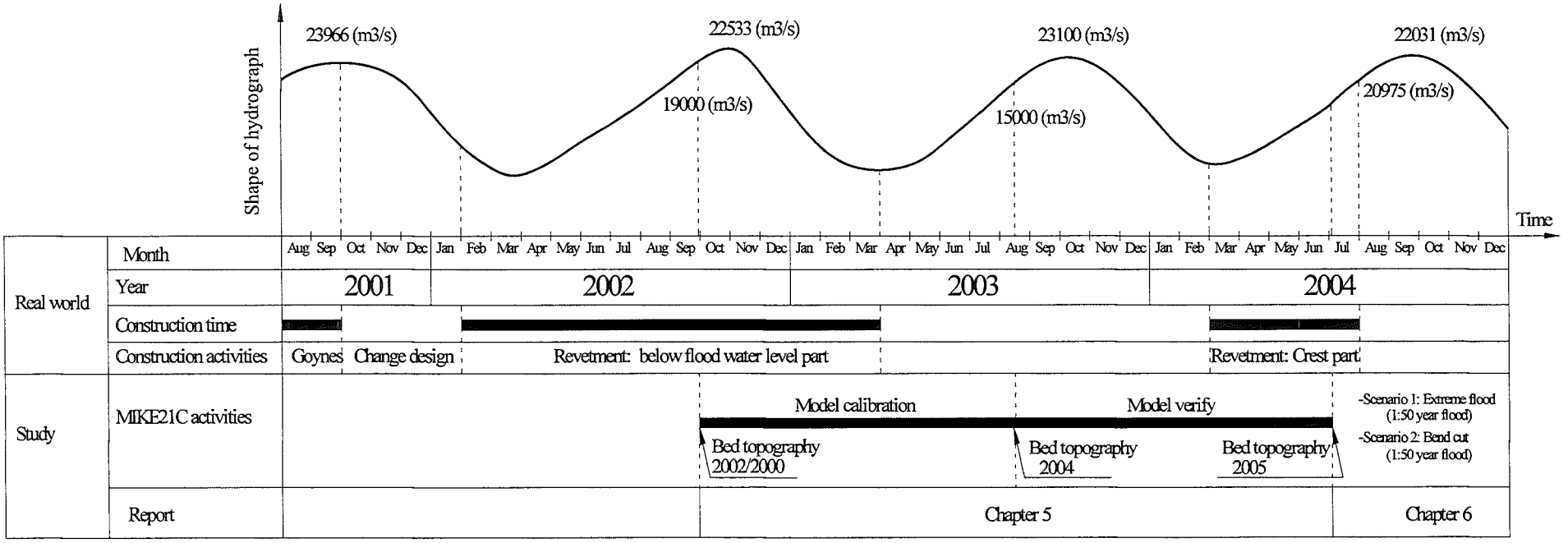

Figure 5.4 The schematization of activities for Tan Chau area.

5.3 Model description

5.3.1 Governing flow equations

MIKE21C used the simplification of Navier-Stokes equations into two-dimension equations of conservation of momentum and mass in two horizontal directions n and s as shown in figure 5.5 below. The secondary flow is introduced by three – dimension in the separate part of flow module in MIKE 21C, under the assumption of similarity of the vertical distribution of the flow velocities.

In Fig 5.5, at a particular point, the flow parameter is denoted by P (mass fluxes in the direction of s) and Q is mass fluxes in the direction of n, and the flow depth H at one computation point.

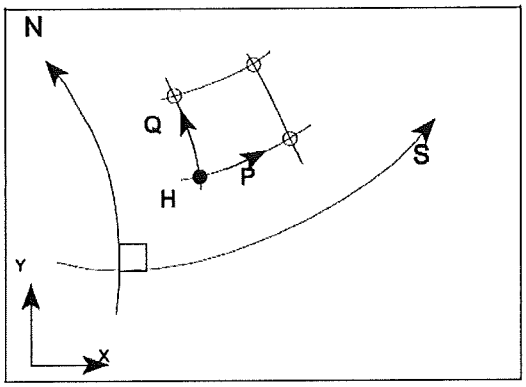

Figure 5.5 Location of flow parameters: Fluxes P and Q, and flow depth H in the curvilinear coordinate system (s,n) in comparison with Cartesian coordinate (x,y)

The equations solved in the curvilinear hydrodynamic model are:

$$\frac{\partial p}{\partial t}+\frac{\partial}{\partial s}\left(\frac{p^2}{h}\right)+\frac{\partial}{\partial n}\left(\frac{pq}{h}\right)-2\frac{pq}{hR_n}+\frac{p^2-q^2}{hR_s}+gh\frac{\partial H}{\partial s}+\frac{g}{C^2}\frac{p\sqrt{p^2+q^2}}{h^2}=RHS \qquad (5\text{-}1)$$

$$\frac{\partial p}{\partial t}+\frac{\partial}{\partial s}\left(\frac{pq}{h}\right)+\frac{\partial}{\partial n}\left(\frac{q^2}{h}\right)+2\frac{pq}{hR_s}-\frac{q^2-p^2}{hR_n}+gh\frac{\partial H}{\partial s}+\frac{g}{C^2}\frac{q\sqrt{p^2+q^2}}{h^2}=RHS \qquad (5\text{-}2)$$

$$\frac{\partial H}{\partial t}+\frac{\partial p}{\partial s}+\frac{\partial q}{\partial n}-\frac{q}{R_s}+\frac{p}{R_n}=0 \qquad (5\text{-}3)$$

Where:

s, n Co-ordinates in the curvilinear co-ordinate system.
p,q mass fluxes in the s – and n direction, respectively
H Water level
h Water depth
g Acceleration of gravity
C Chezy roughness coefficient
Rs, Rn Radius of curvature of s and n-line, respectively
RHS the right hand side in the force balance, which contains (among, others) Reynolds stresses (see below), Coriolis force and atmospheric pressure.

The Reynolds stresses, included in the RHS terms, can be described in a curvilinear grid assuming a smooth grid (Rs and Rn large and slowly varying). For the p – direction:

$$\frac{\partial}{\partial x}\left(E\frac{\partial p}{\partial x}\right)+\frac{\partial}{\partial y}\left(E\frac{\partial p}{\partial y}\right)=\frac{\partial}{\partial s}\left(E\frac{\partial p}{\partial s}\right)+\frac{\partial}{\partial n}\left(E\frac{\partial p}{\partial n}\right)-\frac{2E}{R_s}\frac{\partial q}{\partial s}-\frac{\partial E}{\partial s}\frac{q}{R_s}-\frac{2E}{R_n}\frac{\partial q}{\partial n}-\frac{\partial E}{\partial n}\frac{q}{R_n} \quad (5\text{-}4)$$

(P, Q) are fluxes described in a Cartesian (x,y) system and (p,q) are fluxes described in curvilinear
(s,n) co-ordinate system. A similar equation is found for the q-direction:

$$\frac{\partial}{\partial x}\left(E\frac{\partial Q}{\partial x}\right)+\frac{\partial}{\partial y}\left(E\frac{\partial Q}{\partial y}\right)=\frac{\partial}{\partial s}\left(E\frac{\partial q}{\partial s}\right)+\frac{\partial}{\partial n}\left(E\frac{\partial q}{\partial n}\right)+\frac{2E}{R_s}\frac{\partial q}{\partial s}+\frac{\partial E}{\partial s}\frac{p}{R_s}+\frac{2E}{R_n}\frac{\partial q}{\partial n}+\frac{\partial E}{\partial n}\frac{p}{R_n} \quad (5\text{-}5)$$

The curvature of the co-ordinate lines gives rise to additional terms in the partial differential equation for flow. The equations are solved by an finite difference technique with variable (water flux density P and Q in two horizontal direction and water depth H) defined on a space staggered computation grid, as shown in Fig 5.5

In Fig 5.6, the helical flow describes the physical flow insight of water motion in the bend. When the water flows into a river bend, an imbalance of centripetal force starts to generate and outward motion near the free surface and an inward motion near the bed. The reason is that the main stream velocities in the upper part of the flow are greater than lower part of the flow. Therefore, water particles in the upper part of water column must follow a part with a lager radius of curvature than water particles in the lower part to maintain nearly constant centripetal force over the depth. With the velocity v and radius of curvature R, centripetal acceleration is v^2/R.

Simultaneously with generation of helical motion, a lateral free surface slope is created to maintain the equilibrium between lateral pressure force, centripetal force and lateral shear force from friction along the river bed. This spiral (or helical or second) flow pattern can be considered as the sum of main flow and circulation in a plane perpendicular to the main flow direction. The secondary flow is directed towards the centre of curvature near the bottom and outwards in the upper part of the cross-section as illustrated in Fig 5.6.

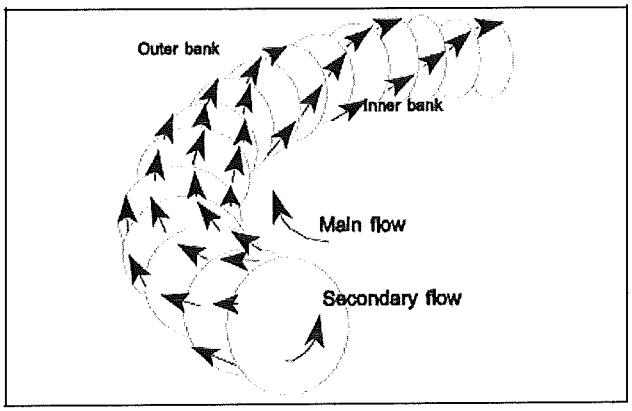

Figure 5.6 The helical flow in the bend

The intensity of the helical flow is the magnitude of the transverse velocity component. It is defined below by equations

$$i_s = u.\frac{h}{R_s} \qquad (5\text{-}6)$$

where
u main flow velocity
R_s radius of curvature of streamlines
i_s helical flow intensity
h, the average water depth in bend

5.3.2 The sediment transport equations

5.3.2.1 Suspended load transport

The partial differential equation that governs the transport of suspended load sediment by convection and turbulent diffusion is:

$$\frac{\partial c}{\partial t} + u\frac{\partial c}{\partial s} + v\frac{\partial c}{\partial n} + w\frac{\partial c}{\partial z} = w_s\frac{\partial c}{\partial z} + \frac{\partial}{\partial s}(\varepsilon\frac{\partial c}{\partial s}) + \frac{\partial}{\partial n}(\varepsilon\frac{\partial c}{\partial n}) + \frac{\partial}{\partial z}(\varepsilon\frac{\partial c}{\partial z}) \qquad (5\text{-}7)$$

where
z vertical co-ordinate
c Concentration of suspended sediment
ε turbulent diffusion coefficient
w_s fall velocity of sediment particles in suspension
u,v,w, flow velocity in s,n,z direction, respectively.

5.3.2.2 Bed load transport

In contrast to the suspended load, it is assumed that the bed load responds immediately to changes in local hydraulic conditions. Thus, there is no need for advection-dispersion modeling in connection with bed load. However, two effects must be taken into account:
1. The deviation of the direction of the bed shear stress from the mean flow direction due to helical flow; and
2. The effect of a sloping river bed.

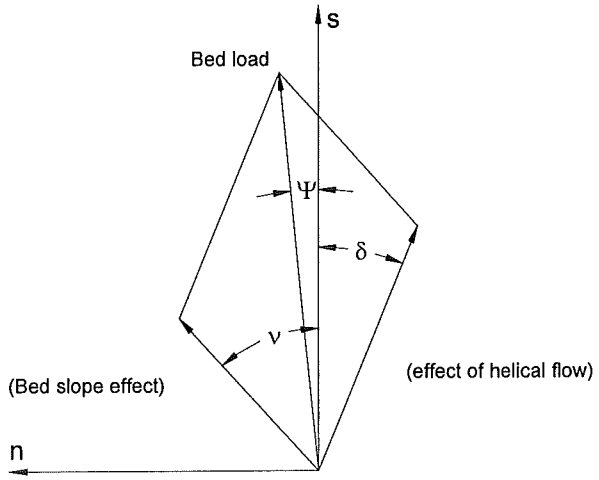

Figure 5.7 Direction of bed load transport influenced by helical flow and transverse slope

The effect of helical flow needs the separate helical flow module as mention above. The bed slope influences the sediment transport rate and direction
In Mike21C, the bed load transport is divided into several components, one is S_n across the stream line was determined in below equation:

$$S_n = \left(\tan \delta_s - G.\theta^{-a}.\frac{\partial z^*}{\partial n} \right) s_{bl}$$

where:
G - transverse slope coefficient
a - transverse slope power differ somewhat the various authors.
$\tan\delta_s$ - the helical flow strength
θ -Shields parameter

$$\frac{\partial z^*}{\partial n} = \frac{\partial z}{\partial y}\cos\phi - \frac{\partial z}{\partial y}\sin\phi$$

z^* Bed level at the centre point in the numerical scheme
n, The horizontal co-ordinate in the transverse direction
x, y, co-ordinate system.
ϕ - The angle between direction and the x-axis.

The other is the bed load transport along the streamline is given as:

$$S_s = \left(1 - e.\frac{\partial z^*}{\partial s} \right) s_{bl}$$

where e is longitudinal slope coefficient
From the experiences and laboratory test, these parameters below are some suggestions:

- Engelund-Fredsoe: G=0.625, a=0.5
- Kikkawa: G = 0.6
- Bendegom: G=0.667, a=1.
- Struiksma: G=0.588, a=0.5 or G=1.176, a=0.5

5.3.2.3 Sediment continuity equation

The sediment continuity equation compute the bed material (bed load and suspended load), the bed level change can be computed from the equation:

$$(1-n)\frac{\partial z}{\partial t} + \frac{\partial S_x}{\partial x} + \frac{\partial S_y}{\partial y} = \Delta S_e \qquad (5\text{-}8)$$

Where
S_x Total sediment transport in s-direction
S_y Total sediment transport in n-direction
n bed porosity
z bed level
t time
(x,y) the Cartesian co-ordinate system
ΔS_e Lateral sediment supply from bank erosion.
For the curvilinear co-ordinate is slightly difference with (5-8)

The total sediment transport is the sum of bed load and suspended load. For a curvilinear (s, n) grid, Eq (5-8) is slightly different due to curving gird lines. This is handle numerically by using different Δs and Δn at inflow and outflow boundaries to each grid cell, see figure 5.8

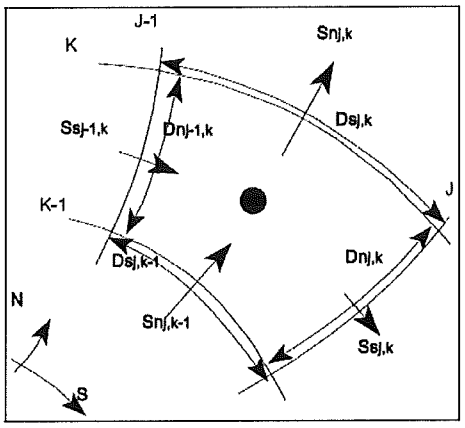

Figure 5.8 Sediment continuity equation defined in curvilinear grid

A space centre – time forwarded difference scheme is applied. The time step is limited by the courant criterion, i.e. that Courant number should be less than 1. The wave celerity number can be estimate by considering the one –dimensional version of Eq (5-8)

$$\frac{\partial z}{\partial t}+\frac{\partial S}{\partial x}=\frac{\partial z}{\partial t}+\frac{\partial S}{\partial z}*\frac{\partial z}{\partial x}=0 \qquad (5\text{-}9)$$

by assuming $dh/dt = -dz/dt$ and that sediment transport is a function of Shields stress (θ) only, the celerity c_{bw} of bed form waves is found to be:

$$c_{bw}=\frac{\partial S}{\partial z}=-\frac{\partial S}{\partial h}=\frac{\partial z}{\partial t}=\frac{\partial S}{\partial \theta}*\frac{\partial \theta}{\partial h} \qquad (5\text{-}10)$$

see page 59

If the Chezy number is assumed constant, then θ is inversely proportional to h^2, i.e. $d\theta/dh = -2\theta/h$. For the transport formula of the Engelund and Hansen Formula, we get:

$$c_{bw}=\frac{2{,}5S}{\theta}*\frac{2\theta}{h}=5\frac{S}{h} \qquad (5\text{-}11)$$

Where

S Sediment transport rate
h Water depth
c_{bw} Roughly estimated bed form celerity

Based on the notations shown in figure 5.9, the continuity equation for the sediment in a curvilinear grid can be expressed by the following difference equation:

$$(1-n)\frac{z_{j.k}^{n+1}-z.j.k^{n}}{\Delta t}+\frac{Ss_{j.k}\Delta n_{j.k}-Ss_{j-1.k}\Delta n_{j-1.k}+Sn_{j.k}\Delta s_{j.k}-Sn_{j.k-1}\Delta s_{j.k-1}}{0.25(\Delta s_{j.k}+\Delta s_{j.k-1})(\Delta n_{j.k}+\Delta n_{j-lk})} \qquad (5\text{-}12)$$

Where:

Ss	Sediment transport rate in *s*-direction
Sn	Sediment transport rate in *n* – direction
n	Bed porosity
t	Time
(s,n)	Curvilinear co-ordinates
Δs	Space step in s- direction
Δn	Space step in n- direction
(j,k)	Grid co-ordinates

To close the system a boundary condition is required at the upstream boundary. Two options are possible: specification of the rate of the bed level change (dz/dt), or simply the transport rate (*S*) into the system.

Theoretically, only upstream sediment transport boundary conditions are required. However, as the model allows change in the flow direction during a simulation, the sediment transport is specified at all boundaries. Each specific boundary condition becomes active only during inflow into the model domain.

5.3.3 Bank erosion equations

The bank erosion is computed by MIKE21C in the following expression:

$$E = -\alpha \frac{\partial z}{\partial t} + \beta \frac{q_s}{h} + \gamma \qquad (5\text{-}13)$$

where the parameters α,β,γ can be specified for each eroding bank.
The first term stems from the link between scour and bank erosion. This means that the bank erosion and scour are directly proportional. The value α is theoretically the transverse slope (1: α), but it should be calibrated for the particular application.
The second term expresses that a certain fraction (β) of sediment transport capacity is used for the transporting the material eroded from a bank.
The third term (γ) is simply constant bank erosion rates (m/s), that means the bank erosion can be from other causes. In other words, bank erosion is not influence due to flow, and sediment transport in front of eroded bank. In figure 5.3, there are five locations of bank erosion, however there is only one riverbank erosion (number 4 – at Hong Ngu town) was used in the simulation. We used river bank number 4 to check the sensitive of three parameters: α,β and γ coefficient as the early state of riverbank erosion prediction by mathematical modelling.

5.4 Schematization

Because of vast the computational area, the boundary had to be simulated from one dimension model (MIKE11). This model was also calibrated and validated. The more details are reported in appendix A3, MIKE11.
In figure below, the one-dimensional model is included two-dimensional model area.

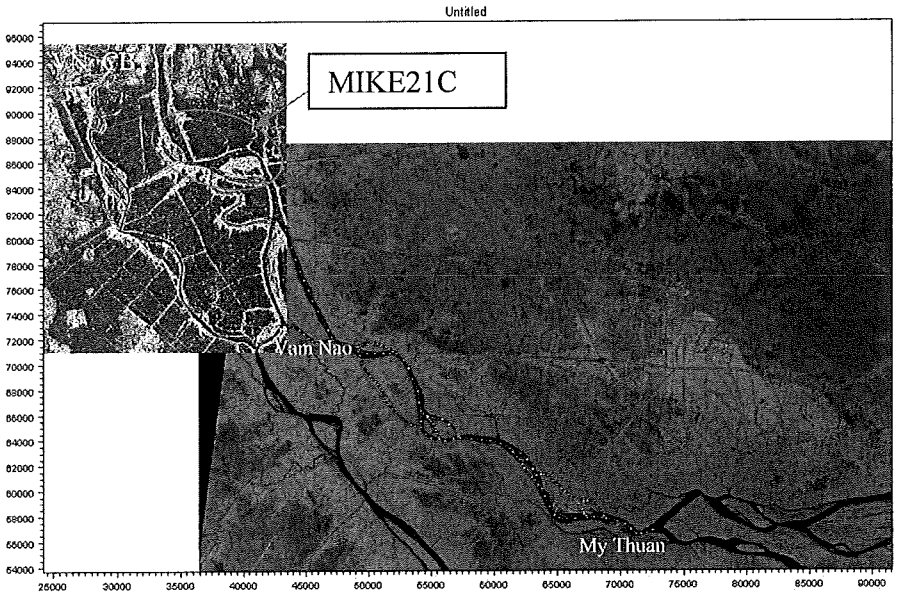

Figure 5.9 Area of computational in MIKE11 and MIKE21C

The computation time schedule based on the available data is described in figure 5.10. In this figure, the simulation of MIKE11 is longer than MIKE21C because of available data at the boundary condition. Moreover, the bed topography surveyed for this wide area is only found in the year 1996, and updated in the year 2003 at some small branches.

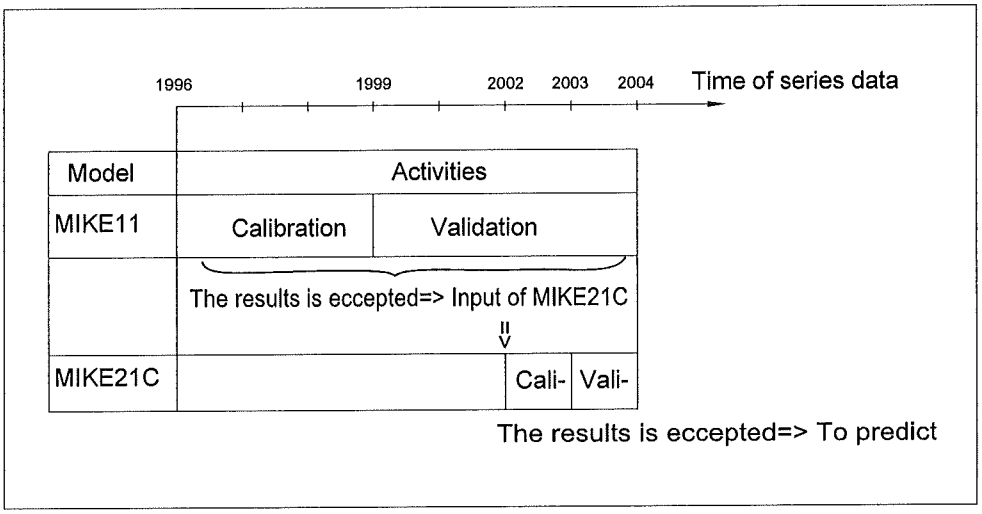

Figure 5.10 Time and activities of simulation

5.5 Initial condition and boundary conditions

5.5.1 Initial condition

An initial state was established before the fully computation of hydrodynamic and morphology process. This step checked whether flood wave, and hydrodynamic condition is available for computation or not.

The topography is from survey data at 29th September, 2002. The end of this simulation is 14 August, 2003.

The upstream boundary discharge is equal to maximum discharge in the simulation period. Q_{max}= 22200m^3/s at 18^{h}00 30th September, 2002.

Correspond to the maximum discharge, the water level in downstream is at the same time found WL=3.95m (amsl).
The result is a hot-start simulation, and after check all the results is stability, the next step is to calibrate the model.

5.5.2 Boundary conditions

The boundaries condition were determined from MIKE11, the results of MIKE11 is shown in the appendix A3. MIKE 11.
In the table below, the boundary conditions are reported.

Terms	Chainage from the sea (km)	Boundaries	Time
Upstream	248 (Vietnam –Cambodian frontier at Km250)	hourly discharge	From 29th September 2002 to 14th August 2003
Downstream	218 (Hong Ngu town)	hourly water level	From 29th September 2002 to 14th August 2003
Upstream	248	hourly sediment discharge (m^3/s)	From 29th September 2002 to 14th August 2003
Downstream	218	hourly sediment discharge (m3/s)	From 29th September 2002 to 14th August 2003

Table 5.3 The boundary conditions of model

The discharges, water level and sediment transport boundaries are determined by using MIKE11(the more detailed see appendix A3. MIKE 11).

5.6 Model calibration

5.6.1 Hydraulics

5.6.1.1 Eddy viscosity coefficient

In MIKE21C, the flow equations for the flow in the longitudinal, s, and the transverse direction, n, expressed:

$$u\frac{\partial u}{\partial s}+v\frac{\partial u}{\partial n}+w\frac{\partial u}{\partial z}+\frac{uv}{R}+\frac{1}{\rho}\frac{\partial P}{\partial s}=\frac{\partial}{\partial z}\left(E\frac{\partial u}{\partial z}\right)$$

$$u\frac{\partial v}{\partial s}+v\frac{\partial v}{\partial n}+w\frac{\partial v}{\partial z}-\frac{u^2}{R}+\frac{1}{\rho}\frac{\partial P}{\partial s}=\frac{\partial}{\partial z}\left(E\frac{\partial v}{\partial z}\right)$$

(5-10)

see page 56

where

ρ	Density of water
u	Velocity in longitudinal flow direction
v	Velocity in transverse flow direction
w	Velocity in vertical direction
P	Pressure
s	Co-ordinate in stream wise direction
n	Co-ordinate in transverse direction
z	Vertical co-ordinate
R	Radius of curvature of the main streamline
E	Turbulent (eddy) viscosity coefficient

Because the computational area is wide where includes the bend, bifurcation, confluence, and island, so that eddy viscosity is took an important parameter in the results of model.
Base on the data of velocity survey by ADCP in the area, the eddy was calibrated at some cross-section, the results are listed in figure 5.11 a,b,c.

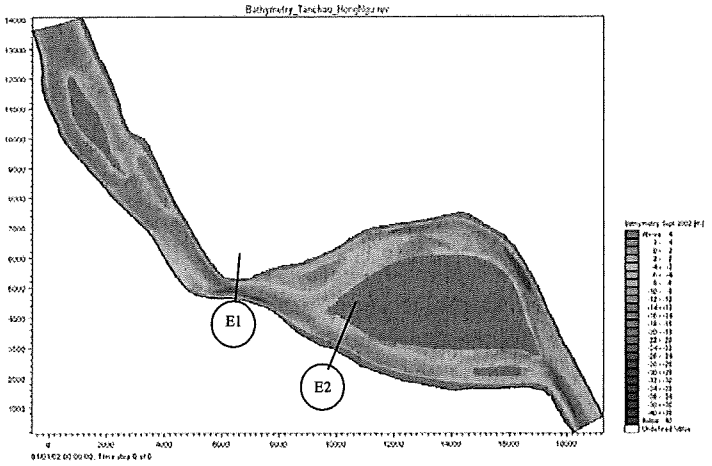

Figure 5.11a The location of cross-section calibrate the velocity distribution

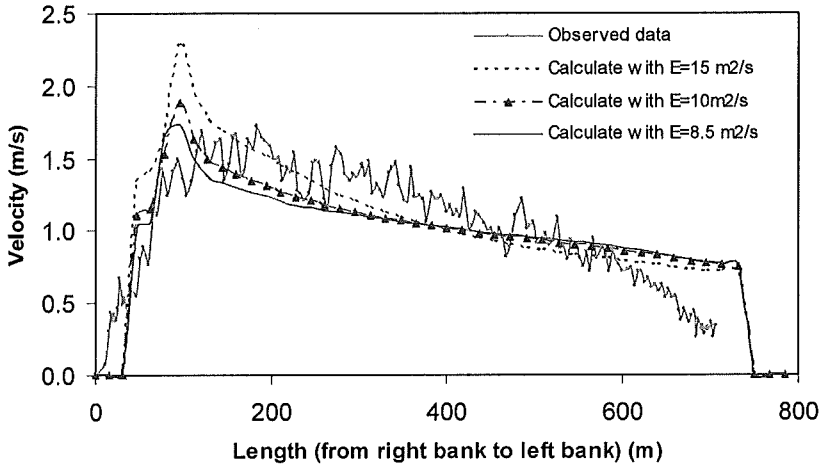

Figure 5.11b The velocity distribution of cross-section E1 (correspond grid cells J=288, K=0-45) in different eddy viscosity coefficient.

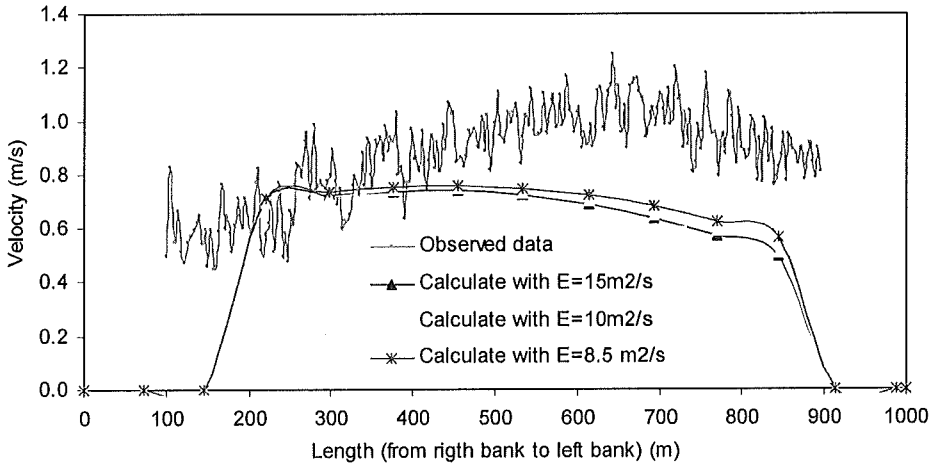

Figure 5.11c The velocity distribution of cross-section E2 (correspondence to grid cells J=369, K=0-14) in different eddy viscosity coefficient.

The results in the figure 5.11. a), b), c) reported that the different eddy viscosity affected to the velocity distribution. The cross-section E2 in figure 5.11.c, there are some errors, it may be the influence due to the bifurcation. However, the eddy viscosity is affected by the topography and the intensity of turbulent of water body. It is very difficult to find the good results. Above result is reasonable for the eddy viscosity coefficient E=8.5m^2/s.
The model chose E=8.5m2/s as a constant value for the computational area.

5.6.1.2 Roughness coefficient and bed form.

The Chezy coefficient is chosen for this simulation. The constant value for the entire area is used because of vast area, and because the topography changed rapidly between riverbank and main channel. The value is estimated based on the Engelund-Hansen(1967) predictor formula, and Van Rijn (1984) predictor formula (see appendix A4).Bed form and roughness. However, the comparing between the computed water level, discharge and observed data, the reasonable Roughness coefficient is found.

By using the Engelung-Hansen (1967) the Chezy coefficient found is 94.2 $m^{1/2}$/s and by applying Van Rijn (1984), the Chezy coefficient found is 83.9 $m^{1/2}$/s, more detail see appendix A4.
The different can be understand that, according to Van Rijn method, the roughness depends mainly on three parameters, the bed form height, the bed-form steepness and the bed-form shape, and most of case use Van Rijn when the bed form is dunes. However, in this case,T parameter is lager than ten, so that the ripple vanish is the state of bedform.

Nevertheless, the roughness coefficient is much more complicate, it is not the constant value as the assuming above but it depend on the time, space itself. In such complicated parameters, to simplify the model by calibrate the water levels, and discharge with many roughness coefficient, and the reasonable roughness coefficient is found C=90 $m^{1/2}$/s. This value was used for initial state of hydraulic calibration, but it depends on the result, the roughness coefficient could be found from next step.
The result between them are shown in water level and discharges calibration below

5.6.1.3. Water level calibration.

The water level observed station is showed in figure 5.12a) below.
By changing the Chezy roughness coefficient, the water affected in the table below.

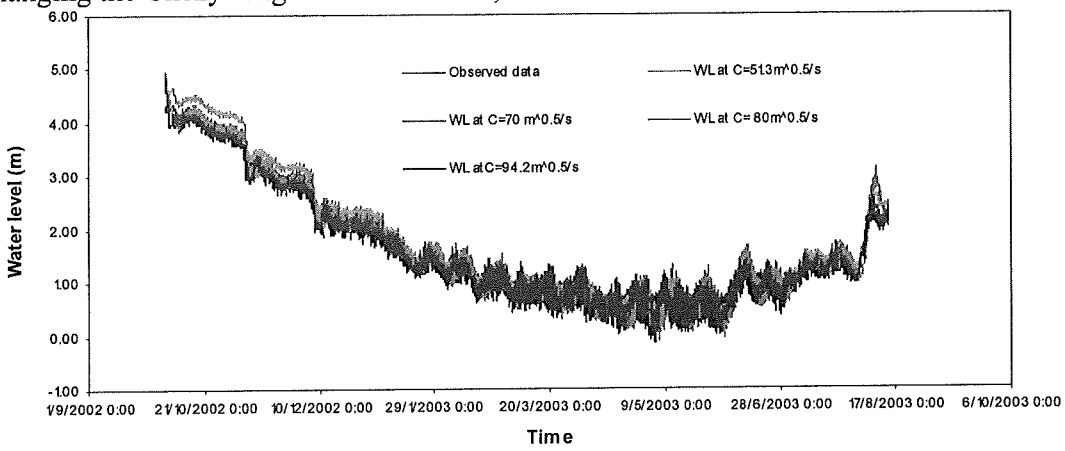

Figure 5.12a Water level calibration from 4th October,2002 to 14th August,2003 at Tan Chau station

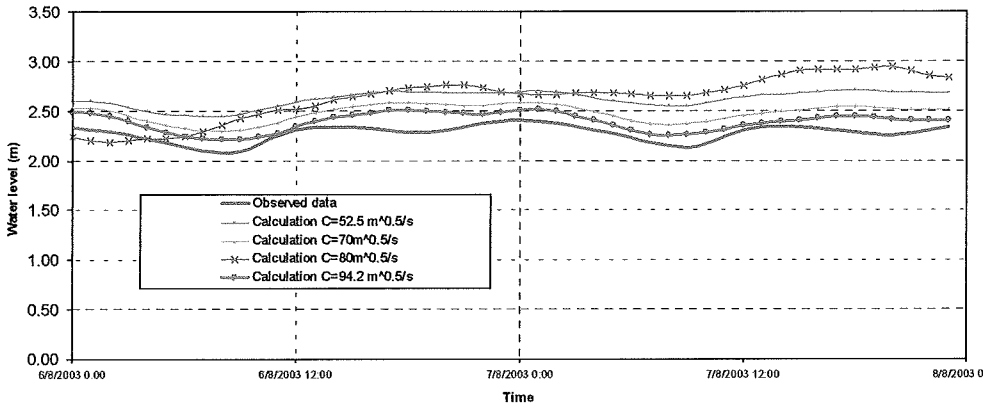

Figure 5.12b Water level calibration from 6th August 2003 to 7st August,2003 at Tan Chau station.

5.6.1.4 Discharge calibration

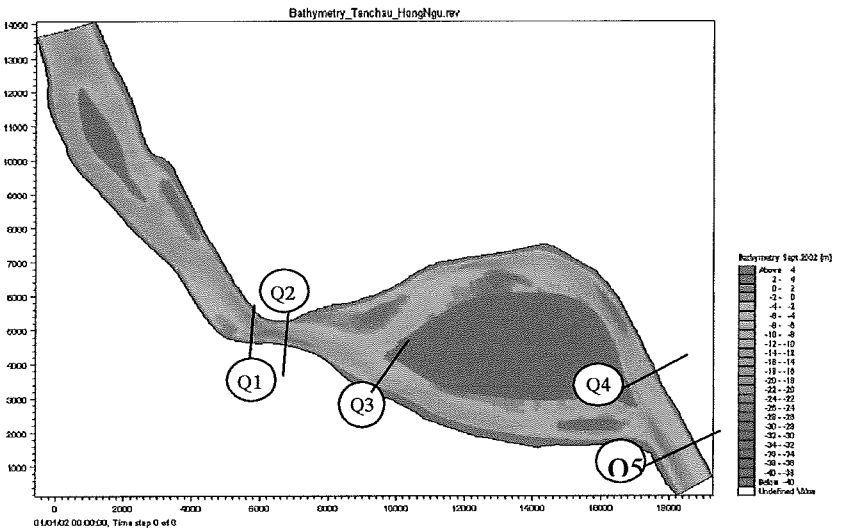

Figure 5.13 Location of discharge observation

Cross-section	Time observed discharge	Discharge (m^3/s)				
		Observed	Calculation, C=51.3 ($m^{1/2}/s$)	Calculation, C=55 ($m^{1/2}/s$)	Calculation, C=49 & C=56 $m^{1/2}/s$	Calculation, C=90$m^{1/2}/s$
Q1	9h05' 6th, August 2003	14260	11415	11356	11457.5	10903
Q2	8h40' 6th,August 2003	14148	11355	11326	11367	11286.6
Q3	9h14' 7th, August 2003	6370	6357	6524	6334	7168
Q4	16h47' 7th,August 2003	6957	7266	7496	7270	8186
Q5	17h05' 7th, August 2003	13593	13741	14030	13527	15753

Table 5.4 The discharge calibration

5.6.2 Sediment transport

The sediment transport data is not available in the lower Mekong river. The relationship between discharge and observed suspended load has been established. In this relationship should takes into consideration of wash load influence. The suggestion takes into computation with only 50% of amount sediment from relationship is suspended load for MIKE21C simulation (see the appendix A.1, available data, that relationship were reported).

Based on the Engelund and Hansen (1967) and Van Rijn (1984), the sediment transport in the Tan Chau area were determined (see appendix A.4). The results show in table 5.5 below, it seems that the Engelund and Hansen (1967) has more reasonable than Van Rijn (1984).

However, lack of observed data, strong influence of wash load, those thing make the calibration of the sediment transport becomes more complex and difficult task in this study. In other words, which theory is suitable for lower Mekong would be checked carefully.

Basically, the sediment transport is proportion with velocity in below equation:

$$S=m.u^n$$

Where

m - parameter depend on bed material characteristic(e.g the grain size, density, porosity)

n- parameter depend on the theory (n=3-5)

Using Engelund-Hansen n=5 and Van Rijn n=4.

From the observed data is available in 1998 at cross-section Tan Chau with the same time measurement, the velocity and the total load has been checked below.

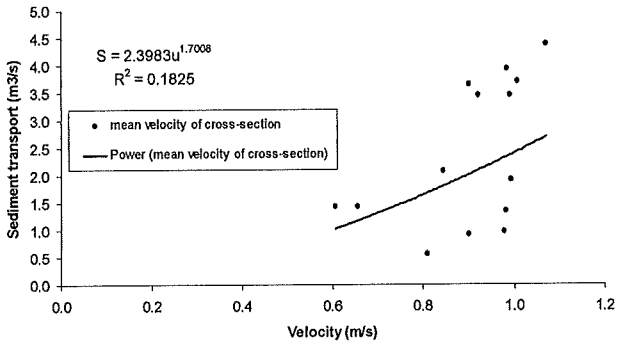

Figure 5.14 The relationship between velocity and sediment transport at Tan Chau,1998

Herein fig 5.14 the most important value is n≈1.7 <<3 (theory index should be larger than three). Let assuming the survey data is correct, what can be causes by that different. The only remaining answer is by wash load impact.

Moreover, the suspended load taken into account as the certain mainly impacts in lower Mekong with 72 percent and only 28 percent of bed load should take into simulation (see appendix A-4).

The results of MIKE21C were compared with the suspended load, which were derived from above relationship. After comparing, the results of MIKE21C were smaller than 28 times.

The results show in table 5.5 and figure 5.15 below:

Methods	Bed load (m3/s)	Suspended load (m3/s)	Sediment transport (m3/s)	Note
Data from relation	-	**1.030**	-	mean value
Van Rijn (1984)	0.0880	0.1270	0.2150	
Engelund – Hansen (1967)	-	-	0.7920	
MIKE21C – Used Van Rijn	0.0022	0.0026	0.0048	mean value
MIKE21C –Used Engelund – Hansen	0.0050	0.0360	0.0410	mean value

Table 5.5 Sediment transport at Tan Chau cross-section

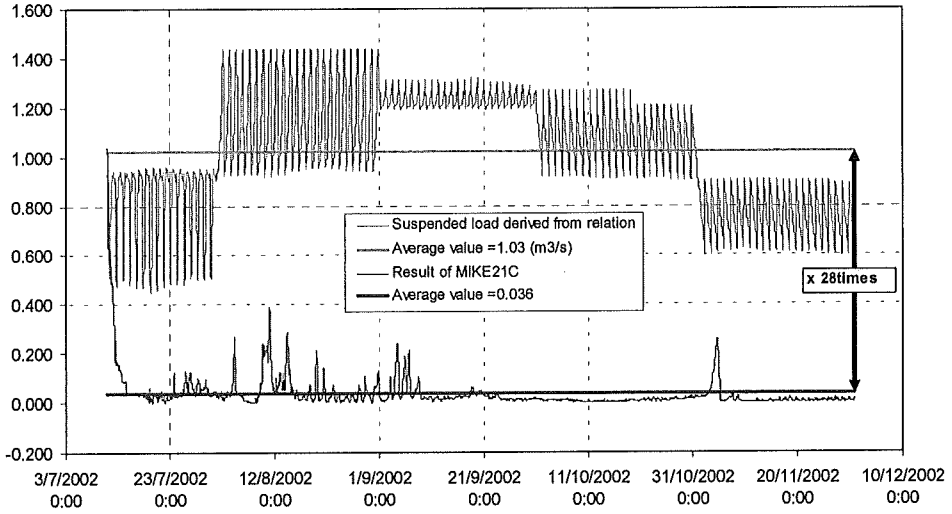

Figure 5.15 The suspended load from simulation and $Q \sim Q_{suspended}$ load relation at Tan Chau

According to the author's point of view, this result is very a strange. However, because of the lack of data, and wash load influence could be causes of this problem.

5.6.3 Morphology

Based on the hydraulic parameters and the sediment transport adjustment above, the morphology modulus have been simulated by changing three parameters: transverse slope coefficient, transverse slope power and longitudinal slope coefficient. These parameters affected to the morphology shows in part 5.3.2.2.

The morphology was calibrated by comparing between the observed topography data in 14thAusgust 2003, and the computational results from MIKE21C.

The results show in figure 5.17 a, b, c,d below with the parameters were found:

- Transverse slope coefficient=1.25
-Transverse slope power=0.5
- Longitudinal slope coefficient=5

The observed data from echo sounding combination with GPS and because of vast area, and the data depend on the vessel tracks shows in figure 5.16 the data of observed 2003, and the tracks of vessel, and the location of compare cross-section.

The bed topography verify in figure 5.17 a,b,c,d below is acceptable for calibration model
In order to verify the model, all above parameters should taken into account the verification parameters in the part below.

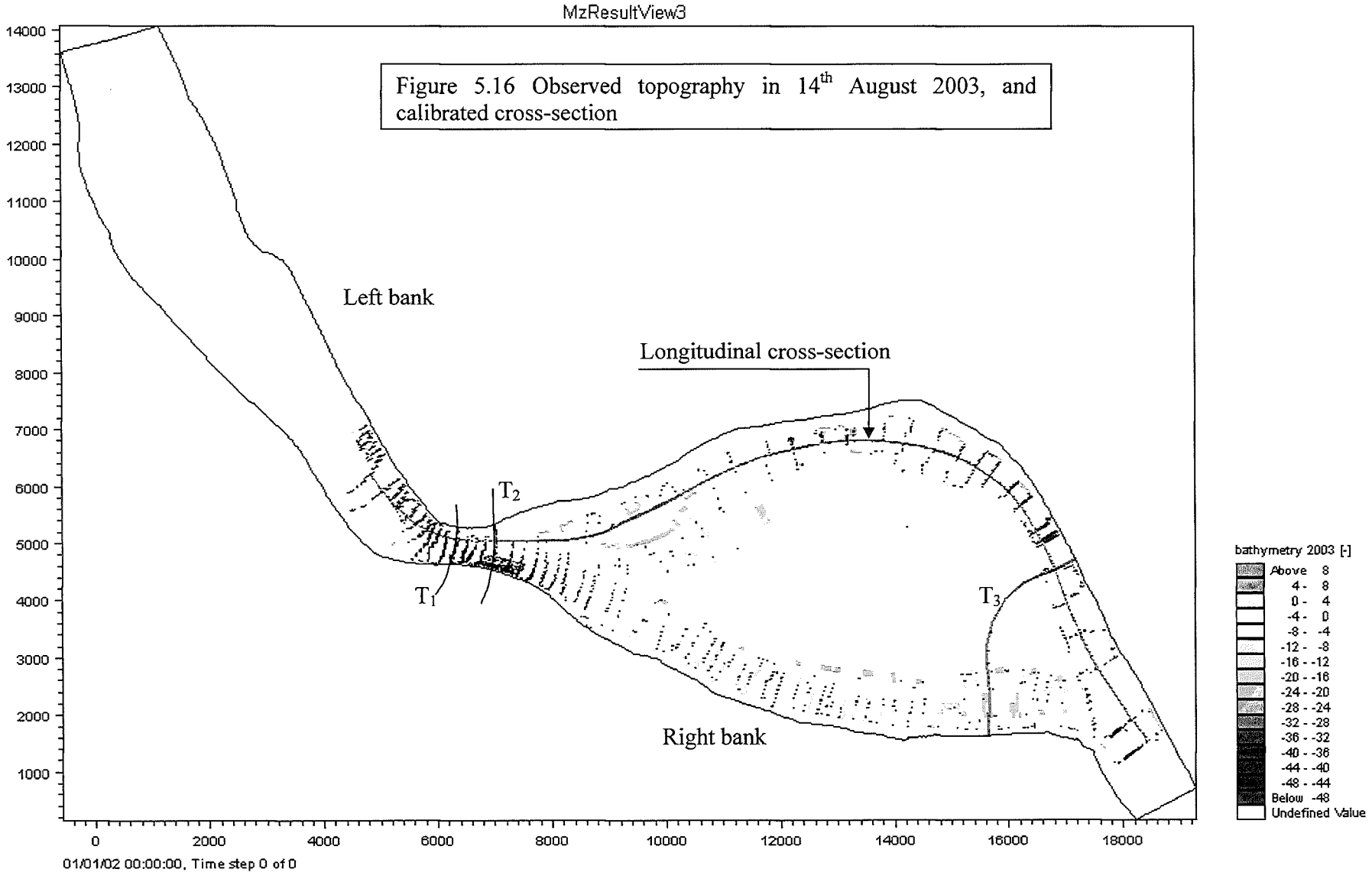

Figure 5.16 Observed topography in 14th August 2003, and calibrated cross-section

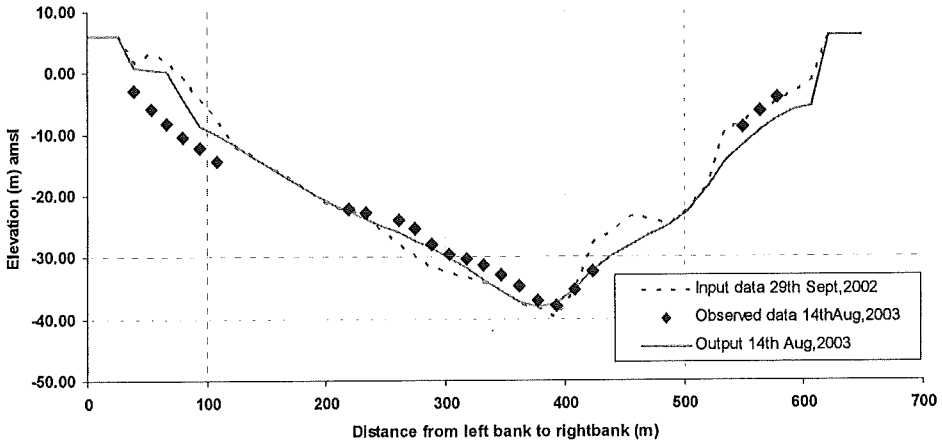

Figure 5.17a The bed comparison between observed data and MIKE21C results at cross-section T1 (from J=270, K=0-45, see fig 5.14)

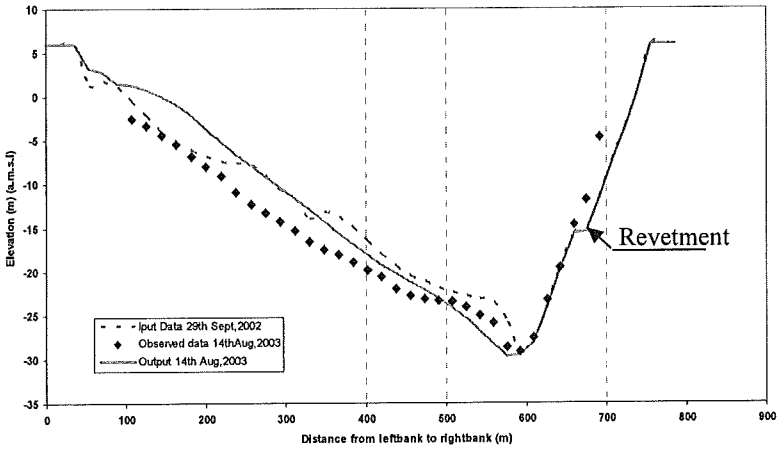

Figure 5.17b The bed comparison between observed data and MIKE21C results at cross-section T2 (from J=288, K=0-45, see fig 5.14), the cross-section at revetment

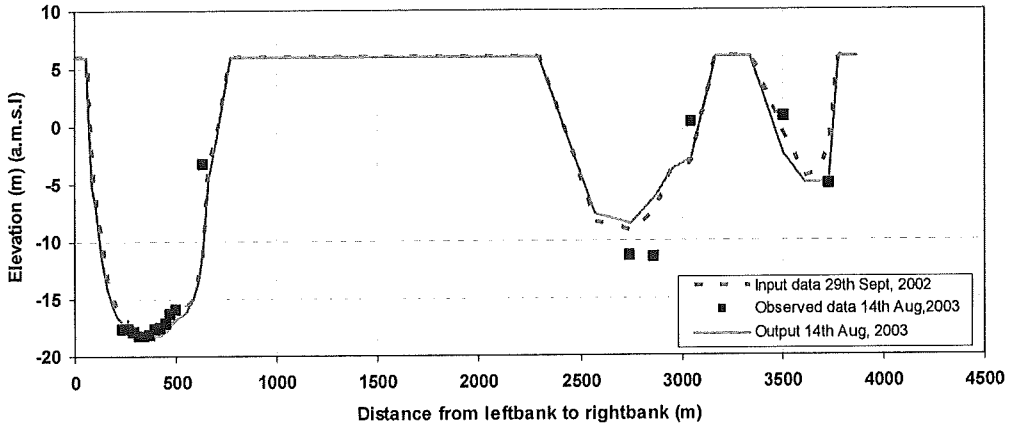

Figure 5.17c The bed comparison between observed data and MIKE21C results at cross-section T3 from (J=458, K=0-45, see fig 5.14)

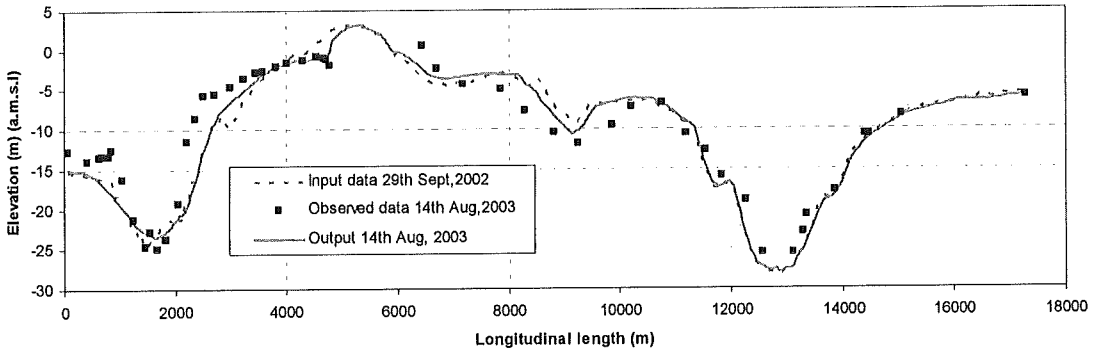

Figure 5.17d The bed comparison between observed data and MIKE21C results at longitudinal cross-section (J=225-503, K=30, see fig 5.14)

5.6.4 Bank erosion

As early state to simulate the riverbank erosion in this area, there are three calibration parameters taken into account they are α,β,γ (see eq 5-13 above). Those parameters were taken extremely important part in riverbank erosion model. However, the sensitive of those parameters and the influence to the results of simulation is still need to improve in this model. Although the area has 5 locations of riverbank erosion, but this study only simulate for one single bend erosion (number 4 in fig.5.3 above) at Hong Ngu town.

Previous study had done by Olesen and Tjerry (2002) at Chaktomuk Junction upstream of lower Mekong in Phnom Penh, Cambodia. This study suggested that $\beta = 0.3$ should take into simulation for this area.
The riverbank erosion from J=398 to J=442 at K=42 (land value) was determined in the model. The maximum erosion rates is approximately 0.1m/day (≈36.5m/year)

The results of sensitive of erosion parameters in the table blow.

Riverbank erosion	Calibration parameters				E (m/yr)
				h (m)	
J=398-443,K=43	10	0.3	0.1	1.5	44.43
J=398-443,K=44	0	0.3	0	1.5	6.50
J=398-443,K=45	5	0	0	1.5	0.00
J=398-443,K=45	0	0	0.1	1.5	36.50

Table 5.6 The result of river bank prediction by change the different parameters

The results of riverbank erosion in table 5.6 suggest that, it would be consider in the development this model. The influence of independent parameter γ in riverbank erosion process is dominant than the other parameters. It can be understand that, the sediment transport is so small near the bend Hong Ngu (J=398-443, K=43), and the bed level change at the grid in front of bend is not so much.(see more detail in part 5.5.3)

In conclusion, this model should not take into account the riverbank erosion modulus. In other words, the riverbank erosion could be studied based on the small scale of computational, which has fine grid cell and more detail bathymetry. However, by checking the sensitive of calibration parameters of riverbank erosion equation (5-13), the riverbank erosion can be computed by MIKE21C.

5.7 Model verification

The calibration process brings the adjustment parameters (e.g. roughness, eddy viscosity, sediment motivation factor, etc) for the model. At the end of calibration, the result from model is computed bathymetry at 14th August 2003. Then, the model has to verify against with the observed data in the year 2004(see Fig.5.5 for more detail information)

The bathymetry from computed at 14th August 2003 is used for verification process. The hydraulic boundary taken from MIKE11 model (see appendix A-3).
The calibration parameters were found in calibrating process should be keeps the same in verification model.
In table 5.7 shows the information of the conditions, parameters for the verification model.

A summary input condition of verify model in table below:

Terms & coefficients	Time & value of coefficient	Unit
Bathymetry	Result of calibration model at 14th August 2003	m
Grid	Grid base on bank line 2002 J x K=518x45 (J is the number of grid along river bank, and K is number of grid transverse)	cells
Upstream boundary From MIKE21C	1.Discharge from 14th august 2003 to 03rd July 2004 2.Sediment transport 14th august 2003 to 03rd July 2004 Results of model multiply with motivation factor (28times)	m^3/s m^3/s
Downstream boundary From MIKE21C	1. Water level from 14th august 2003 to 03rd July 2004 2.Sediment transport 14th august 2003 to 03rd July 2004 Results of model multiply with motivation factor (28times)	m m^3/s
Eddy viscosity	E=8.5	m^2/s
Chezy coefficient	C=90	$m^{1/2}/s$
Morphology	G=1.25 transverse slope coefficient a=0.5 transverse slope power (see part 5.3.2.2) e=5 longitudinal slope coefficient	

Table 5.7 Summary condition and factors of model verify

5.7.1 Water level

The water level was verified against with observed data at Tan Chau station in figure 5.18.

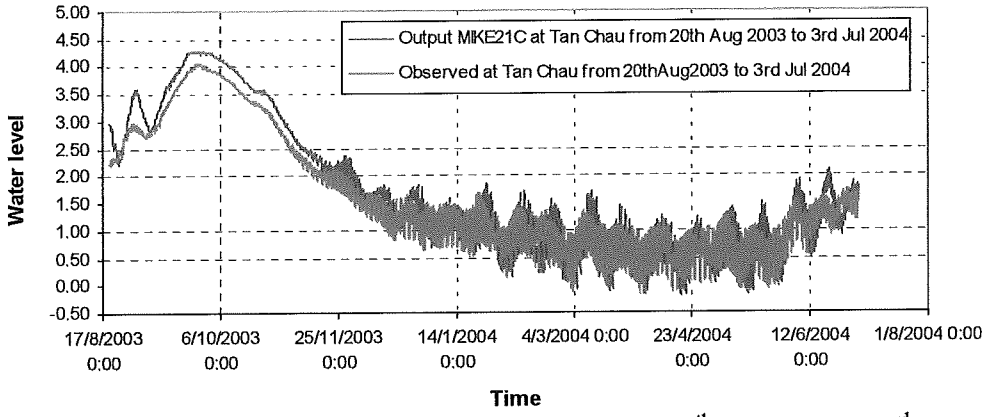

Figure 5.18 Water level verify at Tan Chau station from 20th Aug 2003 to 3rd Jul 2004

5.7.2 Discharge

The discharge distribution by ADCP surveyed is not available in this period of time. There is only one cross-section at Tan Chau revetment was checked the discharge at 14h18, 21st June 2004 shows in figure 5.19

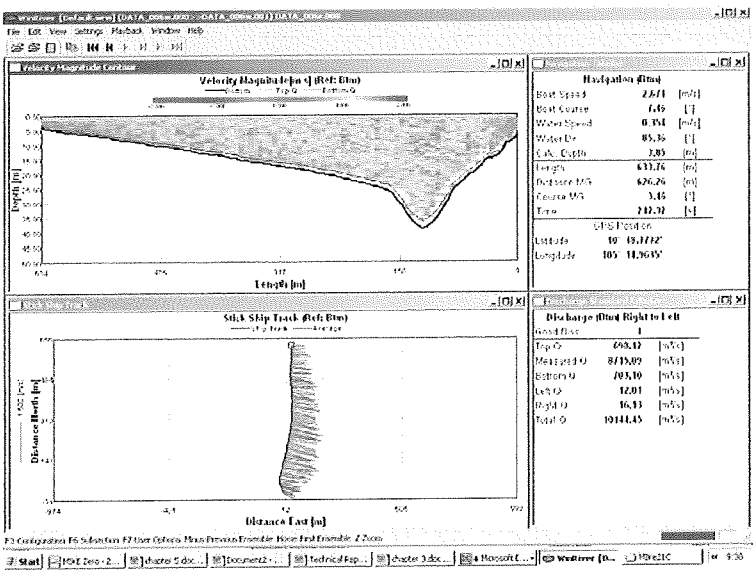

Figure 5.19 The discharge at Tan Chau revetment at 14h 18, 21st June 2004

The observed discharge is 10144m^3/s, and in comparison with results of MIKE21C the discharge at the same time is 9467 m^3/s. This result seems reasonable with the water level result above.

5.7.3 Morphology

Using the same location of cross-section and longitudinal cross-section in calibrate (see. fig 5.16). The results of verification models against with observed data show in figure 5.20 a,b,c,d below.

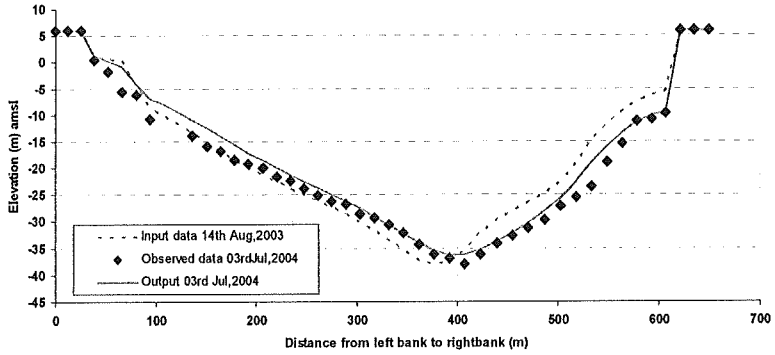

Figure 5.20a) The bed comparison between observed data and MIKE21C results at cross-section T1 (from J=270, K=0-45, see fig 5.16)

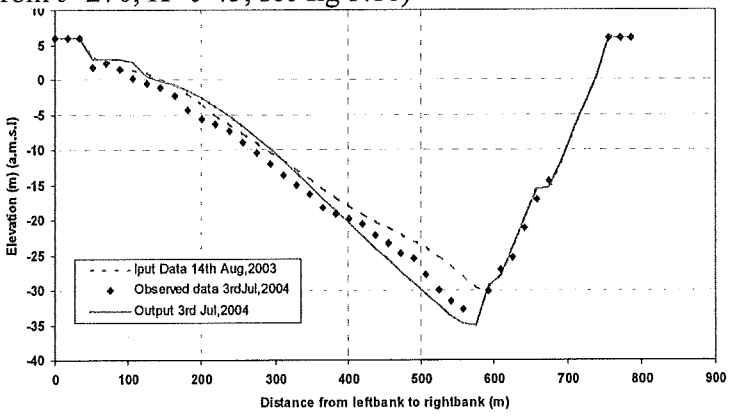

Figure 5.20b The bed comparison between observed data and MIKE21C results at cross-section T2 (from J=288, K=0-45, see fig 5.16)

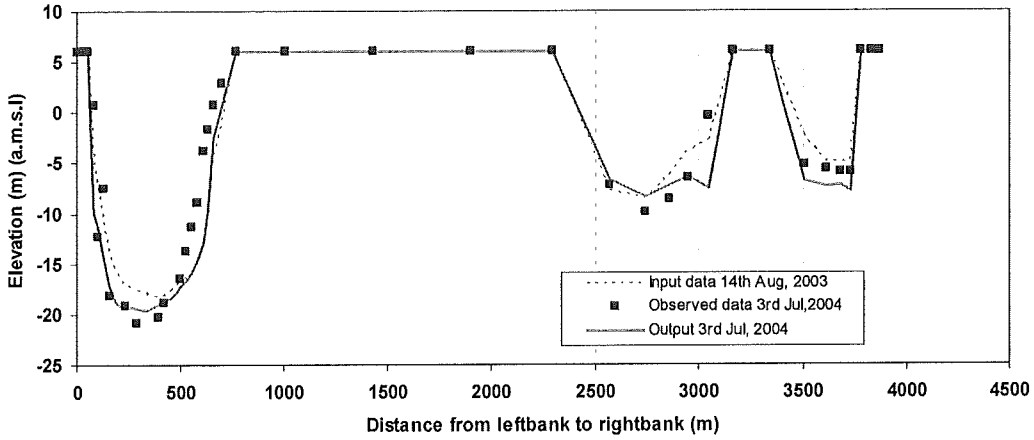

Figure 5.20c The bed comparison between observed data and MIKE21C results at cross-section T3 (from J=458, K=0-45, see fig 5.16)

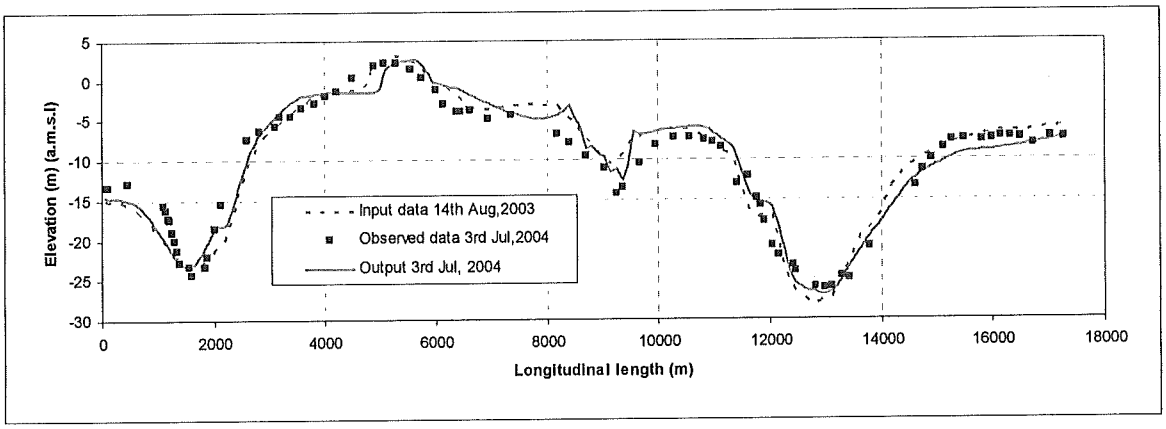

Figure 5.20d The bed comparison between observed data and MIKE21C results at longitudinal cross-section (J=225-503, K=30, see fig 5.16)

5.7.4 Conclusions for calibration and verification model

After the model was established, it was running for the period of calibration from 29th September 2002 to 14th August 2003. The calibration parameters (see table 5.5) were defined with roughness coefficient ($C=90m^{0.5}/s$) is higher than reality range ($30\text{-}80m^{0.5}/s$) but by applying Van Rijn (1984) and Engelund – Hansen (1967) is acceptable (see Appendix A.4). Although, the sediment transport seems quite different between the model and theory, but at least it could be adjustment in the model. The morphology calibration results has some small problem (see Fig. 5.17 a,b,c,d) however, it is acceptable result. The calibration process is reasonable to be continued with model verification process.

The model verification process was taken into account the result of calibration process (table 5.7). The water level is smaller than the observed data about 0.2-0.3m see Fig.5.18. The discharge has only one value of observed data, and it seems that computed value is smaller than observed about 6%. However, it would be better if we have more observed discharge data to verify.
Nevertheless, the results of morphology of verification model (see Fig. 5.20 a,b,c,d). There is some errors but it could be accepted.
In conclusion, model is available to use for some computed scenarios, in order to predict the tendency morphology change in Tan Chau – Hong Ngu area.

6. MITIGATION MEASURES

6.1 Introduction

Riverbank erosion in the lower Mekong area includes land losses, collapsing of houses, human casualties and other social and economic damages. Therefore, the mitigation measures are extremely needed for the lower Mekong river. However, the riverbank protection in general, for preventing of riverbank erosion in particular is a process. This process should take into account the understanding of problem identification e.g. considering whether the current attack is main cause of riverbank erosion or it could be due to surcharge, by waves, navigation, use of banks etc. Based on the understanding of these causes the right mitigation measures can be selected for a particular problem.

Moreover, riverbanks appear in many landforms but commonly they form the transition between land and water. With the water being a dynamic element, it is clear that riverbank also acts dynamically. The design of mitigation structures of riverbank erosion is one of the most challenging activity for an engineer because of multifunctional character and multidisciplinary interactions and responses namely, interaction between complex hydraulic loading, morphology, foundation (geotechnical aspects) and structural elements (stability) (Przedwojski et al., 1995). Therefore, the first law of river engineering by Prof. Watson says: ***"A complex river engineering problems often have simple, easy to understand wrong answers"***. In general, decision maker has always to remember that an effective application of measures is to stop or reduce the gradual erosion. This new situation should be compared with the previous situation. Whether this is acceptable or not depends on the particular case. In addition, before making a final choice of a specific measure, the effectiveness and consequences of applying such a measure should be investigated with all available means. Some of these means (models, empirical relations...) can give probably only a qualitative answer (show tendencies), but still can be a very useful tool in helping to take a right decision.

Starting with identification of the problem, a number of measures can be distinguished. These may be single or combined structural and non-structural measures and their lifetime can be permanent or temporary. The mitigation measures could be active or passive measures. The life time of measures in existing codes of practice or design guidelines often provide some information on the minimum requirements for the design life of hydraulic structures (usually as 20 years for temporary or short term measures, 50 to 100 years for shore protection structures and 100 to 1000 years or more for flood prevention structures). The active measures which are intended to influence the flow conditions or channel properties to decrease the impact. (e.g. upstream reservoir, groyne systems, ...) and the passive measures to protect the actual bank line without relevant active interference on the fluid (e.g. revetments)

The substantial development in society, economy, and environment should be taken into account; those key elements have to be clarified before the choice of alternatives has been made.

Nevertheless, whatever the elements of this complex river engineering can be, in chapter presents the possibility of prevention measures in the lower Mekong river. In addition, some existing measures will be discussed concerning their stability and performance condition.

Especially, Tan Chau is the most critical location in lower Mekong (see Fig 5.3 for location and see section 3.2.1 for more detail information). The existing revetment was checked by using the mathematical model (which was established in chapter 5), concerning the development of scour hole in front of this revetment. Moreover, Bend cut-off and permeable groyne were discussed as other alternatives for this specific location.

In addition, based on the Guideline and design manual for standardized bank protection structures of Ministry of Water Resources Research of Bangladesh, the design of permeable groyne is studied for Tan chau and The guideline of design permeable groyne are study and reported in appendix A- 6.

In conclusion, this chapter conveys the topic, which related to somehow to mitigate the riverbank erosion in lower Mekong river in general, and how to be consider the mitigation measures in specific location which a case study. Tan Chau is an example for other locations in lower Mekong river.

6.2 Existing mitigation measures in lower Mekong

The problems and consequences of riverbank erosion in lower Mekong river are very serious. On the other side, the available budget for preventing these problems is rather limited. In spite of that, the Vietnamese government and local agencies, and people put many efforts to mitigate these problems. The existing mitigation measures can be classified into four classes below.

- Simple measures (very small, small scale)
- Temporary measures (medium scale)
- Permanent measures (large scale)
- Pilot project

6.2.1 Simple measures (very small, small scale)

The budget: supported by farmers, local people
Lifetime: one year or two years
Type: passive measures
Design: base on the living close river experience
Structures: Revetment
Material: Timber pile, sand bag, bamboo
This measure is usually applied on very small scale. It normally implemented by people, who live near riverbank. The main purpose of these measures is to reduce temporary the impacts of currents, waves and therefore to mitigate the erosion. Those structures are not designed, not based on the calculation. However, it just estimated by people according to their living riverine experience. It is shown in figure 6.1 a, b as results of their efforts to mitigate the riverbank erosion impacts.

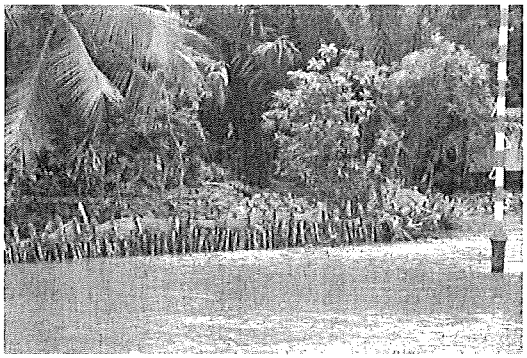

a) The timber poles

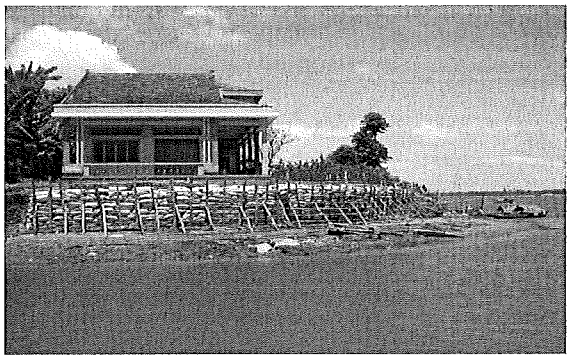

b) The timber poles combining with sand bag

Figure 6.1 The simple measures made by local people in Tien River

These kinds of local mitigation measures are very common in the lower Mekong river, because the government has only budget to implement protection in the critical location of high economical value.

There are a number of locations, where impacts of current and waves is limited where this kind of simple protection can be still effective. However, these measures were built only by the experience of people who live close to the river. They cannot realise that experience is not enough to keep longer lifetime of structures. In other words, for long term of strategy, the government has no budget to protect the riverbank for the whole area, but the government should focus on some selected structures, which people should use for specific locations, they also should guide people how to apply those measures more efficiently. Promising some official guidelines hereabout should be recommended.

6.2.2 Temporary measures (medium scale)

The budget: supported by town, community, or local government.
Lifetime: two years to five years
Type: passive measures
Design: base on experience or very simple design
Structures: revetment (usually)
Material: rock and grout, concrete bocks, gabion, sand bag, bamboo

These temporary measures could be need when the loss of land and economic damage is expected. The local government, local community can support budget to build up this kind of measures. The lifetime of these measures are from two to five years, and the material is normally rock, or concrete blocks. The purpose of these measures is to reduce the erosion gradually at specific locations. This design does not take into account the impacts to other area. The approach by means mathematical modeling and/or physical modeling is not applied in these measures. The designer only focuses on the stability of structures and the amount of available budget. In figure 6.2, the temporary measures to mitigate the riverbank erosion were made by concrete piles and concrete facing.

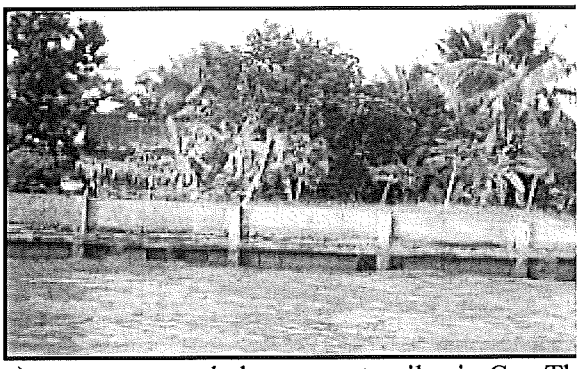

a) revetment made by concrete piles in Can Tho

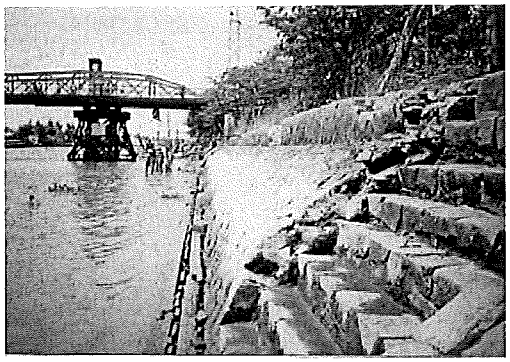

b) revetment made by grout and rock

Figure 6.2 The temporary measures made by local government at Can Tho city

6.2.3 Permanent measures (large scale)

The budget: supported by provincial government, Ministry of Rural and Agriculture Development, or Vietnamese government, ODA, Foreign funds
Lifetime: twenty years to thirty years
Type: active or passive measures
Design: base on design standards, guidelines, approach with physical and mathematical modeling
Structures: Revetment, groyne system, closure dam, Bend cut-off, etc.
Material: rock, concrete bocks, gabions
These measures are used to protect the economic, urban, and cultural areas due to strong impacts of riverbank erosion. In lower Mekong river, there are some locations such as Vinh Long (built in 1996), Tan Chau (built in 2002), Long Xuyen (built in 2002), Sadec (built in 2003) where this kind of measures have been applied. These measures normally follow the design process from problem identifications, the pre-feasibility study, feasibility design, final design, construction, operation, and maintenance. However, this design process needs more practice and more deepening in understanding both aspects of physic and clear design standards. The cost of this kind of measure is relatively high. However, normally in lower Mekong the cost and benefit approach is still not applied for design and selection of these.

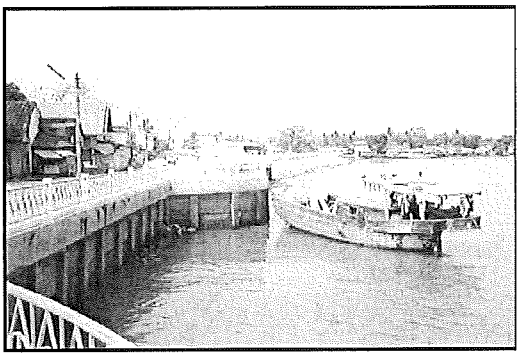

a) Vinh Long revetment built in 1996

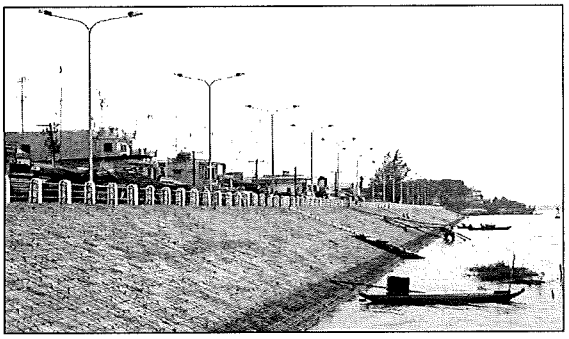

b) Tan Chau revetment built in 2002

Figure 6.3 The permanent measures in lower Mekong

In figure 6.3a, the revetment was constructed in 1996 in Vinh Long to protect the city and 6.3b, the revetment in Tan Chau build in 2002, where many comments above is applicable to this critical location.

6.2.4 Pilot projects

The budget: supported by province government, Ministry of Science & Technique, or Vietnamese government.
Lifetime: twenty years to thirty years
Type: active or passive measures
Design: design standard
Structures: revetment, groyne system, closure dam, Bend cut-off.
Material: Concrete mattresses, sheet pile
The number of pilot structures in lower Mekong is limited. The example of that is concrete mattresses as implemented in Rach Gia, Kien Giang province, see figure 6.4. This measure is a trial project to investigate the ability of this solution for some small canals, and reaches.

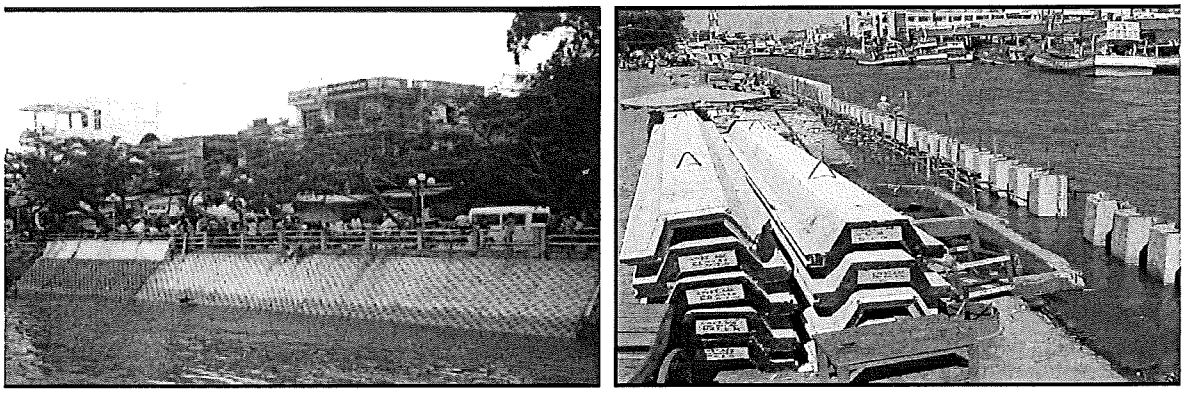

a) Concrete mattresses in Kien Giang province b) Sheet ~~pipe~~ piles in Kien Giang province

Figure 6.4 The pilot project use in lower Mekong river

6.3 Overview of possible preventive measures

There is a large variety of possible erosion impact in the lower Mekong river. Therefore, the various measures can be applied, from small scale (simple) to large-scale measures (more complicated). Some of above existing measures need improvement, and other need better understanding and clear standard guidelines.

The small-scale measures can be applied at some locations, which are not so strong impacts and local people can make it. Still there is a guideline to increase the efficiency of these measures. Traditional practice is shown in figure 6.1 a, b where the measures are made by wooden poles, and sand bags.

The large-scale (permanent) measures form the main interest in this study. Especially for critical locations, their design must be adequate for the high water levels, depth water depth, high velocity (e.g Tan Chau h = 40m, u=3m/s, see more in part 4.3 chapter 4, river characteristic) and their construction can be more difficult and expensive. In addition, unstable of soil condition of alluvial river may lead to the expensive construction foundation. These measures have to take into account the long-term strategy, which included economic analysis, stability of structures, environment, maintain and operation. Moreover, the question whether implement these measures or removes people and their property to other place should be answered before making a decision; this question needs considering the cost benefit analysis.

Figure 6.5 shows the possible preventive measures in lower Mekong along two lines, one is non-structure measures, and the other is structures measures. Non-structures such as reforest to mitigate the flood from upstream, regulation as navigation, construction, and sand excavation are activities of people on the river, which have to be regulated. The education is also an important measure, because people can understand the dangerous effects of riverbank erosion and try to limit the damage. Moreover, the planning should include future developments, clear strategy based on master plan for the area. The resettlement is also a measure, which should be taken into consideration when the erosion area is not quite valuable or too costly for protection.

The structure measures can be divided into passive and active measures. The passive measures as usual are vegetation, which was applied in small reaches, canals, (such as vetiver grass), and revetment. Revetment is very common measures in lower Mekong river, with different kind of rip-rap and other materials. The active measures are normally applied to change flow conditions in order to mitigate the riverbank erosion. These measures could be groyne system (permeable, impermeable, and both in combination) or closure dam, upstream reservoir, and flow guiding structures. All of those structures can be possible as preventive measures in lower Mekong river.

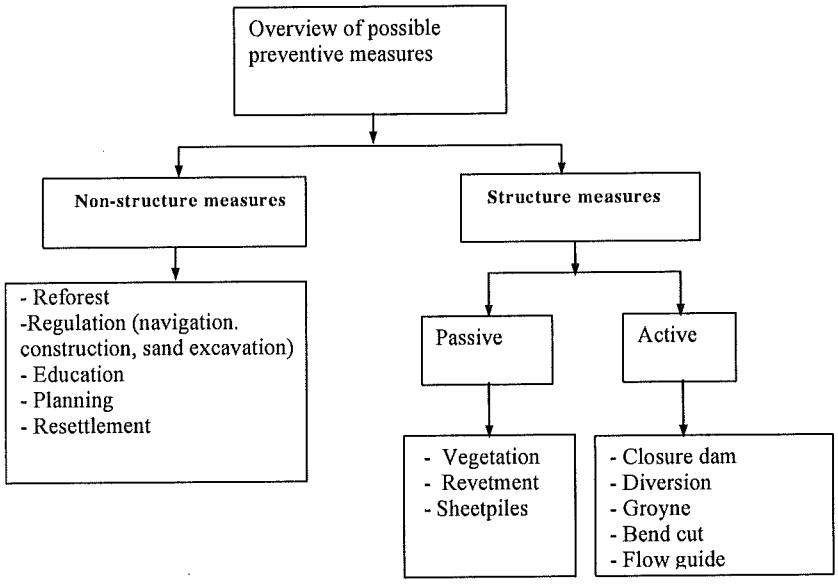

Figure 6.5 The overview of possible preventive measures in lower Mekong

6.4 A case study for Tan Chau

6.4.1 Introduction

Tan Chau is high economic value, urban area and crowded town. The riverbank erosion occurred extremely in this location (see Fig 5.3 for location and see section 3.2.1 for more detail information).

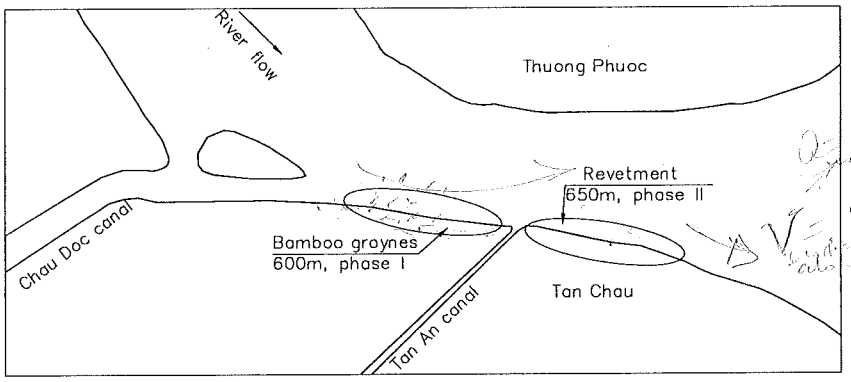

Figure 6.6 Construction stretch

Therefore, on September 2001, a project was implemented in order to protect the Tan Chau town. The first phase included three bamboo groynes from Chau Doc canal to Tan An canal with a length 600m. The second phase is six impermeable groynes from Tan An canal to down stream with a length 650m (see figure 6.6). The structures were started at beginning of the 2001 flood season (August 2001). The structures was implementing in flood condition with the poor equipment. Due to these difficulties, the construction had to stop to change the design after two months of constructing. It was re-started again on February 2002, and finished the under water part on August 2002 (Ngo Thi Nguyet (2004)).

The observation of stability of revetment was implemented on December, 2002. It found that the maximum bed level change in front of revetment about 8-10m. Therefore, the additional material for the toe protection of revetment costs about 250,000EUR more (Ngo Thi Nguyet (2004)). The upper water part was implementing on Mach 2004 and it was completed on August 2004. At the end, the cost of construction is about nine million euro, which was about twice times of initially estimate cost.
The view of construction after finish shows in figure 6.7.

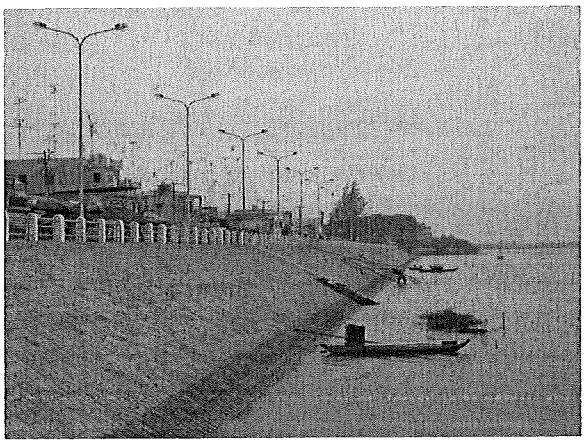

Figure 6.7 Tan Chau revetment

Example of the revetment at Tan Chau is given in figure 6.8, the revetment was made by sand bag, and riprap material is gabion 10x2x0.5m.

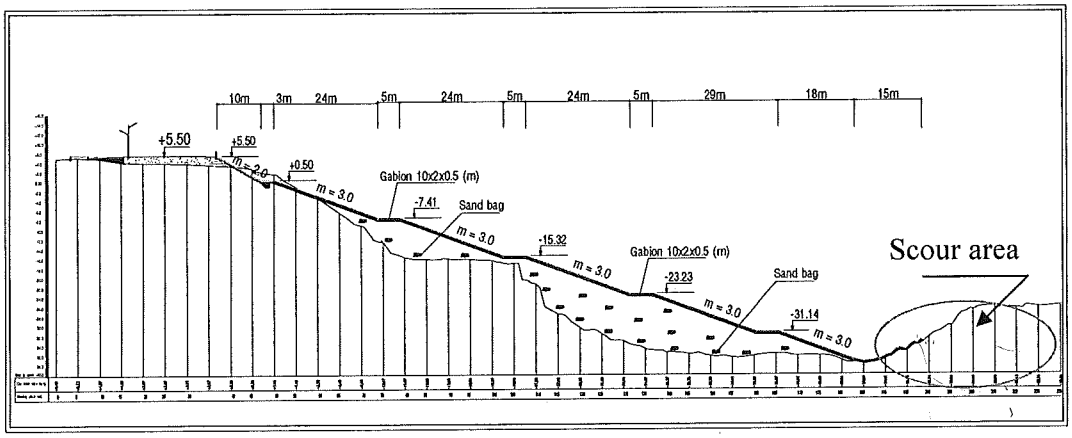

Figure 6.8 The Tan Chau design cross-section
(Source: An Giang provincial consultant company)

6.4.2 Stability of Tan Chau revetment

The river cross-section was narrowed by construction. It would be a cause of scour hole in front of this revetment in such sharp bend in the Tien river. The question is how deep will be the scour hole in front of this revetment. This question could be answered by using MIKE21C simulation (model have been established in chapter 5), and some empirical methods.
The simulation of extreme flood was studied in order to predict how the scour hole would develop on one hand and other hand by using the Maynord and USACE formula, which used to predict the scour hole in river bend (see part 4.4.2 chapter 4).

6.4.2.1 Extreme flood and model input

The extreme flood is defined based on the limited data of observed maximum discharge at Tan Chau station (see figure 6.9) and the results of applying Pearson type III method (see figure 6.10).

Apply Pearson type III, with skew coefficient G = - 0.753 (From table 13-4. page 363, Hydrology for Engineers, Linskey.R.K et al(1982)

$$LogQ=\overline{LogQ}+K\sigma_{logQ}$$

n^0	Year	Qmax	$(Q-Qmean)^2$	m (rank)	logQ	$(logQ-mean_{logQ})^2$	$(logQ-mean\sigma_{logQ})^3$	P%	Tr (yr)
1	1982	22000	79868	13	4.342	6.82439E-05	5.63762E-07	54.2%	1.8
2	1983	19800	3676389	17	4.297	0.001405988	-5.27196E-05	70.8%	1.4
3	1984	22400	465955	11	4.350	0.00025877	4.16266E-06	45.8%	2.2
4	1985	21200	267694	16	4.326	6.12437E-05	-4.79283E-07	66.7%	1.5
5	1986	21900	33346	14	4.340	3.94688E-05	2.4796E-07	58.3%	1.7
6	1987	19300	5843781	19	4.286	0.002362386	-0.000114822	79.2%	1.3
7	1988	16700	25174216	23	4.223	0.012420038	-0.001384154	95.8%	1.0
8	1989	19000	7384216	20	4.279	0.003070057	-0.000170106	83.3%	1.2
9	1990	22800	1172042	9	4.358	0.000565163	1.34357E-05	37.5%	2.7
10	1991	24300	6669868	3	4.386	0.002646545	0.00013615	12.5%	8.0
11	1992	18900	7937694	21	4.276	0.003329277	-0.000192099	87.5%	1.1
12	1993	19600	4483346	18	4.292	0.001756081	-7.35897E-05	75.0%	1.3
13	1994	23200	2198129	7	4.365	0.000981337	3.07416E-05	29.2%	3.4
14	1995	22200	232911	12	4.346	0.000148627	1.81196E-06	50.0%	2.0
15	1996	23700	3930737	5	4.375	0.001647276	6.68574E-05	20.8%	4.8
16	1997	23300	2504650	6	4.367	0.001101857	3.65753E-05	25.0%	4.0
17	1998	17200	20406824	22	4.236	0.009728517	-0.000959555	91.7%	1.1
18	1999	22700	965520	10	4.356	0.000478042	1.0452E-05	41.7%	2.4
19	2000	26000	18340737	1	4.415	0.006530524	0.000527742	2.4%	24.0
20	2001	23900	4763781	4	4.378	0.001956842	8.65633E-05	16.7%	6.0
21	2002	24400	7196389	2	4.387	0.002833234	0.000150808	8.3%	12.0
22	2003	23100	1911607	8	4.364	0.000867319	2.55428E-05	33.3%	3.0
23	2004	21900	33346	15	4.340	3.94688E-05	2.4796E-07	62.5%	1.6
	Σ	499500			99.7	0.05430	-0.00186		
	Mean	21717			4.33				
	σ_Q	2390.07							
	σ_{logQ}					0.0497			
	G						-0.753		

Where: Σ : sum, Mean= average value; σ_Q standard deviation Q value; σ_{logQ} standard deviation logQ value; G- skew coefficient

P(%)=m/n+1 – Probability of occurrence, m-rank, n=23 number of samples. T_r – return period (year) T_r=1/P

For extremely value probability of occurrence can be computed:

$$P(\%)=\frac{m-0.44}{n+0.12}$$

Table 6.1. Flood discharge data at Tan Chau from 1982 to 2004 for analysis Pearson type III

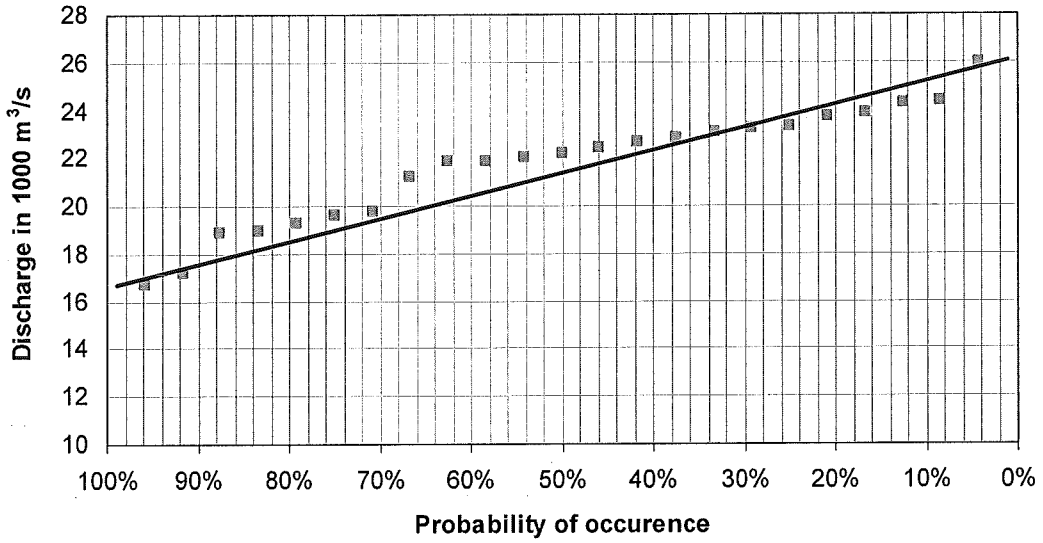

Figure 6.9 The occurrence of maximum water level at Tan Chau station according to Pearson type III method

In figure 6.9, the maximum discharge in the year 2000 is 2600m^3/s correspond to around the return period of 50 years.

In conclusion, the hydrograph of the year 2000 is chosen to predict the scour hole in front of revetment. The boundary condition, the bathymetry and the model parameters was summarized in table 6.2.

Terms & coefficients	Time & value of coefficient	Unit
Bathymetry	Result of verification model at 3rd July 2004	m
Grid	Grid base on bank line 2002 J x K=518x45 (J is the number of grid along river bank, and K is number of grid transverse)	cells
Upstream boundary From MIKE21C	1. Discharge from 3rd July 2004 to 31st October 2005 2. Sediment transport 3rd July 2004 to 31st October 2005	m^3/s m^3/s
Downstream boundary From MIKE21C	Water level from 3rd July 2004 to 31st October 2005 Sediment transport 3rd July 2004 to 31st October 2005	m m^3/s
Eddy viscosity	E=8.5	m^2/s
Chezy coefficient	C=90	$m^{1/2}/s$
Morphology	G=1.25 transverse slope coefficient a=0.5 transverse slope power (see part 5.3.2.2) e=5 longitudinal slope coefficient	

Table 6.2 Summary model input for scour hole prediction

It is noted in table 6.2 that, the time of period from 1st January 2005 to 31st October 2005 is prediction time correspond to 1:50 year flood discharge (flood 2000). In other words, it is the prediction time, which corresponds to the value of discharge or sediment or water level is the value of the year 2000.

6.4.2.2 The results of model

The results of model are reported more in the appendix A-5. In figure 6.10 the change of scour depth in time at grid point (J=276, K=19) where is the close point with revetment area (J=274-292, k=0-18).

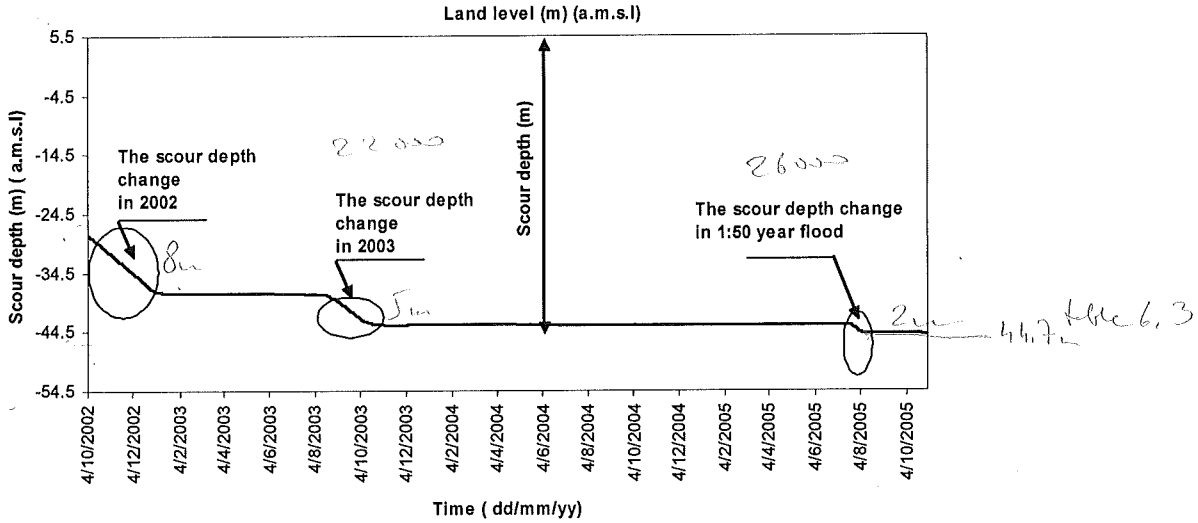

Figure 6.10 The change scour depth in time at grid point, which is close to revetment (J=276, K=19)

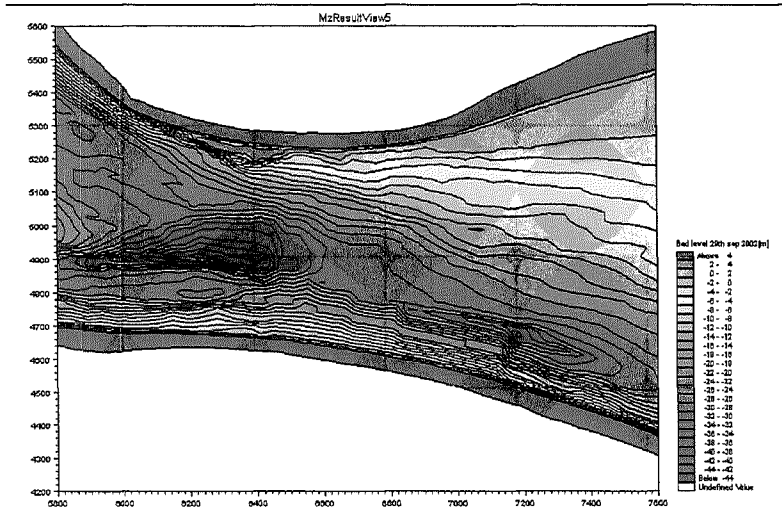

a) The initial bed level on 29th September 2002

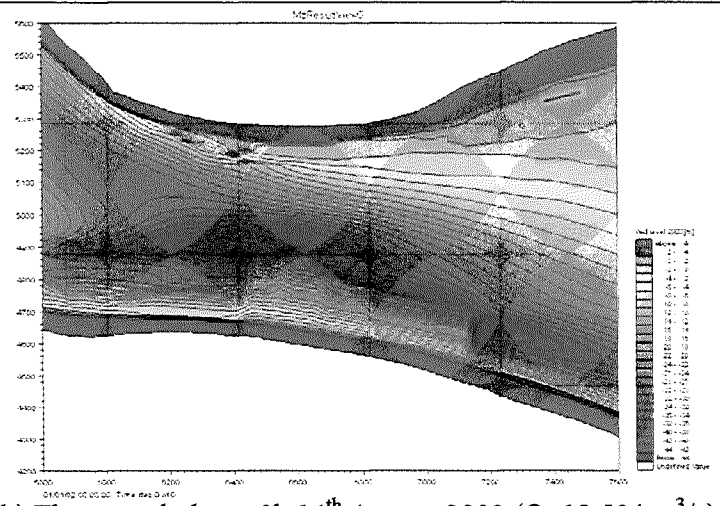

b) The scour hole on 0h 14th August 2003 (Q=13,504 m^3/s)

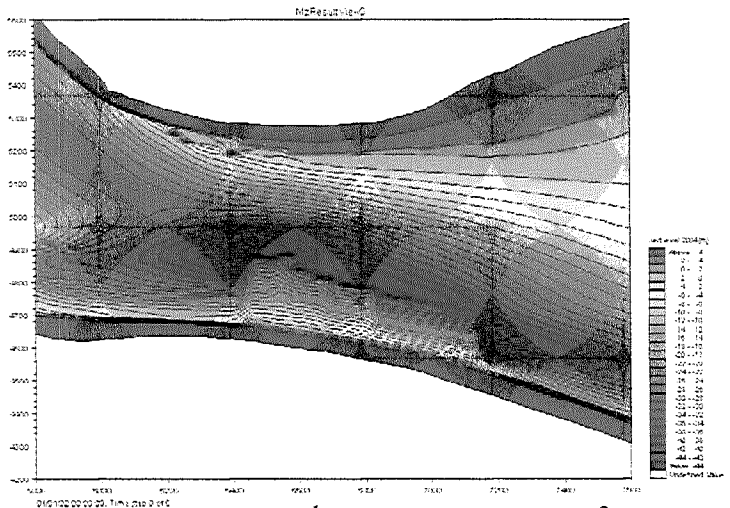

c) The scour hole on 0h 3rd July 2004 (Q=9,786 m^3/s)

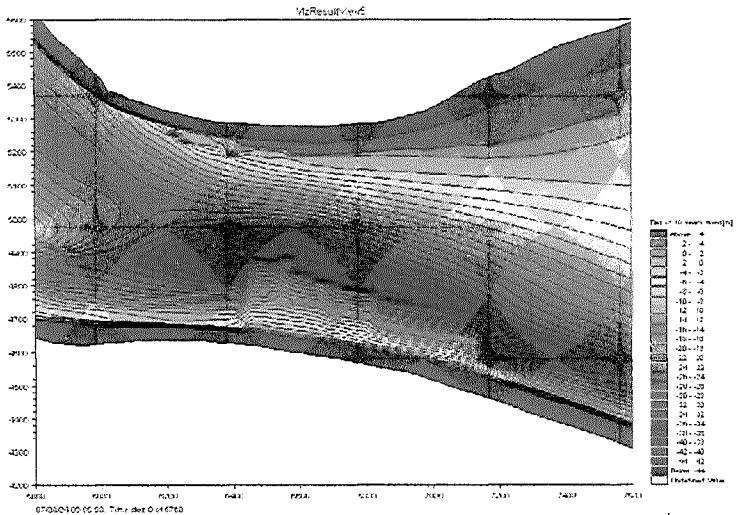

d) The scour hole at the end of 1:50 year flood 0h 31st October 2005 (2000) (Q=16,000m^3/s)

Figure 6.11 The plan view of scour hole in front of revetment

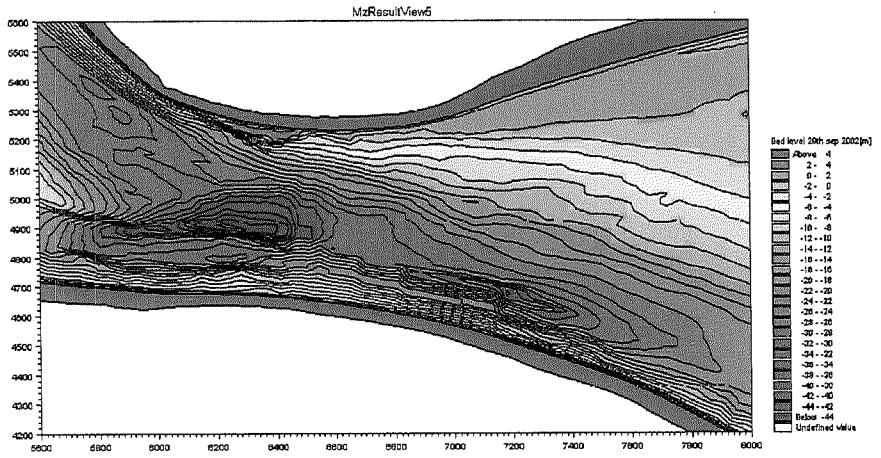

a) The initial bathymetry on 29th September 2002

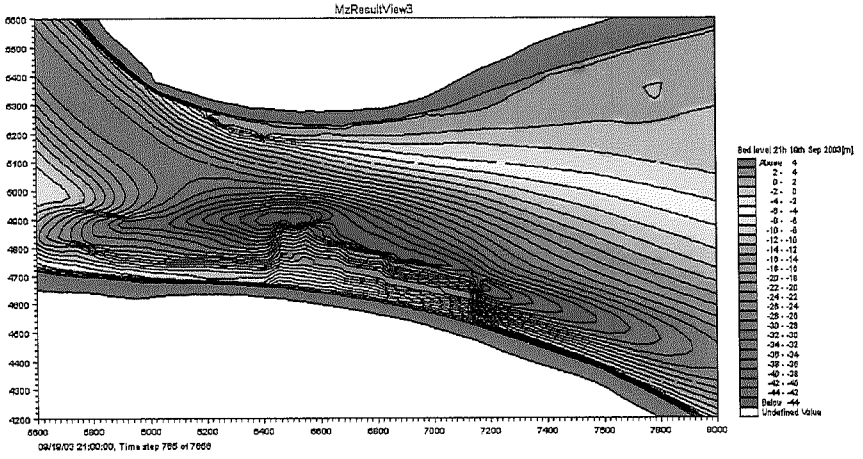

b). Bed level at flood peak on 21h 19th September 2003, Q=23,185m^3/s

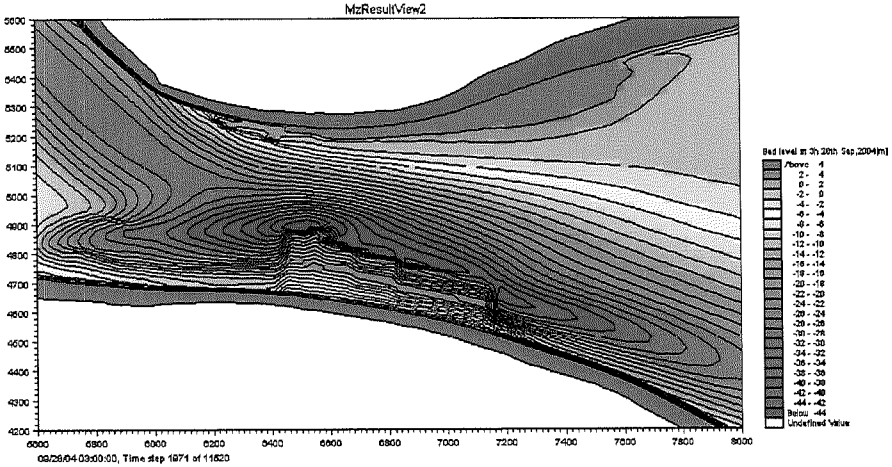

c) Bed level at flood peak on 3h 28th September 2004, Q=22,031m^3/s

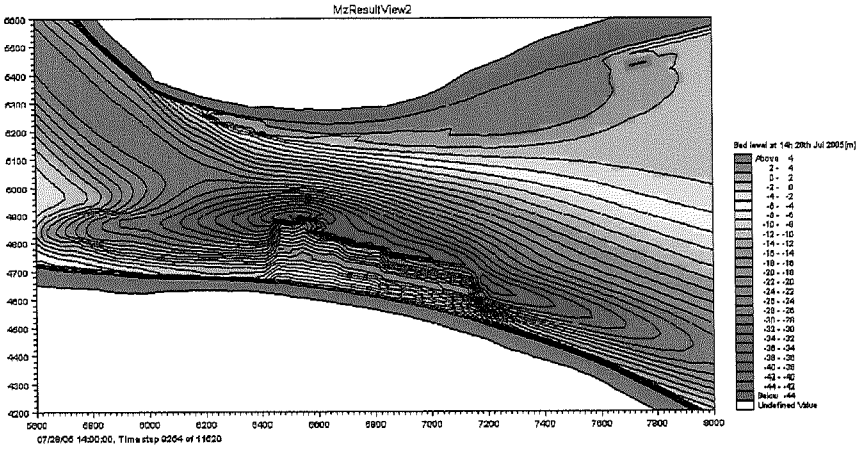

d) Bed level at flood peak on 14h 28th July 2005 (2000), Q=26,000m^3/s

Figure 6.12 The scour hole in flood peak

In Figure 6.13 a, b, c, d are the results of cross-section change in period 2002, 2003, 2004 and the 1:50 year flood prediction for upstream revetment, and revetment, downstream revetment cross-section.

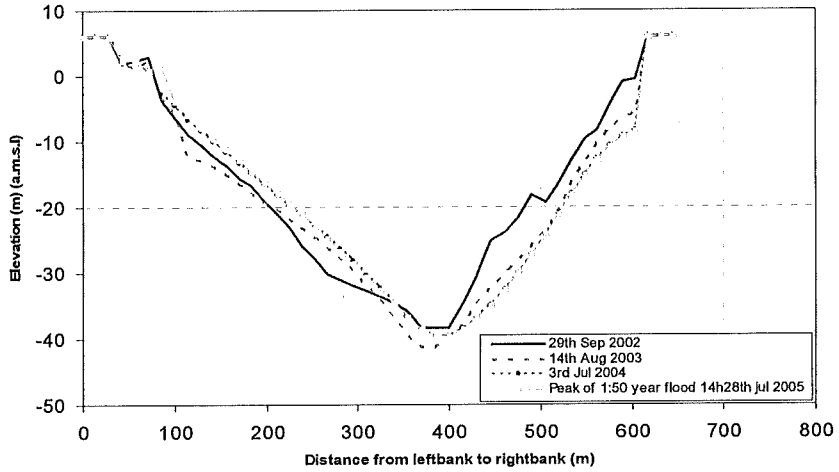

a) The cross-section upstream revetment (J=272, K=0-45)

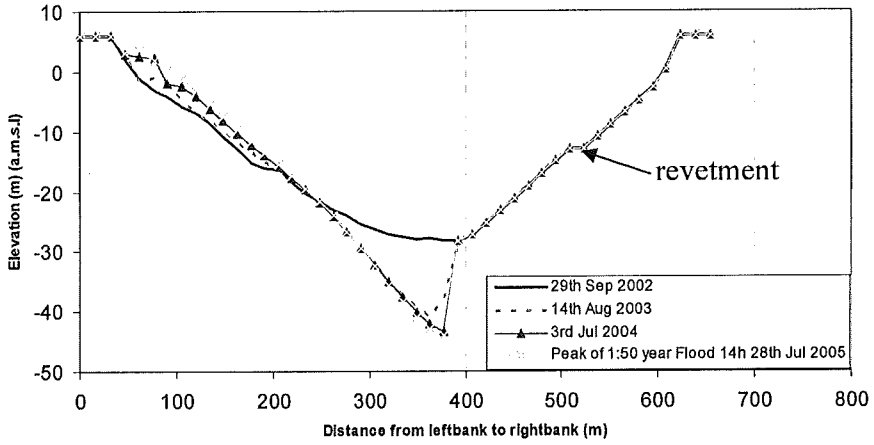

b) The cross-section revetment where the deepest scour hole place (J=276,K=0-45)

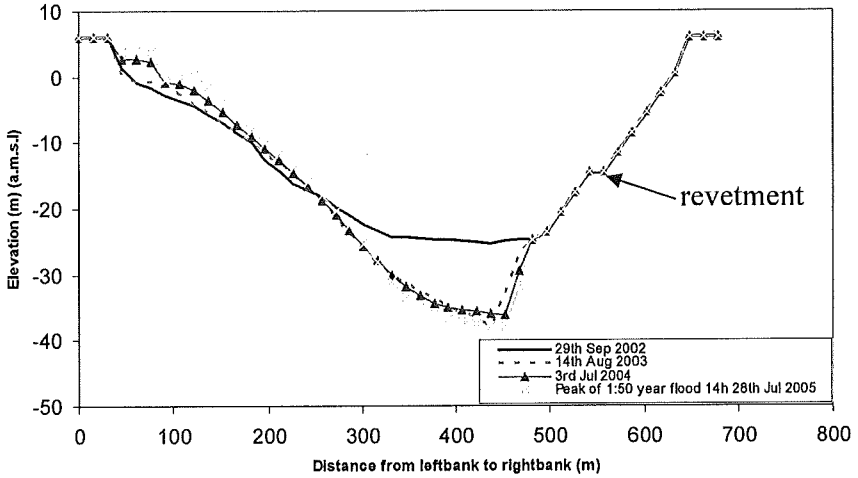

c) The cross-section revetment (J=280,K=0-45)

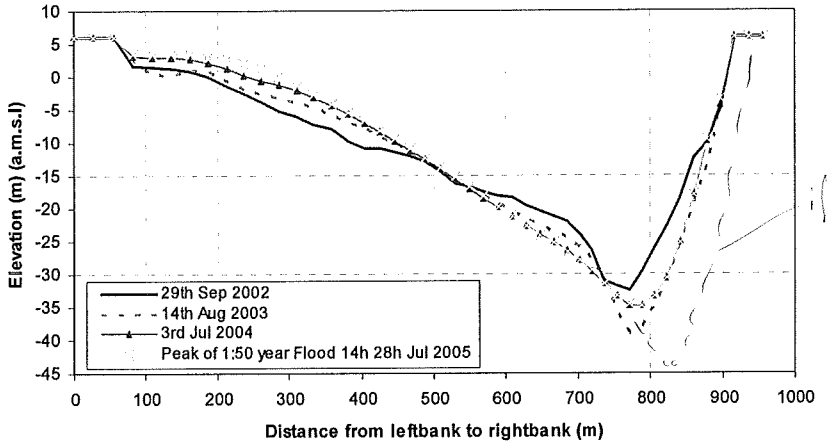

d) The cross-section at downstream of revetment (J=294,K=0-45)

Figure 6.13 The cross-section at Tan Chau revetment

In Table 6.3 is result of by using Maynord and USACE formula and comparison with result of MIKE21C with 1:50 year flood discharge.

Maynord formula:

$$\frac{h_b}{h} = -0.36\ln(\frac{R}{W}) + 2.57 \qquad (6\text{-}1)$$

and the formula of USACE:

$$\frac{h_b}{h} = -0.71\ln(\frac{R}{W}) + 3.377 \qquad (6\text{-}2)$$

where as

h_b – Scour depth in the bend (m)

h – The average water depth at cross-section (m)

R –The radius of curvature of bend (m)

W – The river width (m)

Terms	Radius of curvature (m)	River width (m)	Average water depth h(m)	Scour depth h_b (m)	Notes
Data observed 2004				44.7	Observed
Maynord	2660	619	24.1	49.3	Prediction
USACE	2660	619	24.1	56.4	Prediction
MIKE21C				50.5	Prediction

Table 6.3 The scour hole prediction results

6.4.2.3 The volume of falling apron

Due to the scour depth was developing rapidly during construction and during the 1:50 year flood. According to the model and empirical method, the scour depth is about 15m.

The volume of falling apron is calculated base on the Bangladesh design guideline:

$$V_{FA} = 1.5.D_n.\sqrt{5}.y_{BL}.C_{FA} \qquad (6\text{-}3)$$

Where

V_{FA} - volume of falling apron per linear meter protected length (m^3/m)

D_n - block size ($1.5D_n$ is the proposed layer thickness after scouring without voids) (m)

y_{BL} - vertical distance between base level of falling apron at time of construction and deepest point of the expected design scour hole (m)
C_{FA} – flow attack coefficient: 1.50 (moderate flow attack)
1.75 (strong flow attack) applied for this case
Assuming the falling apron of revetment is filled with cubic cement concrete bock with D_n=0.5m (recommended minimum =0.3m, Bangladesh design guide line)

From (6-3) the volume of falling apron is computed:
$V_{FA} = 1.5.0.5.\sqrt{5}.10.1.75 = 29.3$ (m^3/m)
The number of cubic cement concrete block per linear meter.

$$n = \frac{V_{FA}}{D_n^3} = \frac{29.3}{0.5^3} \approx 235 \text{ blocks/m}$$

The total length of revetment is about 650m so that the number of concrete block needs about 650x235= 152,750 blocks.
Estimate cost: 152,750x3e per block ≈ 460,000 euro.

This price is rather high than 250,000euro for toe protection at the end of flood 2002 (reported by Ngo Thi Nguyet, 2004). It can be explained that, the cost is higher because of different protection material used for falling apron and with this result is taken into account the scour depth of the year 2003, and 1:50 year flood.

6.4.2.4 Result discussion

From figure 6.11, the bed level change at one point (J=274, K=19) in time are reported. It seems reasonable result, because of the bed level changed rapidly during the construction time (flood season 2002). The maximum bed level change in this period is about 10m, and it is comparable with the observation data (from 8-10m reported by Ngo Thi Nguyet, 2004).

In flood 2003, the scour depth was developing again, which was estimated about 6m (see Fig.6-10, 6-11, 6-12). The scour hole became very close to the revetment. However, in the report of Ngo Thi Nguyet (2004), there was no observation after flood of 2003. That means, in the flood 2002 the scour depth in front of revetment was observed and additional material for toe protection, but at the end of flood 2003, this step was not implemented. The results suggest that it might be important to implement the observation and maintain of revetment.

Moreover, the simulation of 1:50 year flood, the results of bed level does not change so much. It is about 2m at point (J=276, K=19). However, the important thing that, the scour hole was moving very close with revetment toes with 1:50 year flood condition.

Although, the model was calibrated and verified against with observed data (chapter 5), but it is still need improvement. It would be interesting for further study with fine grid, and more sufficient data for calibration and verification. Nevertheless, the results derived from model of MIKE21C shows the tendency of how the scour hole process and how deep it would be. It points out the important of observation and maintenance for revetment stability. Especially, it should be more detail observation in the upstream of revetment part.

In addition, by applying Maynord, and USACE formula the prediction of scour hole would be more deeper (see Table 6.3). Although this results is not taken into account the influence of revetment, but the equilibrium state of scour in bend will reaches when its depth of about

50m. These results recommend that, the observed activities for revetment have to be implemented every month during flood season.

6.4.3 Bend cut-off

The revetment is existed to protect Tan Chau town in such sharp bend and strongly currents due to yearly flood. However, the need of discussion and learning from doing is much more important. In other words, the other possibility of alternatives could be discussed, and checking by numerical model. The revetment cost about nine million euro, and it may be need more in future for observation and maintenance action. From author point of view, it would be nice if the bend cut-off and the permeable groynes were considering alternatives for Tan Chau bend.

The bend cut-off solution can be reduced the erosion attack to Tan Chau town as well as the development of scour hole.

In theory, a channel was excavated in full dimensions as a pilot channel, which is eroded to the final extend during rising water level stages, provided that the existent sediment is fairly mobile sandy soil. The rate of flow directed in to the pilot channel should be at least 25-30% of the bankfull discharge of main channel. The creation of a bend cut-off results in an increase in water slope, bed slope and flow velocity, in parallel the water depth will decrease, which usually lead to local erosion. The eroded material is normally deposited in the reach downstream from the bend cut-off.

However, the fixed bank channel was study instead for mobilization bank of channel due to time limited in this thesis. The length of channel is about 2.5km with trapezium shape, the channel level is -10m (a.m.s.l) with side slope m=3. The soil is movable due to high velocity in this region.

The volume of excavated soil is estimated:
$V = L.A$ (m^3)
L= 2.5 km is length of pilot channel.
A= 736m^2 the area of cross-section.
$V = L.A$ =2500x736 =1,840,000 (m^3)
Estimate cost: 1,840,000x2euro/m^3 =3,680,000 EUR

The drawing of design of the bend cut-off and the curvilinear grid cells at Tan Chau bend cut-off are shown in figure 6.14.

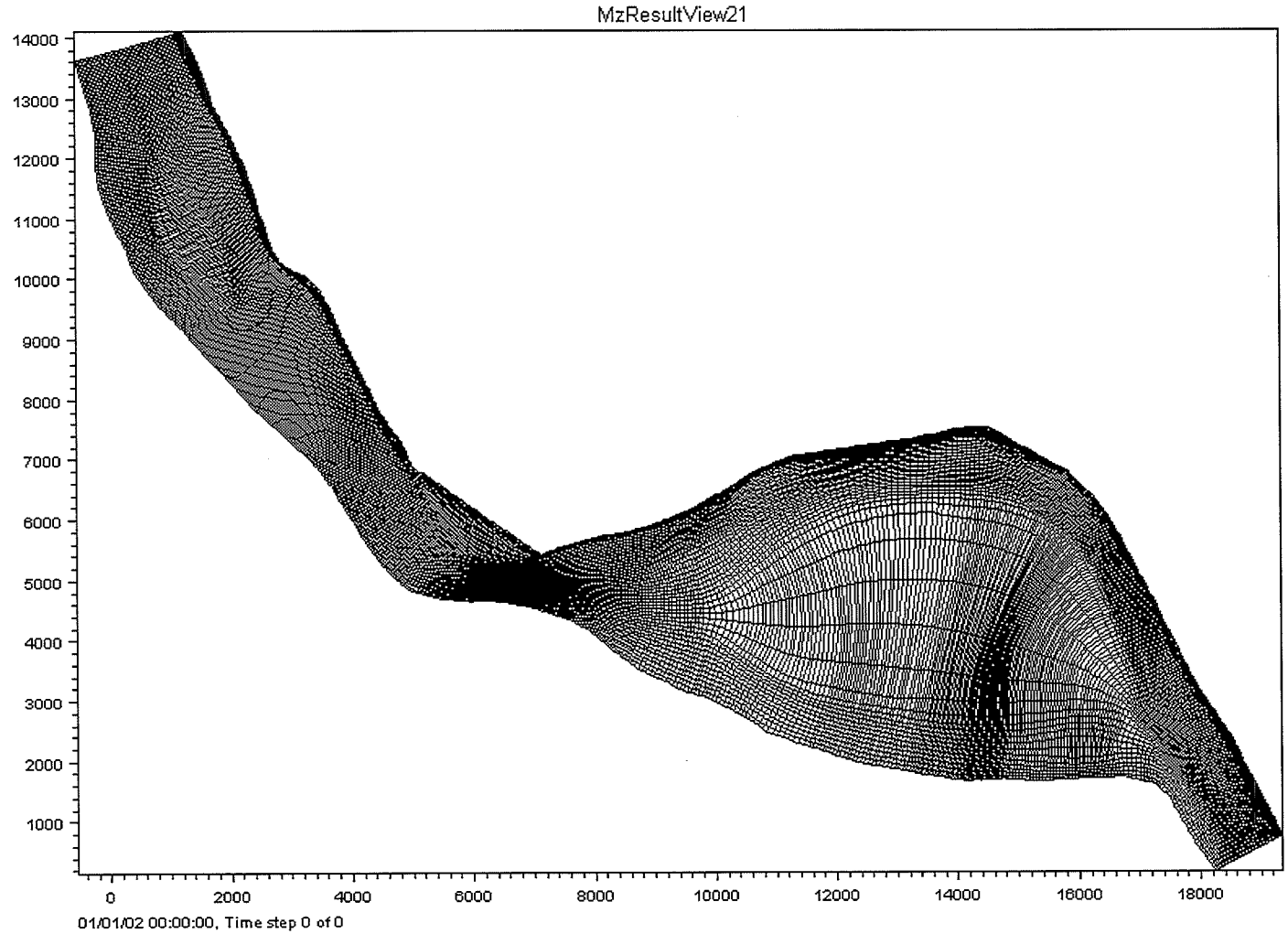

Figure 6.14 a) The curvilinear grid of Bend cut-off solution

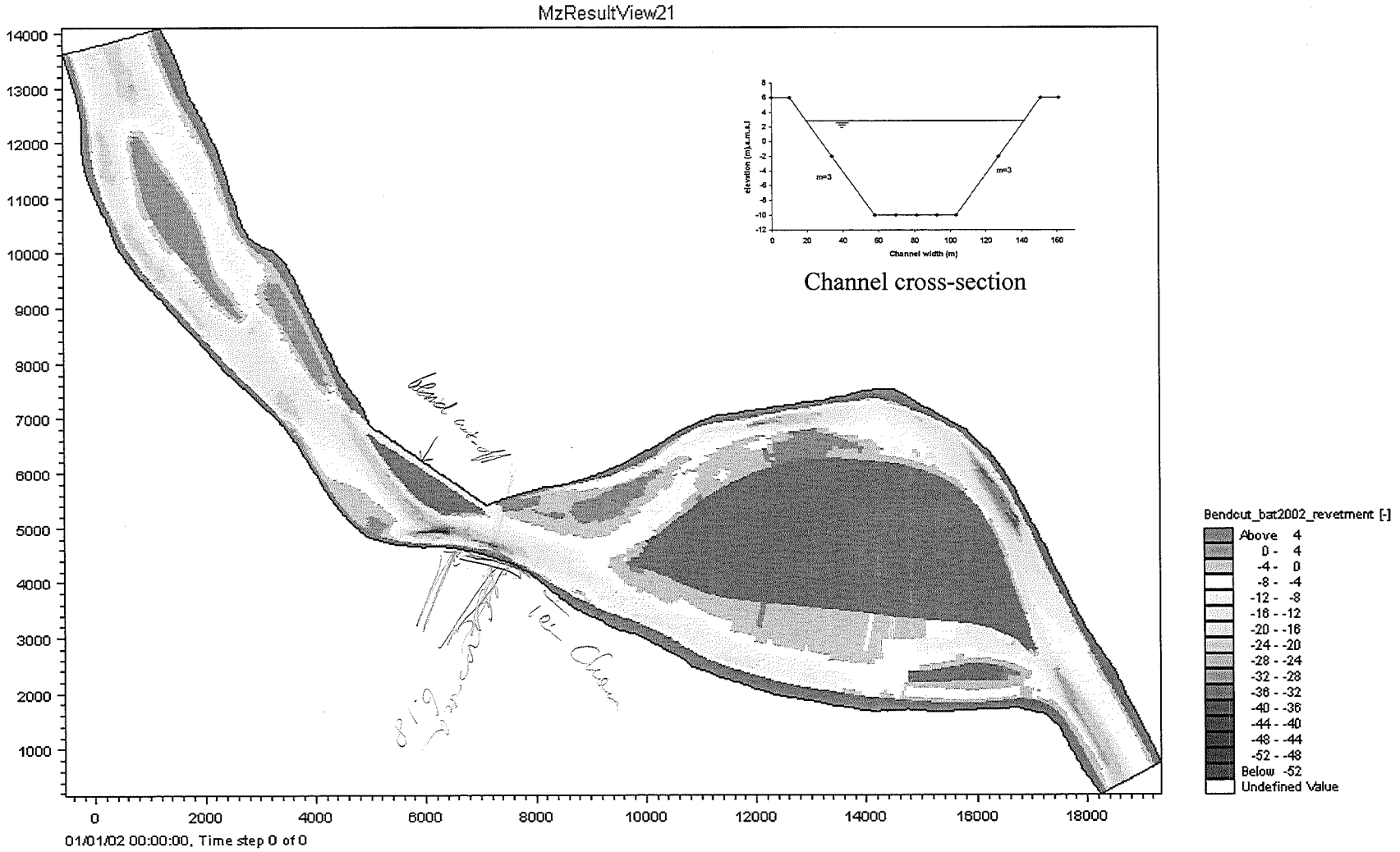

Figure 6.14 b) Bathymetry of bend cut-off solution

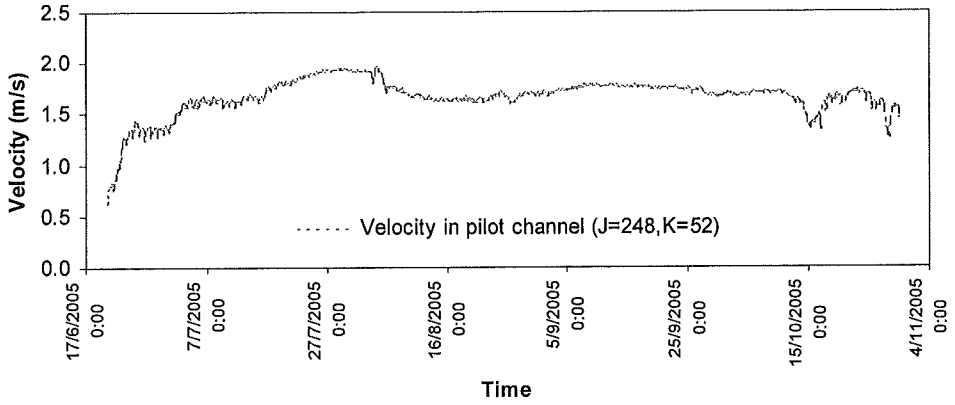

Figure 6.15 a) The velocity at point in the middle pilot channel during flood (J=248, K=52)

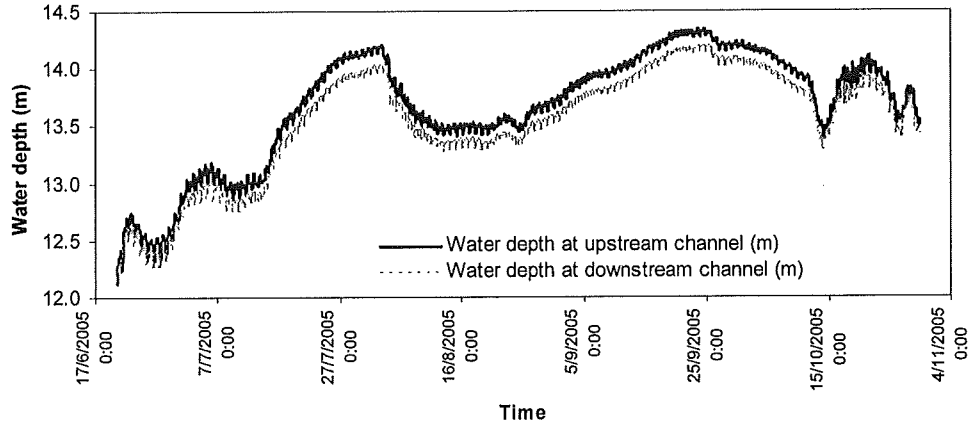

Figure 6.15 b) The water depth at upstream and downstream of pilot channel during ten-year flood

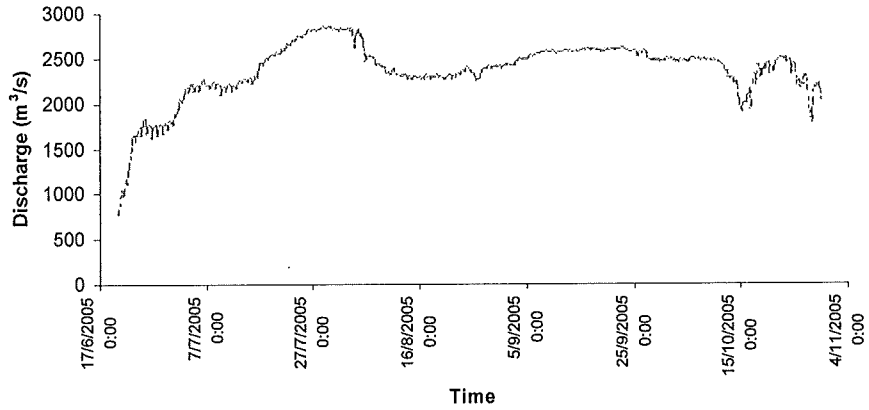

Figure 6.15 c) The discharge of pilot channel during ten-year flood

In figure 6.15 a, b and c) reported by the velocity, the water depth and discharge in the pilot channel. The velocity is rather high about 1.5-2.0m/s during flood it could lead erosion in pilot channel. The slope in the channel is increased about 5.5 times in comparison with river slope ($4x10^{-5}$), the different water depth in 2.5km in length of channel shown in figure 6.15b.

Normally, the discharge in the pilot channel required at least about 25% of bankfull discharge in main channel for the cut off case (Q_{bf}=19000m^3/s, see table A.2.4 appendix A-2). However, in this case, the bend cut-off is only to reduce the flow in the bend. In the figure 6.15c, the discharge is about 2500m^3/s (15% of bankfull discharge).It is accepted because in the model, the fixed bank of pilot channel was simulate but in it is movable in reality.

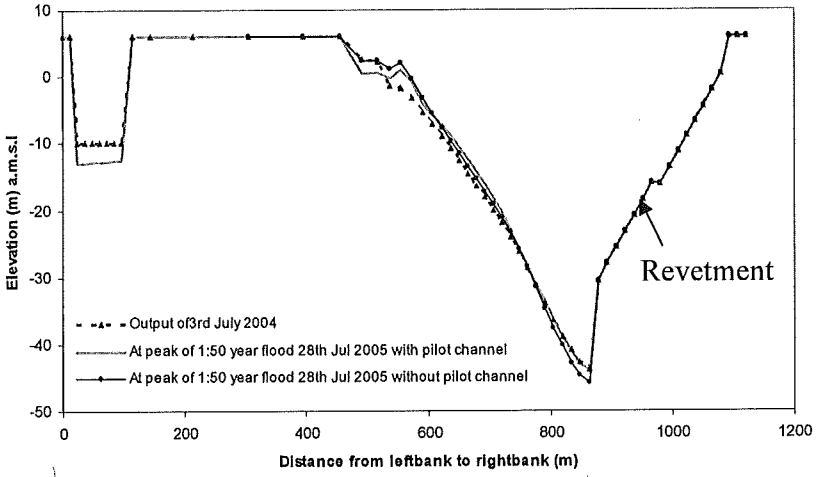

Figure 6.16 a) Bed level change in cross-section of pilot channel and river (J=274, K=0-57)

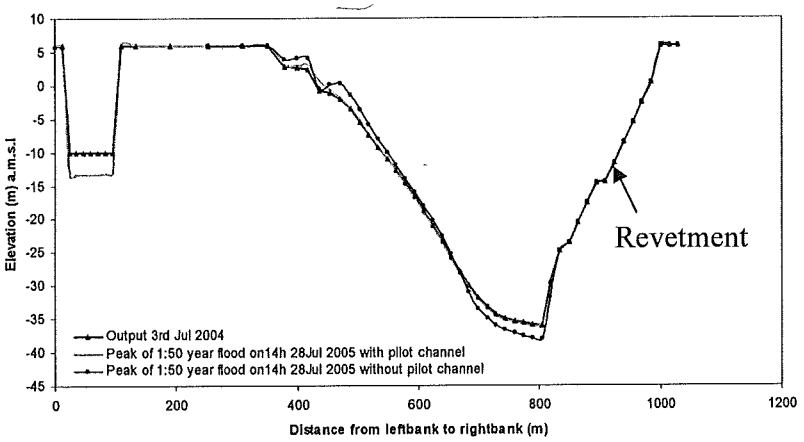

Figure 6.16 b) Bed level change in the pilot channel and river (J=280, K=0-57)

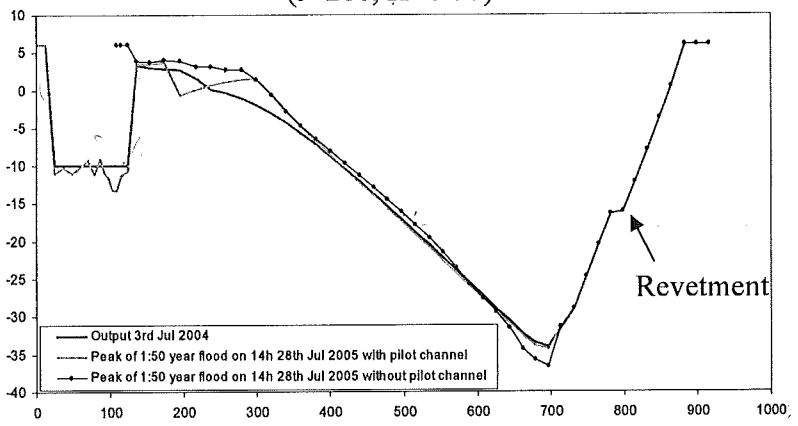

Figure 6.16 c) Bed level change in the pilot channel and river (J=290, K=0-57)

The bed level changes in cross-section during 1:50 year flood was not changing when the pilot channel implemented (see figure 6.16, a, b, c). This seems reasonable, when the amount of flood peak about 3000m^3/s was conveyed through pilot channel. However, in this simulation, the bend cut-off was not reaching the equilibrium state, which means the effective of bend cut-off measure to the river bend will be more strongly.

In addition, the bend cut-off is a good measure to reduce the hydraulic load in the Tan Chau bend, but its material from erosion of pilot channel might be a cause for complex change in downstream from it. The downstream pilot channel is the island where the discharge distribution (see figure 6.14 b), hence the pilot channel could be make a complex thing to down stream of Tan Chau bend.

In conclusion, the bend cut-off measure is very useful measure in order to mitigate the scour in bend, and the bank erosion in outer bend but it needs study more in detail, which take into account the long-term effects.

6.4.4 Permeable groynes

6.4.4.1 General

The permeable groynes are rarely application in lower Mekong river in comparing with revetment. Up to now, there is only one implemented permeable groyne in downstream of My Thuan bridge, Vinh Long province, see figure below.

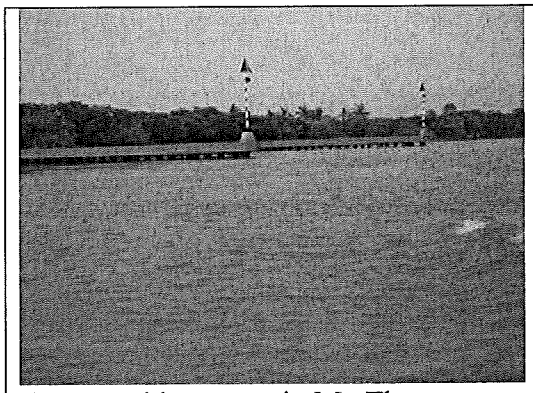

a) Permeable groyne in My Thuan

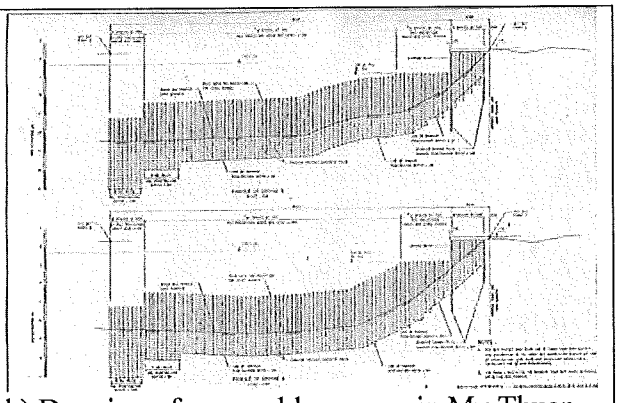

b) Drawing of permeable groyne in My Thuan

Figure 6.17 Permeable groynes in lower Mekong

In principle, permeable groynes generally consist of one or several rows of timber piles, steel piles or reinforced concrete piles, which must be designed to resist the expected hydraulic loads and additional forces induced by floating debris and ship impacts. The main goal of permeable groyne is reduction the velocity near riverbank, where it located. In table 6.4 the advantage and disadvantage were listed.

Advantage of permeable groyne	Disadvantage of permeable groyne
- Reduce the velocity near outer bend - Possibility to use the local material - Construction into the river under moderate flow conditions - Lower cost of construction - Lower cost of repair and maintenance	- Local scour - Narrow the river - Construction side

Table 6.4 . The advantage and disadvantage of permeable groyne.

However, due to the limited time, this study focused more on the design aspect and permeable groyne was not study in numerical model.

6.4.4.2 Design Tan Chau permeable groyne

Hydraulic and morphological design parameters
- Design discharge.

The lower Mekong river, especially at Tien river, the flood discharge does not vary so much in time. Base on the data and analysis in the design discharge is 1:50 year flood, base on the table 6.1 and figure 6.9.

The discharge of the year 2000 is chosen for design permeable groyne.

Q_{ch}=26000m^3/s
- Design water level

The water level is observed during flood 2000. The design water level is corresponded to design discharge of 26,000m^3/s. From the data observation, design water level is about 5.06m. (a.m.s.l)
- Waves

There is no observation of wind data at Tan Chau station. However, in this design the estimate the high of wind is about 1m for 1:50 year.
- Design cross-section from morphological analysis

For the conceptual planning of a protection structure, a design cross-section of the channel has to be determined. A morphological analysis of data available from the monitoring, which contained: Bankfull width, bankfull depth, and the curvature of bend from satellite image.

However, the revetment is existed in this location, that means the bankfull width and bankfull depth is changed.

The design cross-section could be considered from data of 1996 and 2002 when the revetment was not implemented.

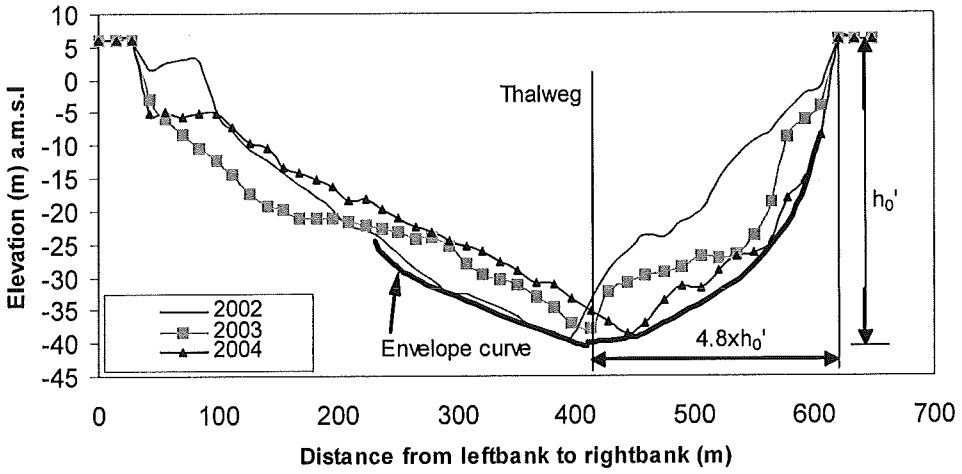

Figure 6.18 The envelope curve of measured cross-section of channel bend

The food plain level: +5.50 (m) a.m.s.l
The bankfull width: B_{ch} = 650 m
The area of cross-section: A_{ch} =16550 m^2
The average water depth at bankfull level: h_{ch}= 25.5m
- Scour

Bend scour:

By applying Maynord formula above, the bend scour is about: h_b = 49.3m.
The bend scour depth y_s=h_b-h_{ch} =49.3-25.5= 23.8 (m)

Local scour:

The local scour depends on the design structure; herein the permeable groynes are going to design, which are proposed single – pile – row-groynes.

Base on Bangladesh guideline:

$$h_1 + y_{s,local} = K\left(h_1 u_1 \frac{B_{ch}}{B_{ch} - b}\right)^{\frac{2}{3}} \qquad (6\text{-}4)$$

Where:

K =$K_{structure}$.$K_{bed\ protection}$.$K_{floating\ debris}$=2.4 x 1.0 x 1.0=2.4 ($s^{0.67}/m^{0.33}$) with assuming there is no bed protection at goyne head, without floating debris.

h_1 =16.5 the upstream of scour hole average water depth (m).
u_1 =1.5 the upstream of scour hole average velocity (m/s).
B_{ch} =650 the width of main channel (m).
$b \geq 4.8h_0'$ =4.8x49.3=236, chose b=150(m) assuming the length of groyne (m).

From (6-4) the local scour was computed:
$y_{s\ local}$ =7.8 (m)

The total scour depth:

The factor 1.2 times is added for total scour due to the combination of different scour types.

$y_{s,0}$=0.2.$y_{s,bend}$+1.2. $y_{s,local}$ =0.2x23.8+1.2x7.8= 14.1 (m)

- Overall length, alignment, and termination of groyne fields

The length, alignment, and termination of permeable groyne are very similar with those elements of revetment. However, the structural layout of groyne field bears a substantially layer number of possible variations of different structure components due to the strong

interference between the most important characteristic properties (porosity, spacing, individual length, etc).

The standard layout of a groyne field consist of a central section with a series of at leats 3 groynes similar in composition and length plus an upstream and downstream termination with shorter groynes (with decreasing length).(see appendix A-6)

Application for Tan Chau case, the protection length is about 1500m with nine groynes. Five groynes are the same length in central section, upstream and downstream termination contains four other groynes. See figure 6.20

- Permeability of groynes

The permeability of groyne is defined base on Bangladesh guideline

The permeability P of a groyne is defined by the ratio of open (non-blocked) area to the total area, which can be expressed by the quotient of internal width s and the distance e between the axis of two adjacent piles (P=s/e, see figure 6.19)

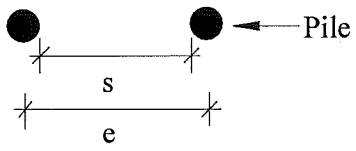

Figure 6.19 Definition of groyne permeability

The optimum permeability of a groyne is dependent on various boundary parameters (flow velocities, local turbulence, grain size distribution, etc) and is strongly interrelated with structural conditions of groyne field (number and length of groynes, spacing in flow direction).

Based on the research result of Bangladesh guideline the permeability of groyne recommended in the table below.

Section	Permeability (%)
First pile near the river bank (groyne root)	
0 to 0.25L_G	50
0.25 to 0.50L_G	60
0.50 to 0.75L_G	70
0.75 to 1.00L_G	80
Last pile in river (groyne head)	

Table 6.5 Recommended pile arrangement for a permeable groyne (L_G is length of groyne)

The minimum permeability of P=0.5 (50%) show in table should kept for constructional reason because of increased pile-driving resistance). Moreover, due to of main goal of permeable groyne is reduction of flow near banks, there for P>60% in this area should be avoided.

- Orientation of groynes

The deviation of the streamline is mainly dependent on the structure included blockage of flow cross-section, which can be described by the length and permeability of structure in relation to the geometrical channel properties. In comparison with the impermeable, spurs groyne, the orientation of permeable groyne is not so important. Because of economical reason, the orientation of permeable groynes is perpendicular with river bank (see figure 6.19)

- Crest level

In order to restrict the hydraulic loads (currents, waves) at higher water levels, groyne may be designed as submerged structure (during peak flood). To reduce this influences, the groynes can be designed with a negative freeboard, they act as slightly submerged groynes and towards the groyne root, the crest level of piles should increase to meet the elevation of the embankment. In case of partly or completely submerged groynes (during high flood level), the installation of navigation signal at the groyne's head is obligatory.

The crest level of permeable groyne can be submerge.

Application for Tan Chau case, using the submerged groynes is used because of economic reason and the specific condition at Tan Chau as well.

The groynes was divided into three part. See figure 6.21

Part one: near the riverbank, the crest level =1.60m (mean water level)

Part two: middle part of groynes, the crest level = - 4.0m (depend on the design cross-section)

Part three: Groyne head part, the crest level = -14.0m (depend on the design cross-section)

- Design of individual groynes

Groyne length:

The groyne length can be computed based on following equation

$$L_G \geq \Delta L + n.(h_0' + y_{s,0}) + 0.5.l_s.\tan(\beta + \theta) \quad (6\text{-}5)$$

and $L_G \leq 0.2$ to $0.4\ B_{ch}$ (6-6)

where

L_G effective length of groyne (perpendicular to the embankment) (m)

ΔL safety margin (minimum ΔL=10) (m)

n cotangent of natural slope of the bed material 1(V):n(H) for Tan Chau n= 3.0

h_0' water depth at the thalweg referred to flood plain level, h_0'= 49.7(m).

$y_{s,0}$ maximum total scour depth related to the thalweg of the undisturbed river bed, $y_{s,0}$ =33.2m

l_s length of scour hole perpendicular to the groyne axis with first estimate $l_s=4y_s$ (m)

θ angle of flow attack between flow line and bankline θ =45 (^{0})

β fictitious angle of flow separation , assuming that β=2 (^{0}), then later it was checked again.

B_{ch} average width of the approach channel B_{ch}=650 (m)

Apply equation (6-5):

$L_G \geq$ 10+3(49.7+14.1)+0.5x4.7.8.tan(45+2)=194 (m)

And apply (6-6)

$L_G \leq$ 0.2x650 to 0.4x650

The length of individual permeable groynes was determined **L_G=195(m)**

Because the length is too large, so that in this condition the submerge permeable groyne is applied more valuable.

- Spacing of permeable groynes

The minimum spacing of permeable groynes determined from formula (see more detail in appendix A.6)

$$S_G = \frac{2}{3}.\frac{L_G}{\tan(\theta+\beta)} \qquad (6\text{-}7)$$

Where: S_G - Effective length of permeable groyne (m)

θ - angle of oblique flow attack (^{0}), in this case assuming is 45^0

β - fictious separation angle (^{0}), $\beta=2^0$

L_G - The length of groynes, L_G=195(m)

So that, minimum of spacing S_G = 121 (m)

The maximum spacing of permeable groynes can be determined:

$S_G=2/3\,\lambda_w$

$$\lambda_w = c_5\frac{C^2h}{2g}$$

where

λ_w relaxation length (m)

C- Chezy coefficient, in the assumption value, C=50 ($m^{\wedge 0.5}/s$), later have to check again.

g acceleration due to gravity, g=9.81 (m/s^2)

h local water depth, h=25.5 (m)

c_5 (-) empirical coefficient for channel properties, c_5=0.85 (see appendix A.6)

so that, λ_w=2437 (m) => S_G=1625 (m)

The fictitious separation angle is determined as function below:

$\tan\beta = c_5.2g.\frac{L_G}{C^2h}$ => $\beta = 3.4^0$ is very close with assumption value above if this value is not close with assumption, then recalculation with new β until it fit.

The distance between two groynes is varied from 121m to 1625 m, so that it is important to make the physical modeling to check and find which distance is more economic and sufficient. However, in this case, the practice design will chose the distance S_G = 300m for safety reason only.

- Design pile:

Due to the limited time, the design of pile is not considering in this study. However, base on the recommended of Bangladesh guideline, the concrete pile was used which has diameter about 1.0m.

In conclusion, the design of permeable groyne parameters are shown in table below.

Terms	Value, define	Notes
1. Design water level		
Low water level	+0.5m	above mean sea level
Design water level	+5.06m	1:50 year flood
Flood plain level	+5.50m	No flooded area
2. Design cross-section		
River width at bankfull discharge	650m	
Channel area	16550 m^2	
Averaged water depth of channel	25.5m	
Relative bend radius R_c/B_{ch}	1.25	measured
3. Design water depth		Maynord formula
Water depth at thaweg	h_0=49.3m	Relate to design water level
	h_0'=49.74m	Relate to design water level
4. Design scour depth		
Total water depth ($h_0 + y_{s,0}$)	63.4m	Relate to design water level
Total design scour depth	14.1m	

Table 6.6 Summary information of permeable groyne design

The groyne length and permeability and crest level shown in table 6.7

Permeability				Crest level	
Chainage	Number	Length (m)	Permeability (%)	Chainage	Level (m)
Ch.00				0	
0 to 0.25 L_G	1	48.75	50%	0 to 30m	+1.60
0.25 to 0.50 L_G	2	48.75	60%	30 to70m	-4.0
0.50 to 0.75 L_G	3	48.75	70%	70 to 195	-14.0
0.75 to 1.L_G	4	48.75	80%		
Ch.End					
Total		195		195	

Table 6.7 Permeability and crest level of permeable groynes.

The design was shown in figure 6.20, 6.21.

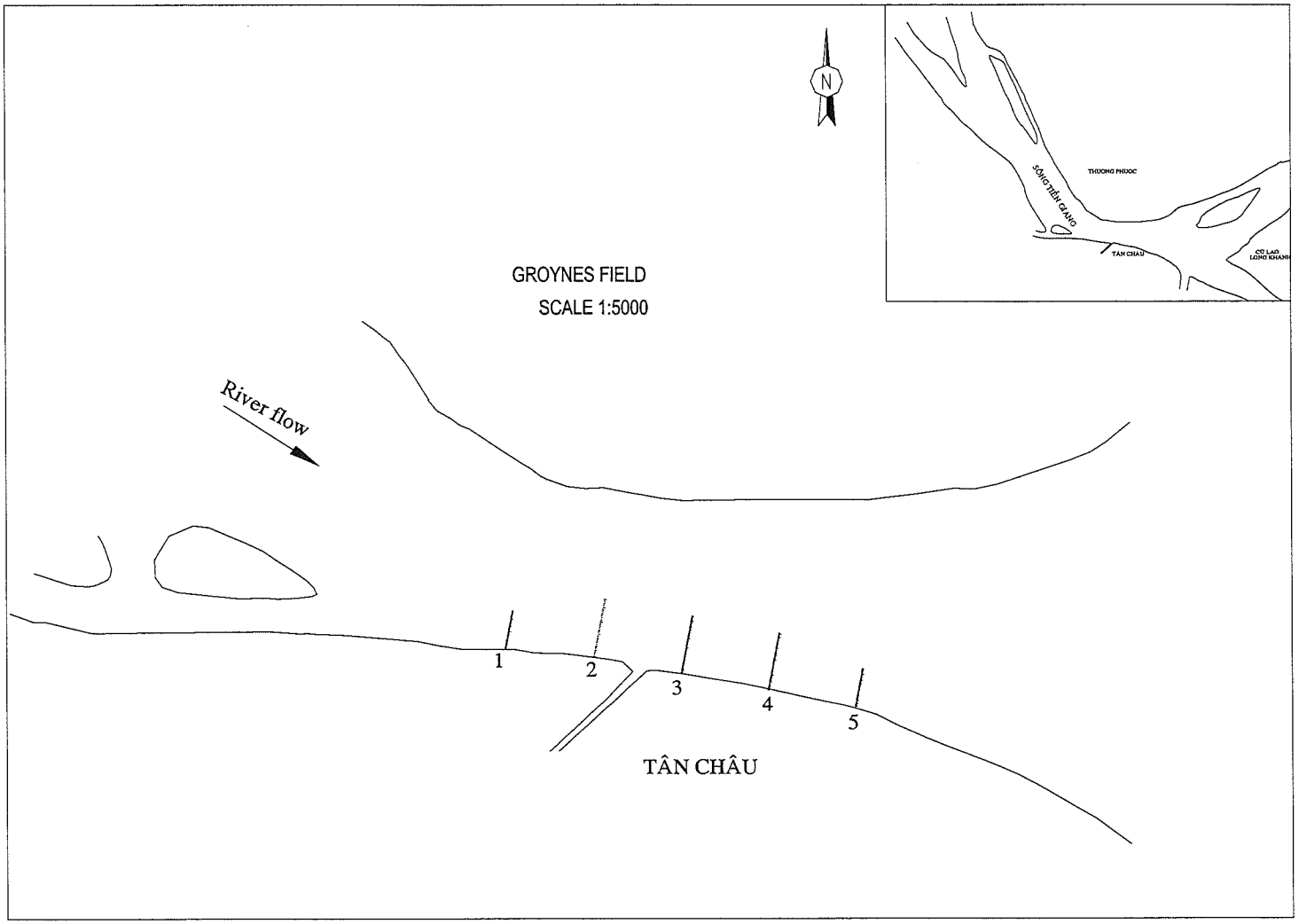

Figure 6.20 Groynes fields at Tan Chau bends

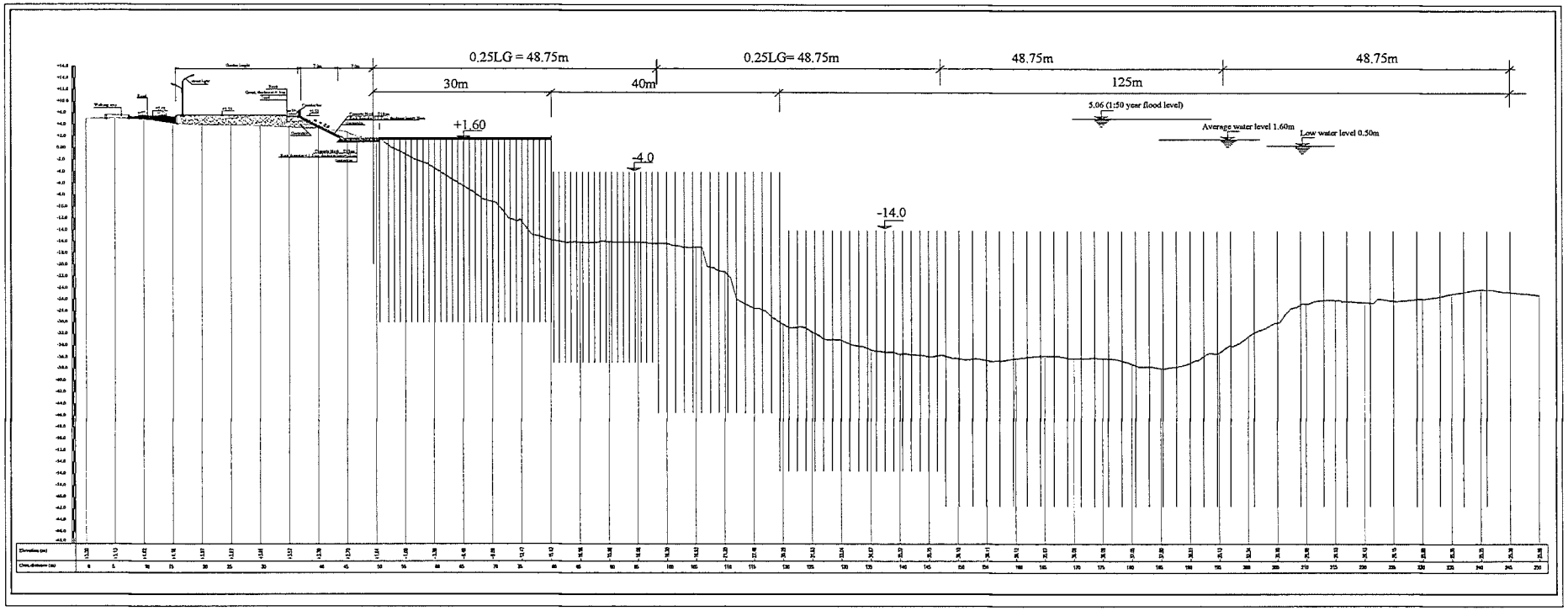

Figure 6.21 Design cross-section of permeable groyne

7. DISCUSSION

7.1 Data and data management

7.1.1 The data of in the lower Mekong river

The study was used many kinds of data, which are different quantity and quality in the lower Mekong river.

First of all the satellite images: This kind of data normally depends on the pixels size, if the quality is high, the pixels size is small, and hence the price is high. In this study, satellite images were collected. The resolution is not so good, that leads much more difficulties during data analysis and GIS analyses steps. Moreover, the map of the year 1937 and 1966 are poor quality, which also produced many difficulties to get the river bankline in the same view in GIS system.

Secondly, the cross-section data used for one dimension simulation (MIKE11) is extracted from the map of 1995, 1996 and at some reaches is updated in 2000. This mixing data can be cause of one-dimension model errors. Moreover, the bank hight (h_b) - one of variable in empirical method improvement were also taken from this cross-section data.

Thirdly, the sediment transport data is limited, based on some observed suspended load (included wash load) in Tan Chau station to establish the relationship between suspended load and water discharge (after reduce the wash load). However, the relation is poor correlation but there is no way in this study. In addition, the geology studies are needed in the lower Mekong river, in particular of tectonic faults.

In conclusion, the data and the data management in lower Mekong need improvement in concerning of quantities and qualities. The data uniform (time and space) is also taken important role in this process. In other words, it is time to make a database bank with contains all data, information related to Mekong river. This database bank is managed by government organization and it can be shared to every professional organization and public. The data and data management is still have many thing to do in lower Mekong river.

7.1.2 The data for Tan Chau- Hong Ngu area

There is no doubt, that Tan Chau- Hong Ngu is one of location in lower Mekong, which has more data than other location. In this study, the topography was used in every year from 2002 to 2004. However, the quality of data is still need improvement. In addition, the lack of geology data and information is one of other reason that leads to the lack analysis in Tan Chau case study (Chapter 6). Moreover, the data of discharge distribution in different reaches of this area is also important key but it was missed.

For future study, data improvement should be the first task in this location; it helps very much for the quality of study.

7.2 Riverbank erosion prediction

7.2.1 Application and improvement of Hickin & Nanson (1984)

Nickin & Nanson (1984) give a method to predict the bank migration in Canada based on 189 observed bends, they reported that, the rates of riverbank erosion depend on the ratios between the radius of curvature and river width at the bend. And they found that the maximum rates occurs when this ratios equal to 2.5 (E_{max} when R/W=2.5)

However, based on the data from satellite images and old map, the application of this method to the lower Mekong river are not fair. Therefore, the reasons could be the local conditions of the lower Mekong are different with Canadian rivers. It might be a strong impact of tectonic faults, the mixing soil in alluvial area such as clay box, sandy, muddy, was discussed in this study.

Moreover, from the author point of view, the adjustment of Hickin & Nanson (1984) was reported based on locally condition of the lower Mekong river. Especially, based on the data of 15bends in different time of observation and the different bank high of river bend was taken into consideration. The bankfull discharge was taken into computation of this improvement in concerning of stream power. At least, there is an adjustment of Hickin & Nanson (1984) for the lower Mekong river.

Nevertheless, the riverbank erosion prediction is very difficult task of river engineering. The simplifying by application of empirical method is still a tricky and using for locally.

In order to predict, a general method of riverbank prediction of lower Mekong is needed in future. The data should be adequate and sufficient, the need of observed near bank velocity and bank material at some places in lower Mekong river have to taken into this general process.

In conclusion, there are only 15 bends in different period of time is not enough data to improve or to establish the riverbank prediction in the lower Mekong river. The improvement Hickin & Nanson (1984) is an initial step of prediction of riverbank erosion. It needs more data to calibrate and verify. The used of data from satellite images is very good ideas, because of in future the satellite images will have an acceptable cost and higher resolution.

7.2.2 Bank erosion modulus in MIKE21C

The numerical model was treated as other hand of riverbank erosion in this study. The equation of riverbank erosion in MIKE21C reported that:

$$\frac{\partial E}{\partial t} = -\alpha \frac{\partial z_b}{\partial t} + \beta \frac{\partial q_s}{h_b} + \gamma \qquad (7\text{-}1)$$

Where as:

$\frac{\partial E}{\partial t}$ - The riverbank erosion rates

$\frac{\partial z_b}{\partial t}$ - The bed level in front of riverbank term

$\frac{\partial q_s}{h_b}$ - The sediment capacity term

α - The calibration parameter

β - The calibration parameter

γ - the independent bank erosion term, this parameter is proposed the bank erosion is not depend on the flow, or sediment transport.

The equation pointed out clearly that, the riverbank erosion rate depended on the calibration parameters. However, in an early state of numerical model development, bank erosion prediction along the lower Mekong river was tested with the model. The the sensitive of calibration parameters above were checked.
From author point of view, the riverbank erosion module in MIKE21C need very fine grid cells and very detail of bathymetry. The influence of α, β calibration parameters in this process is not so stronger than γ in this model.

The riverbank erosion module computed the update grid in every time step it needs and takes a larger of hard disk capacity. Moreover, it must be careful with the area of update grid in the model, otherwise it becomes unstable model due to grid change (see figure 7.1 and 7.2)

The calibration step will be more difficult to manage all calibration parameters because of erosion material from bank erosion module.

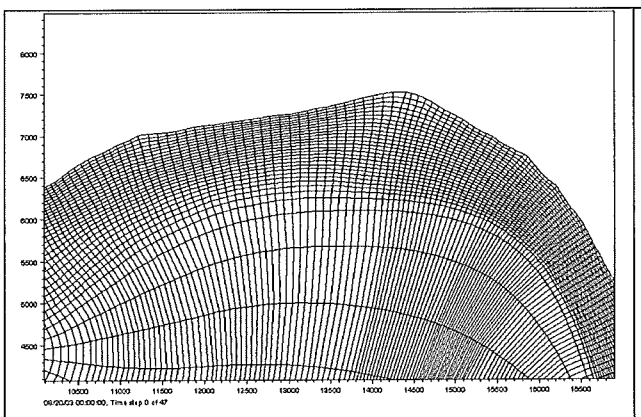

Figure 7.1. Initial grid at Hong Ngu bend

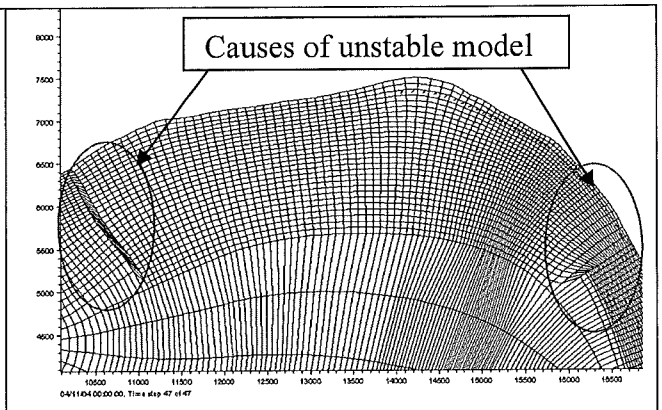

Figure 7.2. Update grid in unstable case

In conclusion, this module should be separately study and more detail in future, and the location of study area have to be available data in detail.

7.3 Model calibration and verification

Working with numerical model, the most challenge is calibration model. In other words, how hard the model was built the difficulty of calibration a model would be.

The calibration of model that needs modeller's understanding of system works in numerical process as well as physic of phenomena in real world. Due to the lack of data, information, and author knowledge, the calibration spent a lot of time but the result only give the tendency of real world situation.
The area of simulation - Tan Chau, which included bend, island, bifurcation and confluence, the lack of sediment transport, lead many difficulties in this process.

The lesson learnt from the calibration process of this study that, it is important to implement systematically (step by step). In other words, the hydraulic model is calibrated first, then helical model. After helical flow module calibration is sediment transport module. At the end, the morphology is calibrated. By doing so, the people can avoid the mixing understanding in the system and they can manage the calibration parameters. The calibration was stop when the acceptable fit of model and real world.

During the study, there is a big problem with sediment transport, the computational results is so smaller than the observed data. According to author's experience, it is normal when the sediment transport is different between computed results and observed, but this different is around ten times. Here in this model, it found that about 28 times. The reason can be explained that: due to lack of sediment transport data, the input of model is derived from a relationship between discharge and sediment transport (this relationship is not good).

In addition, verification is also very important step. The main goal of this step is the results checking. If the results are acceptable thence it is stopped, if not, the calibration has to be implemented again.

In practice, the calibration is very difficult task of numerical model. The acceptable results have to be based on a number of things, which could be the certainty of surveyed data, the good schematization, the effect of constructing revetment at Tan Chau, the effect of hydrograph and the model adjustment. During the study, the calibration step has problem with sediment transport, but at the end, the morphology result is acceptable. It could be called a properly calibration under lack of data and knowledge.

7.4 Mitigation measures and case study at Tan Chau

The mitigation measures in concerning of bank erosion or bank protection have a process, which included the understanding of problem, pre-feasibility design, feasibility design, final design, construction, operation and maintenance. Through those steps, the mitigate measure is decided for the particular location. However, there are a number of riverbank erosion locations in the lower Mekong river, the government should have a plan where is critical or moderate problem in order to preventive urgently or gradually.

Moreover, to mitigate the riverbank erosion in the lower Mekong is costly because of the vast area with many locations. The rates of riverbank erosion are different. The simple measures would be very economical measures, which made by local people such as timber poles, sand bags, etc. These measures are needed to study and guide to the public. The local government should plan where these kinds of measures can be implemented in order to increasing the effects of simple measures.

7.4.1 Revetment

The revetment is common measure in the lower Mekong river. However, the design of this measure is always narrow the river cross-section in this area, which leads to scour in front of revetment. In other words, the cost for the falling apron has to be included during considering process, it is not extra cost of construction at all.

In this study, base on numerical simulation, the Tan Chau revetment was installed in the model and it leads about 10m scour in depth in front of this revetment. The different cost (ending cost is about twice times of initial cost) of this construction have to be draw the lesson.

In addition, the maintenance has to be implemented at Tan Chau revetment. It is not only observed in yearly flood but it is important to make measurement before and after flood season. The material need available to fill the scour hole before flood season, and end of flood season should has to taken into account in maintenance process. The government should prepare some additional material for to fill the scour hole in emergency case at Tan Chau revetment.

The cost of revetment is not only at Tan Chau but also other locations have to take into account the maintenance cost.

7.4.2 Bend cut - off

The bend cut -off and permeable groyne are two kinds of possibility of preventive measures in lower Mekong river. However, the use these measures have to be study carefully, which takes into account the effect in long term.

Especially, the bend cut seems an economical measure but its effective depend on the river change in time. This study was simulating the bend cut solution but it is fixed bank simulation by use of pilot channel. In practice, the bank and bed level of pilot channel are movable, which leads to increase the conveyance capacity in the pilot channel until it matches the equilibrium state. However, the bend cut-off is also a risky measure; the deposition area in downstream and the risk of sand bar in upstream of pilot channel could be reasons.

7.4.3 Permeable groyne

The permeable groyne is a very good measure but it need more detail study to apply it in the lower Mekong river. This study based on the Bangladesh guideline to make a roughness design of Tan Chau revetment. The basic of calculation reported in appendix A-6. However, it appeared that less suitable in specific location at Tan Chau. This reason can be explained that, the river is quite depth, the scour depth is also large, the velocity is rather high, and the river is narrow.

7.4.4 Estimate cost

Herein the table 7.1 the cost was estimate in comparison with three kind of measures. The impacts to the environment, the impact to the society, etc are not comparable in this table. The only construction cost estimations proposed to mitigate the Tan Chau bend are reported.

Type of structures	Cost (million euro)	Order	Note
Permeable groyne	-	1st	Not available but estimate based on real conditions
Revetment	9	2nd	Existing
Bend cut-off	2.5	3rd	Propose

Table 7.1. The cost estimates for different kind of mitigation measure at Tan Chau

In conclusion, it is not only Tan Chau but also other locations, the study on all possibility measures should taken into account in bank protection project in the lower Mekong river. Whether bend cut-off or permeable groynes, or revetment or others have to be studied carefully before making decision. Although, the study was only focus on Tan Chau locations, which three kinds of measures but this process could be apply for other critical location such as Long Xuyen, Sa Dec or Vinh Long.

8. CONCLUSION AND RECOMMENDATION

8.1.Conclusion

• The data in the lower Mekong river needs a improvement in terms of quantity, quality and a sufficient management.

• The application of empirical method (Hickin &Nanson (1984)) has not so good results, the modified version is still a question mark because of lack data. It appears that, the local conditions such as: active tectonic faults, clay box, sandy and muddy soil have strong influence to a general empirical method. In conclusion, a general empirical method for particular condition of the lower Mekong river is needed.

• The ideas of use satellite images for establish the riverbank erosion is very good. Nowadays, many satellites were launch, hopefully the price become reasonable with a high quality of satellite image.

• The bank erosion can be predicted by MIKE 21C, but this numerical model needs very fine grid, detail information at the river bank (near bank velocity, sediment...). It should be implemented by a separate study.

• The simple measures (timber poles, sand bags, etc), which make by local people are very useful in the lower Mekong river. However, it needs more detail study and clarify in terms of sufficient use. In other words, the government should guide people where, and how to apply this kind of measure in order to get high sufficiency.

• The falling apron have to take into the design process as the part of the revetment construction, it is completely not the extra cost, which happens during the constructing time.

• The maintenance takes an extremely important part in the mitigation measures in the lower Mekong river. Especially, the Tan Chau revetment needs observations, maintenance. It is not only observation before flood season, but also after flood season.

• The bend cut is possible alternative in the lower Mekong river, but it needs very careful study, which takes into consideration long term effects.

• The permeable groynes are very good measures in term of mitigate the river bank erosion, however it appears less suitable for particular condition as Tan Chau (depth water, high velocity, large scour hole).

• It is not only for Tan Chau, but also for other locations, it is better to take into consideration whether a revetment, a bend cut-off or a permeable groynes before making decision.

To prevent (predict and mitigate) of riverbank erosion is very challenging task in river engineering, especially in case of insufficient data and lack of knowledge. Therefore, many limitations and constraints can be shortly listed as follows

• There is no double that there are many uncertainties for the satellite images and old map data (resolution, cloud matters, geo-correction, and tidal influence).

• It is clear that there are many uncertainties for the hydrological data (river discharge, water level, sediment transport) relating to the methods of estimation and measurement of data. Effects of tidal are not profoundly studied in this thesis. In practice, these effects can also make riverbank erosion problems more serious.

• The dynamic flow regimes in lower Mekong river, which is a typical transition zone between rivers and the sea, are very strong and steady flow computations will hardly simulate exactly. The model adjustment can be other effects to the result of simulation models.

• The simulation was established during the construction time, which means the effect of constructing structures effect to the model results.

8.2 Recommendation

8.2.1 Data and data management

• The data of study was collected from many sources in many different organizations. It is essential to establish the database bank, and the data have to be uniform in time and space.

• The satellite images is taken extremely important part of study on master-plan, the high resolution is more essential.

• There is a need for better monitoring of eroding riverbanks and yearly reporting on bank erosion and progress of bank protection works.

• There are only five key hydrological stations in lower Mekong are not adequate data to study for the lower Mekong river. It is recommended that to establish the network of hydrological observation in lower Mekong have to be taken into account.

8.2.2 Prediction of riverbank erosion

• The empirical method takes an important role in order to predict the riverbank erosion. The ideas used of satellite images are very good for the lower Mekong river. Nowadays, there are many satellites have been established, promising that the acceptable prices and high accuracy images are available in futures. However, it should be combined with many observed data such as soil material, hydrology, and geology for riverbank prediction.

• The MIKE21C can predict the riverbank erosion but it needs more detail study. This study should be done individually.

• The prediction of riverbank erosion needs a general method for particular condition in the lower Mekong

8.2.3 Mitigation measures

• It is clear that, master plan are important part of future development of the lower Mekong river. An integrated plan for bank protection should take into account the long term, short term, socio-economic and environment aspects, while not neglecting the importance of the rivers and canal system for inland navigation should be recommended. This master plan should include: water management, drinking water supply, floods, dikes, bank erosion, zoning

along the rivers (free space for natural developments), navigation, ecology, relocation of riparian people to other areas, legislation for living along riverbank, sand excavation, etc.

- More clarity in non-structural measures and procedures (early warming, evacuation plans, compensation, etc)
- There is a need for improvement of design and maintenance guideline.

- There are three kinds of mitigation measures could be more focus study in detail, and it should be taken into consideration in lower Mekong river are revetment, bend cut-off and permeable groynes.
- The falling apron have to be take into account during the design process for revetment. The better prediction of scour hole development is recommended.

REFERENCE

Allmendinger.N.E, et al (2005) "Geological Society of America; January/February 2005 vol117, no.1/2

ASCE, (1998) Task committee on Hydraulics, Bank mechanics, and Modeling of River Width adjustment, River Width Adjustment, II Modeling, ASCE, 124, 903-917

DWW/MARD (2003), "Bank erosion in Mekong delta and along Red River in Vietnam", *Mission report*, Delft, The Netherlands. (2003)

Darby.S.E and Thorne.C.R (1996), "Development and testing of riverbank –stability analysis", *ASCE*, 122, 443-454.

Edited by Thorne.C.R et al(1993)," River, Coastal and shoreline protection"

Engelund, F., and Fredsoe, J. (1982). *''Sediment ripples and dunes.''* Annu. Rev. Fluid Mech., 14, 13–37.

Julien, P. Y., and Klaassen, G. J. (1995). *''Sand-dune geometry of large rivers during floods''* J. Hydraul. Eng., 121(9), 657–663.

Government of Bangladesh, Ministry of Water Resources (2001) *"Guidelines and design manual for standardized bank protection structures"*

Hagerty.D.J at al(1991), "Piping/Sapping erosion I: Basic considerations", *ASCE*, 117, 991-1008.

Hickin.E.J and Nanson.G.C (1984) "Lateral Migration rates of river bends" *ASCE*, 110, 1557-1567.

Hudson.P.F and Richard.H.K(2000)." Channel migration and meander-bend curvature in the lower Mississippi River prior to major human modification", Geology: Vol. 28, No. 6, pp. 531–534.

Hoang Dinh Co / Mekong river, Potential life and threats for Vietnam

Klaassen.G.J and Masselink.G (1992), "Planform changes of a braided river with fine sand as bed and bank material", *5th International symposium on river sedimentation*, Karlsruhe, Germany.

Klaassen.G.J, Mosselman.E and Bušhl.H (1993), "On the prediction of plan form changes in braided sand-bed rivers", *Hydrolic and enginerring*, Washington, USA.

Hydraulic

Keller .R.J. (2005) *"Guideline for design of bank stability and protection using rip-rap"* CRC for Catchment Hydrology, Australia 2005

Louis Delaporte / Francis Garnier. "A Pictorial Journey On The Old Mekong: Cambodia, Laos, Yunnan". *The Mekong Exploration Commission Report(1866-1868)_ Volume 3.* White Lotus Press 1998, Bangkok Thailand

Le Manh Hung, et al (2003), "Prediction of Riverbank sliding and deposition in lower Mekong delta, mitigations measurement strategies" *National project,* Ho Chi Minh city, Vietnam.

Linsley.K.R, et al (1982), "Hydrology for Engineers", Third edition, International student edition.

Mosselman.E (1992). "Mathematical Modeling of morphology processes in River with erodible cohesive bank." PhD thesis, Delft Univ.of Techno., Delft, The Netherlands.

MIKE21C – Scientific documentation DHI water & Environment, .

Nagata.N, Hosoda.T and Muramoto.Y (2000) "Numerical analysis of river channel process with bank erosion", *ACSE*, 126, 243-252.

Ngo Thi Nguyet (2004) " Constructing observation and stability assessment of Tan Chau revetment", construction report, Nation project Code KC08-15, Technology and Science Ministry, Vietnam.

Osman, A.M., and Thorne, C.R. 1988. *"Riverbank stability analysis"* I: Theory. Journal of Hydraulic Engineering, 114(2), 134-150.

Olesen.K.W &Tjerry.S (2002), "Morphological Modelling of Chaktomuk Junction"

Pilarczyk.K.W (2004) "River bank protection workshop", *Presentation of short course,* Hanoi, Vietnam.

Przedwojski, B., Blazejewski, R. and K.W. Pilarczyk, 1995, RIVER TRAINING TECHNIQUES; Fundamentals, Design and Applications, *A.A. Balkema Publisher*, Rotterdam.

Pilarczyk, K.W., (editor) (1998), Dikes and revetments, Published by A.A Balkema, Rotterdam.

Sarker.M.H et al (2002). "Developing and updating empirical methods for predicting morphological changes of the Jamuna River"

Struiksma.N and Crosato.A (1989)." Analysis of a 2-D bed topography model for rivers", American Geophysical Union, River Meandering Syunsuke Ikeda and Gary Parker editors, 157-180.

Thorne, C.R., and Tovey, N.K (1981)." Stability of composite river banks" Erth Surface processes and Landforms, 6, 469-484

Thoma.D.P, Gupta.S.C, Bauer.M.E (2001), "Quantifying River Bank Erosion with scanning laser altimetry" International archives of Photogrammetry and Remote Sensing, Volume XXXIV-3/W4 Annapolis,MD,22-24 Oct,2001.

Van Rijn, L. C. (1984a) *''Sediment transport, Part I: Bed load transport.''* J. Hydraul. Eng., 110(10), 1431–1456.

Van Rijn, L. C.(1984b). *''Sediment transport, Part II: Suspended load transport.''* J. Hydraul. Eng., 110(11), 1613–1641.

Van Rijn, L. C. (1984c). *''Sediment transport, Part III: Bed forms and alluvial roughness.''* J. Hydraul. Eng., 110(12), 1733–1754.

Appendix A-1
AVAILABLE DATA

A.1.1.Topography data

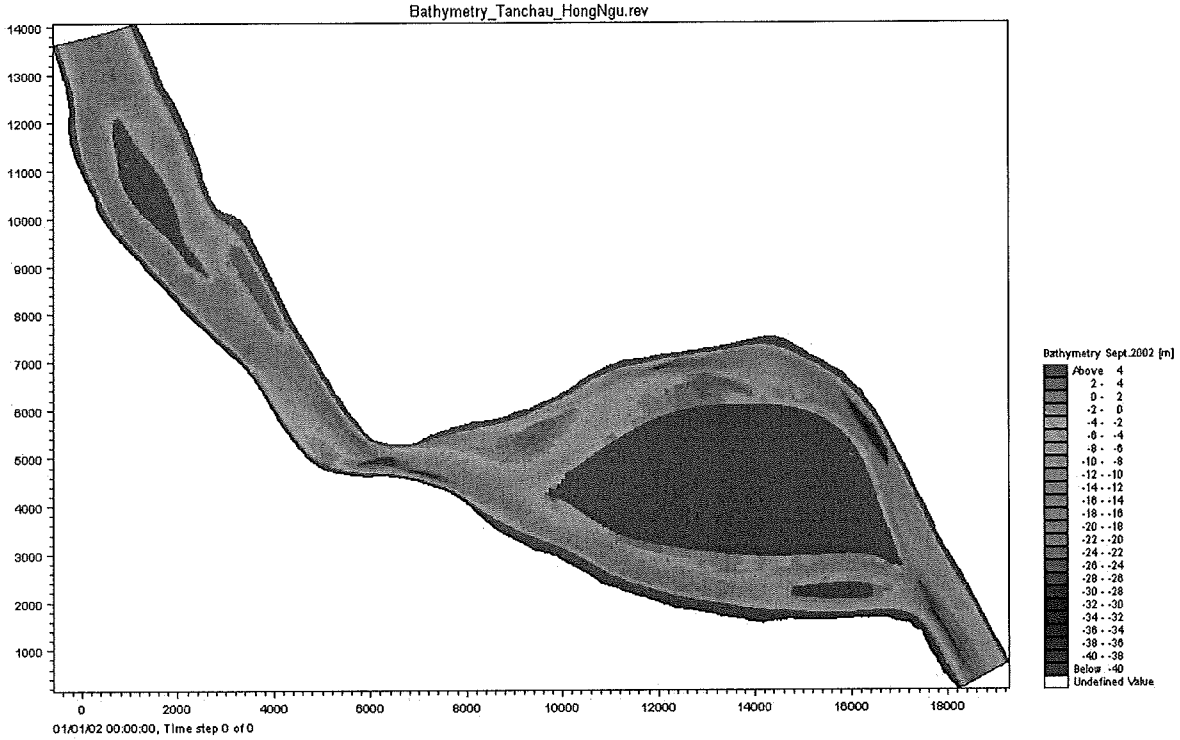

Figure A.1. 1. Bathymetry 2002

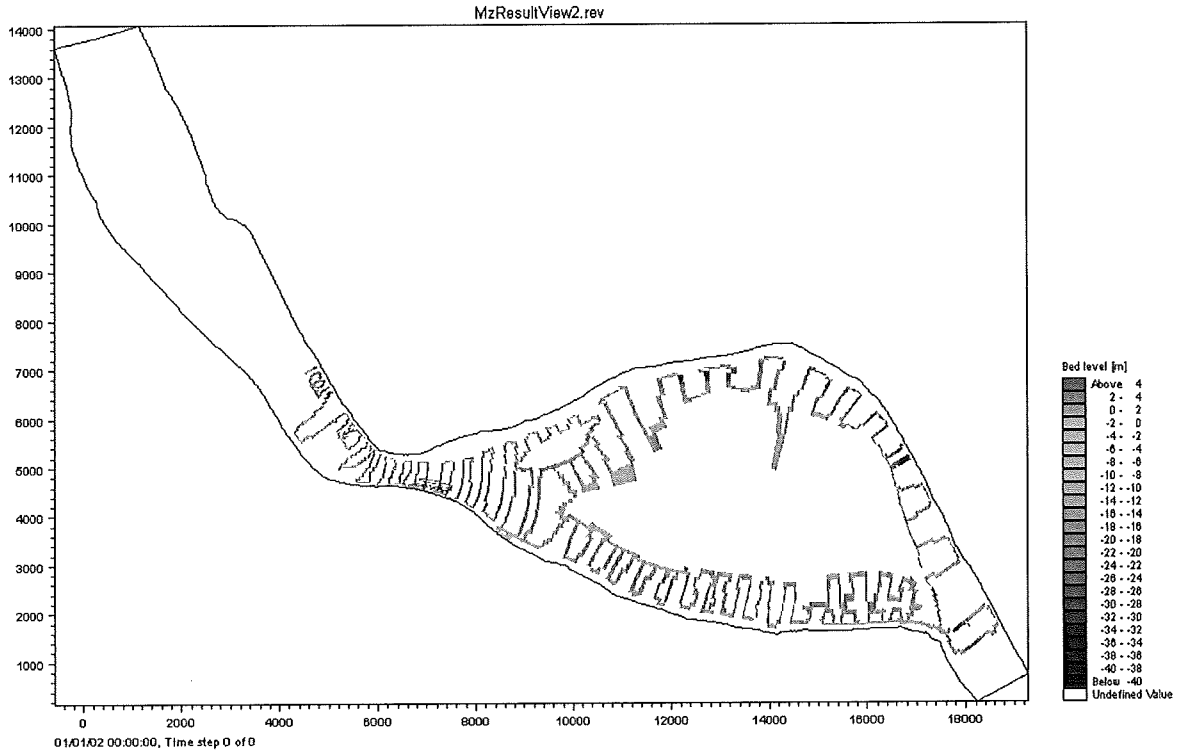

Figure A.1.2. Bathymetry 2003

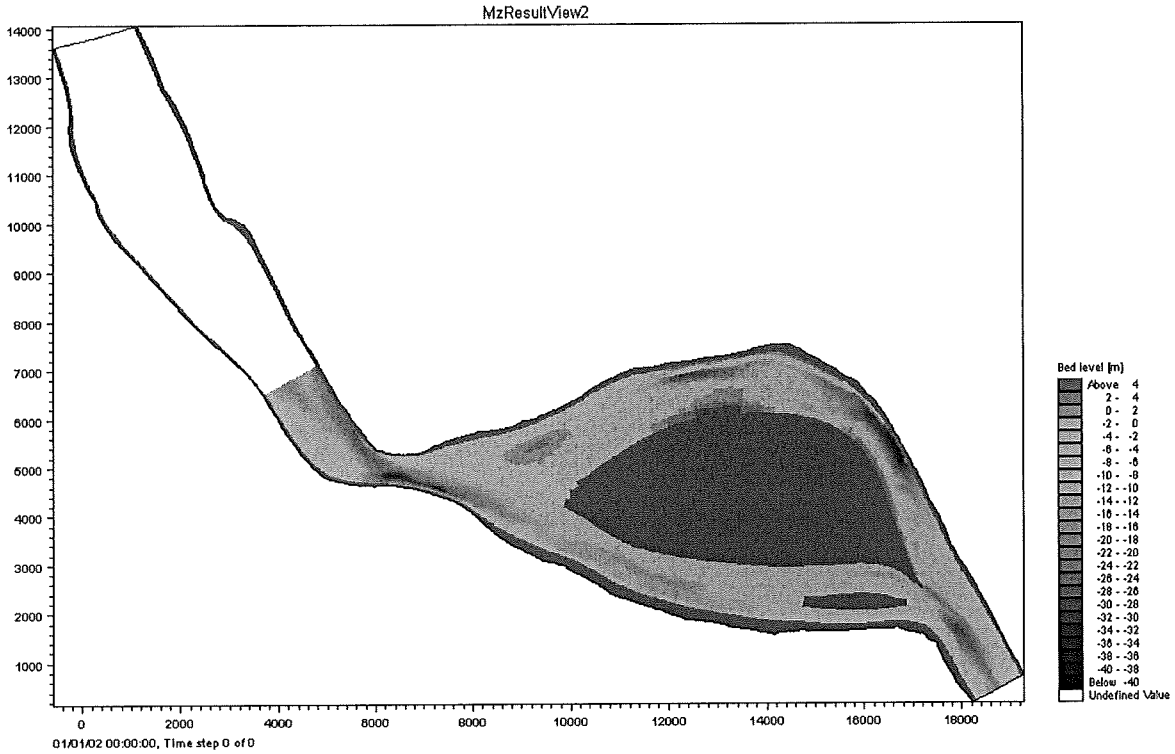

Figure A.1.3. Bathymetry 2004

A.1.2. Hydrology

A..1.2.1. Discharge

The discharge at Tan Chau from 1996 to 2004 hydrograph

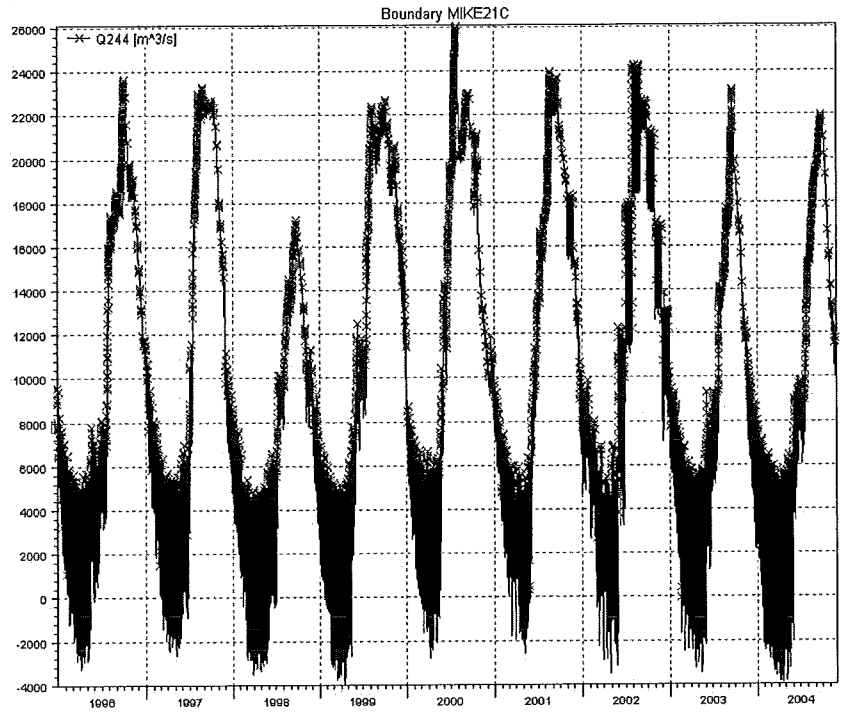

Figure A.14. Discharge at Tan Chau station from 1996 to 2004

A.1.2.2. The ADCP surveyed at Tan Chau –Hong Ngu area

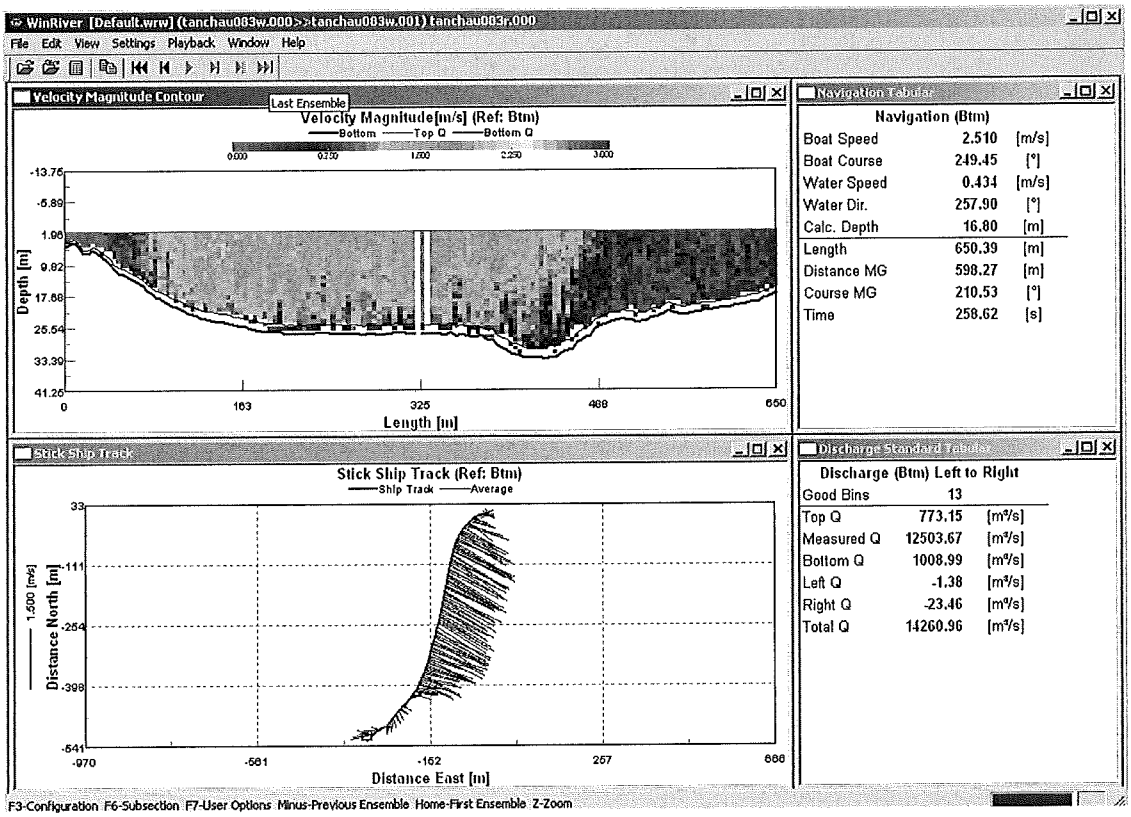

Figure A. 1.5. Discharge observation at Cross-section Q1.

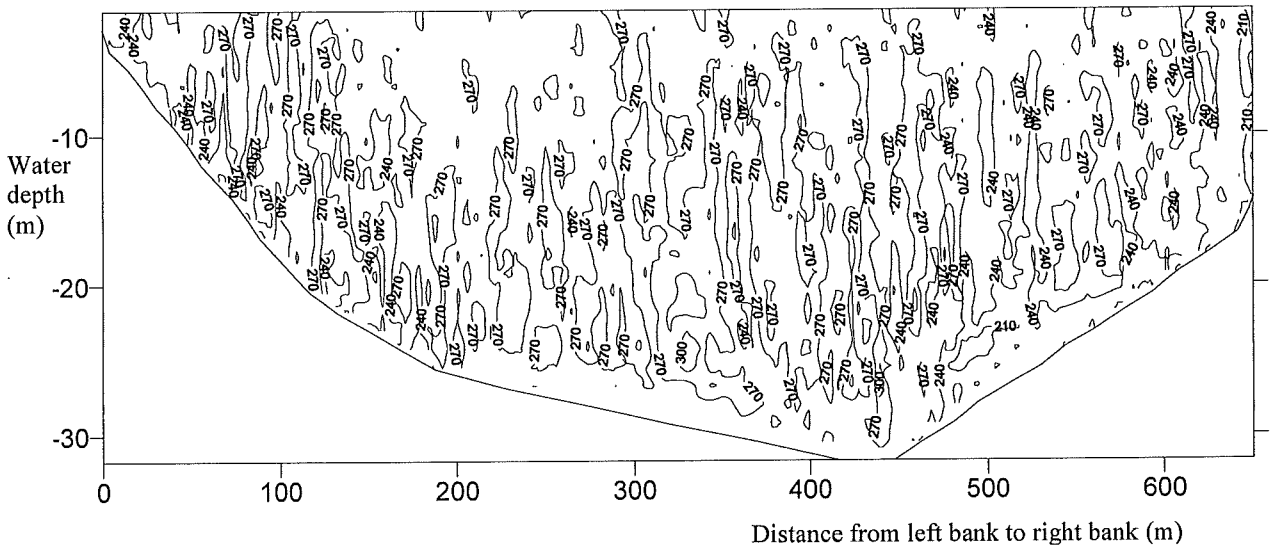

Figure A. 1.6. Velocity contour in cross-section Q1, surveyed 9h05'6th, August 2003.

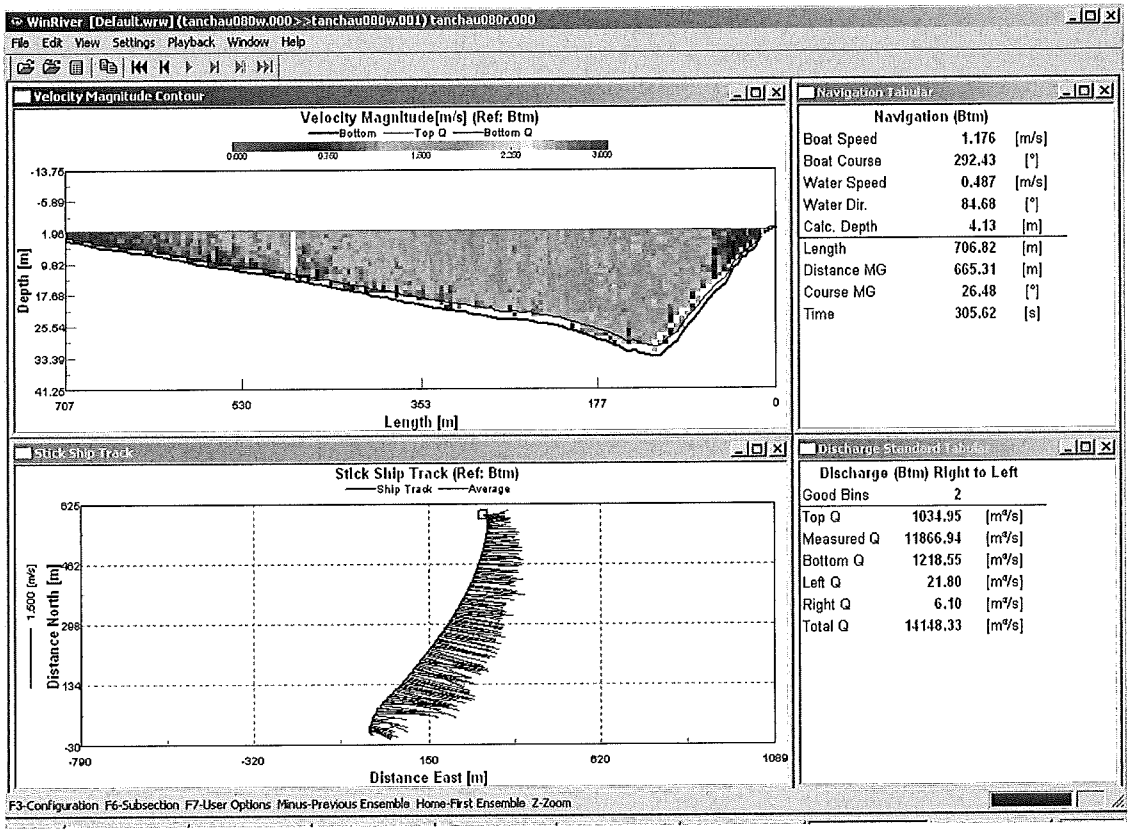

Figure A.1.7. Discharge observation at Cross-section Q2.

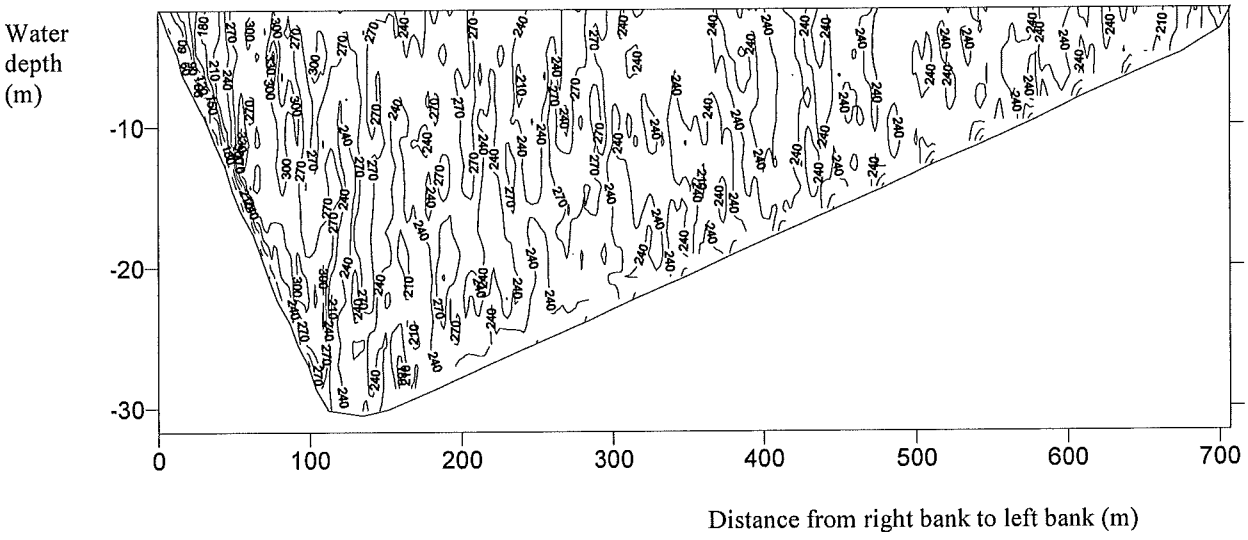

Figure A.1.8.Velocity contour in cross-section Q2, surveyed 8h40'6th, August 2003.

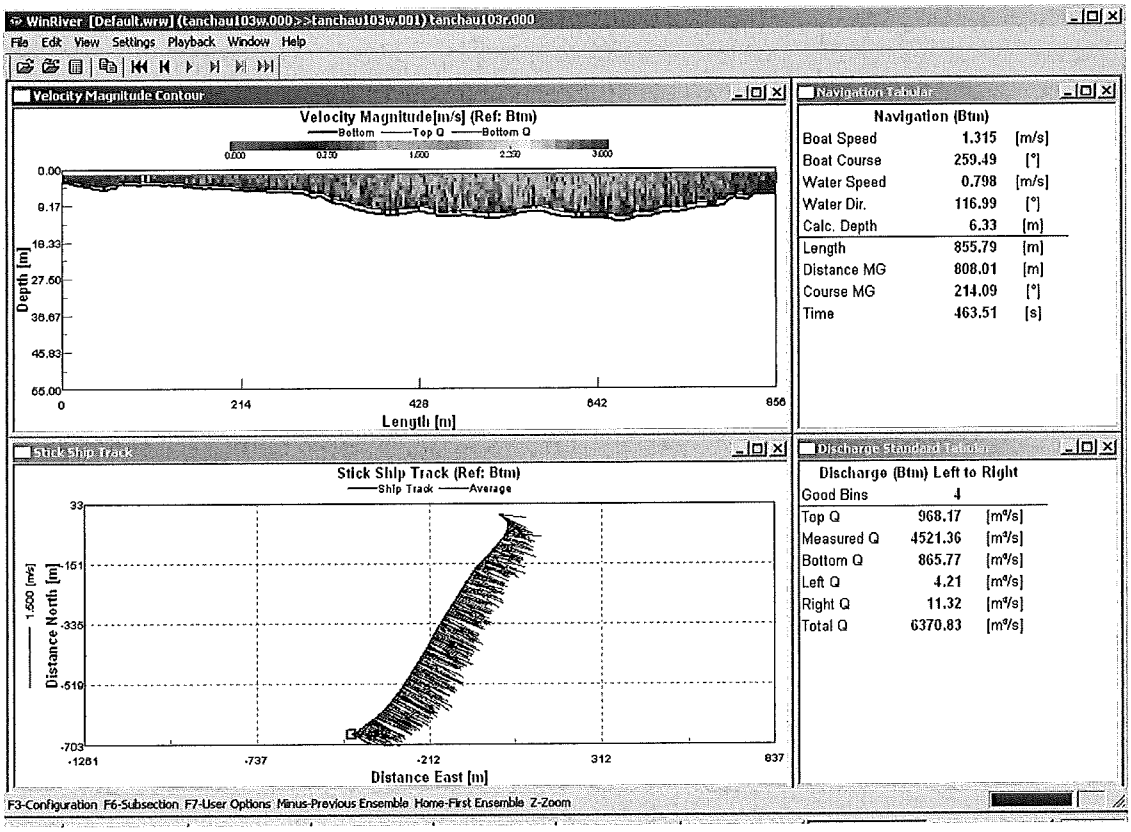

Figure A.1.9. Discharge observation at Cross-section Q3.

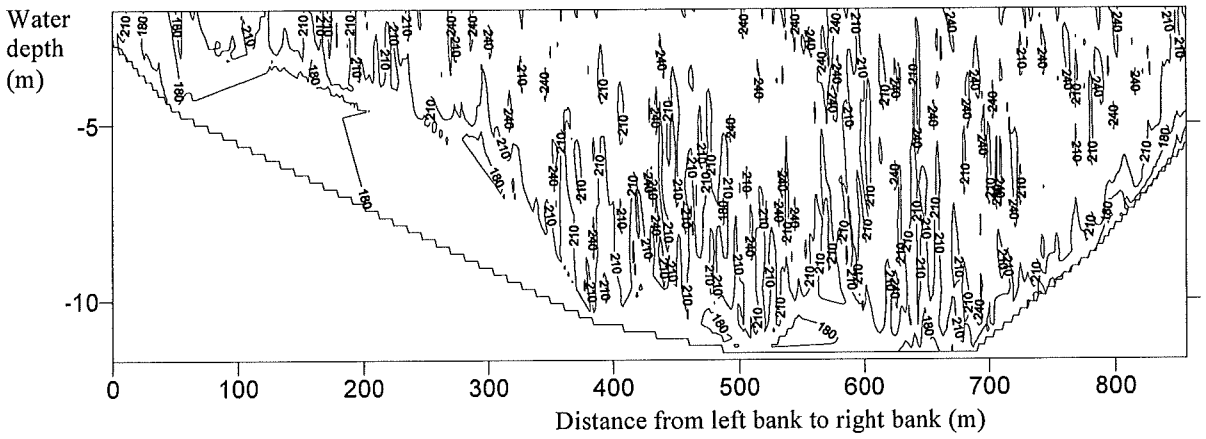

Figure A. 1.10. Velocity contour in cross-section Q3, surveyed 9h14'7th, August 2003.

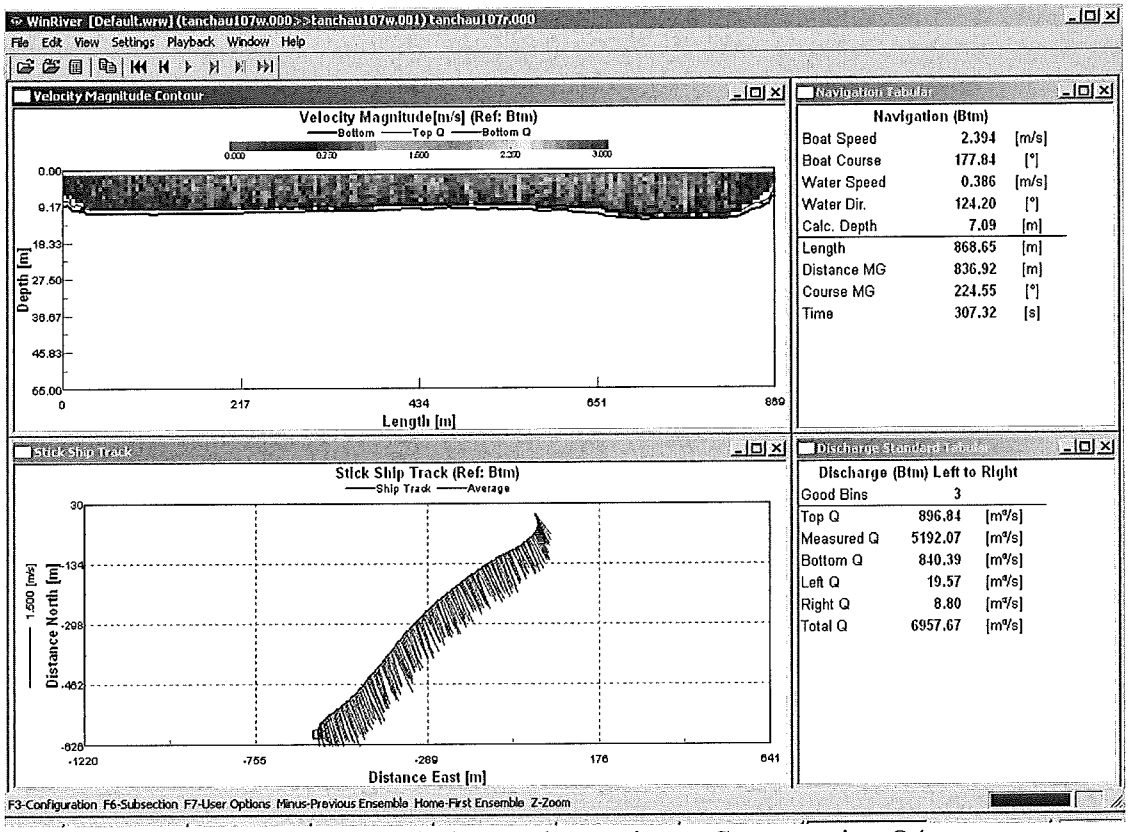

Figure A. 1.11. Discharge observation at Cross-section Q4.

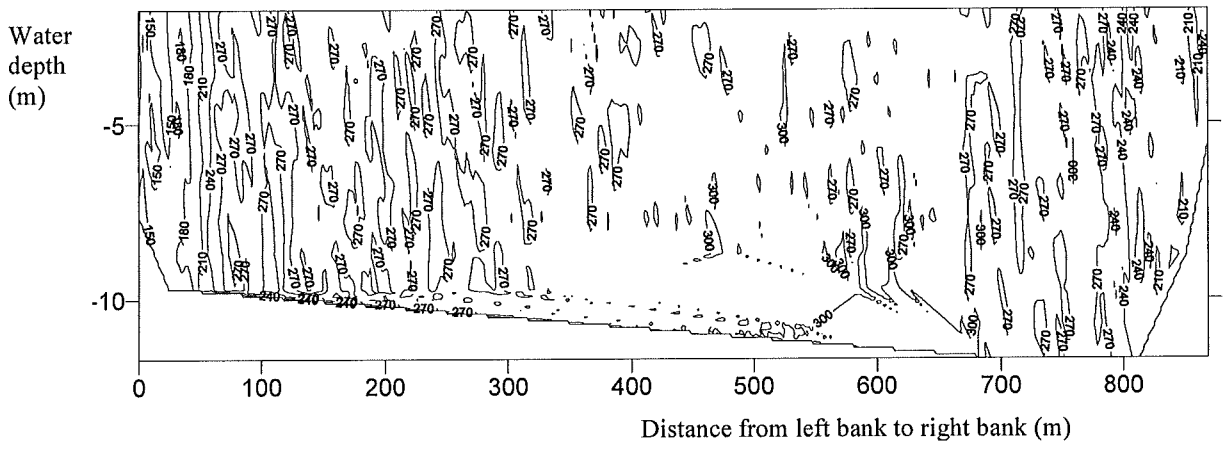

Figure A.1. 12. Velocity contour in cross-section Q4, surveyed 14h47'7th, August 2003.

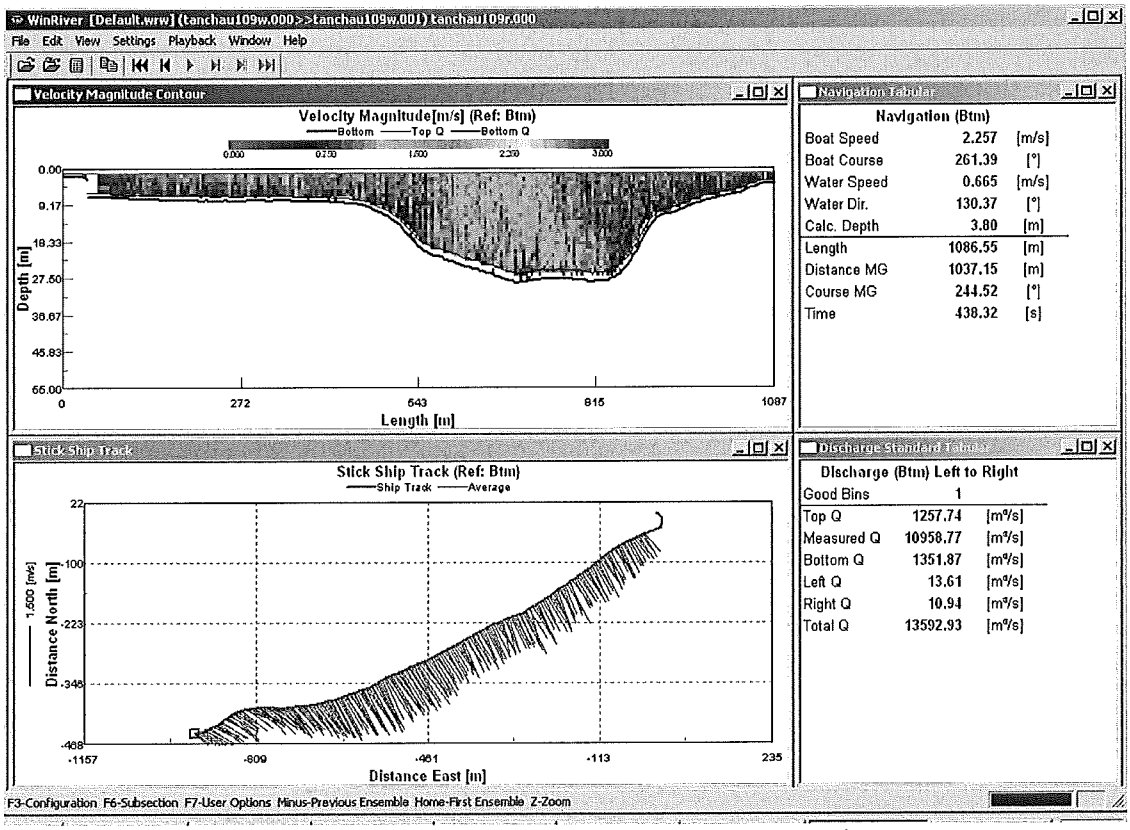

Figure A. 1.13. Discharge observation at Cross-section Q5.

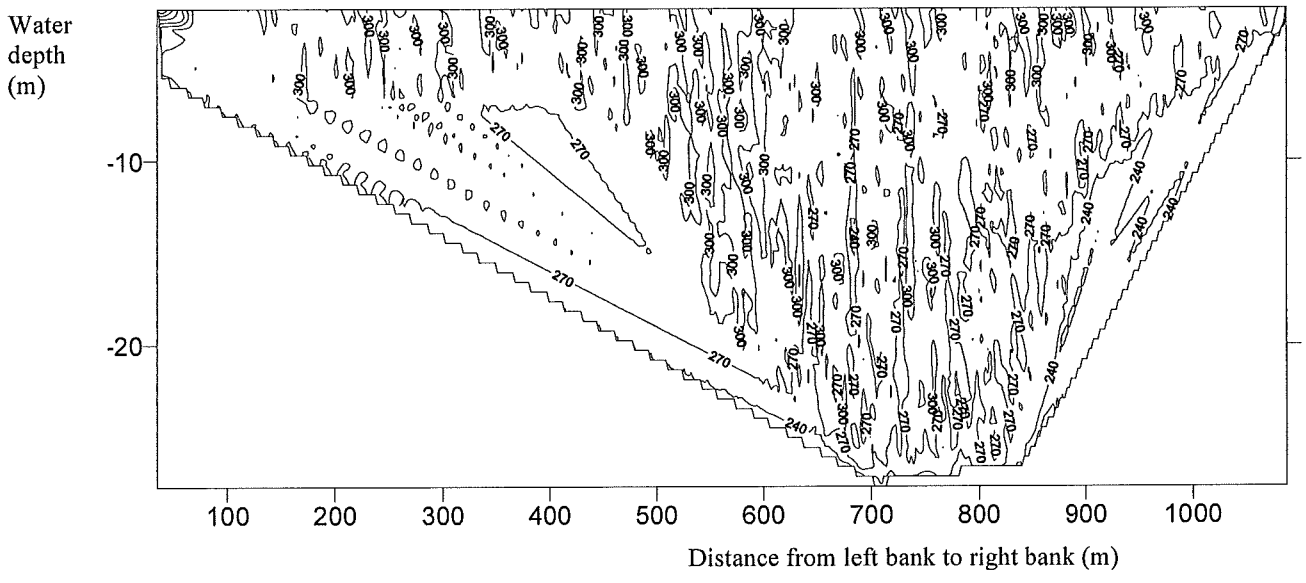

Figure A.1.14. Velocity contour in cross-section Q5, surveyed 17h05'7th, August 2003.

A..1.2..3. Water level

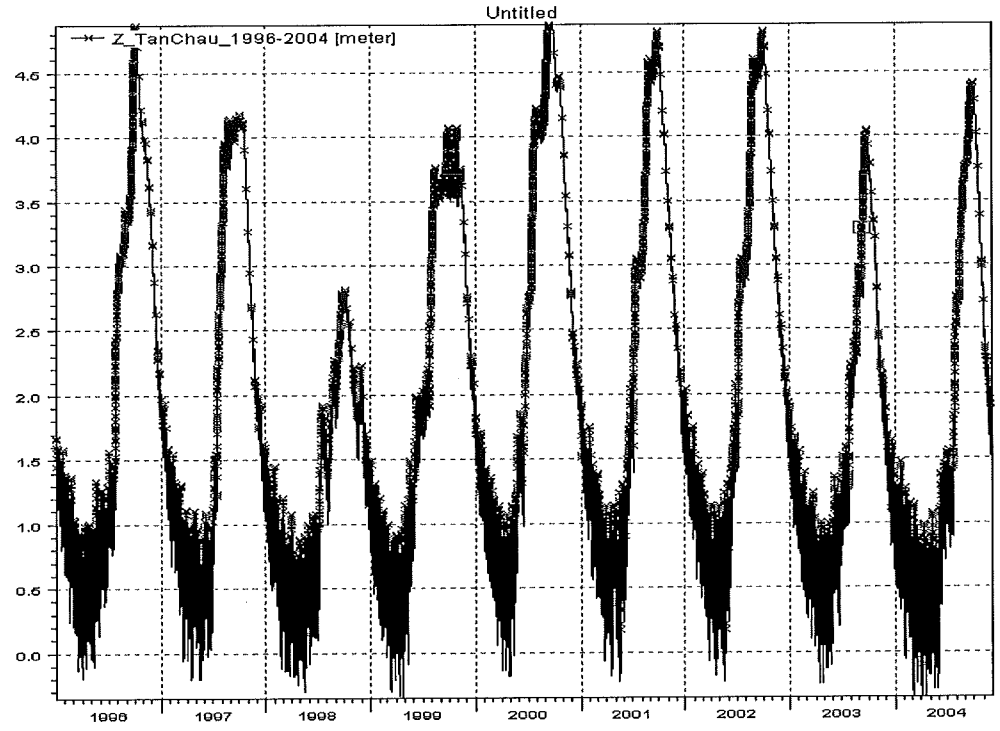

Figure A. 1.15. Water level at Tan Chau from 1996 to 2004

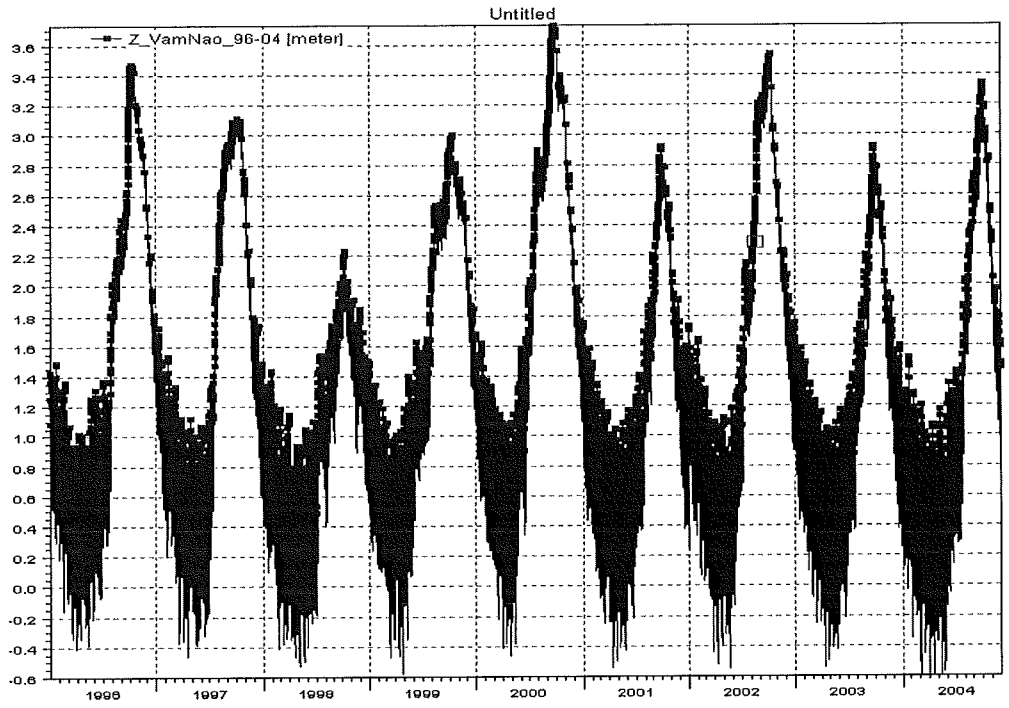

Figure A.1.16. Water level at Vam Nao from 1996 to 2004

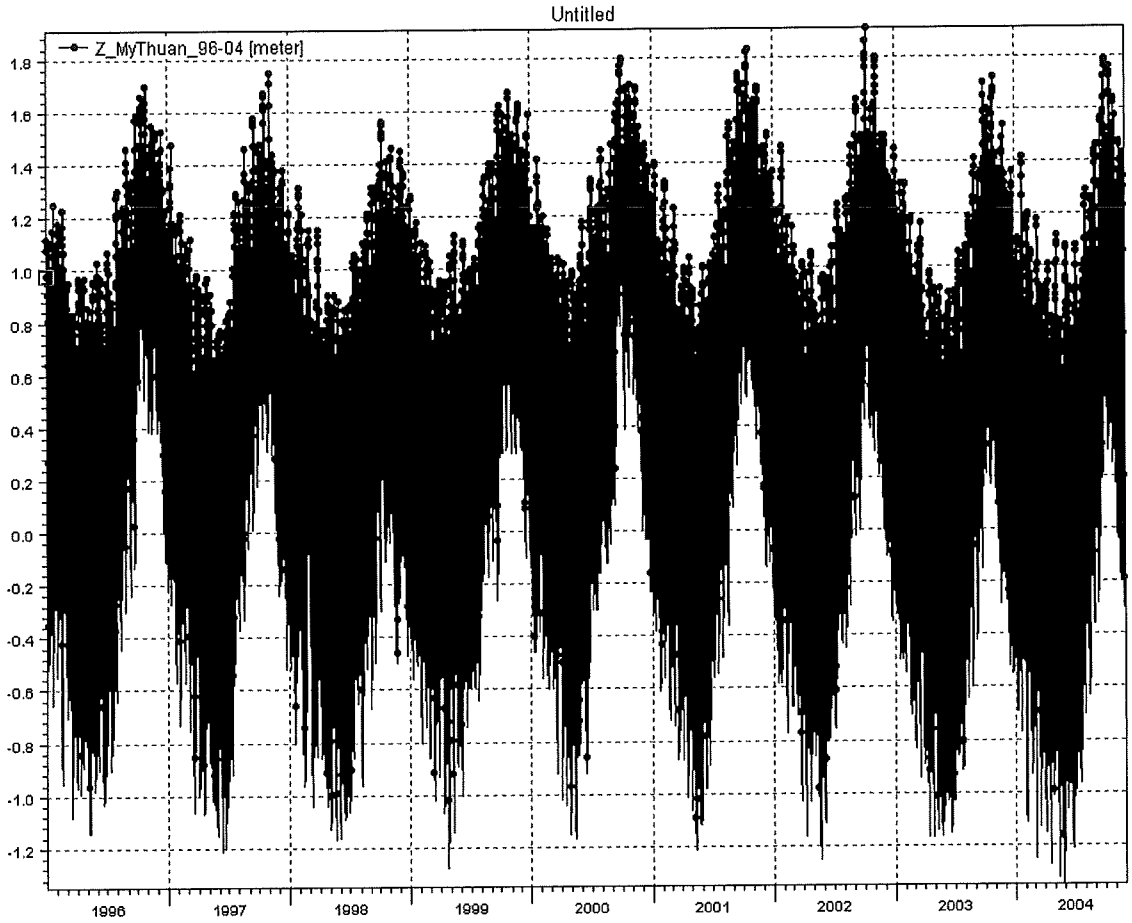

Figure A.1.17. Water level at My Thuan from 1996 to 2004

A.1.2.4 Sediment transport

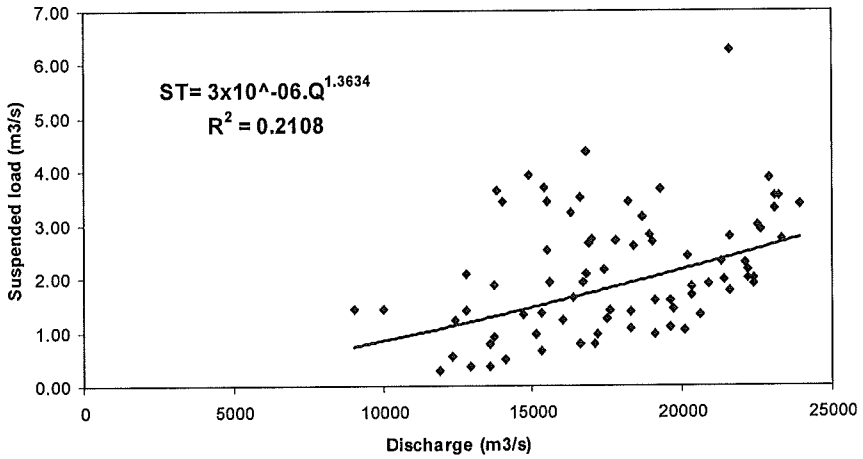

Figure A.1.18. Relation between suspended sediment discharge and water discharge at Tan Chau, period1998-2003

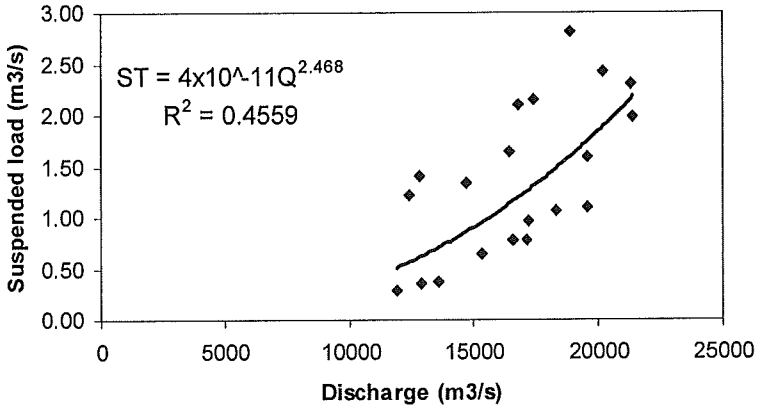

Figure A.1. 19. Relation between suspended sediment discharge and water discharge at Tan Chau, in the year 2003

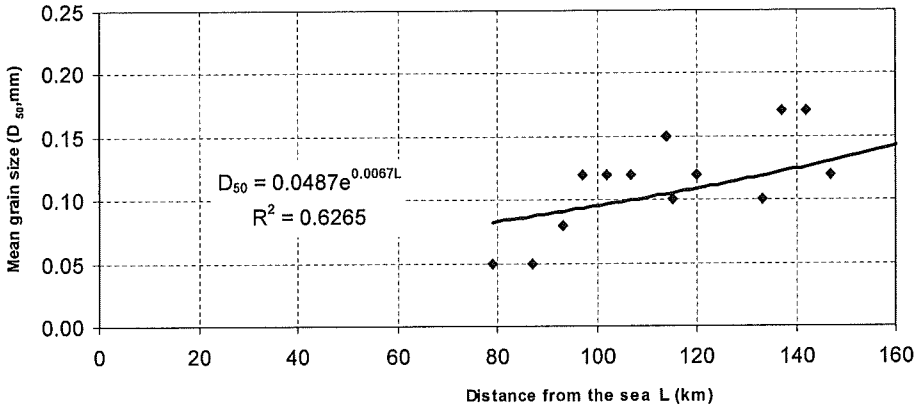

Figure A.1.20. Grain size distribution along Tien River.

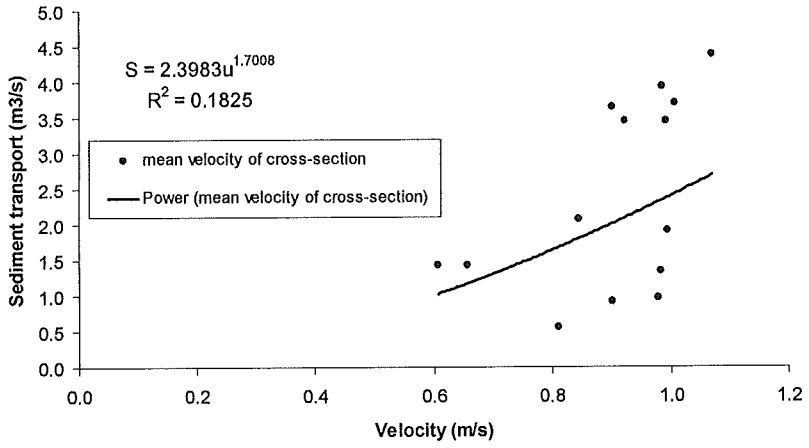

Figure A.1. 21. The relationship between sediment transport and velocity.

A.1.3. Geology and soil sample

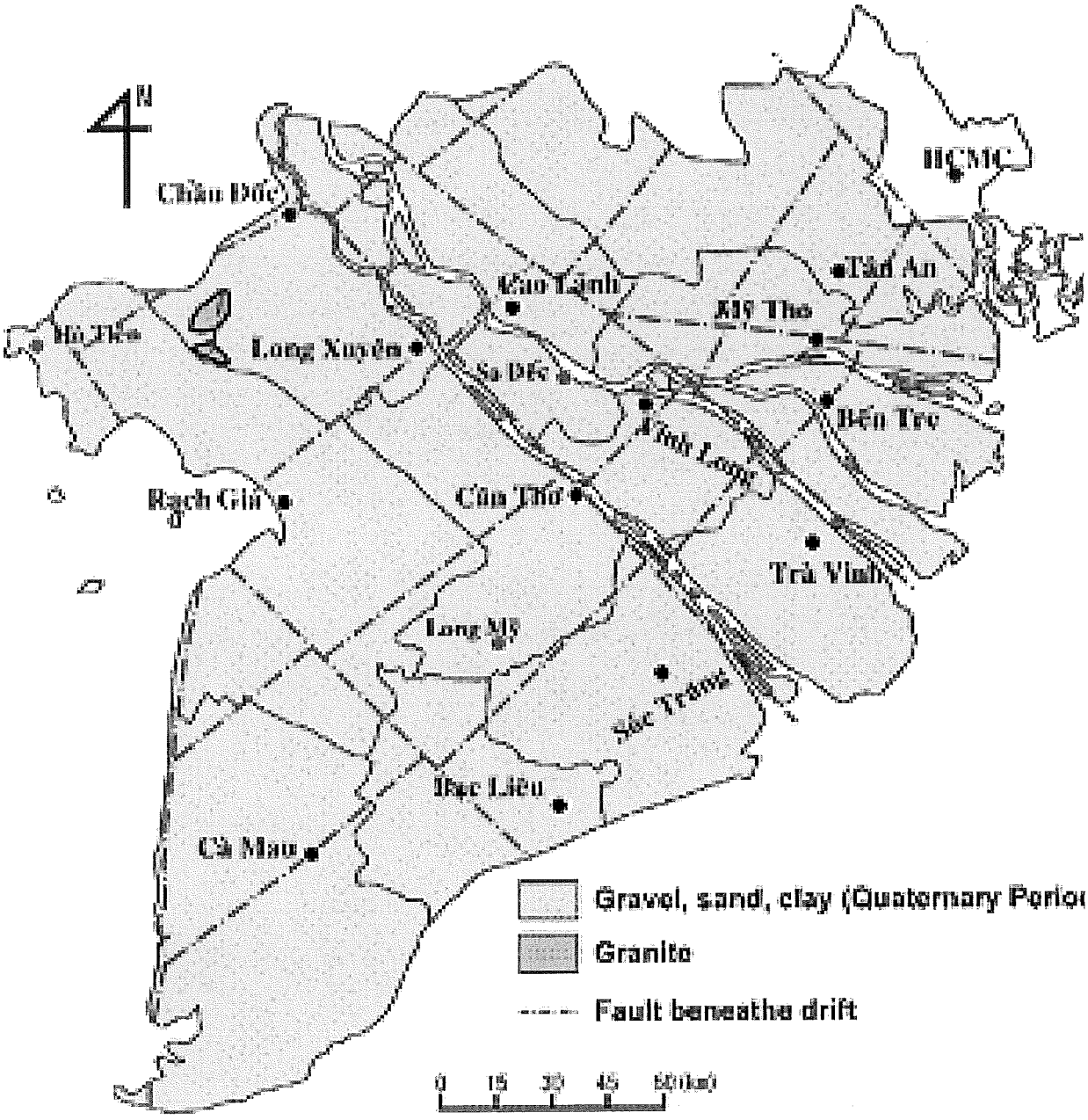

Figure A.1.22. The geo tectonich faults in lower Mekong (source: SIWRR)
(Sourthern Institute of Water Resource Research, Vietnam)

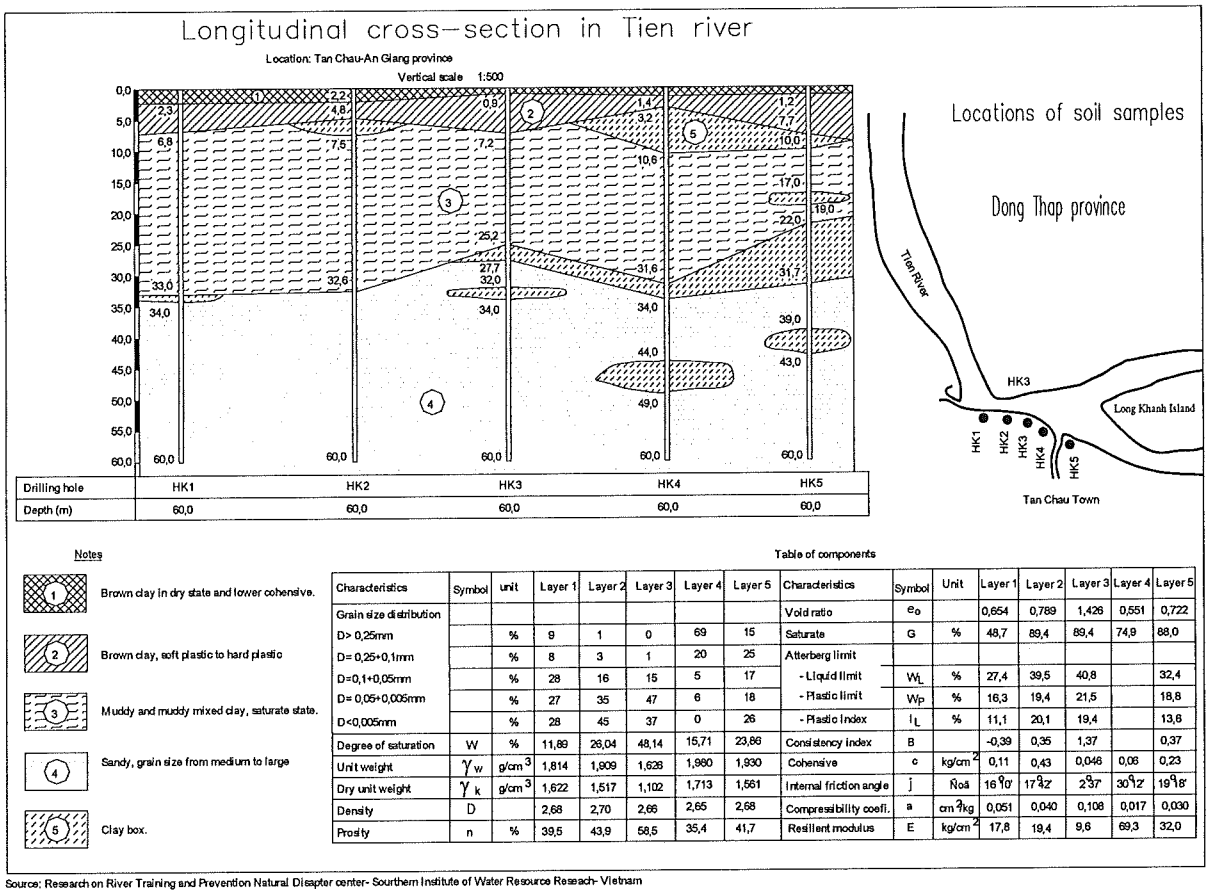

Characteristics	Symbol	unit	Layer 1	Layer 2	Layer 3	Layer 4	Layer 5
Grain size distribution							
D> 0,25mm		%	9	1	0	69	15
D= 0,25÷0,1mm		%	8	3	1	20	25
D=0,1÷0,05mm		%	28	16	15	5	17
D= 0,05÷0,005mm		%	27	35	47	6	18
D<0,005mm		%	28	45	37	0	26
Degree of saturation	W	%	11,89	26,04	48,14	15,71	23,86
Unit weight	γ_w	g/cm^3	1,814	1,909	1,628	1,980	1,930
Dry unit weight	γ_k	g/cm^3	1,622	1,517	1,102	1,713	1,561
Density	D		2,68	2,70	2,66	2,65	2,68
Prosity	n	%	39,5	43,9	58,5	35,4	41,7

Characteristics	Symbol	Unit	Layer 1	Layer 2	Layer 3	Layer 4	Layer 5
Void ratio	e_o		0,654	0,789	1,426	0,551	0,722
Saturate	G	%	48,7	89,4	89,4	74,9	88,0
Atterberg limit							
- Liquid limit	W_L	%	27,4	39,5	40,8		32,4
- Plastic limit	W_P	%	16,3	19,4	21,5		18,8
- Plastic Index	I_L	%	11,1	20,1	19,4		13,6
Consistency index	B		-0,39	0,35	1,37		0,37
Cohensive	c	kg/cm^2	0,11	0,43	0,046	0,06	0,23
Internal friction angle	j	Rad	16°0'	17°2'	2°37'	30°12'	19°8'
Compressibility coefi.	a	cm^2/kg	0,051	0,040	0,108	0,017	0,030
Resilient modulus	E	kg/cm^2	17,8	19,4	9,6	69,3	32,0

Source: Research on River Training and Prevention Natural Disapter center- Sourthern Institute of Water Resource Reseach- Vietnam

Figure A.1.23. The Soil sample at Tan Chau- Tien River
(source: Resear on River Training and preventive natural disaster Centre- Southern Institute of Water Resource Research, Vietnam)

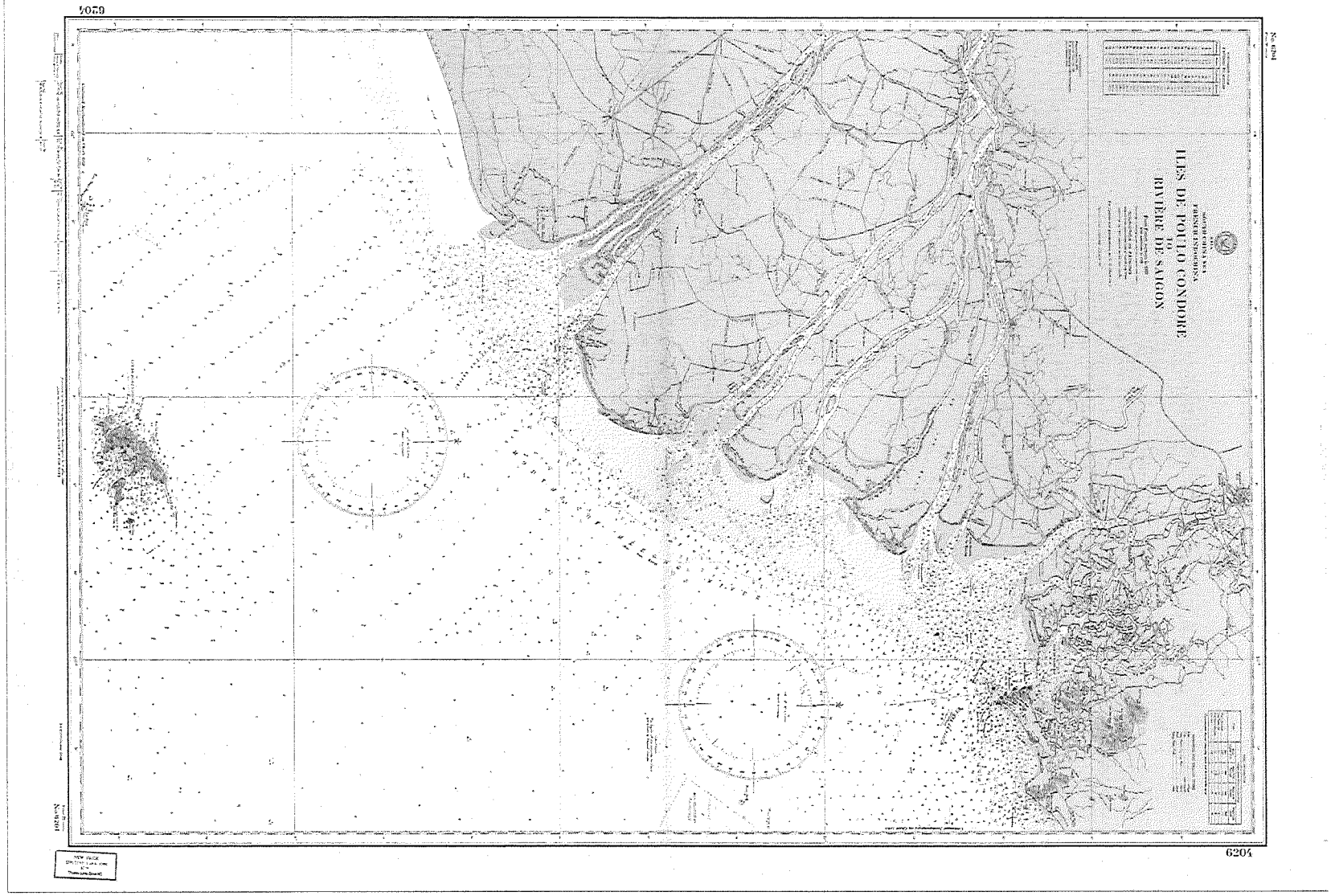

Figure 24. The map of Mekong river in 1937

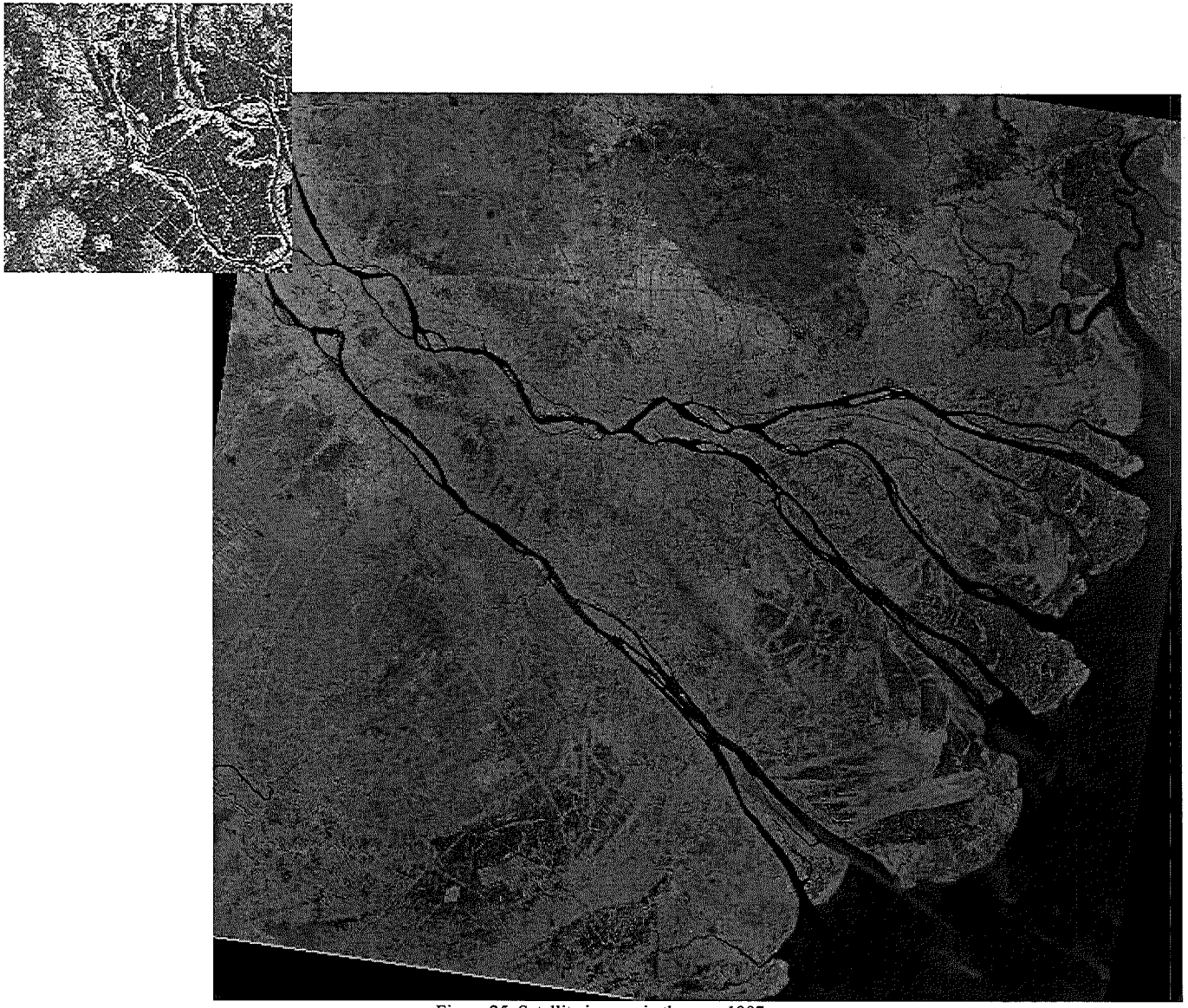

Figure 25. Satellite images in the year 1987

Figure 26. Satellite images in the year 1987

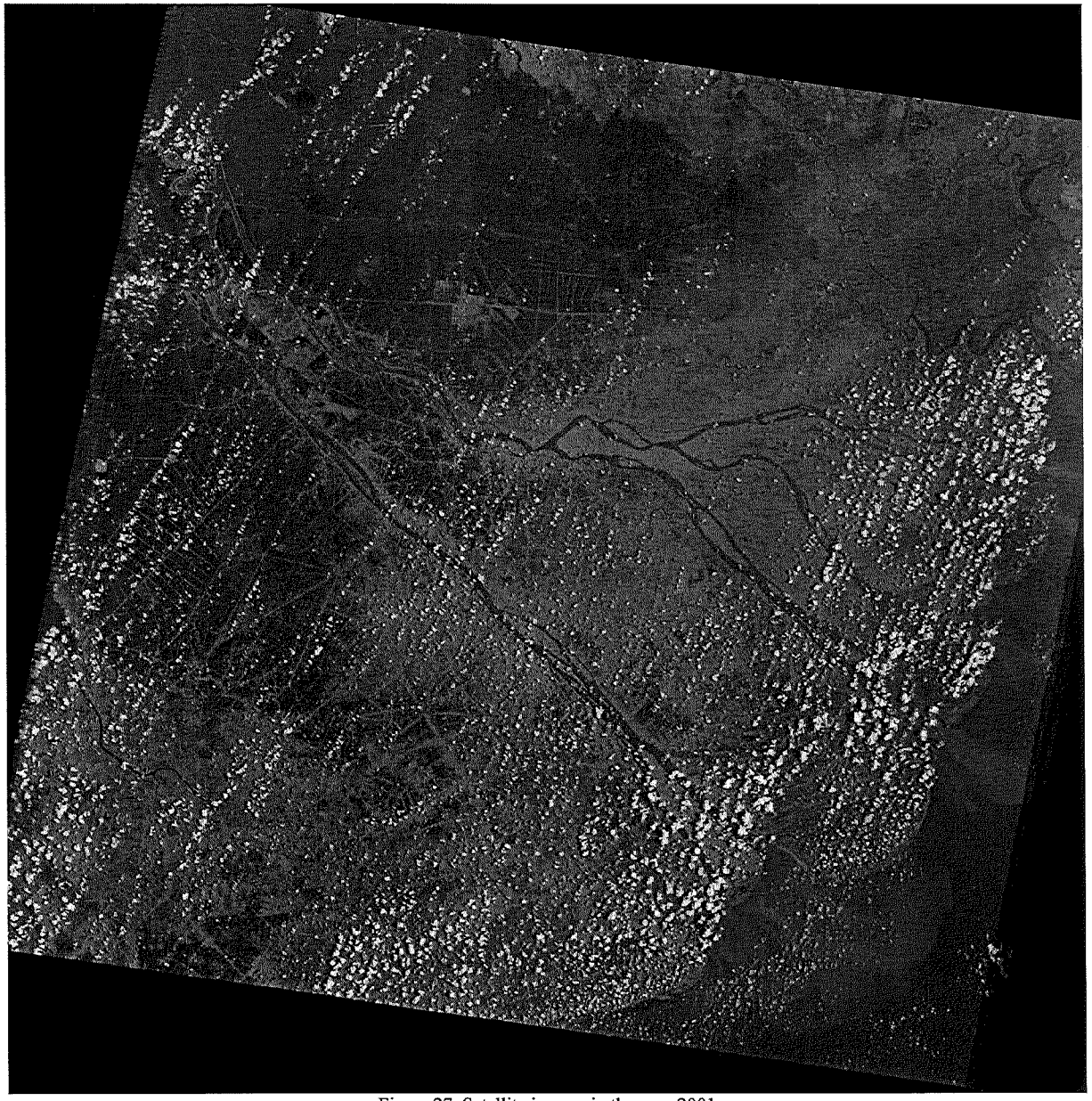

Figure 27. Satellite images in the year 2001

APPENDIX A.2

RESULTS OF GIS ANALYSIS

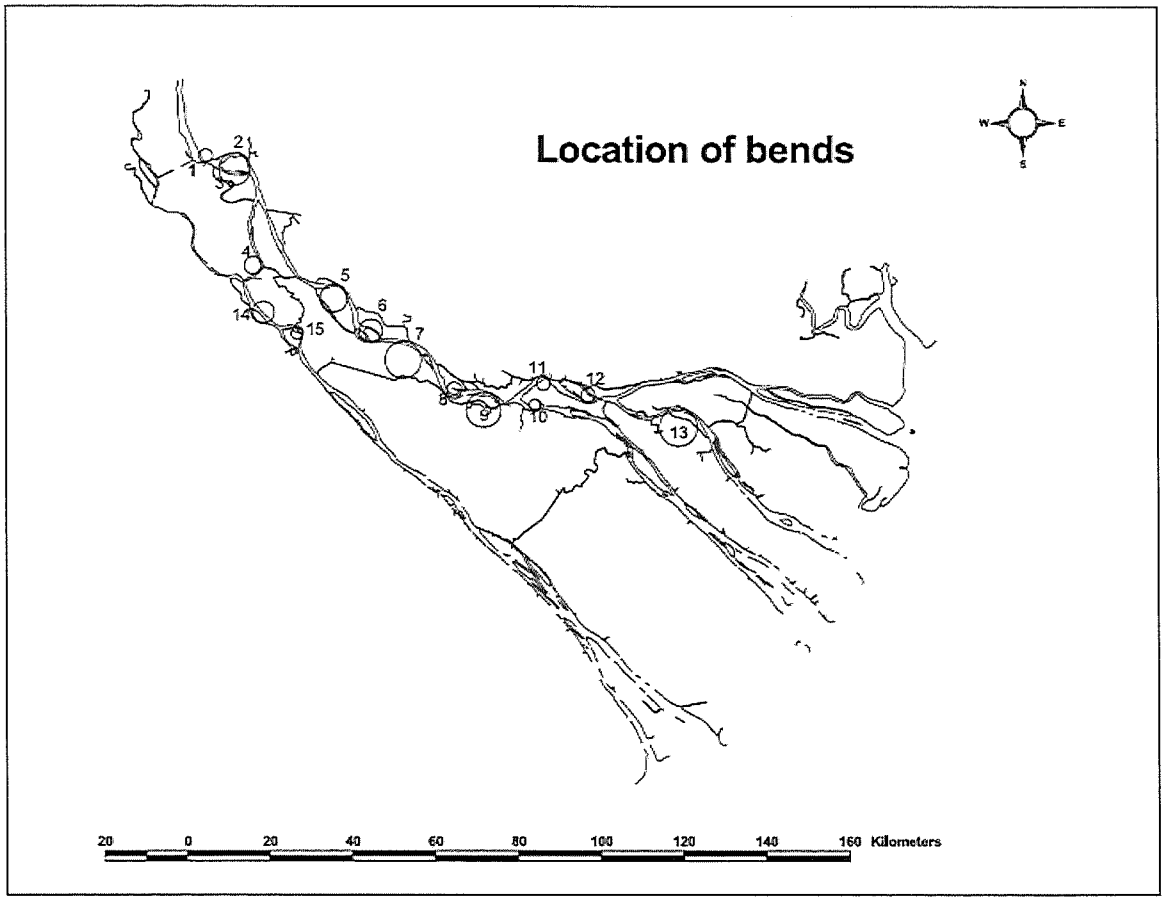

Figure A.2.1. Overview of bends locations

Nº	Location of bends	1937			1966			1987			1996			2001			2003		
		R	W	Q_5	R	W	Q_5	R	W	Q_5	R	W	Q_5	R	W	Q_5	R	W	Q_5
1	Tan Chau _ outer bend										1470	1208	22000				1634	1267	22000
2	Hong Ngu-Dong Thap				1577	537	6534				1286	608	4390	2304	1082	5072	2560	1096	5072
3	Phu An _ Lach Vung _ An Giang				664	165	2000							670	172	2000			
4	Vam Nao Upstream				2118	750	7000							2050	809	7000			
5	Thanh Binh - Dong Thap				5046	590	10000	3572	454	10000	3302	573	10000	3405	557	10000			
6	My An _ Lap Vo_Dong Thap				2075	458	7333	1958	510	7333	1538	678	7333	2210	526	7333			
7	My Xuong -Cao Lanh - Dong Thap				5616	1121	15000	4660	1169	15000	4238	1070	15000	4310	1086	15000			
8	Sadec -Dong Thap				1830	1260	15000	1739	964	15000	1804	1144	15000	1798	1240	15000			
9	Chau Thanh - Dong Thap				4829	717	14000	5177	744	14000	4582	760	14000	4222	850	14000			
10	Vinh Long							1353	680	5000	1280	545	5000						
11	Hoa Khanh _ Cai Be- Tien Giang	1241	571	10000	1663	672	11551	1658	687	11551				1637	692	11551			
12	Tan Thanh - Cho Lach - Ben Tre				1609	806	7000	1570	735	7000	1769	652	7000	1742	662	7000			
13	An Hiep -Chau Thanh - Ben Tre	4533	1055	15000	4300	1046	15000	4342	1068	15000	4404	1047	15000	4603	1107	15000			
14	Binh An - Long Xuyen - An Giang				2633	180	3000							2650	190	3000			
15	An Thanh Trung-Long Xuyen-An Giang				938	1027	4000	1397	1018	4000	1405	1108	4000						

Table A.2.1. The basis data at bends

Notes: R - Radius of cavatures (m)
W - Bankfull width (m)
Q_5 - Estimated five year flood discharge (m^3/s)

Nº	Locations	1937-1966 (29 yr)			1966-1987 (21yr)			1966-1996 (30yr)			1987-1996 (9yr)			1987-2001 (14yr)			1996-2001 (5yr)			2001-2003 (2yr)			
		E (m/yr)	R/W	E/W	E (m/yr)	R/W	E/W	E (m/yr)	R/W	E/W	E (m/yr)	R/W	E/W	E (m/yr)	R/W	E/W	E (m/yr)	R/W	E/W	E (m/yr)	R/W	E/W	
1	Tan Chau _ outer bend																			22.86	1.25		(1996-2003)
2	Hong Ngu-Dong Thap							3.90	2.50	0.0073							15.33	2.12	0.025	28.67	2.23	0.026	
3	Phu An _ Lach Vung _ An Giang																			3.43	3.96		(1966-2001)
4	Vam Nao Upstream																			9.66	2.67		(1966-2001)
5	Thanh Binh - Dong Thap				5.14	8.25	0.009				8.89	6.69	0.036				13.20	5.94	0.066				
6	My An _ Lap Vo_Dong Thap				6.67	4.17	0.015				8.11	2.94	0.016				9.00	3.11	0.013				
7	My Xuong -Cao Lanh - Dong Thap				6.62	4.49	0.006				13.00	3.97	0.011				13.16	3.96	0.012				
8	Sadec -Dong Thap				37.33	1.60	0.030				40.00	1.68	0.042				51.20	1.51	0.045				
9	Chau Thanh - Dong Thap				10.62	6.85	0.015				7.78	6.49	0.010				13.50	5.47	0.015				
10	Vinh Long										5.78	2.15	0.009										
11	Hoa Khanh _Cai Be- Tien Giang	7.45	2.34	0.013	5.86	2.44	0.009							3.86	2.39	0.006							
12	Tan Thanh - Cho Lach - Ben Tre				2.38	2.06	0.003				14.11	2.41	0.019				7.00	2.67	0.0111				
13	An Hiep -Chau Thanh - Ben Tre	4.10	4.20	0.004	2.14	4.09	0.002				2.56	4.14	0.002				10.92	4.18	0.0104				
14	Binh An - Long Xuyen - An Giang																			3.69	14.28		(1966-2001)
15	An Thanh Trung-Long Xuyen-An Giang				2.48	0.96	0.002				15.00	1.32	0.015										

Table A.2.2. The observed riverbank erosion rates, width, radius of curvature and data analysis.

Notes: ☐ The erosion rates related to the periods in the horizontal rows
Number of bends related with figure A.2.1 above

No	Locations	Observed Time	E (m/yr)	R/W	Q_5 (m^3/s)	Ω (watt/m)	D50 (mm)	Yb (N/m2)	h_b (m)	$M_{2.5}$ (m/yr)	$f_{(R/W)}$	Results of H&N (1984) (m/yr)
1	Tan Chau _ outer bend	1996-2003	22.86	1.25	22,000	8,800	0.25	60.00	44.00	3.33	0.17	0.56
2	Hong Ngu-Dong Thap	1966-1996	3.90	2.50	5,462	2,185	0.22	55.00	28.61	1.39	1.00	1.39
		1996-2001	15.33	2.12	4,731	1,892	0.22	55.00	28.61	1.20	0.75	0.90
		2001-2003	28.67	2.23	5,072	2,029	0.22	55.00	28.61	1.29	0.82	1.06
3	Phu An _ Lach Vung _ An Giang	1966-2001	3.43	3.96	2,000	800	0.22	55.00	6.10	2.38	0.63	1.51
5	Thanh Binh - Dong Thap	1966-1987	5.14	8.25	10,000	4,000	0.17	50.00	18.60	4.30	0.30	1.30
		1987-1996	8.89	6.69	10,000	4,000	0.17	50.00	18.60	4.30	0.37	1.61
		1996-2001	13.20	5.94	10,000	4,000	0.17	50.00	18.60	4.30	0.42	1.81
6	My An _ Lap Vo_Dong Thap	1966-1987	6.67	4.17	7,333	2,933	0.15	48.00	20.40	3.00	0.60	1.80
		1987-1996	8.11	2.94	7,333	2,933	0.15	48.00	20.40	3.00	0.85	2.54
		1996-2001	9.00	3.11	7,333	2,933	0.15	48.00	20.40	3.00	0.80	2.41
7	My Xuong -Cao Lanh - Dong Thap	1966-1987	6.62	4.49	15,000	6,000	0.14	47.00	20.03	6.37	0.56	3.55
		1987-1996	13.00	3.97	15,000	6,000	0.14	47.00	20.03	6.37	0.63	4.01
		1996-2001	13.16	3.96	15,000	6,000	0.14	47.00	20.03	6.37	0.63	4.02
8	Sadec -Dong Thap	1966-1987	37.33	1.60	15,000	6,000	0.13	46.00	21.90	5.96	0.40	2.40
		1987-1996	40.00	1.68	15,000	6,000	0.13	46.00	21.90	5.96	0.45	2.70
		1996-2001	51.20	1.51	15,000	6,000	0.13	46.00	21.90	5.96	0.34	2.03
9	Chau Thanh - Dong Thap	1966-1987	10.62	6.85	14,000	5,600	0.12	45.00	17.00	7.32	0.37	2.67
		1987-1996	7.78	6.49	14,000	5,600	0.12	45.00	17.00	7.32	0.39	2.82
		1996-2001	13.50	5.47	14,000	5,600	0.12	45.00	17.00	7.32	0.46	3.35
14	Binh An - Long Xuyen - An Giang	1966-2001	3.69	14.28	3,000	1,200	0.17	50.00	9.60	2.50	0.18	0.44
15	An Thanh Trung-Long Xuyen-An Giang	1966-1987	2.48	0.96	4,000	1,600	0.16	49.00	10.37	3.15		
		1987-1996	15.00	1.32	4,000	1,600	0.16	49.00	10.37	3.15	0.21	0.67

Table A.2.3. The results of application of Hickin & Nanson (1984).

No	Locations	Observed Time	E (m/yr)	R/W	Q_{bf} (m3/s)	Ω (watt/m')	Yb (N/m2)	hb (m)	f(R/W)	E2.5	E_H&N(1984) (m/yr)	E_Improve H&N (m/yr)
1	Tan Chau _ outer bend	1996-2003	22.86	1.25	19,112	7,645	60.00	44.00	0.17	2.90	0.49	22.68
2	Hong Ngu-Dong Thap	1966-1996	3.90	2.50	6,348	2,539	55.00	19.67	1.00	2.35	2.35	14.08
		1996-2001	15.33	2.12	6,348	2,539	55.00	19.67	0.75	2.35	1.76	14.00
		2001-2003	28.67	2.23	6,348	2,539	55.00	19.67	0.82	2.35	1.93	14.07
3	Phu An _ Lach Vung _ An Giang	1966-2001	3.43	3.96	2,000	800	55.00	6.10	0.63	2.38	1.51	2.31
5	Thanh Binh - Dong Thap	1966-1987	5.14	8.25	15,106	6,042	50.00	18.60	0.30	6.50	1.97	2.64
		1987-1996	8.89	6.69	15,106	6,042	50.00	18.60	0.37	6.50	2.43	3.82
		1996-2001	13.20	5.94	15,106	6,042	50.00	18.60	0.42	6.50	2.74	4.80
6	My An _ Lap Vo_Dong Thap	1966-1987	6.67	4.17	9,178	3,671	48.00	20.40	0.60	3.75	2.25	6.31
		1987-1996	8.11	2.94	9,178	3,671	48.00	20.40	0.85	3.75	3.19	15.02
		1996-2001	9.00	3.11	9,178	3,671	48.00	20.40	0.80	3.75	3.01	12.98
7	My Xuong -Cao Lanh - Dong Thap	1966-1987	6.62	4.49	19,390	7,756	47.00	20.03	0.56	8.24	4.59	11.53
		1987-1996	13.00	3.97	19,390	7,756	47.00	20.03	0.63	8.24	5.18	15.31
		1996-2001	13.16	3.96	19,390	7,756	47.00	20.03	0.63	8.24	5.20	15.40
8	Sadec -Dong Thap	1966-1987	37.33	1.60	17,542	7,017	46.00	21.90	0.40	6.97	2.81	41.21
		1987-1996	40.00	1.68	17,542	7,017	46.00	21.90	0.45	6.97	3.16	42.54
		1996-2001	51.20	1.51	17,542	7,017	46.00	21.90	0.34	6.97	2.37	39.00
9	Chau Thanh - Dong Thap	1966-1987	10.62	6.85	21,485	8,594	45.00	17.00	0.37	11.23	4.10	6.10
		1987-1996	7.78	6.49	21,485	8,594	45.00	17.00	0.39	11.23	4.33	6.73
		1996-2001	13.50	5.47	21,485	8,594	45.00	17.00	0.46	11.23	5.14	9.35
14	Binh An - Long Xuyen - An Giang	1966-2001	3.69	14.28	14,260	5,704	50.00	9.60	0.18	11.88	2.08	2.03
15	An Thanh Trung-Long Xuyen-An Giang	1966-1987	2.48	0.96	15,915	6,366	49.00	10.37		12.53		
		1987-1996	15.00	1.32	15,915	6,366	49.00	10.37	0.21	12.53	2.66	28.07

Table A.2.4. The results of improvement of Hickin & Nanson (1984) for lower Mekong river.

Bend Nº	Locations	Distance*(km)	W_{bf} (m)	A_{bf} (m^2)	H_{bf} (m)	i (-)	d50 (mm)	u_* (-)	θ (–)	θ' (-)	H' (m)	C ($m^{1/2}/s$)	Qbf (m^3/s)
1	Tanchau outer bend	236	2265	18795	8.30	0.00004	0.237	0.058	0.85	0.35	3.41	55.81	19112
2	Hong Ngu -Dong Thap	228	2560	10847	4.24	0.00004	0.224	0.041	0.46	0.14	1.33	44.95	6348
3	Phu An _ Lach Vung _ An Giang	No available data- value is estimated											2000
5	Thanh Binh - Dong Thap	185	699	7988	11.43	0.00004	0.168	0.068	1.65	1.35	9.37	88.44	15106
6	My An _ Lap Vo_Dong Thap	168	1100	6365	5.78	0.00004	0.150	0.048	0.93	0.93	5.78	94.81	9178
7	My Xuong -Cao Lanh - Dong Thap	158	1151	11169	9.71	0.00004	0.140	0.062	1.68	1.36	7.89	88.10	19390
8	Sadec -Dong Thap	140	1374	10969	7.98	0.00004	0.124	0.057	1.56	1.31	6.73	89.50	17542
9	Chau Thanh - Dong Thap	133	1512	13227	8.75	0.00004	0.119	0.059	1.79	1.40	6.87	86.84	21485
14	Binh An - Long Xuyen - An Giang	147	831	8295	9.98	0.00004	0.130	0.063	1.86	1.43	7.68	86.04	14260
15	An Thanh Trung-Long Xuyen-An Giang	137.5	1440	10323	7.17	0.00004	0.122	0.054	1.42	1.25	6.30	91.04	15915

Table A.2.5 The bankfull discharge at bends

Notes: Bend number is related to figure A.2.1

Distance*(km) is the distance counted from the sea.

Nº	Bends	h_b/h	R/W (average)	E (average)	H_b	Y_b (N/m^2)	D_{60} (mm)	L(km)
1	Tan Chau _ outer bend	**4.81**	**1.25**	22.86	**44.00**	**9.77**	0.25	0.00
2	Hong Ngu-Dong Thap	**4.15**	**2.37**	15.97	**28.61**	**3.64**	0.22	10.90
3	Phu An _ Lach Vung _ An Giang	**1.41**	**3.96**	3.43	**6.10**	**6.40**	0.22	10.70
5	Thanh Binh - Dong Thap	**1.53**	**6.96**	9.08	**18.60**	**10.50**	0.17	53.25
6	My An _ Lap Vo_Dong Thap	**1.92**	**4.78**	7.93	**20.40**	**7.02**	0.15	69.70
7	My Xuong -Cao Lanh - Dong Thap	**1.86**	**4.14**	10.93	**20.03**	**14.63**	0.14	78.00
8	Sadec -Dong Thap	**2.27**	**1.60**	42.84	**21.90**	**13.38**	0.13	95.10
9	Chau Thanh - Dong Thap	**2.27**	**6.27**	10.63	**17.00**	**16.08**	0.12	104.16
14	Binh An - Long Xuyen - An Giang	**2.29**	**14.28**	3.69	**9.60**	**6.10**	0.17	49.50
15	An Thanh Trung-Long Xuyen-An Giang	**2.43**	**1.14**	8.74	**10.37**	**7.53**	0.16	60.80

Table A.2.6. The bank hight h_b, and stream power Y_b by apply Hickin & Nanson (1984)

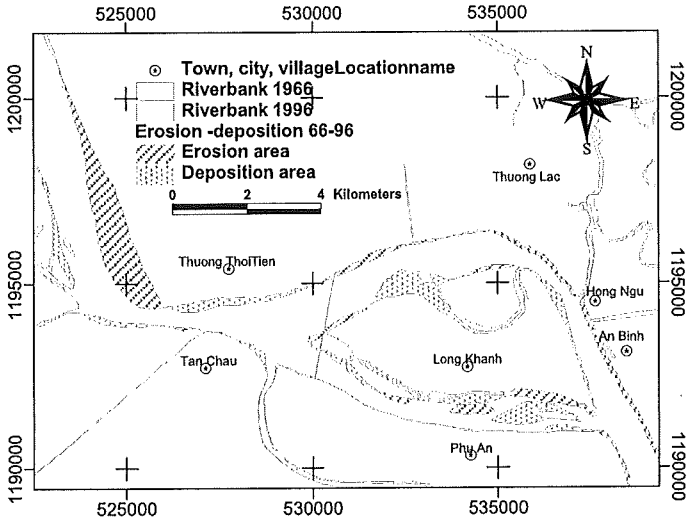

(a) From 1966 to 1996

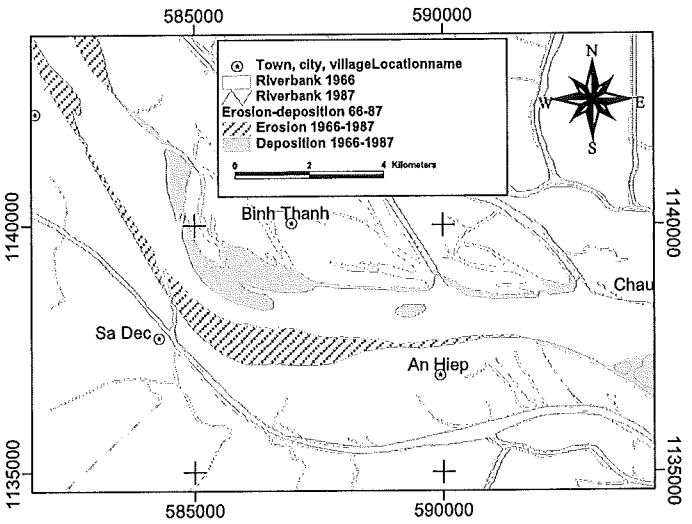

(a) From 1966 to 1987

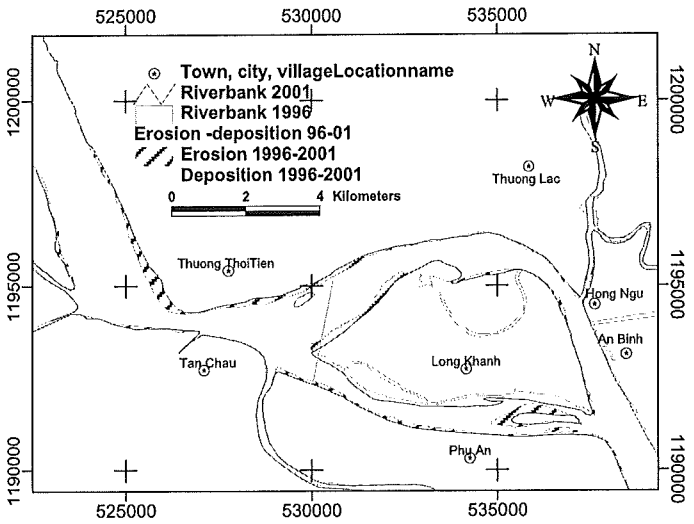

(b) From 1996 to 2001

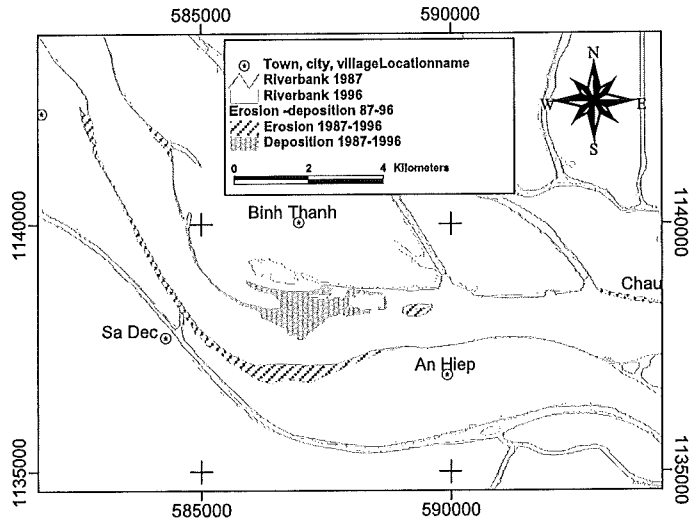

(b) From 1987 to 1996

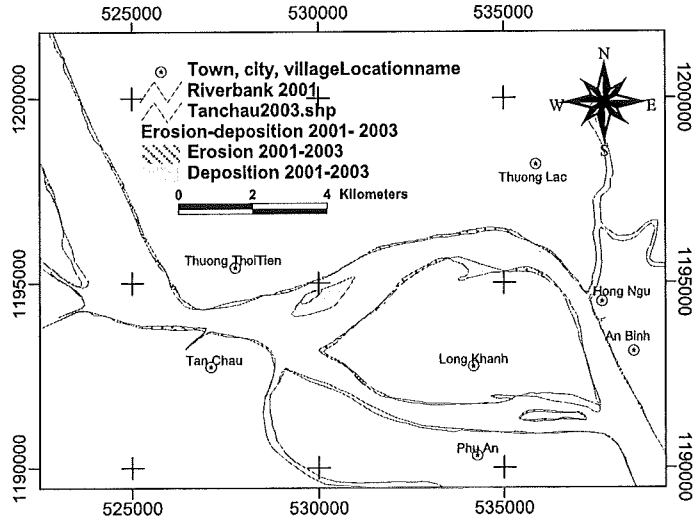

(c) From 2001 to 2003

Figure A.2.7. Erosion and deposition area in Tan Chau-Hong Ngu

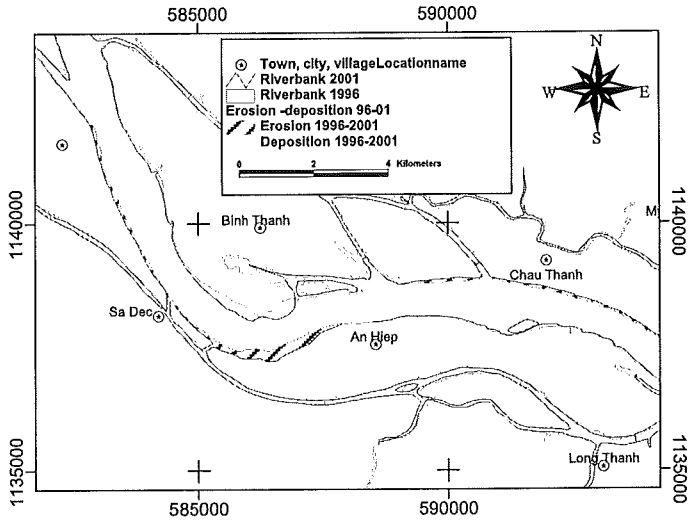

(c) From 1996 to 2001

Figure A.2.8. Erosion and deposition area in Sadec

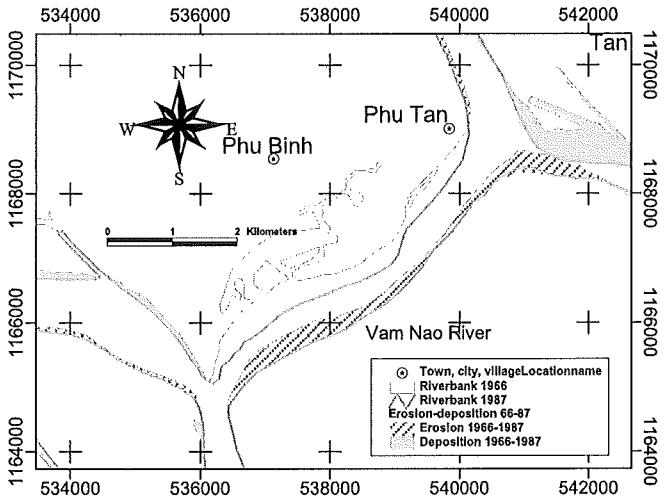

(a) From 1966 to 1987

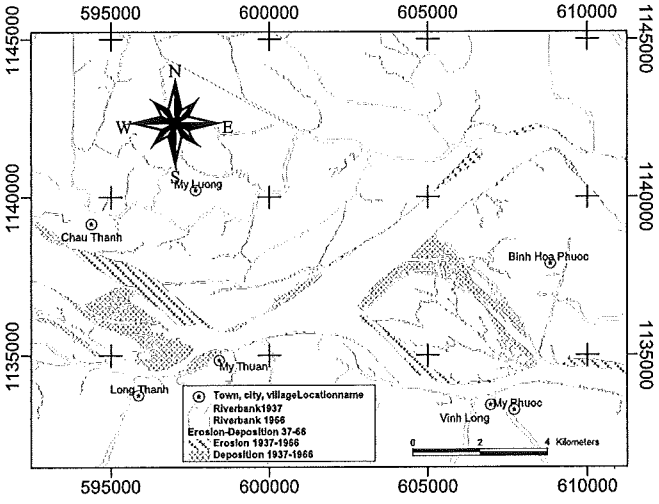

(a) From 1937 to 1966

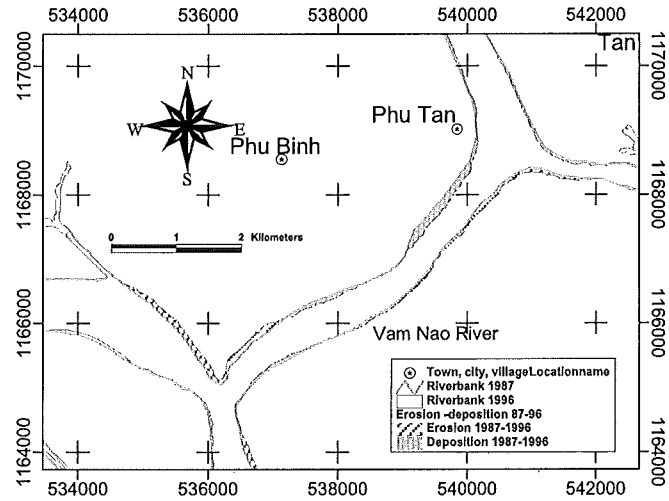

(b) From 1987 to 1996

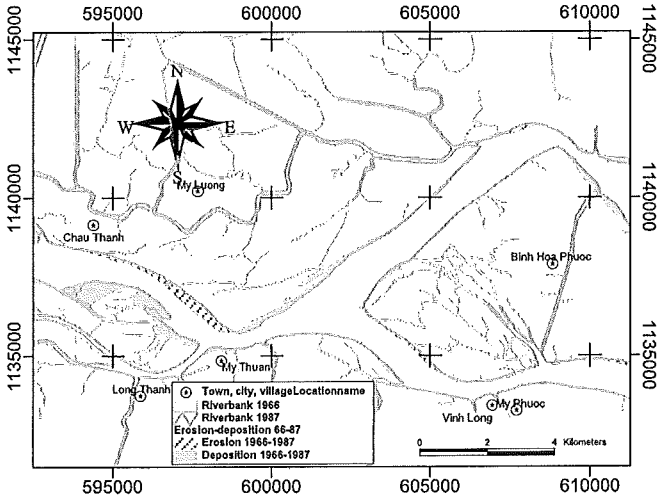

(b) From 1966 to 1987

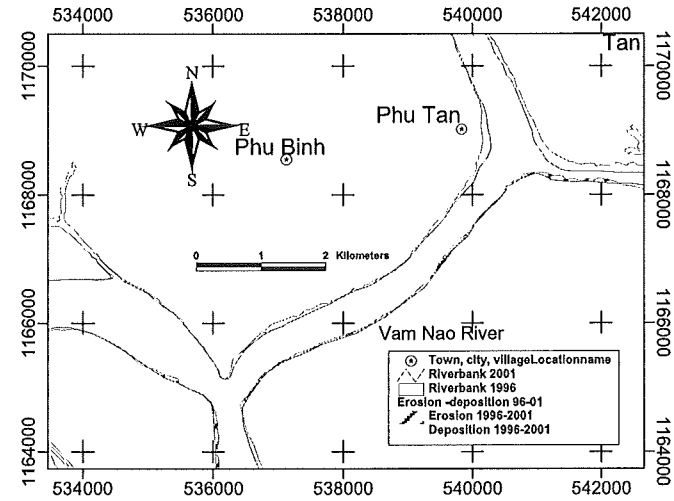

(c) From 1996 to 2001

Figure A.2.9. Erosion and deposition area in Vam Nao

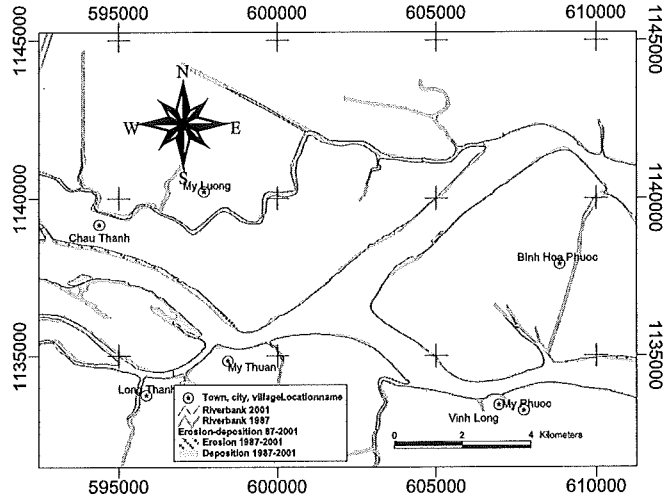

(c) From 1987 to 2001

Figure A.2.10. Erosion and deposition area in My Thuan

Appendix A- 3

MIKE11 Simulation

A.3.1. Model decription

The objective of using MIKE11 for this study to compute the boundary condition for MIKE21C.

The one –Dimension only focus on the main channel of Tien river from Vietnam-Campodian frontier to My Thuan in Tien branch and Vam Nao conection branch, see figure A.3.1

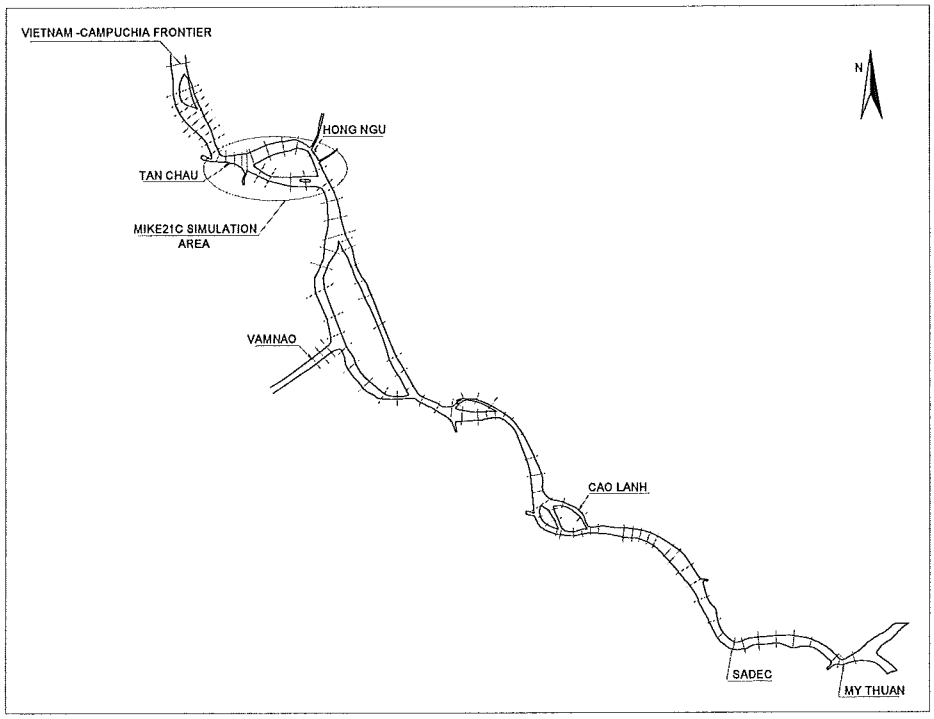

Figure A.3.1: Network system of Simulation and cross-section.

The cross-section base on the topography surveyed in 1996 for navigation and updated some small cannals in 2004.

The boundary condition use the upstream boundary is hourly discharges from 1996 to 2004, and the downstream boundary are My Thuan hourly water level, and Vamnao hourly water level.

A.3.2. Model Calibration

The model was calibrated by adjust the roughness coefficients, and comparision between observed data and computed data.
The duration of time for calibration in this model is from October,1996 to November 1999.

Because of lack discharge observed data, the calibration was only implemented by comparing some value, at some surveyed locations.

On the table A.3.1, the discharge comparison was accepted with the roughness coefficient n=0.022 $m^{1/3}/s$ for all cross-section. It seems very good results

The water level calibrations at TanChau, and Caolanh stations see figure A.3.1 for location and A.3.2, and A.3.3 for calibration results.

Date	Discharge distribution								Data types
	Tan Chau		Hong Ngu		Long Khanh		Cai Vung		
	Q(m3/s)	%	Q(m3/s)	%	Q(m3/s)	%	Q(m3/s)	%	
Flood-1996	23876	100	14229	59.6	7344	30.8	2295	9.6	Obsevation
Q_{Max} 1996	23500	100	14000	59.6	7200	30.6	2300	9.8	Calculation

Table A.3.1: The discharge distribution results at Hong Ngu, Long Khanh and Cai Vung channels

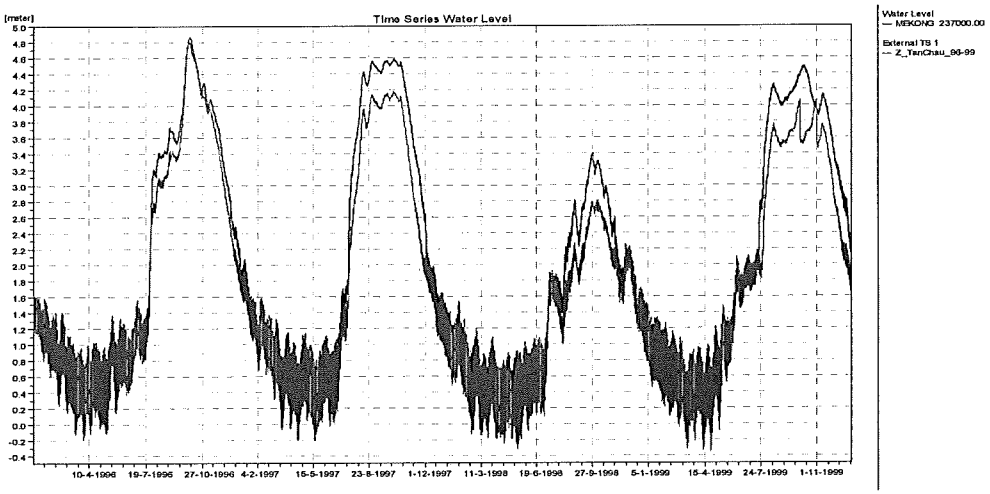

Figure A.3.2: The water level calibration at Tan Chau, period 1996-1999

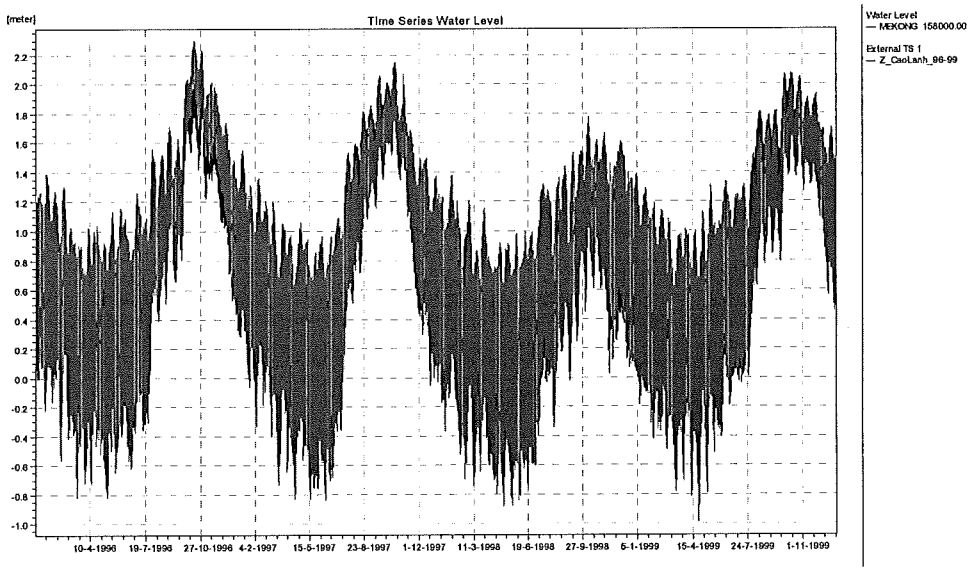

Figure A.3.3: The water level calibration at Cao Lanh, period 1996-1999

A.3.3. Model validation

The model validation in the period of 2000 to 2003 with the calibration parameters. The results of validation shows below.

Date	Discharge distribution								Data types
	Tan Chau		Hong Ngu		Long Khanh		Cai Vung		
	Q (m3/s)	%	Q (m3/s)	%	Q (m3/s)	%	Q (m3/s)	%	
Oct-01	**17286**	**100**	**8232**	**47.6**	**7783**	**45**	**1271**	**7.4**	**Obs.**
25/10/01	19000	100	12000	63.2	5800	30.5	1500	7.9	Calc.
Mar-03	**4290**	**100**	**1825**	**42.5**	**2183**	**50.9**	**270**	**6.3**	**Obs.**
9/3/2003	5400	100	4200	77.8	1800	33.3	200	3.7	Calc.

Table A.3.2 : Discharge distribution, period 2000-2003

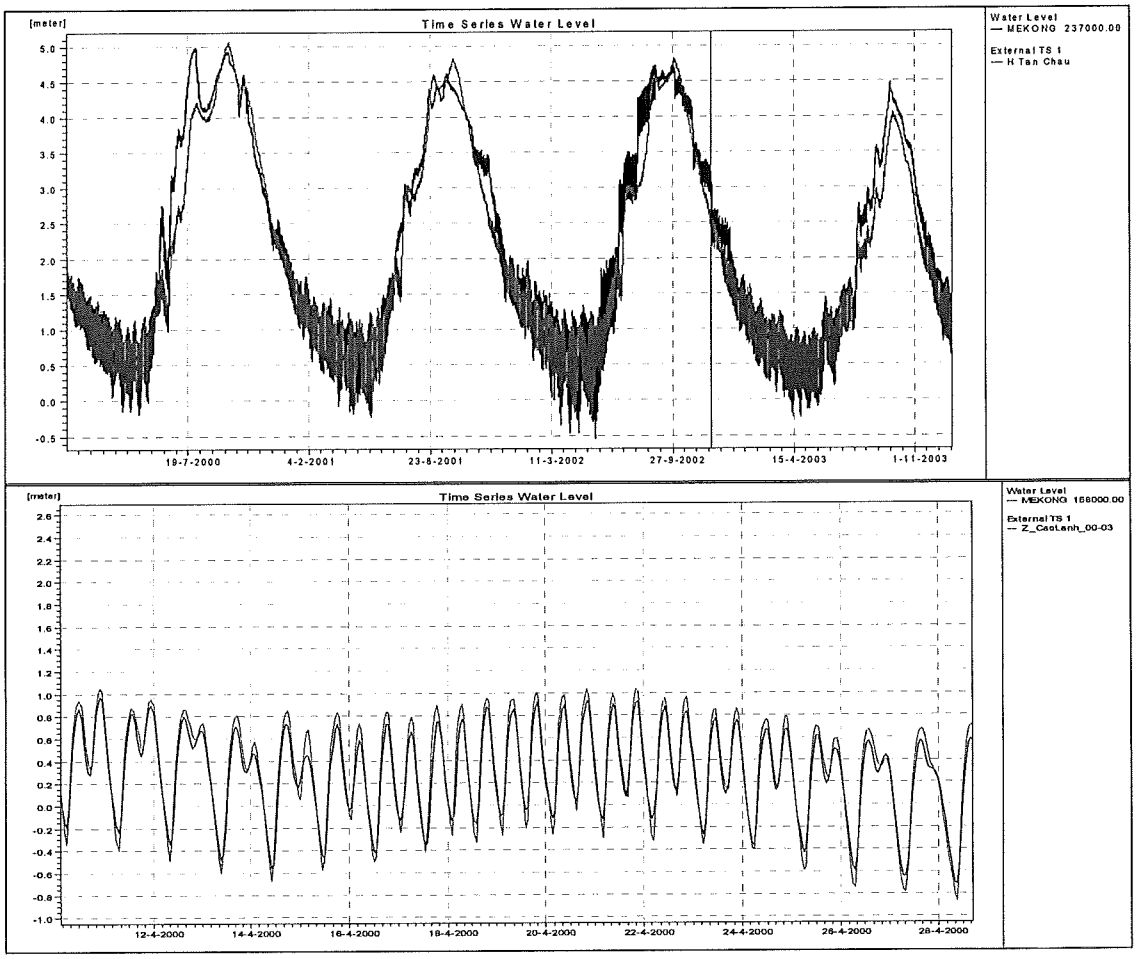

Figure A.3.4 Water level validation at Tan Chau and Cao Lanh, period 2000-2003

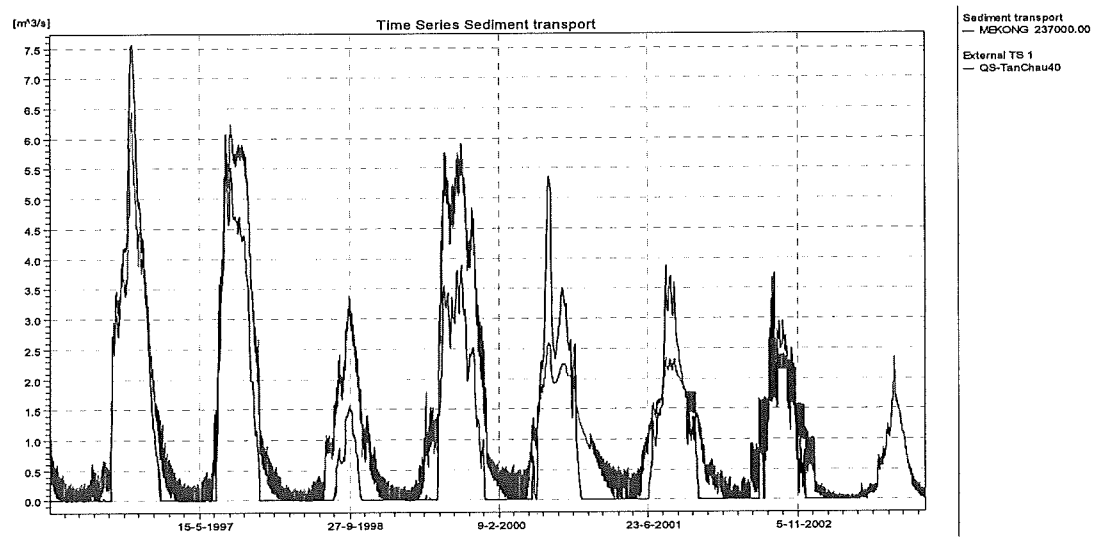

Figure A.3.5. Suspended sediment discharges – the calibration and observation values at Tan Chau

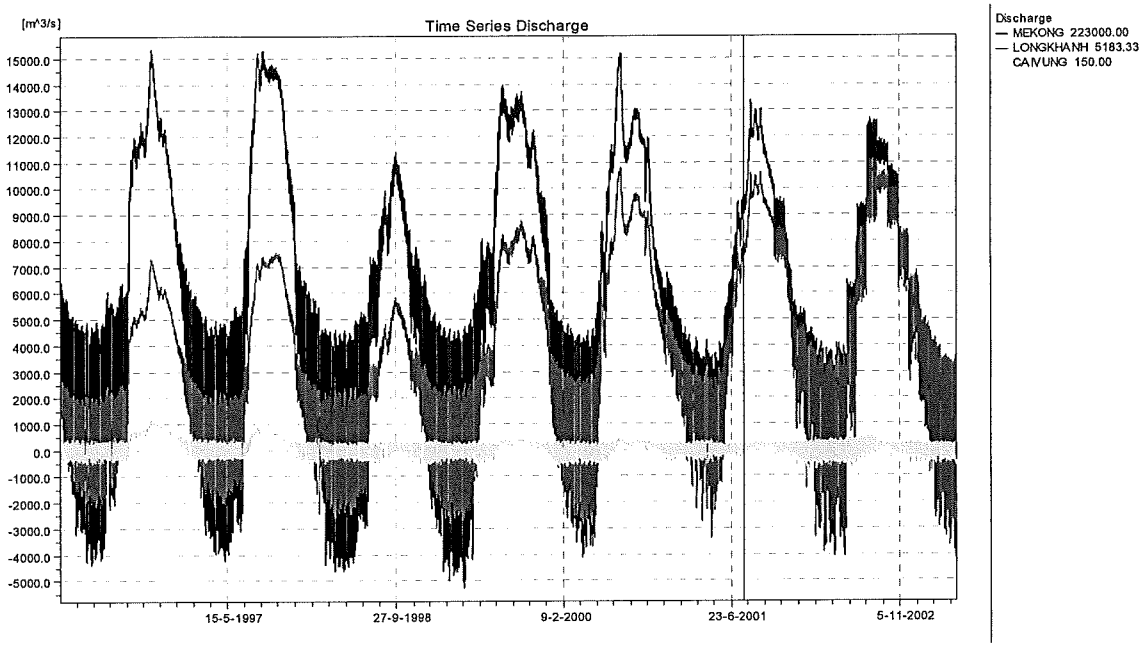

Figure A.3.6: The discharge increase and decrease at Long Khanh and Hong Ngu respectively, period 1996-2003

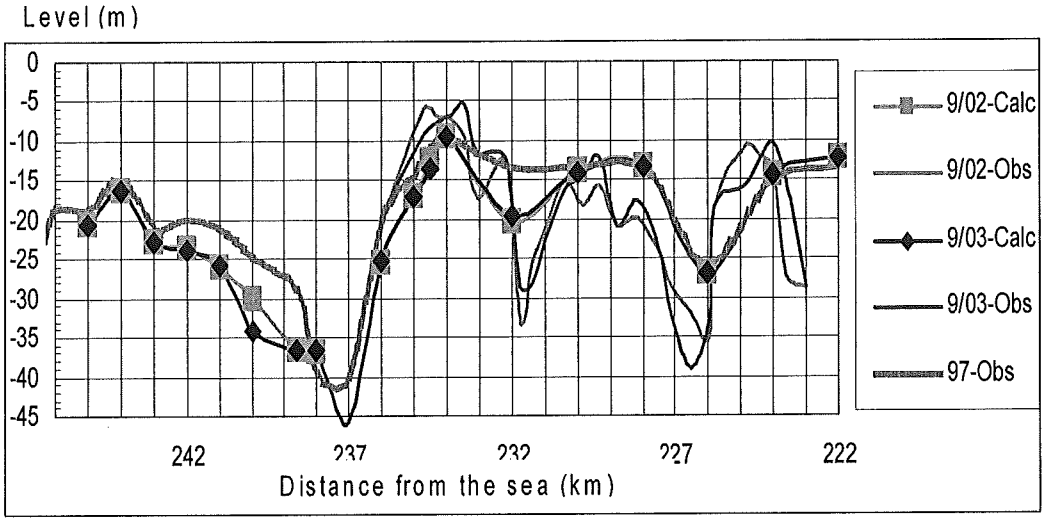

Figure A.3.7 : River bed (talweg) simulation and Observation from Vietnam – Cambodia border- Tan Chau – Hong Ngu (Hong ngu channel)

Appendix A - 4
Roughness coefficient, bed form, helical flow and sediment transport

A.4.1. Input data

Base on the topography 2002, and the hourly water level from 1996 to 1999:
Average water level above mean sea level: + 1.66m
Average bed level: -9.87m (abmsl)
The average water depth for the whole area: h=1.66+9.87= 11.5m and slope $i=4x10^{-5}$, D_{50}=0.25mm, D_{90}=1mm, $\nu=10^{-6}m^2/s$, $g=10m/s^2$, $\Delta=1.65$, $\rho = 1000kg/m^3$.

A.4.2. Roughness coefficient

The shear stress velocity: $u_* = \sqrt{ghi} = \sqrt{10x11.5x4x10^{-5}} = 0.068$ (m/s) (5-11)

- Fall particle velocity: from D_{50}=0.25mm in the figure 2.5 Sediment transport in river lectures note the fall velocity for particle is found w_s=0.031(m/s)
- Checking the bed form is whether in motion or not by used fig 3.1 Shields diagram.

$$\left.\begin{aligned} R_e &= \frac{u_* D}{\upsilon} = \frac{0.068x0.25x10^{-3}}{10^{-6}} = 17 \\ \frac{hi}{\Delta D} &= \frac{11.5x4x10^{-5}}{1.65x0.25x10^{-3}} = 1.12 \end{aligned}\right\} \Rightarrow \text{Motion}$$

✓ **Apply Engelund and Hansen (1967)**

$$C = 18\left(\frac{h'}{h}\right)^{0.5} \log\frac{12h'}{2.5D_{50}} \quad (5\text{-}12)$$

where

C - Chezy roughness coefficient ($m^{1/2}/s$)
h - water depth (m)
D_{50} – mean diameter of particle (m)
h' is parameters (m)

$$h' = \left(\frac{\theta'}{\theta}\right)h \quad (5\text{-}13)$$

$$\theta = \frac{u_*^2}{\Delta g D_{50}} = \frac{0.068^2}{1.65x10x0.25x10^{-3}} = 1.12 > 1.0 \quad (5\text{-}14)$$

$$\Rightarrow \theta' = (0.3 + 0.7.\theta^{-1.8})^{-0.56} = 1.08$$

from (5-13) h'=11.09 (m)
from (5-12) **C = 94.2** ($m^{1/2}/s$)

✓**Apply Van Rijn (1984)**

$$C = 18\log\left(\frac{12h}{k_s}\right) \quad (5\text{-}15)$$

where γ_d=0.7 for field data.
Assuming initial Chezy coefficient C=94.2 ($m^{1/2}/s$)
$\Rightarrow$ u =C$\sqrt{hi}$ = $94.2x\sqrt{11.5x4x10^{-5}}$ =2.02 (m/s)

Then $T = \left(\tau_0^{'} - \tau_{0,cr}\right)/\tau_{0,cr}$ (5-16)

Where $\tau_{0,cr}$ is the critical shear stress as a function of grain size (quoted from Breusers,1986)

Correspond D_{50}=0.25mm => $\tau_{0,cr}$=0.18 (N/m^2)

$$\tau_0^{'} = \rho g\left(\frac{u}{C'}\right)^2 \quad (5\text{-}17)$$

$$C' = 18\log\frac{12h}{3D_{90}} = 18\log\frac{12x11.5}{3x1x10^{-3}} = 83.93$$

Apply equation (5-17) => $\tau_0^{'} = 1000x10\left(\frac{2.02}{83.93}\right)^2$ =5.79(N/m^2)

From (5-16) T computed:

$T = \left(\tau_0^{'} - \tau_{0,cr}\right)/\tau_{0,cr}$ =(5.79 -0.18)/0.18= 31.17>10=> Ripples vanish

$k_s = 3D_{90}$ =3x1x10^{-3} = 0.003

From equation (5-15)

$$C = 18\log\left(\frac{12h}{k_s}\right) = 18\log\left(\frac{12x11.5}{0.003}\right) = 83.9 \text{ m}^{1/2}/\text{s}$$

=> u =C$\sqrt{hi}$ = $83.9x\sqrt{11.5x4x10^{-5}}$ =1.8 (m/s)

Base on the application of both method, we choose C=90m$^{1/2}$/s for simulation.

A.4.3. Bed form.

✓ Apply the Criteria for bed forms [after Simons et al (1961)]:

$$\left.\begin{aligned}\frac{u_*}{w_s} &= \frac{0.068}{0.031} = 2.19\\ \frac{u_* D}{\upsilon} &= \frac{0.068x0.25x10^{-3}}{10^{-6}} = 17\end{aligned}\right\} \Rightarrow \text{Plane bed or standing waves}$$

A.4.4. Helical flow.

The intensive of helical flow is estimate equal to ten times of ratios water depth over radius of curvature. Herein doing the calibration for helical flow by checking the estimation:

✓ Tan Chau bend: Radius outer bend =3073m, Radius inner bend =1536m, average depth equal 20.96(m), so that:

$i_s = \frac{10h}{R}$ => i_s=0.068 for outer bend and i_s=0.136 for inner bends.

✓ Hong Ngu bend: Radius outer bend =2116m, Radius inner bend =1715m, average depth equal 17.15 (m), so that:

$i_s = \frac{10h}{R}$ => i_s=0.084 for outer bend and i_s=0.104 for inner bends.

A.4.5. Sediment transport predictor.

✓Bed load and suspended load factor:
In sediment transport, the ratio between current related bed-shear velocity over partical fall velocity taken an important parameters to consider whether the bed-load or suspended load important. Herein the A.4.3 denoted:

$\frac{u_*}{w_s} = \frac{0.068}{0.031} = 2.19 >> 1$ **so that, the suspended load is more important than bed-load.**

In the 7.3.16 Ratio of suspended and total load transport, Principle of sediment transport in rivers, estuaries, Coastal Seas and Ocean (Van Rijn) denoted that:

Corresponding to $\frac{u_*}{w_s} = 2.19$

Van Rijn (1984): => ratio suspended and total $q_s/q_{total}=0.72$
Laursen (1958): => ratio suspended and total $q_s/q_{total}=0.58$

✓ Bed load computed by Van Rijn:

Apply Van Rijn (1984a)
$q_b = 0.1.\Delta^{0.5}.g^{0.5}.D_{50}^{1.5}.D_*^{-0.3}.T^{1.5}$ for T≥ 3

Wherein: q_b : volumetric bed load transport rate (m^2/s).

D_{50} : Average diameter of bed material (m). $D=0.25x10^{-3}(m)$.

D_* : Particle parameter.

$$D_* = D_{50}\left[\frac{\Delta g}{\upsilon^2}\right]^{1/3} = 6.36$$

v : Kinematic viscosity coefficient $=10^{-6}$ (m^2/s)

Δ : Specific density. $\Delta=1.65$

g : accelerate of gravity (m^2/s). $g=9.81(m^2/s)$.

T : Transport stage parameter, T=31.17 see A.4.2

=> $q_b=0.00016$ (m^2/s)

$\mathbf{S_{bed\text{-}load}} = q_b \times B = \mathbf{0.00016x550=0.088}$ (m^3/s)

✓ Suspended load computed by Van Rijn:
Using the simplified method was given by Van Rijn (1984b)

$$\frac{q_s}{uh} = 0.012\left(\frac{u-u_{cr}}{\Delta g d_{50}^{0.5}}\right)^{2.4}\left(\frac{D_{50}}{h}\right)\left(\frac{1}{D_*}\right)^{0.6}$$

wherein:

q_s : volumetric suspended load transport rate (m^2/s).

u_{cr} : $u_{cr}=0.015$(m/s), base on Critical shear velocity as function of grain size for sand (Breusers,1986)

u : depth average velocity, u=C(hi)^0.5=1.93 (m/s)

h : average water depth, h=11.5m

i : slope $i=4x10^{-4}$

D_{50} : Average diameter of bed material (m). *$D=0.25x10^{-3}(m)$.*

D_* : $D_*=6.36$ Particle parameter, see above.

Δ : Specific density. *$\Delta=1.65$*

g : accelerate of gravity (m^2/s). *$g=9.81(m^2/s)$.*

=> $q_s=0.00023$ (m^2/s)

$\mathbf{S_{suspended\text{-}load}} = q_s \times B = \mathbf{0.00023x550=0.127}$ (m^3/s)

✓Total load computed by Van Rijn and Englund-Hansen:

Apply Van Rijn method:

$q_{total}=q_{suspended\ load}+q_{bed\text{-}load}=0.00023+0.00016=0.00039$ (m^3/s)

$S_{total}=S_{suspended\ load}+S_{bed\text{-}load}=0.127+0.088=0.215$ (m^3/s)

Apply Engelund –Hansen (1967)

$$s = \frac{0.05}{1-\varepsilon} \times \sqrt{g \times \Delta \times D_{50}^3} \times \left(\frac{h \times i}{\Delta \times D_{50}} \right)^{2.5} \times \frac{C^2}{g} \quad (m^3/s/m).$$

The sediment transport in (m^3/s):

$\mathbf{S} = s \times B\ (m^3/s)$

Wherein:

B : width of the channel (m) at Tan Chau . *$B=550(m)$.*

h : water depth (m) for whole area is 11.5m.

i : slope of river . *$i=4x10^{-5}$.*

D_{50} : Average diameter of bed material (m). *$D=0.25x10^{-3}(m)$.*

C : Chezy coefficient ($m^{1/2}/s$). *$C=90\ (m^{1/2}/s)$ in A.4.2*

ε : Porosity of bed material. $\varepsilon=0.4$

Δ : Specific density. *$\Delta=1.65$*

g : accelerate of gravity (m^2/s). *$g=9.81(m^2/s)$.*

=> $s= 0.00144\ m^3/s/m$

$\mathbf{S_{total}} = s \times B = \mathbf{0.00144x550=0.792}$ (m^3/s)

Appendix A-5.
Scour hole computation, results of MIKE21C

A.5.1. Scour hole computation

Terms	Radius of curvature (m)	River width (m)	Average water depth h(m)	Scour depth h_b (m)	Notes
Data observed 2004				44.7	Observed
Maynord	2660	619	24.1	49.3	Prediction
USACE	2660	619	24.1	56.4	Prediction
MIKE21C				50.5	Prediction

Table: A.5.1 The results of prediction bend scour and MIKE21C

A.5.2. More MIKE21C results of revetment

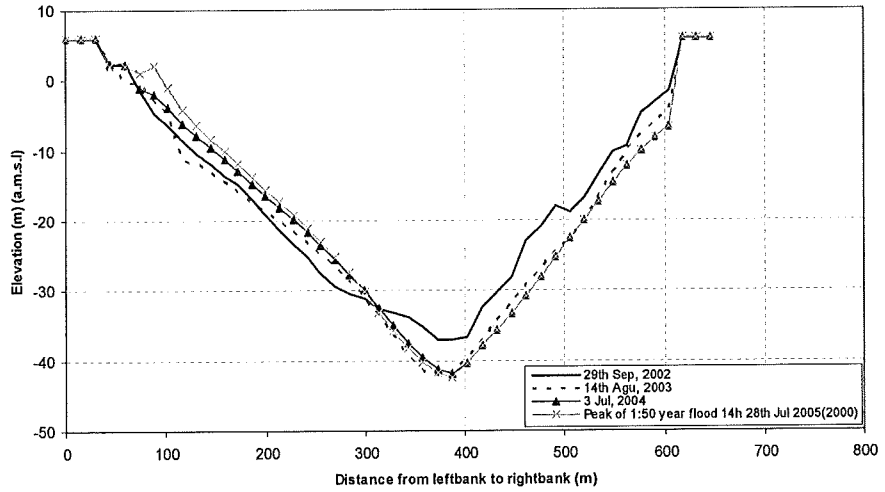

A.5.1. The bed level change at J=273, K=0-45 upstream of revetment

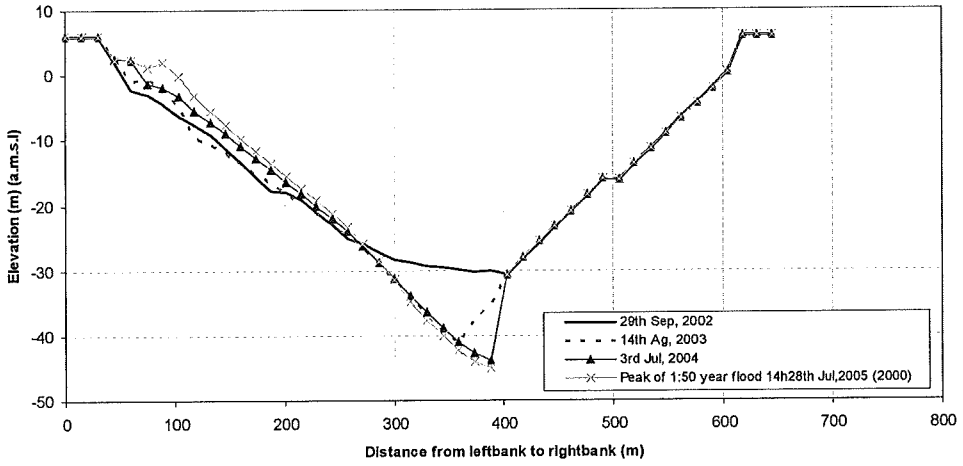

A.5.2. The bed level change at J=274, K=0-45 revetment

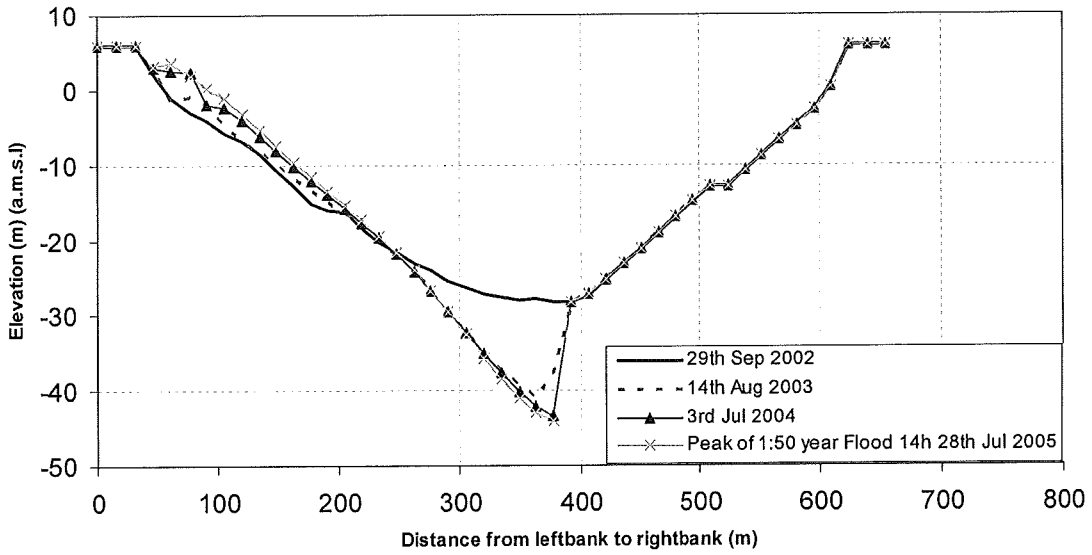

A.5.3. The bed level change at J=276, K=0-45 revetment

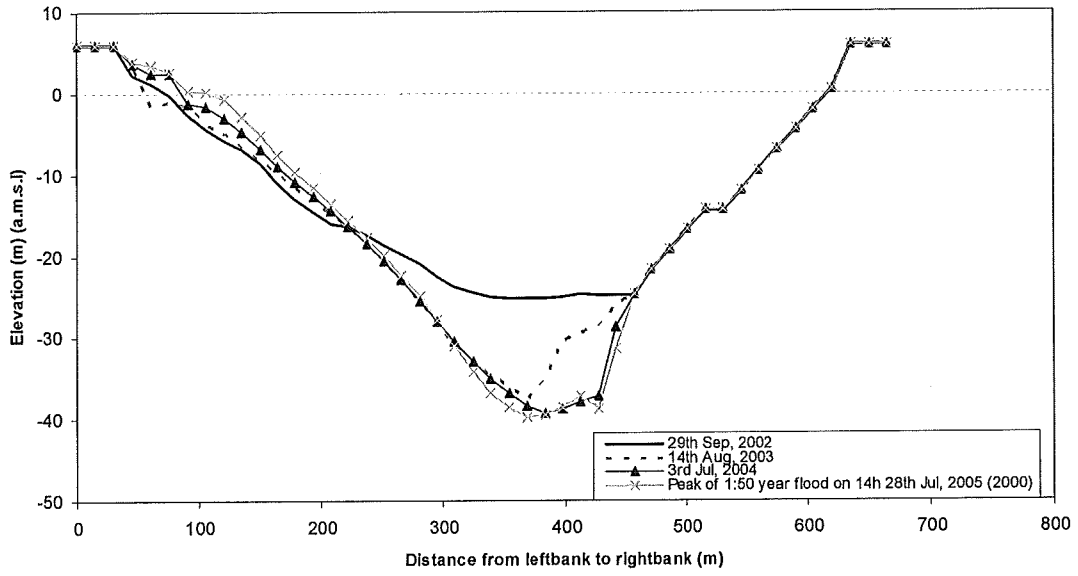

A.5.4. The bed level change at J=278, K=0-45 revetment

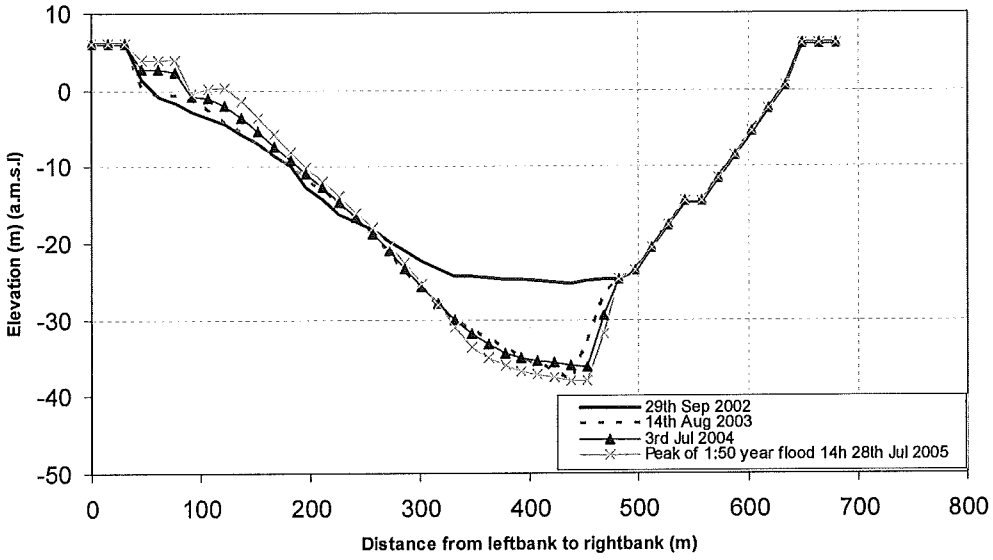

A.5.5. The bed level change at J=278, K=0-45 revetment

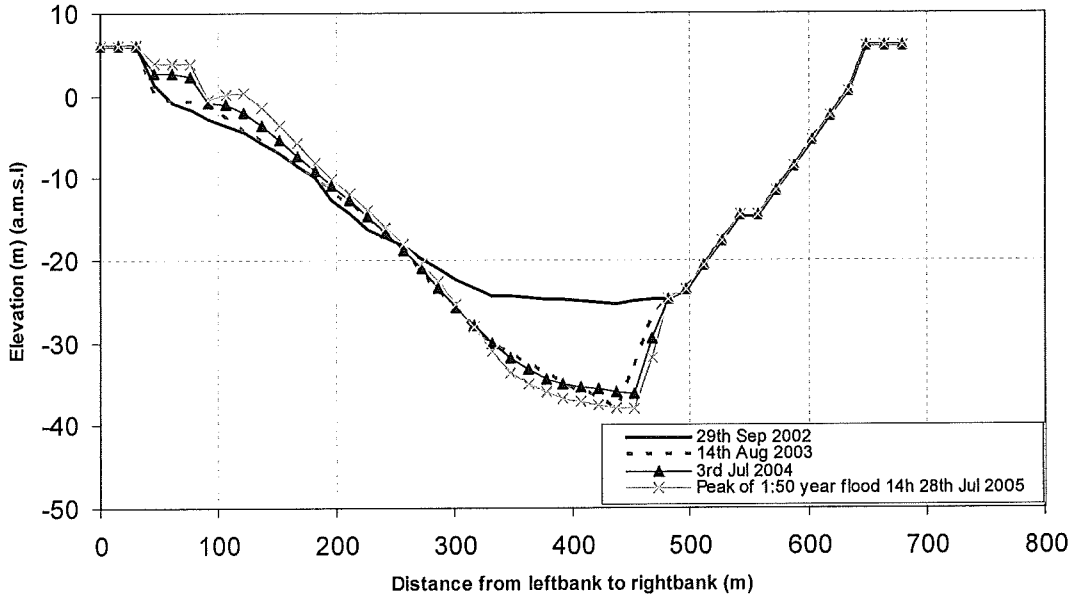

A.5.6. The bed level change at J=280, K=0-45 revetment

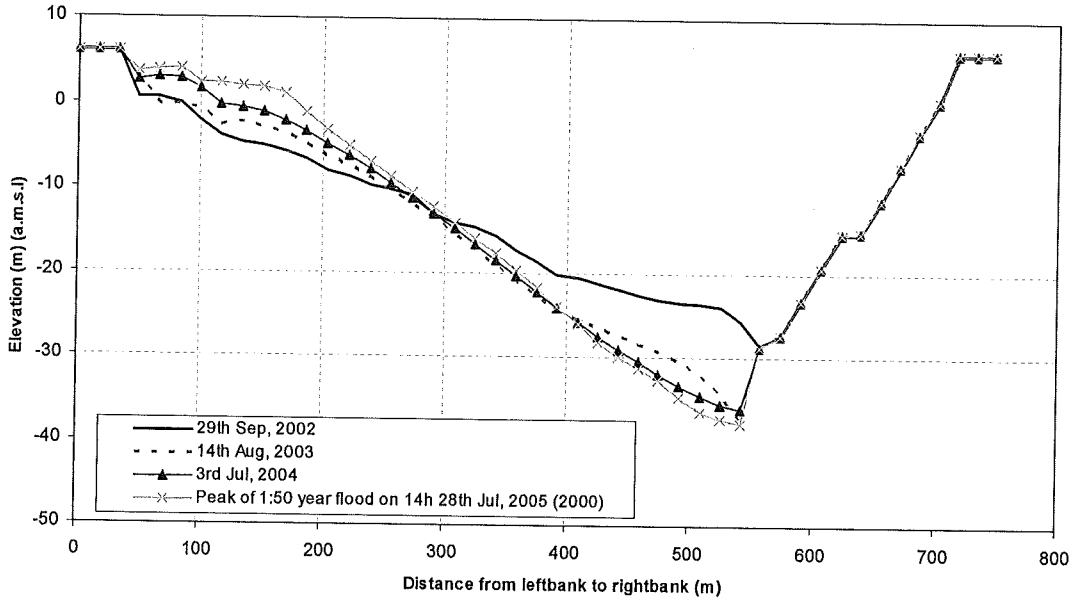

A.5.7. The bed level change at J=286, K=0-45 revetment

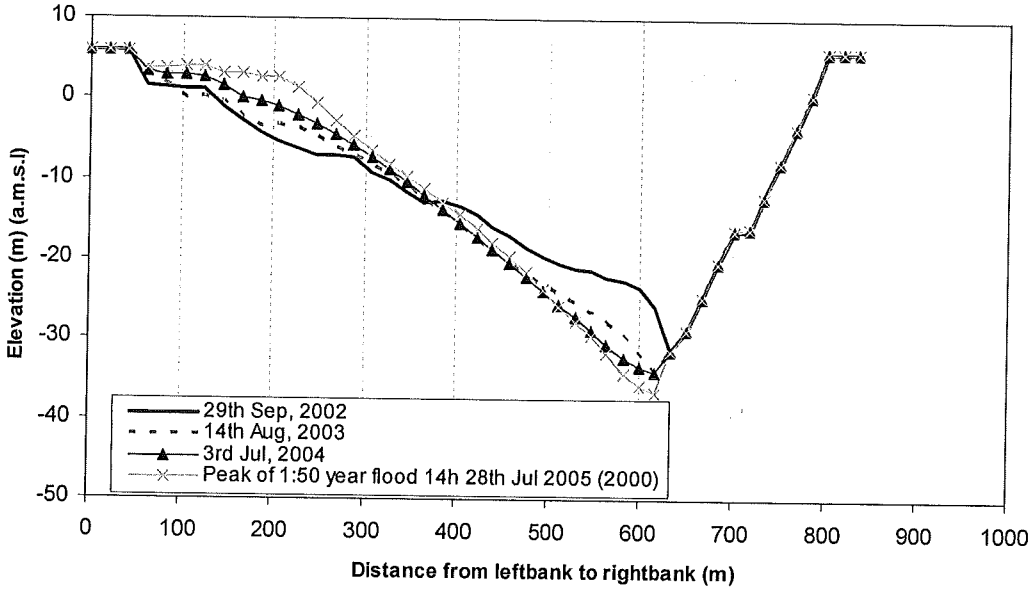

A.5.8. The bed level change at J=290, K=0-45 revetment

A.5.3. More MIKE21C result of Bend cut-off

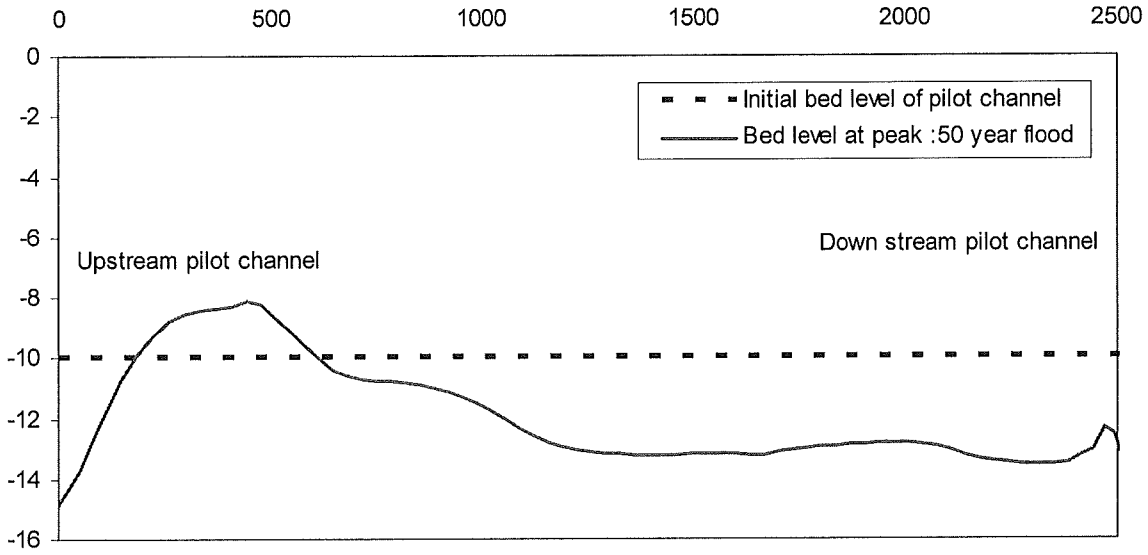

A.5.9. The bed level change in pilot channel during 1:50 year flood

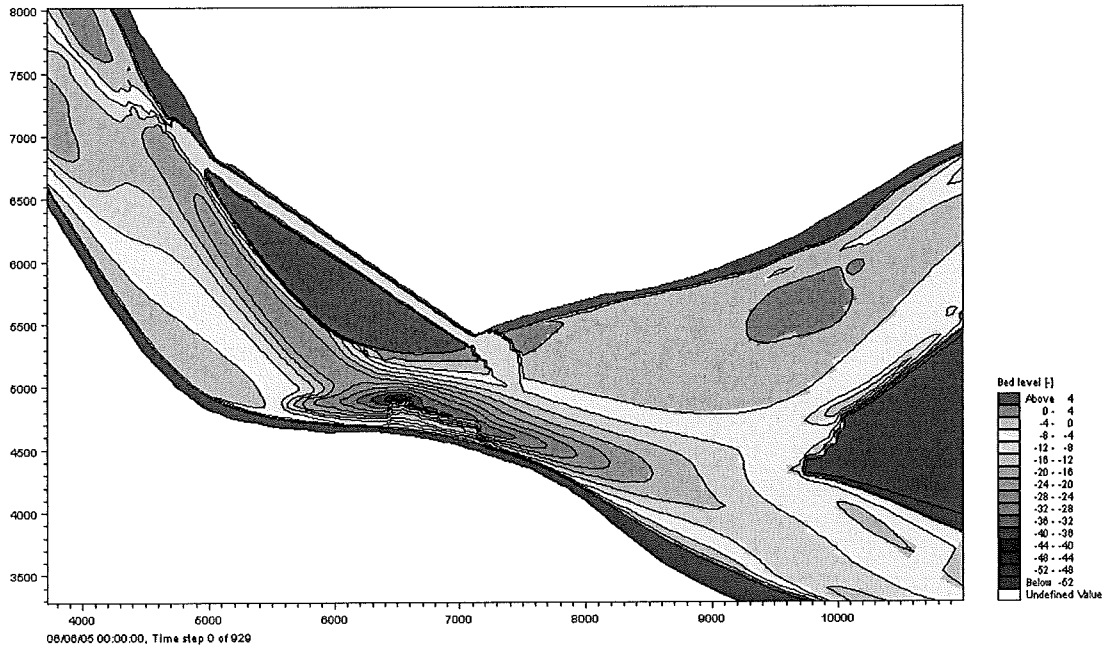

A.5.10. Before open the pilot channel during

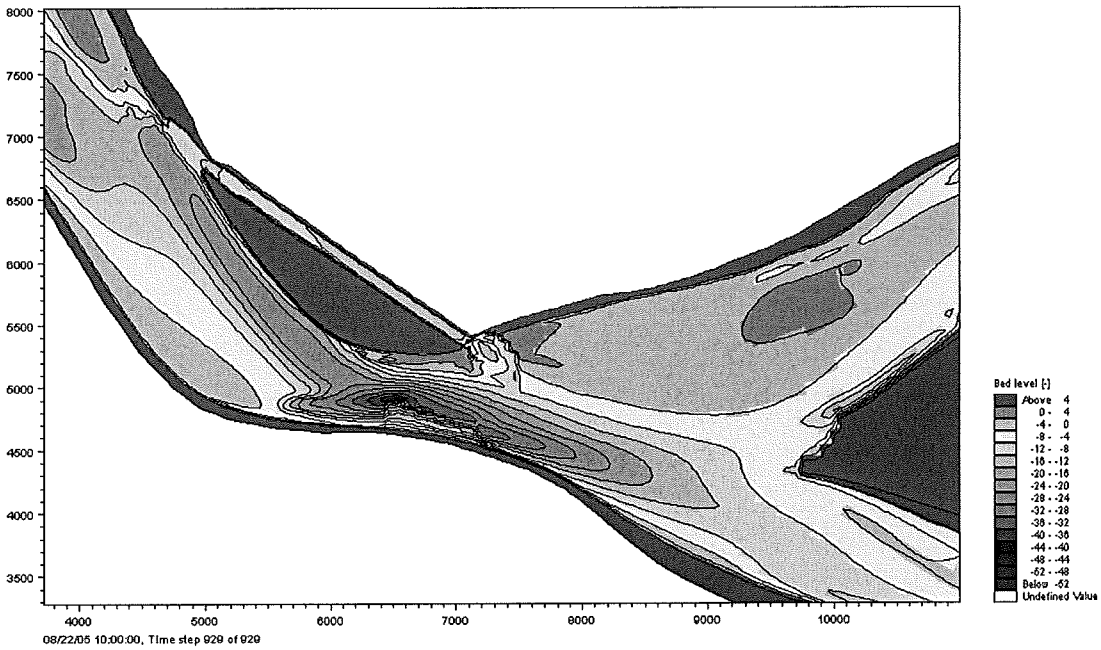

A.5.11. Bed level change at the peak of flood

Appendix A-6
GUIDELINE PERMEABLE GROYNE DESIGN

A.6.1. Overall length, alignment and termination of groyne fields

The length, alignment, and termination of permeable groyne are very similar with those elements of revetment. However, the structural layout of groyne field bears a substantially layer number of possible variations of different structure components due to the strong interference between the most important characteristic properties (porosity, spacing, individual length, etc).

The standard layout of a groyne field consist of a central section with a series of at leats 3 groynes similar in composition and length plus an upstream and downstream termination with shorter groynes (with decreasing length). See figure A.6.1

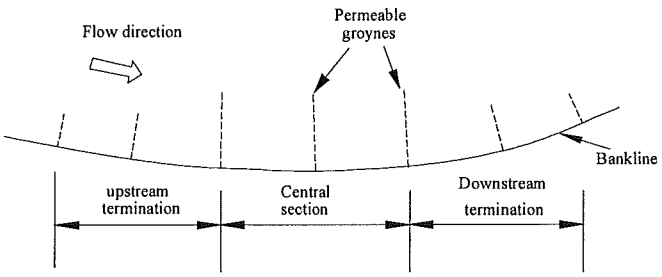

Figure A.6.1: Schematic layout of permeable groyne field.

A.6.2. Permeability of Groynes

The permeability P of a groyne is defined by the ratio of open (non-blocked) area to the total area, which can be expressed by the quotient of internal width s and the distance e between the axis of two adjacent piles (P=s/e, see figure A.6.2)

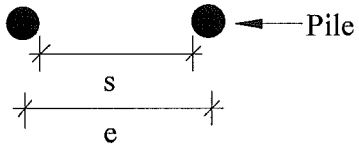

Figure A.6.2. Definition of groyne permeability

The optimum permeability of a groyne is dependent on various boundary parameters (flow velocities, local turbulence, grain size distribution, etc) and is strongly interrelated with structural conditions of groyne field (number and length of groynes, spacing in flow direction).

Base on the research result of Bangladesh guideline the permeability of groyne recommended in the table below.

Section	Permeability (%)
First pile near the river bank (groyne root)	
0 to 0.25L_G	50
0.25 to 0.50L_G	60
0.50 to 0.75L_G	70
0.75 to 1.00L_G	80
Last pile in river (groyne head)	

Table A.6.1. Recommended pile arrangement for a permeable groyne (L_G is length of groyne)

The minimum permeability of P=0.5 (50%) show in table should kept for constructional reason because of increased pile-driving resistance). Moreover, due to of main goal of permeable groyne is reduction of flow near banks, there for P>60% in this area should be avoided.

A.6.3. Orientation of groynes

The deviation of the streamline is mainly dependent on the structure included blockage of flow cross-section, which can be described by the length and permeability of structure in relation to the geometrical channel properties. In comparison with the impermeable, spurs groyn, the orientation of permeable groyne is not so important. Because of economical reason, the orientation of permeable groynes is perpendicular with river bank.

A.6.4. Crest level

In order to restrict the hydraulic loads (currents, waves and floating debris) at higher water levels, groyne may be designed as submerged structure (during peak flood). To reduce this influences, the groynes can be designed with a negative freeboard, they act as slightly submerged groynes and towards the groyne root, the crest level of piles should increase to meet the elevation of the embankment. In case of partly or completely submerged groynes (during high flood level) the installation of navigation signal at the groyne's head is obligatory.

A.6.5. Design of individual groynes

A.6.5.1. The groyne length

The effective length of a groyne L_G is defined as the length on a theoretical line perpendicular to the riverbank. For orthogonal groynes, the effective length and the linear groyne length are identical. The main design aspect regarding the minimum effective groyne length L_G is to sustain the embankment stability with regard to the developing scour hole downstream from the groyne head.

Assuming a natural scour slope (dependent on the existing subsoil) developing from the deepest point of the scour hole towards the bankline, the minimum groyne length can be calculated according to figure A.6.3 The actual location of the scour hole will shift towards the embankment, in case oblique flow attack is prevalent.

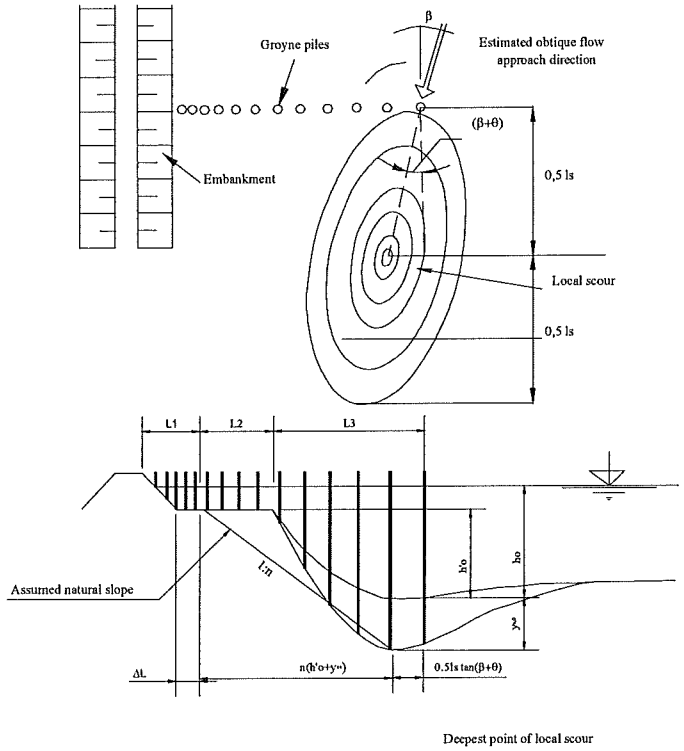

Figure A.6.3. Assumed scour development at the groyne head

According to the figure 6.9, the effective length of groyne calculate in following equation (6-1) and the upper limit in equation (6-2) to possible negative impacts at opposite bank line:

$$L_G \geq \Delta L + n.(h_0^{'} + y_{s,0}) + 0.5.l_s.\tan(\beta + \theta) \qquad (6\text{-}1)$$

and $L_G \leq 0.2$ to $0.4\ B_{ch}$ (6-2)

where

L_G (m) effective length of groyne (perpendicular to the embankment)

ΔL (m) safety margin (minimum ΔL=10m)

n (-) cotangent of natural slope of the bed material 1(V):n(H) for sandy, non-cohesive soils n=5.5 is recommended.

h_0' (m) water depth at the thalweg referred to flood plain level.

$y_{s,0}$ (m) maximum total scour depth related to the thalweg of the undisturbed river bed

l_s (m) length of scour hole perpendicular to the groyne axis with first estimate l_s=4y_s

θ (^{0}) angle of flow attack between flow line and bankline

β (^{0}) fictitious angle of flow separation (see figure A. 6.4.)

B_{ch} (m) average width of the approach channel

A.6.5.2. Spacing of permeable groynes

From the economical point of view, the spacing should be as large as possible. However, the efficiency of groyne field as a whole shall not be affected by too large spacing.

A groyne can be considered as a disturbance of the flow field, which diminishes in downstream direction and finally becomes neutralized after a certain distance, called the relaxation length λ_w. The relaxation length follows from a linear balance between the convective term and the friction term in a one dimensional momentum equation, which is defined for a bank parallel flow as:

$$\lambda_w = c_5 \frac{C^2 h}{2g} \qquad (6\text{-}3)$$

where

$\lambda_w (m)$ relaxation length

C ($m^{\wedge 0.5}/s$) Chezy coefficient

g (m/s^2) acceleration due to gravity

h (m) local water depth

c_5 (-) empirical coefficient for channel properties

Channel alignment	Water depth in groyne field	Scour hole	Coefficient c_5
Bend	deep	deep	0.85
Straight	deep	Moderate/deep	0.70
straight	Half of main channel depth	No/moderate	0.50

Table A.6.2. Recommended values for c_5 dependent on local situation

The spacing of permeable groyne is recommended at a value of approximate SG=2/3 λ_w (e.g. Jansen et al.,1979). A factor 2/3 has been taken into account with respect to keep the separating flow line at a certain distance from the bank line.

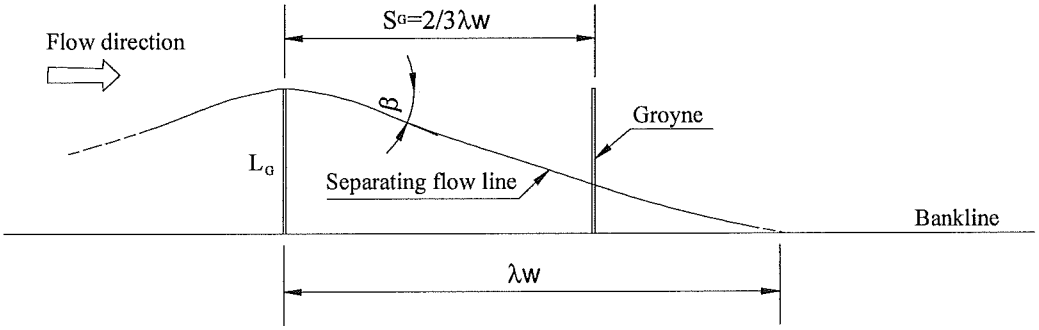

Figure A.6.4. Theoretical separating flow line (bank parallel flow)

In equation (6-1) the fictitious separation angle β defined base on figure A.6.4

$$\tan\beta = \frac{L_G}{\lambda_w} = c_5.2g.\frac{L_G}{C^2 h} \qquad (6\text{-}4)$$

It is obvious, that using (6-4) for calculation the relaxation length is not consistent with physics. Introducing a potential angle of oblique flow attach, the minimum spacing S_G between two adjacent groynes is given by:

$$S_G = \frac{2}{3}.\frac{L_G}{\tan(\theta+\beta)} \qquad (6\text{-}5)$$

where

L_G(m) effective length of permeable groyne

θ (^{0}) angle of flow attack between flow line and bankline

β (^{0}) fictitious angle of flow separation

A.6.6. Design of piles

The individual goyne must be existent load due to current, waves and floating debris. Furthermore, loads resulting from ship impacts or earthquakes might be of importance, but are not included here.

Pile design comprises the determination of required embedment length, which is needed to transmit the loads acting on the pile structure into the subsoil as well as the dimension of the required pile diameter and wall thickness.

A.6.6.1 Loads

*** Current induced loads**

The single piles to withstand the forces resulting from the flowing water. Due to the effect of the groynes, the flow velocities –and thereby the corresponding loads to the piles-are reduced along the groyne axis towards the embankment. Base on how reduction of average velocity nearby the river bank, so in the figure A.6.5 show the recommendation of reduce velocity along the axis of groyne.

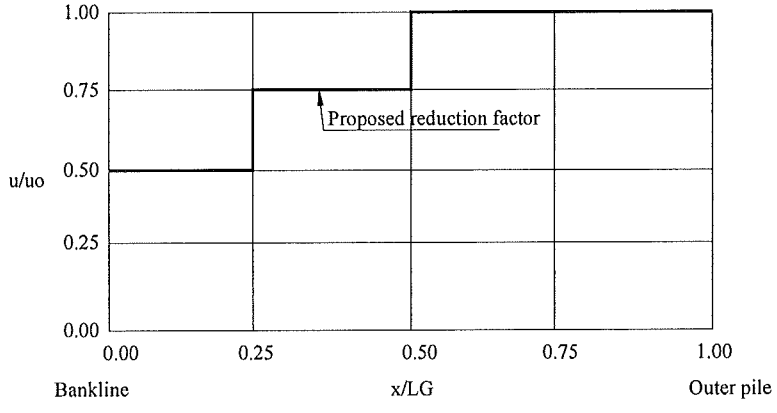

Figure A.6.5. The recommended reduction of flow velocities along groyne axis

The current induced load on a single pile can be determined by a momentum approach, based on the velocity distribution over the water depth:

$$p(z) = \int_{z=0}^{z=h} C_D 0.5.\frac{\gamma_w}{g} D.u_1^{\,2}(z)dz \qquad (6\text{-}6)$$

where

C_D (-) drag coefficient to characterize the structure fluid interaction (friction, viscosity, and turbulence (C_D=0.7 for circular piles).

γ_w (KN/m^3) density of water

g (m/s^2) acceleration due to gravity

D (m) diameter of pile

$u_1(z)$ (m/s) the velocity depend on the flow depth

The flow velocity distribution over the water depth is given by a logarithmic profile as function below;

$$u_1(z) = u_1 \frac{\ln\left(30\frac{d_1 - z}{k_s}\right)}{\ln\left(11.\frac{d_1}{k_s}\right)} \qquad (6\text{-}7)$$

where

u_1 (m/s) average upstream flow velocity

d_1 (m) the average depth in upstream

h (m) average water depth

z (m) depth at the velocity $u_1(z)$

k_s (-) coefficient of roughness for the river bed

Due to narrowing of the cross-section between adjacent piles of a permeable groyne a local water level set up upstream from the structure occurs which is followed by a decrease in the upstream velocity. Based on the assumption of constant water level gradient at the structure, the water level difference h_s can be calculated by the REHBOCK formula:

$$h_s = \alpha.[\delta - \alpha(\delta - 1)](0.4 + \alpha + 9\alpha^3)\left(1 + \frac{u_2^2}{g.d_2}\right)\frac{u_2^2}{2g} \qquad (6\text{-}8)$$

where

h_s water level difference at pile (m)

α α=1-P, blockage (-)

D Diameter of piles (m)

e distance between two adjacent piles (m)

δ shape coefficient (δ=2.10 for round, δ=3.80 for square piles) (-)

d_2 (m) undisturbed downstream design water depth

u_2 (m/s) average undisturbed downstream velocity

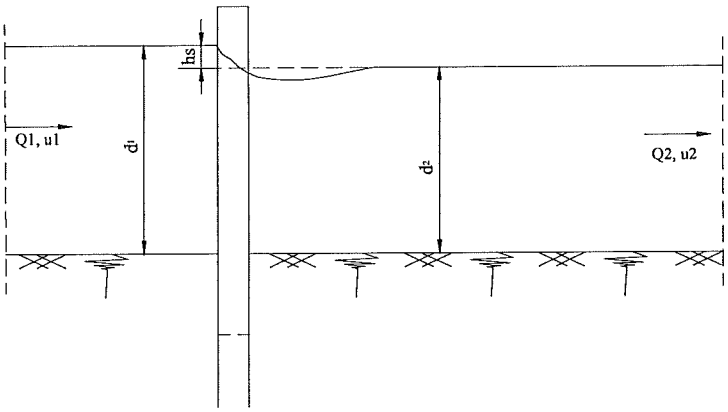

Figure A.6.6. Current induced water level set-up upstream of a single pile

With the simple relation $d_1=d_2+h_s$ and with $Q=d_1.u_1=d_2.u_2$ (continuity equation, constant channel width) the average upstream flow velocity can be calculated.

$$u_1 = \frac{u_2 d_2}{d_1} \tag{6-9}$$

*** Wave induced load**

The wave included load resulting from progressive waves consists drag forces due to velocity components and inertia forces which are generated by acceleration components of the orbital motion. Due to the fact, that the maximum of drag and inertia forces under a progressive wave occur at different wave phases (theoretical phase lag of a quarter wave length for linear waves) both load components must be computed and superimposed for different phase angles. For comparatively slender elements ($D/L \leq 0.05$), the resulting non-breaking wave load on a vertical pile can be approximated by the MORISON formula (SPM 1984):

$$p(z) = p_D(z) + p_M(z) = \beta\left(C_D.\frac{1}{2}.\frac{\gamma_w}{g}.D.u(z).|u(z)| + C_M.\frac{\gamma_w}{g}.\frac{D^2\pi}{4}.\frac{du(z)}{dt} \right) \tag{6-10}$$

and

$$p = \int_{z=0}^{z=h} p_D(z) + p_M(z)dz \tag{6-11}$$

where

p(z) depth dependent wave force, (kN/m)
p total resulting wave force on a single pile, (kN)
p_D drag force per unit length of pile, (kN/m)
p_M inertia force per unit length of pile, (kN/m)
C_D drag coefficient (C_D=0.7) (-)
C_M inertia coefficient (C_M=2.0 for circular piles) (-)
g acceleration due to gravity, (m/s^2)
γ_W density of water (γ_W =10 kN/m^2) (kN/m^2)
β (-) correction factor for narrow spaced piles (-)

At alluvial rivers, velocity and acceleration components computed by linear wave theory will provide sufficient accuracy for the calculation of non-breaking wave loads on pile structures.

In case of more severe wave attack is expected (estuaries, etc) a more detailed study of the wave forces might be needed. The phase related velocity and acceleration components under a linear deep water wave are given by:

$$u = \frac{H}{2}\omega.e^{k.z}\cos\upsilon \qquad (6\text{-}12)$$

$$\frac{du}{dt} = \frac{H}{2}\omega^2.e^{k.z}\sin\upsilon \qquad (6\text{-}13)$$

where

d (m) water depth

u (m/s) horizontal component of the orbital velocity

$\frac{du}{dt}$ (m/s^2) horizontal component of the orbital acceleration

H (m) wave height

t (s) temporal co-ordinate

T (s) wave period

ω (1/s) angular wave frequency ω=2π/T

L (m) wave length $L = \frac{g.T^2}{2\pi}$

e (-) base of the natural logarithm (e=2.718…)

k (1/m) wave number k=2π/L

z (m) vertical co-ordinate (z=0, still water table)

υ (-) phase angle υ=k.x-ω.t (describing temporal and spatial development of a progressive wave)

x (m) spatial co-ordinate

The correction factors β for wave loads on narrow spaced pile clusters are adapted from EAU (1996). For a relative spacing between 2< e/D<4 the correction factor β can be calculated by

$$\beta = 2 - 0.25\frac{e}{D} \qquad (6\text{-}13)$$

To keep a certain simplicity, this method was also applied for e/D=1 and the value suggested in table below.

e/D (-)	1	2	3	4
P(%)	50	67	75	80
β (-)	1.85	1.5	1.25	1.0

Figure A.6.3. Correction factor β for different relative spacing e/D

*** Floating debris**

The floating debris induce is considered as a horizontal load F_h computed by equation below:

$$F_h = 0.5.\frac{\gamma_w}{g}.e.h_d.u_s^2 \qquad (6\text{-}14)$$

where

F_h (kN) horizontal force to single pile

h_d (m) thickness of floating debris

u_s (m/s) surface velocity

*** Load combination**

The piles are stressed by current induced load together with forces resulting from either waves or floating debris. Waves are absorbed by the floating debris, so that the forces caused by waves and floating debris do not act simultaneously and only the more unfavourable load has to be considered in the pile design.

A.6.6.2. Pile length

All load acting on a vertical groyne pile must be transmitted into the subsoil. The horizontal force and the bending moment are compensated by the earth pressure which is limited by the embedment module of the soil. The embedment length is the statically required pile length below the design bed level including the design scour depth in figure A.6.7.

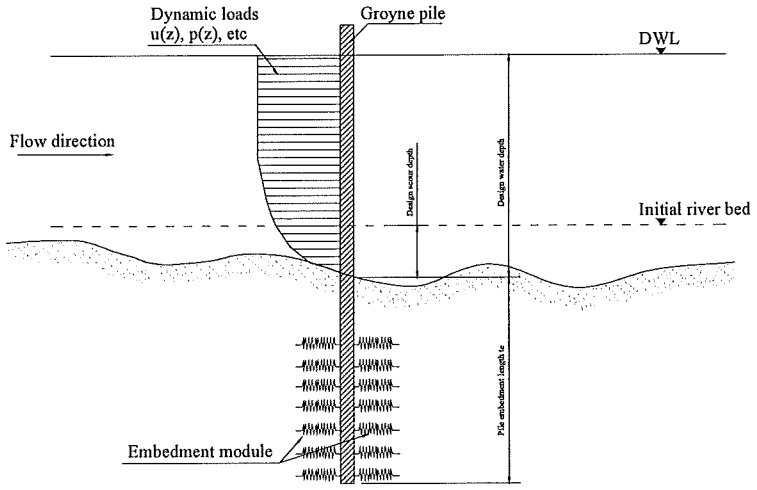

Figure A. 6.7. Definition of pile embedment length

* Blum method.

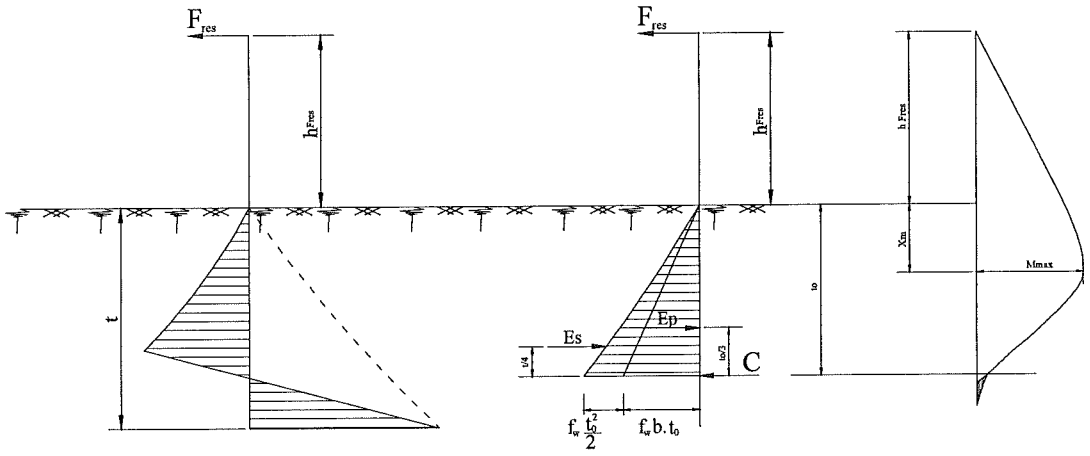

Figure A.6.8. Assumtion and simplication of Blum method (adapted from EAU,1990)

The first step is applying the Blum method to reduce the actual single linear loads to resulting force F_{res} with the lever arm h_{Fres} in relation to the design river bed level. The resulting force is given by:

$$F_{res} = \sum_{z=0}^{z=-h} F_h(current) + F_h(wave) + F_h(floatdebris) \qquad (6\text{-}15)$$

$$M_{res} = \sum F_h(current).z_{sc} + F_h(wave).z_{sw} + F_h(floatdebris).z_{s\,fd} \qquad (6\text{-}16)$$

The lever arm h_{Fres} of the resulting force is defined by:

$$h_{Fres} = \frac{M_{res}}{F_{res}}$$

The minimum embedment length t_e is calculated following the pre-condition that the pile bending moment is equal to zero. Applying the ideal earth pressure distribution, the fictitious embedment length t_0 at the ideal centre of moments (M=0, see figure A.6.8) has to calculated iteratively. Following the definition given in A.6.8 can be derived from:

$$\sum M = 0 \Rightarrow F_{res}(h_{res} + t_0) - f_w \frac{D.t_0^2}{2}.\frac{t_0}{3} - f_w \frac{t_0^3}{6}.\frac{t_0}{4} = 0 \qquad (6\text{-}17)$$

$$\Rightarrow F_{res}(h_{res} + t_0) - f_w\left(\frac{D.t_0^3}{6} + \frac{t_0^4}{24}\right) = 0 \qquad (6\text{-}18)$$

$$\Rightarrow t_0^4 + 4.D.t_0^3 - \frac{24}{f_w}.F_{res}.t_0 - \frac{24}{f_w}.F_{res}.h_{Fres} = 0 \qquad (6\text{-}19)$$

with

D(m) pile diameter

f_w (t/m^3) coefficient of passive earth pressure $f_w = \gamma \tan^2(45^0 + \frac{\varphi}{2})$

γ (t/m^3) density of subsoil

t_o (m) fictitious embedment length at the ideal centre of moments

The quadratic term of t_0 (second term in equation (6-17) considers the linear increase of the earth pressure with depth directly behind the pile (idealized pressure distribution), whereas the cubic term of t_0 (third term in 6-17) considers the exponential increase of the spatial extent of the activated earth pressure.

When talking into account a spatial earth pressure component in transversal direction (parallel to groyne axis), it has to be borne in mind that the initiated spatial earth pressure of two adjacent piles will overlap at a certain critical depth t_{crit}, which must be considered in the computations. Below t_{crit} the earth pressure is increasing only linear with increasing penetration depth of the piles, therefore the assumption regarding the earth pressure distribution in figure 6.14 is not appropriate for narrow spaced groynes. The actual (qualitative) distribution of the passive earth pressure is shown in figure A.6.9

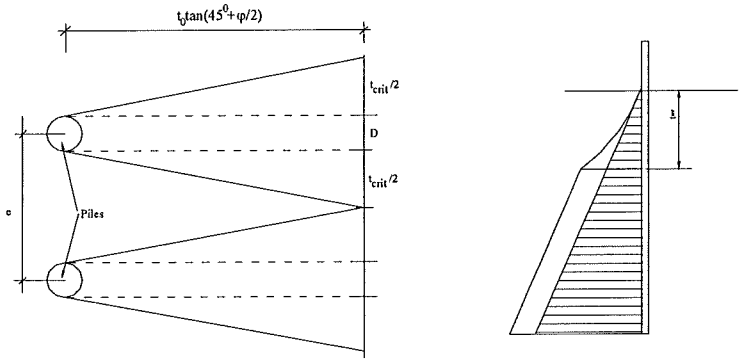

Figure A.6.9. Overlapping spatial earth pressure of adjacent piles at critical depth t_{crit}

For a small permibility of the groyne (P=50-60%) the cubic term in (6-17) can be neglected and instead the diameter D in the quadratic term should be replaced by the distance e between two adjacent piles to derive the minimum theoretical embedment length:

$$\sum M = 0 \Rightarrow F_{res}(h_{res} + t_0) - f_w \frac{e.t_0^2}{2}.\frac{t_0}{3} = 0 \qquad (6\text{-}20)$$

The actual minimum embedment length is given by

$t_e = f.t_0$ (6-21)

The correction factor f is required to approximate the actual moment distribution and earth pressure condition as described in figure A.6.8 and is f=1.2 for normal cases. If no bed protection/ falling apron is provided (compare figure A.6.11) this value should be increase to f=1.5.

To cover inaccuracies in the prevailing boundary conditions the design pile embedment length t_{design} should be determined by the following steps:

(1) Compute the theoretical minimum required pile embedment length [t_e]

(2) add a safety margin of 25% for consideration of variation in the subsoil

(3) Make sure that minimum pile embedment length is always above 5m

$t_{design} = 1.25 t_e \geq 5$m.

A.6.6.3. Pile bending moment

Groyne piles are almost entirely burdened by horizontal loads. These create a bending moment in the pile, which must be designed appropriately.

The bending moment distribution in the pile is given by

$$M_x = F_{res}(h_{Fres} + x) - f_w\left(\frac{D.x^3}{6} + \frac{x^4}{24}\right) \qquad (6\text{-}22)$$

The location x_m of the maximum bending moment below the design reiver bed has to be derived iteratively.

$$\frac{x_m^3}{6} + \frac{D.x_m^2}{2} = \frac{F_{res}}{f_w} \qquad (6\text{-}23)$$

or

$$F_{res} = \frac{f_w}{6}.x_m^2(x_m + 3.D) \qquad (6\text{-}24)$$

so that

$$M_{\max} = \frac{f_w}{24}x_m^2[3x_m^2 + x_m(4.h_{Fres} + 8.D) + 12.h_{Fres}.D] \qquad (6\text{-}25)$$

A.6.7. Bed protection and falling apron

The local erosion of the riverbed near a permeable groyne haed can be prevented by a bed protection or falling apron. A bed protection consist of a cover layer placed on the filter mat, whereas the falling apron material is dumped directly on the riverbed. Since under the prevailing flow conditions the placing of the filter mat is rather complicated, falling aprons are the only practicable solution at present (figure A.6.10). The dimension of the falling aprons units (preferably-cubic concrete blocks) and the respective volume required can be derived from the formulae given in revetment part of this thesis.

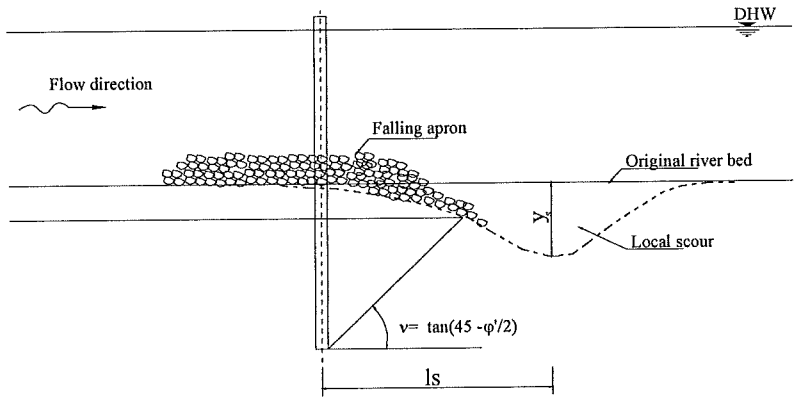

Figure A.6.10. Expected local scour near a groyne head with falling apron